Calcium-montmorillonite and related mixed-layer illite/montmorillonite clays from the UK; the interdependence of physical properties with mineralogy, chemistry and mode of occurrence.

Morgan, D. J

CALCIUM-MONTMORILLONITE AND RELATED MIXED-LAYER ILLITE/MONTMORILLONITE CLAYS FROM THE UK; THE INTERDEPENDENCE OF PHYSICAL PROPERTIES WITH MINERALOGY, CHEMISTRY AND MODE OF OCCURRENCE.

by

D.J. MORGAN

A thesis presented for the degree of Ph.D. of the University of London, 1974.

ABSTRACT

Montmorillonite has certain very important physico-chemical properties, absent or much less pronounced in other clay minerals, which lead to a range of commercial uses. The relationship of these properties to the mineralogical constitution of the clay is not well understood and it is difficult to forecast behaviour in use without recourse to extensive technical testing. In order to throw some light on this problem a number of samples of montmorillonite and interstratified illite/montmorillonite (mainly from Cretaceous and Silurian strata respectively) were examined using various mineralogical, chemical and physico-chemical techniques. The relative merits of certain rapid and simple tests in providing quantitative data (in terms of montmorillonite content) for both original clay samples and purified products is assessed. Emphasis is placed on the extent of particle aggregation in the montmorillonites and the effect of this on the development of some physico-chemical properties.

The clay samples were upgraded by means of a hydrocyclone. Complete chemical analyses and derived structural formulae are given for four of the purified montmorillonites and four purified illite/montmorillonites. Exchangeable cations present in a selection of samples are also tabulated.

Current theories regarding the origin of the Cretaceous montmorillonite deposits of the UK are reviewed and, mainly on the basis of certain features of the trace element assemblage and accessory mineralogy of the present samples, it is suggested that the clays are the alteration products of trachytic ash falls. A pyroclastic source for the Silurian illite/montmorillonites has long been accepted; trace element and accessory mineral data for the present samples suggests that the composition of the original ash was close to that of an alkaline rhyolite or quartz-trachyte. Some of the volcanic centres active in the area of the Welsh Silurian geosyncline can thus be eliminated as possible sources.

ACKNOWLEDGEMENTS

The work recorded here formed part of the research programme of the Mineralogy Unit, Institute of Geological Sciences. The project was originally entitled "The use of certain physico-chemical properties of Ca-montmorillonites as a guide to the assessment of fuller's earth clays in terms of quantitative mineralogy" and it was intended that it should be submitted for the degree of M.Phil. under the regulations governing persons working for a higher degree at research institutions outside the University of London. Work on the project started in January 1970; its scope was subsequently widened and approval for it to be submitted for the degree of Ph.D. was given in March 1973. I am grateful to the Director, IGS, and Mr J.E.T. Horne, Head of the Mineralogy Unit, for initial approval of the project and also for allowing me to devote part of my official time to the preparation of this thesis.

I also wish to record my gratitude to the following:

Professor R.A. Howie, my Director of Studies at King's College.

Mr J.A. Bain, my supervisor at IGS, for his constant interest, support and critical advice throughout the period of research.

Dr J.N. Walsh, King's College, under whose direction many of the chemical determinations recorded in Chapter 5 were carried out.

Colleagues at IGS for advice and assistance, in particular Dr I.R. Basham and Mr D. Bland, Mineralogy Unit, and Mr B.A.R. Tait, Analytical and Ceramics Unit.

The management of Laporte Industries Ltd. for permission to visit their quarries at Redhill and underground workings at Combe Hay. Similarly, the management of the the Steetley Co. Ltd., Berk Mineral Division, for permission to visit their quarries at Woburn.

CONTENTS

CHAPTER 1

FIELD OCCURRENCE AND GENERAL DESCRIPTION OF SAMPLES

1.1 INTRODUCTION

The 35 samples chosen for detailed investigation fall into three groups. The first group (samples A1-17) consists of clays, mainly from the Lower Greensand horizon, in which montmorillonite is the only clay mineral present. The second group (samples B1-15) is composed of members of the interstratified illite/montmorillonite series which were collected almost exclusively from Silurian strata. In the third, and smallest, group (samples C1-3) montmorillonite is accompanied by varying amounts of other clay minerals such as kaolinite and chlorite. Most samples were collected personally during summer 1970 and spring 1971. The exceptions were montmorillonites A1-6, from boreholes in the Baulking and Fernham area, Berks., which had originally been examined by the author during his official duties in the Mineralogy Unit, Geochemical Division, I.G.S., and samples A17 and B15, similarly examined in 1968. Where relevant, results from a small number of additional samples (all encountered during the author's official duties) are also incorporated in this study. The laboratory numbers assigned to these samples on arrival at the Geochemical Division (e.g. 696A) are retained here and therefore they may easily be distinguished (in figures, tables etc.) from samples of the three main groups described above.

In this chapter the general geographical and stratigraphical distribution of montmorillonite and interstratified illite/montmorillonite is described in some detail. Data for the present samples are given mainly in tabulated form. Descriptions of the field occurrence of the interstratified illite/montmorillonite clay horizons are also presented.

1.2 DISTRIBUTION OF MONTMORILLONITE IN UK SEDIMENTS

1.2.1 General

Discrete montmorillonite has not been recorded in sediments earlier than the Devonian (Perrin, 1971). Wilson (1971) found that montmorillonite dominated the clay fractions of some Dittonian sediments from NE Scotland, this author considering that the mineral had formed by alteration of volcanic material. The presence of montmorillonite in the Downtonian Raglan Marls of Monmouthshire has also been noted (Perrin, op. cit.). According to Perrin montmorillonite is rare in the Carboniferous and only sporadic occurrences have been described in either Permian or Triassic sediments.

Montmorillonite is widespread in the Jurassic, occurring in many clay-rich horizons such as the Lower Fuller's Earth and Oxford Clay. In these horizons it is usually present in small amount and is invariably accompanied by other clay minerals, notably clay-grade mica and kaolinite. However a 3m thick bed of montmorillonite, unaccompanied by significant amounts of other clay minerals, does occur in the Jurassic Upper Fuller's Earth horizon at Combe Hay, Somerset. Montmorillonite is extracted from an adit mine at this locality for industrial use.

In the Cretaceous, beds of montmorillonite up to 6m thick are found in the Lower Greensand Sandgate Beds of southern England (Worssam, 1963; Cowperthwaite et al., 1972). The mineral is worked as 'fuller's earth' (see section X1.1 for a definition of this term) at Woburn, Bedfordshire, Nutfield, Surrey, and Maidstone, Kent. Extensive deposits of workable grade have recently been discovered in the Lower Greensand of Berkshire (Poole and Kelk, 1971a, b). Rare occurrences of montmorillonite have also been reported from the Speeton Series of Lincolnshire (Robertson, 1961). Because of their importance in the present study the Lower Greensand occurrences are described in more

detail in the following section. Montmorillonite is present in the clay fractions of the Lower Chalk and Jeans (1968) has suggested that the mineral is of neoformed origin. Marl bands in the Middle Chalk are particularly rich in montmorillonite (Hallam and Selwood, 1968; also present study). Up to 80% of the insoluble residues from samples of the Upper Chalk may be composed of montmorillonite, possibly of authigenic origin (Weir and Catt, 1965). Cowperthwaite et al. (op. cit.) have suggested that the Chalk montmorillonite may have originated by the diagenetic alteration of wind-blown volcanic dust.

With a few exceptions (see Perrin, op. cit.) almost all Tertiary and Quaternary sediments contain montmorillonite, invariably in association with other clay minerals. Gilkes (1968) has suggested that the montmorillonite present in Tertiary sediments of the Hampshire basin originated from erosion of the Chalk.

The stratigraphical distribution of montmorillonite, with its greater preponderance in younger rocks, is not without some considerable significance in diagenetic terms and this feature will be mentioned again in later discussions.

1.2.2 Description of Lower Greensand montmorillonite occurrences

Seams of montmorillonite up to 2m thick are found at Maidstone, Kent. At this locality the area of deposition of the Sandgate Beds, which consist mainly of glauconite silty clays, would appear to have had an east-west extent of about 15 km and, possibly, a north-south extent of 5 km (Worssam, 1963).

At Woburn, Bedfordshire, the montmorillonite and enclosing sediments form an elongate basin which is truncated at depth against the Oxford Clay in the south-west and outcrops in the north and east (Cowperthwaite et al., 1972). Two montmorillonite horizons are recognisable and of these the upper and most prominent varies in thickness

from 2.5 to 3.75 m. Coarse, ferruginous sandy beds (the Woburn Sands) occur abeve and below and main montmorillonite horizon. These sands exhibit strong cross-stratification, a south to north flow being evident from the wave shape.

The montmorillonite-bearing beds of Surrey are lenticular and extend for a distance of 15 km from east to west and attain a maximum thickness, at Nutfield, of 20m. The main (lowest) montmorillonite horizon is 4-5m thick; other thinner seams occur above the main horizon and are separated by beds of sandy limestone.

In the area around Baulking and Fernham, Berkshire (Poole and Kelk,. 1971a, b), deposition of the montmorillonite and associated sediments is thought to have taken place in an irregularly-shaped trench in the Kimmeridge Clay and Corallian Beds rdughly aligned in a north north west to south south east direction. Two montmorillonite beds are present. The lowest is 1 m thick, is generally very pure, and has sharply defined upper and lower limits. The upper bed shows a sharp base, is fairly rich in montmorillonite in the lower portions, but shows a gradual upward increase in sand and silt content into the overlying arenaceous sediments. The montmorillonite-bearing beds may pass laterally into cross-bedded, silty montmorillonitic sands towards the centre of the trench and into similar sands and pebbly, ill-sorted mudstones along the margins.

Two quite different theories of origin for the Lower Greensand montmorillonite have been put forward. Cox (1918), later supported by Newton (1937), Wood (1956), Robertson (1961), and Poole and Kelk ; (1971a, b) suggested that the montmorillonite was a direct chemical precipitate; Kerr (1932), Hallam and Selwood (1968) and Cowperthwaite et al. (1972) favoured derivation from volcanic material. Data which may be relevant to the origin of the Lower Greensand montmorillonites are presented in chapters 4 and 5 and the subject discussed in detail in chapter 6.

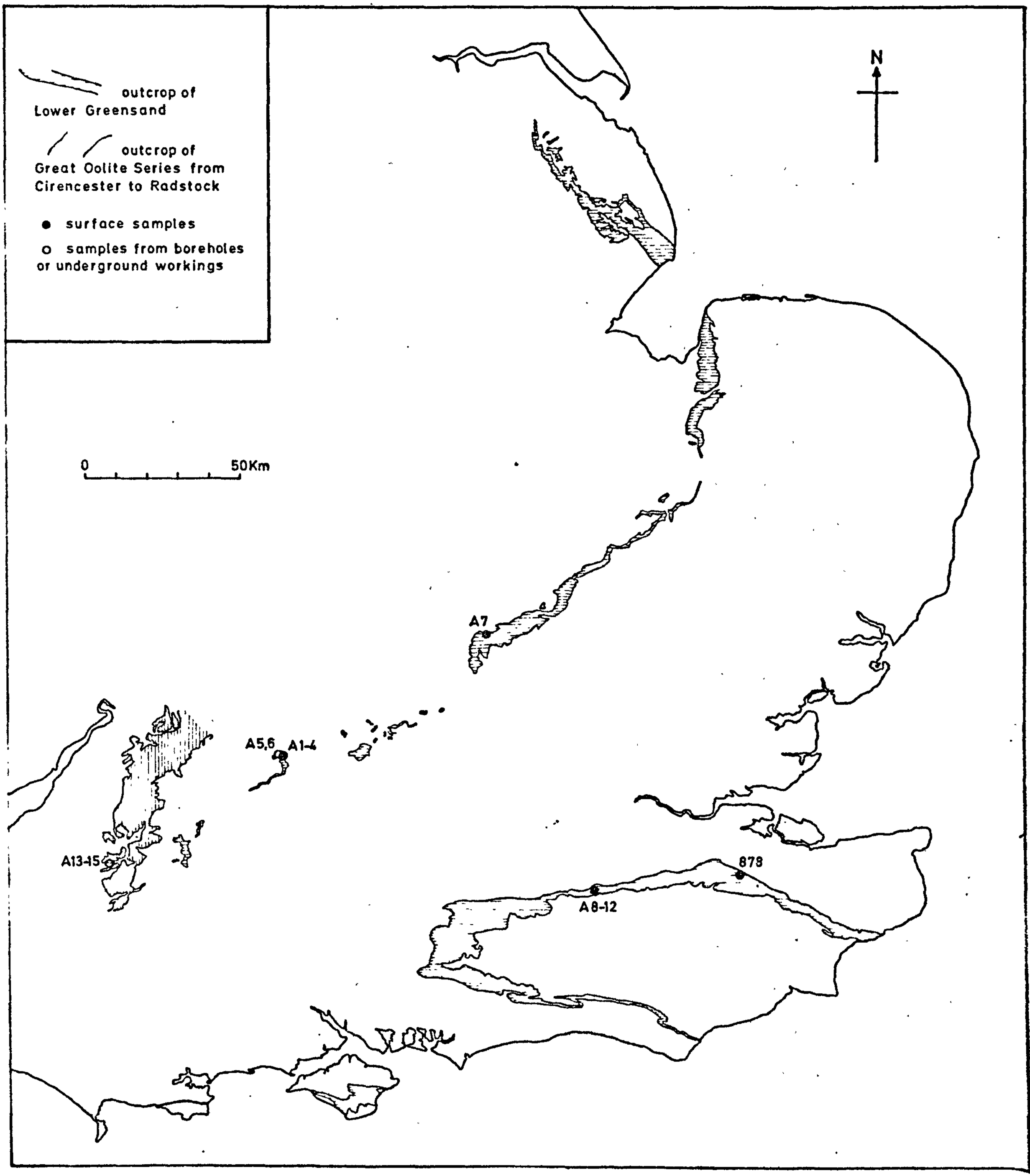

Fig. 1.1 Montmorillonite sample localities

1.3 MONTMORILLONITE SAMPLE LOCALITIES

Table 1.1 gives brief descriptions and location details for the montmorillonite samples examined. Montmorillonites were collected from all the known Lower Greensand occurrences (see previous section) and sample localities, with respect to the outcrop of the Lower Greensand, are shown in fig. 1.1. The other Cretaceous sample (A16) was collected from a poorly exposed marl band in the Middle Chalk (a description of the quarry section is given by Sherlock, 1922). The Jurassic montmorillonite samples (A13-15) were collected from an underground working face at the Combe Hay Mine, Somerset (see fig. 1.1). The grade of the montmorillonite decreased appreciably towards the top of the clay seam. Sample A17 was also obtained from underground workings. It represents the alteration product ('bole') of a Lower Carboniferous lava flow. Normally such boles consist of aluminium hydroxide minerals (eg gibbsite, boehmite etc.) and kaolinite.

1.4 DISTRIBUTION OF INTERSTRATIFIED ILLITE/MONTMORILLONITES IN UK SEDIMENTS

1.4.1 General

In the UK nearly all interstratified illite/montmorillonite clays are found in deposits of the potassium-bentonite type (see Appendix 1 for discussion of this term). Such deposits are widespread in Ordovician and Devonian strata of the eastern and central USA (Huff, 1963; Mossler and Hayes, 1966; Droste and Vitaliano, 1973) and similar occurrences have also been described from the Devonian of Canada (Smith, 1967) and the Lower Palaeozoic of Scandinavia (Bystrom, 1956; Hageman and Spjeldnaes, 1955; Jorgensen, 1964). There is a general consensus of opinion among these authors that the potassium-bentonites represent the alteration

products of fine-grained, wind-transported, volcanic ash which had been deposited in a marine environment. The few workers who have published descriptions of the UK illite/montmorillonite-rich horizons also accept this view.

Published occurrences from strata ranging in age from Ordovician to Carboniferous are summarised below. No occurrences of illite/montmorillonite in sediments younger than the Carboniferous have been noted.

1.4.2 Ordovician

Ball (1968) and Bjorlykke (1971) have identified horizons rich in illite/montmorillonite in Ordovician sedimentary sequences of north and central Wales. Ball described eleven illite/montmorillonite seams interbedded with shaly flags of mid-Caradoc age at Conway, Caernarvonshire, the clay from one of the seams appearing to contain about 10% montmorillonite layers. Bjorlykke found illite/montmorillonite in sediments ranging in age from Arenig to Caradoc at three separate localities (in Anglesey, near Builth Wells and near Llandeilo). From the diffraction traces described by this author the clays may contain between 20 and 30% montmorillonite interlayers.

1.4.3 Silurian

Thin bands of illite/montmorillonite clay are common in Wenlock and Ludlow strata of the Welsh Borderlands. In the past these clays, known as 'Walker's Earth' or 'Walker's Soap' (Murchison, 1839) and locally as 'pudlo' (Mitchell et al., 1961), found restricted use as Fuller's Earth. Frequent mention of these clays is made in the literature dealing with the stratigraphy of the Silurian of the Welsh Borders but comprehensive descriptions of the illite/montmorillonite horizons are rare.

Butler (1937) gave a general account of a number of 'bentonitic' clay bands in a core section from a borehole penetrating Silurian strata at Walsall, Staffs. (Although this author did not specifically recognise interstratified illite/montmorillonite - the first such definitive identification from Silurian strata appears to be that of MacEwan (1956) - there is no doubt from the description of these bands that most, if not all, were composed predominantly of interstratified clay). The clay bands occurred mainly in a Wenlock sequence of shales and mudstones and were concentrated within 60 m either side of the Barr Limestone. Thicknesses were generally 1 cm or less although some up to 5 cm thick were noted. Most were green in colour and had sharply defined upper and lower contacts with the enclosing sediments. A few bands contained flakes of biotite up to 3 mm in diameter. Thin sections showed that the biotite was often chloritized. Biotite flakes were common in the mudstones for a distance up to 2 cm above the illite/montmorillonite bands, Butler suggesting that the 'slow rate of settlement of the biotite flakes led to the concentration of a large proportion at the top of the volcanic deposit, and the slight movement of the waters over the sea floor sufficed to redistribute the flakes in the normal sediment'. Davidson (in an appendix to Butler, op. cit.) noted that the stability range of detrital biotite is not great and also that this mineral is extremely rare in early Palaeozoic sediments. He suggested that the biotite and original material of the enclosing clay bands were deposited from air-borne volcanic dust of acid to intermediate composition.

The field relationships of a number of illite/montmorillonite horizons occurring in the Wenlock Limestone succession near Much Wenlock, Shropshire, have been described by Trewin (1971). This author noted that lower contacts of the clay horizons were usually sharp; upper contacts were often sharp against shale (containing chlorite, muscovite and

quartz) or, alternatively, there might be a zone of mixed shale and illite/montmorillonite grading upwards into shale. In the normal bedded limestone the thickness of the horizon was often variable and in extreme cases they died out laterally and were replaced by shale bands. The horizons generally stopped on reaching the margin of a reef but Trewin described one instance where the illite/montmorillonite did appear to pass over the top of a reef mass. Over the area of the reef the detrital sediment and illite/montmorillonite were mixed; laterally adjacent to the reef the illite/montmorillonite horizon had sharply defined upper and lower limits. Trewin suggested that the activity of the reef organisms was responsible for the mixing of the original volcanic material with the normal detrital sediment of the area.

1.4.4 Dēvonian

Only minor occurrences of illite/montmorillonite have been recorded in strata of Devonian age, these being from Dittonian sediments in north east Scotland (Wilson, 1971) and the Downtonian Raglan Marls of Monmouthshire (Perrin, 1971).

1.4.5 Carboniferous

In Carboniferous strata of the Derbyshire Dome illite/montmorillonite horizons, known as 'wayboards', occur interbedded with both massive shelf limestones and contemporaneous shaly basinal limestones, mainly of D1 and D2 age (Walkden, 1972). This author found that the amount of montmorillonite interlayering in the wayboard clays varied from 10-35% and appeared to be related to the lithology of the enclosing limestones - clays occurring in the thinly-bedded limestones of basinal aspect containing more montmorillonite interlayers than those from the massive shelf limestone sequences. Alteration products of contemporaneous lavas and tuffs were indistinguishable from the wayboard clays on the basis of simple mineralogy, both

containing, in addition to illite/montmorillonite, appreciable kaolinite and anatase. From the evidence available Walkden could not relate the wayboard clays to any known volcanic centre in the Derbyshire Dome. He did suggest however that they might be 'in part the products of as yet undiscovered vents and may be outside the shelf region altogether and which..... never developed much beyond an explosive, probably largely submarine phase'.

Trewin (1968) has described a number of illite/montmorillonite bands from the Namurian (S1, S2) of Staffordshire and Derbyshire. These occurred in a basinal sequence of Carbonaceous shales and mudstones rich in pyrites. Kaolinite usually accompanied the illite/montmorillonite which contained 20-40% montmorillonite interlayers. Trewin noted, but did not discuss further, that black shales adjacent to the illite/montmorillonite horizons also contained appreciable amounts of this mineral.

Spears (1971) found that illite/montmorillonite was the main constituent of a 'tonstein' occurring in the Middle Coal Measures (base of Westphalian C) of north Staffordshire.

1.5 INTERSTRATIFIED ILLITE/MONTMORILLONITE SAMPLE LOCALITIES

1.5.1 General

Table 1.2 gives brief descriptions and stratigraphic locations of the interstratified illite/montmorillonites selected for the present study.

Most of the Silurian samples were collected from inliers of Wenlock and Ludlow rocks of the shelf facies. Localities (fig. 1.2) range from the Usk Inlier, Monmouthshire (B1, 2), one of the southernmost outcrops of Silurian strata in the UK, to Ironbridge, Salop. (786A) which is on the edge of the main area of Wenlock and Ludlow sedimentation, Samples

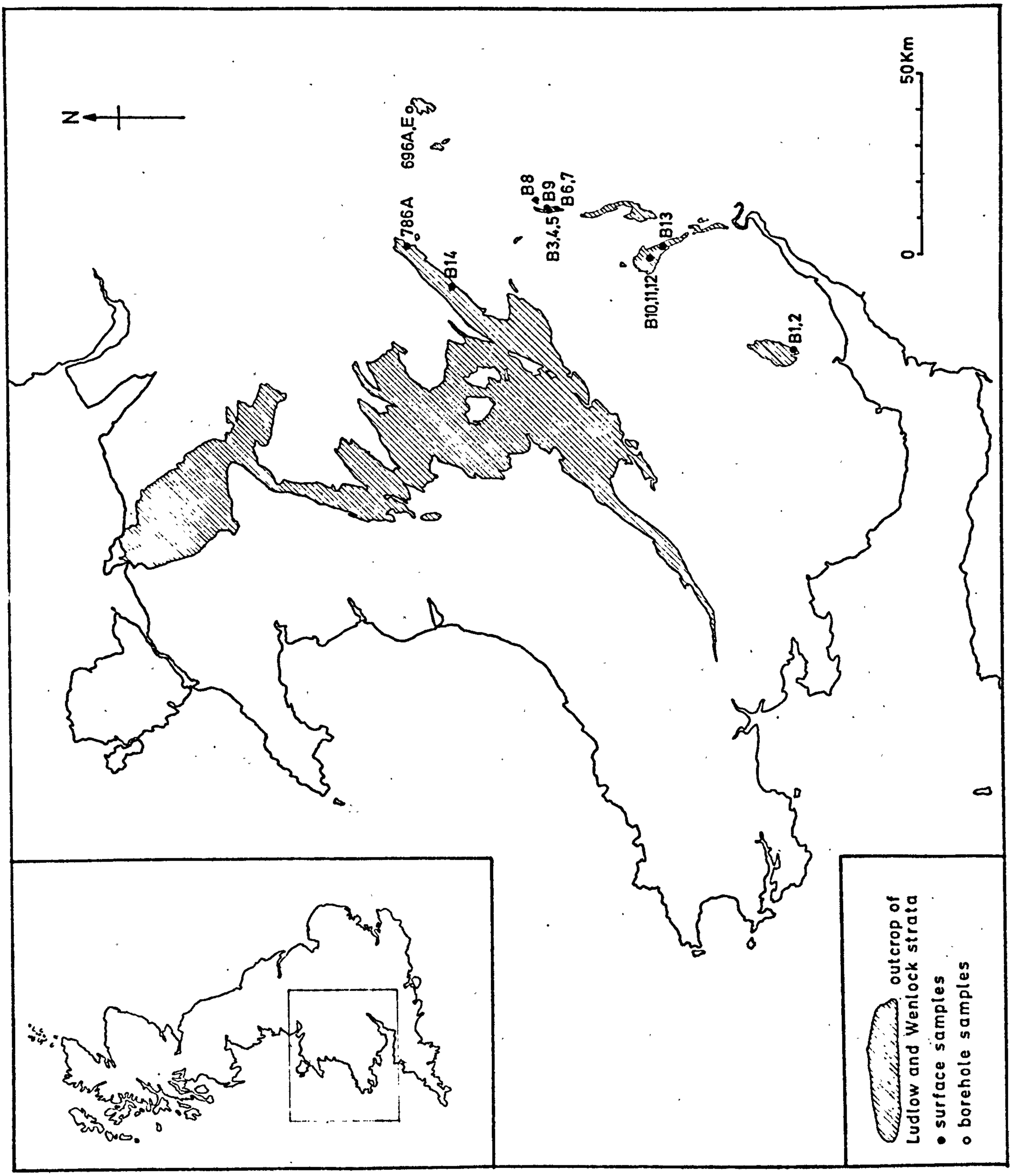

Fig. 1.2 Interstratified illite/montmorillonite sample localities

B3-9 are from the Abberley District, Worcestershire, where highly faulted Silurian strata outcrop along the line of the Malvern axis (Mitchell, et al., 1961). Samples B10-13 are from localities within the Woolhope Inlier, Herefordshire (Squirrell and Tucker, 1960). Stratigraphically, almost all the samples (B1-5, 8, 13), are found in the Middle Ludlow Aymestry Limestone and its time equivalents the Bringewood and Sleaves Oak Beds. The other samples of Ludlow age (B14) is from the Lower Ludlow Shales. Samples of Wenlock age are represented by B6, 7, 9 and 786A (Wenlock Limestone) and B10, 11, 12 (Woolhope Limestone).

Sample B15 is the only interstratified illite/montmorillonite sample from the Carboniferous and shows similarities with the clays of the Carboniferous Limestone 'wayboards' described by Walkden (1972).

1.5.2 Field descriptions of the illite/montmorillonite horizons

Horizons from which the present samples were collected varied in thickness from 1 cm to 0.5 m. Although generally conformable they were seen to vary in thickness or even pinch out along strike due, presumably, to their incompetence in post-tectonic consolidation movements. When freshly exposed the horizons were greyish green to bluish grey in colour and showed a conchoidal to coarse laminar fracture. Weathered horizons were usually buff in colour, contrasting strongly with the drab colours of adjacent strata. Clay from the weathered horizons was usually fairly plastic in its natural state.

Contacts of the clay horizons with adjacent sediments were usually sharp. Sometimes a thin layer of pink calcite was noted near the base of the clay and at Shaver's End, Worcs. (from which locality B8 was collected), a thin layer of euhedral quartz and biotite was visible on the surface of the underlying shaly limestone (compare Smith, 1967, p. 142). Lack of definition and colour lamination in the upper portions of some horizons suggested reworking (see next section).

1.5.3 The succession at Woodbury Quarry, Worcestershire

Details of the section are given in Mitchell et al. (1961). At this locality the succession, consisting of Lower Ludlow Shales, Aymestry Limestone, Upper Ludlow Shales and basal Downtonian, is inverted and shows high apparent dips to the NE. Quarrying (for roadstone) has proceeded mainly in the direction of apparent dip resulting in a steep-sided, horseshoe-shaped embayment into the outcrop. At the time the quarry was visited the NW face was freshly exposed and three clay bands were clearly visible; in the equivalent section of the SE face, which had been temporarily abandoned, the clay bands were less easily distinguished due to the combined effects of weathering and soil-creep.

The bottom clay band as observed on the NW face was 12 cm thick, dark olive green in colour, homogeneous and compact, and showed a marked conchoidal fracture. Both upper and lower contacts were sharp against limestone. Sample B3 (table 1.2) is from this band. The same clay band was also located on the opposite face of the quarry but as a result of recent weathering was much paler in colour and moderately plastic. A sample (B4) from this clay band was also taken in order to compare the physico-chemical properties of compact and weathered clay. (Particle size distribution curves of samples B3 and 4 are shown in fig. 7.6).

The second clay band, 3 cm thick, occurred about 2.5 m above the first and was very similar in appearance. No sample was taken.

The thickest clay band occurred a further 4 m higher in the succession and showed a sharp contact with the underlying shaly limestone. The bottom 30 cm of this band was composed of green compact clay passing gradually upwards through an intermediate bluish green fissile stage (about 10 cm thick) into a fossiliferous bluish grey clay about 20 cm in thickness. Flakes of biotite were prominent throughout, this mineral comprising about 7% of the total horizon. Sample B5 was taken from the bottom 30 cm of green compact clay; subsequent X-ray diffraction

examination established that interstratified illite/montmorillonite was the only clay mineral present in this sample In addition to illite/montmorillonite, X-ray diffraction examination of the clay from the top 10 cm of this horizon identified appreciable amounts of chlorite, mica and quartz (the actual diffraction traces are similar to the top three traces illustrated in fig. 3.8). This fossiliferous blue clay is considered to represent the reworked top of the interstratified illite/montmorillonite horizon.

A dark grey fossiliferous mudstone containing prominent pyrite and biotite occurred about 3 m above the top of the third clay band. Illite/montmorillonite, chlorite, mica and quartz were found to be major components of this mudstone and it would appear to represent a completely reworked illite/montmorillonite horizon.

Table 1.1. Details of occurrence of montmorillonite samples

LOCALITY	SAMPLE NO.	DESCRIPTION	STRATIGRAPHIC HORIZON
IGS Borehole B1, near St Nicholas' Church, Baulking, Berkshire. SU 3222 9063		olive green compact clays	
	A1	sample from 77-82 ft.	Sandgate Beds (Lower Greensand)
	A2	" " 83-84 ft.	
	A3	" " 87-88 ft.	
	A4	" " 96-99 ft.	
IGS Borehole F9, near Sands Farm, Shellingford, Berkshire. SU 3087 9179	A5	brown sandy clay (recovery sample from 10-15 ft.)	Lower Greensand
IGS Borehole F11, near St John's Church, Fernham, Berkshire. SU 2877 9305	A6	iron oxide-stained blocky clay from 18-19 ft.	Sandgate Beds (Lower Greensand)
Fuller's Earth Quarry, Woburn, Bedfordshire SP 959 319	A7	yellow blocky clay from working face	Sandgate Beds (Lower Greensand)
Fuller's Earth Quarries, Nutfield, Surrey			Sandgate Beds (Lower Greensand)
Paddock quarry TQ 285 504	A8	massive blue clay from working face	
	A9	massive yellow clay from working face	
Beachfield quarry TQ 292 506	A10	massive green/blue clay from working face	
Patteson Court quarry TQ 294 505	A11	massive blue clay from working face	
	A12	massive green/blue clay from 'bunkum' seam	
Underground Fuller's Earth workings, Combe Hay, Bath Somerset. ST 724 596		3m seam of grey/blue massive clay	Jurassic, Upper Fuller's Earth (Retrocostatum Zone)
	A13	top 1m	
	A14	middle 1m	
	A15	bottom 1m	
Disused chalk quarry, Frith Hill, Great Missenden, Bucks. SP 900 015	A16	grey/white plastic clay from 3-6 cm 'marl' layer	Cretaceous, Middle Chalk (Terebratulina Zone)

Workings for Strathblane-Balmore tunnel, Stirlingshire. NS 5894 7643	A17	red hard compact clay	Lower Carboniferous
Fuller's Earth Quarry, Grove Green Maidstone, Kent. TQ 783 568	878	green massive clay from working face	Sandgate Beds

Table 1.2. Details of occurrence of interstratified illite/ montmorillonite samples

LOCALITY	SAMPLE NO.	DESCRIPTION	STRATIGRAPHIC HORIZON
Disused quarry near Llangibi Castle, Monmouth ST 3655 9777	B1	5 cm grey/buff plastic clay	Upper Bringewood Beds (Ludlow)
	B2	8 cm mottled grey/buff friable clay	
Working (roadstone) quarry, Woodbury, Worcs. SO 741 635	B3, 4	12 cm green clay (compact and weathered samples)	Aymestry Limestone
	B5	30 cm olive green compact clay	
Working (roadstone) quarry, Penny Hill, Martley, Worcs. SO 751 616	B6	15 cm blue plastic clay	Wenlock Limestone
	B7	12 cm pale grey plastic clay	
Working (roadstone) quarry, Shavers End, Abberley, Worcs. SO 771 680	B8	15 cm mottled grey/ buff plastic clay	Aymestry Limestone
Disused quarry, Wallhouse Plantation, Shelsley Beauchamp, Worcs. SO 751 637	B9	15 cm pale grey/buff plastic clay	Wenlock Limestone
Disused quarry, N of Overbury Farm, Woolhope, Hereford. SO 611 366	B10	8 cm white plastic clay	Woolhope Limestone
	B11	2 cm white plastic clay in soil/limestone rubble	
	B12	8 cm mottled white/ buff clay in soil slip	
Disused quarry, Deans Place, Much Marcle, Hereford. SO 6365 3150	B13	15 cm friable buff clay	Sleaves Oak Beds (Ludlow)
Stream section, 500m NW of Upper Millichope, Salop. SO 520 896	B14	3 cm pale green clay	Lower Ludlow Shales
IGS Borehole No. 1 Manor Farm, Rushall, Staffordshire SK 035 009	696A	pale green brecciated clay (sample from 59 ft 2 ins)	Wenlock
	696E	grey compact clay (Sample from 144 ft. 9 ins)	

Gleedon Hill Quarry, Ironbridge Salop. SO 633 017	786A	pale green laminated clay	Wenlock Limestone
Stream section, Marples Plantation, Kedleston, Derbyshire SK 3098 4234	B15	mottled orange/white clay	Shales with limestones (Carboniferous Limestone)

Table 1.3. Details of occurrence of mixed-assemblage clays.

LOCALITY	SAMPLE NO.	DESCRIPTION	STRATIGRAPHIC HORIZON
Disused sand pits, Chadwell St Mary, Essex TQ 648 784	C1	3 cm lenses of grey/ green plastic clay	Thanet Sands
Cliff section, Walton-on-the-Naze, Essex. TM 260 223	C2	dark grey plastic clay from slumped mass	London Clay
IGS Borehole near Gaskill's Farm, Winstone, Gloucs. SO 9510 0913	C3	dark grey compact clay (sample from 133-135 ft.)	Jurassic, Lower Fuller's Earth

CHAPTER 2

SEPARATION OF CLAY FRACTIONS USING A HYDROCYCLONE

2.1 INTRODUCTION

2.1.1 General

The hydrocyclone is used extensively in mineral technology for desliming operations prior to ore recovery and it also has numerous applications in other fields (Bradley, 1965). Although used in the commercial refining of kaolinite (Naylor, 1958) it has found little application in general laboratory clay separation in the U.K. and in the few recorded instances of its use, e.g. Bidwell et al. (1970), only kaolinitic clays have been separated. Scattered references to the use of the hydrocyclone on a laboratory scale are found in the Hungarian literature; Nemecz (1962) states that montmorillonites have been separated by this technique but the products appear to have a large upper size limit of 20 microns.

In this study separation of the clay fractions was carried out exclusively with the hydrocyclone as it was considered to have many advantages over the more commonly used methods such as sedimentation/ decantation and the supercentrifuge. Before discussing the general features and operating conditions of the hydrocyclone the advantages and disadvantages of using this technique will be considered in some detail.

2.1.2 Advantages of the hydrocyclone

One of the main advantages of using the hydrocyclone is that large amounts of relatively concentrated clay suspension may be dealt with in a short time. Typical slurry densities used in this investigation were between 5 and 10% solids - these figures may be compared

with the maximum of 1-2% solids during sedimentation/decantation (to minimize hindered settling effects) and the much lower concentrations employed during supercentrifugation (Mungan and Jessen (1963) quote a figure of 0.01% solids). Clay recovery from suspension is rendered easier and more efficient when high initial slurry densities are used.

The other important advantage is that the high shear forces encountered by the clay suspension on passing through the cyclone maintain, and often further promote, dispersion. This effect is enhanced if the suspension is allowed to circulate within the system for some minutes prior to separation. The shear forces also minimise thixotropic effects which is a factor of additional merit when dealing with montmorillonite suspensions. In the sedimentation/decantation method a dispersing agent is normally added to produce a stable suspension and, once clay separation is complete, the salt of a divalent cation is added to flocculate and recover the clay. The clay product is then washed with water to remove excess salt and finally washed with a polar organic liquid, e.g. ethanol, and dried. This procedure is time consuming and not feasible for preparation of large amounts of clay. It is also out of the question if clay products containing the same cation assemblage as the original deposit are required. No dispersing agents are necessary when separations are made with the hydrocyclone as the clay is dispersed more than adequately by the shear conditions within the cyclone.

2.1.3 Disadvantages of the hydrocyclone

As gravitational forces are involved, the hydrocyclone separation technique suffers from the same disadvantages as sedimentation/decantation and the centrifuge in that the separation is influenced by the specific gravities of the particles. In practice this effect is not serious for clay minerals, and other minerals commonly found in clay deposits, and is dealt with in more detail when discussing the operating parameters of the

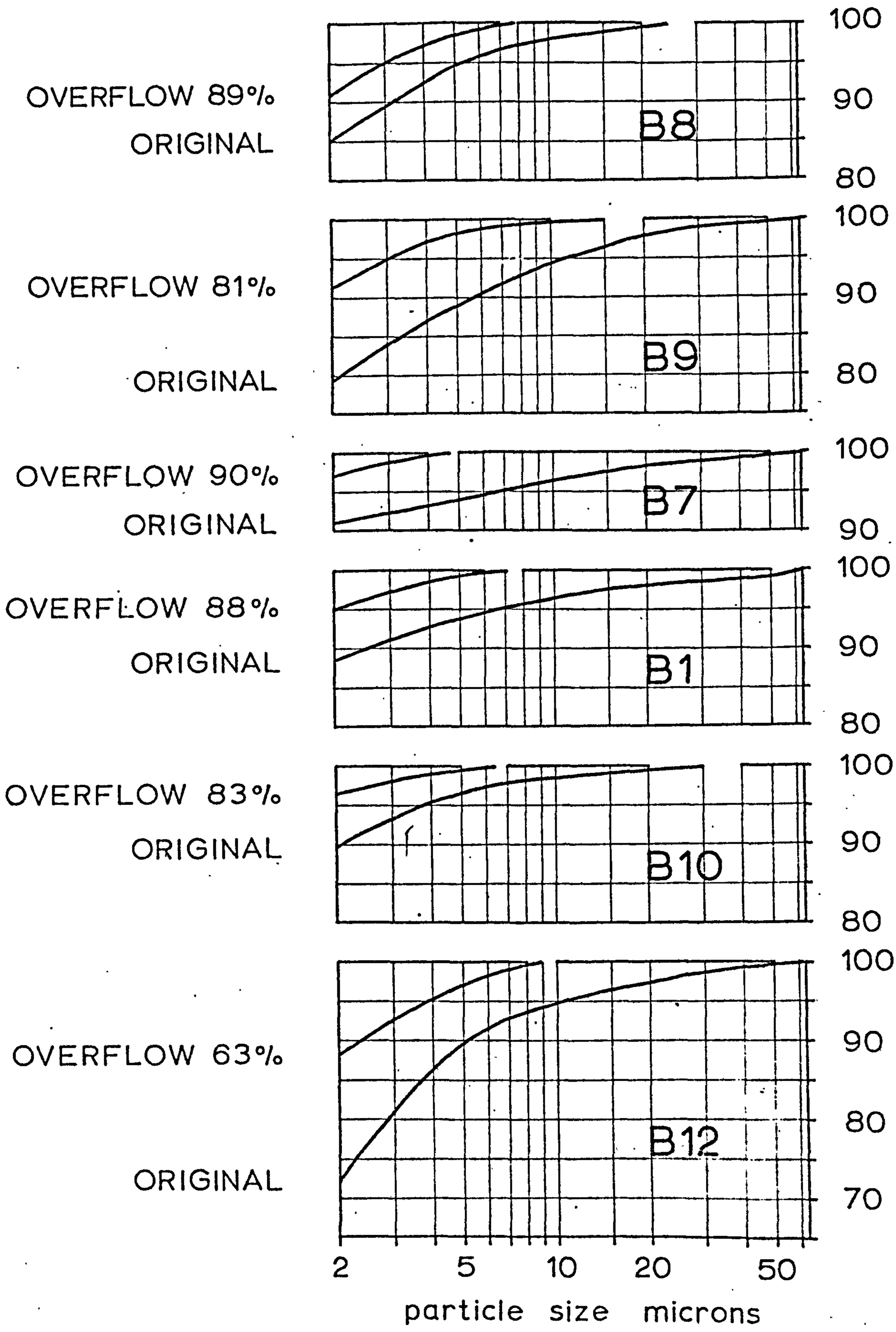

Fig. 2.1 Particle size analyses of original samples and hydrocyclone overflow products from a selection of interstratified illite/montmorillonites

hydrocyclone.

The separation size (defined later) varies to some extent with the size distribution of the feed and, in general, the finer the feed the finer will be the resulting clay product (see fig. 2.1). Products with a cut-off size at 10 microns are easily obtained but separations become more difficult below this figure. Fineness of separation may be improved by recycling the first clay product but the sharpness of separation then decreases and recovery is diminished. In this study the cut-off size under the most favourable conditions was 5 microns (clay aggregates usually accounted for most of the material in the 2-5 micron range however). In this respect sedimentation/decantation methods (usually separating at 2 microns - the accepted upper limit for clay size material) and the supercentrifuge (capable of separations in the sub-micron size range) are superior to the hydrocyclone.

In the hydrocyclone separation procedure the bulk of the water reports with the clay product. Thus any soluble salts present in the original sample would, on drying, be concentrated in the clay product. This is an important potential disadvantage of the hydrocyclone. The appreciable mechanical shear experienced by the slurry during hydrocycloning may also lead to the solubilisation of minerals such as gypsum. Chemical analyses of original samples and hydrocyclone products have shown this factor to be of only minor importance in the present investigation.

2.2 GENERAL FEATURES AND OPERATION OF THE HYDROCYCLONE

2.2.1 Description of apparatus

The hydrocyclone vessel used in these investigations is shown in diagrammatic form in fig. 2.2a. It consists of an inverted cone, made of pyrex glass, open at the apex and cylindrical for a short distance at its widest point. A narrow, hollow, tube called the vortex finder

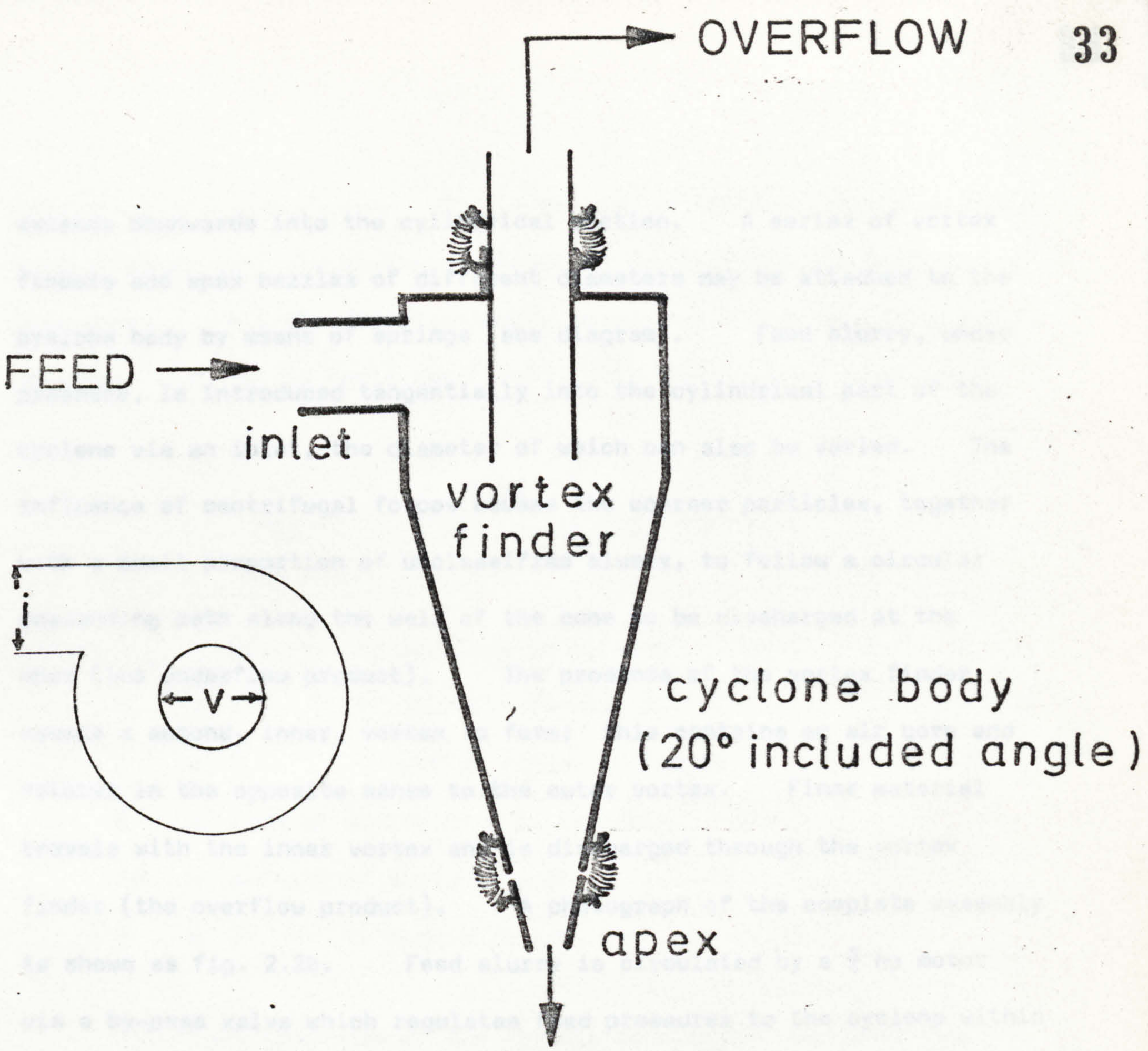

Fig. 2.2 (a) diagram of cyclone vessel (i = inlet, v = vortex finder) (b) photograph of complete hydrocyclone separation system used in this study.

extends downwards into the cylindrical section. A series of vortex finders and apex nozzles of different diameters may be attached to the cyclone body by means of springs (see diagram). Feed slurry, under pressure, is introduced tangentially into the cylindrical part of the cyclone via an inlet, the diameter of which can also be varied. The influence of centrifugal forces causes the coarser particles, together with a small proportion of unclassified slurry, to follow a circular descending path along the wall of the cone to be discharged at the apex (the underflow product). The presence of the vortex finder causes a second, inner, vortex to form; this contains an air core and rotates in the opposite sense to the outer vortex. Finer material travels with the inner vortex and is discharged through the vortex finder (the overflow product). A photograph of the complete assembly is shown as fig. 2.2b. Feed slurry is circulated by a $\frac{3}{4}$ hp motor via a by-pass valve which regulates feed pressures to the cyclone within the range 5-40 lbs/sq. in. Capacity of the system is 4 litres, and the feed densities were in the range 5-10% solids.

The particle size at which the separation is affected depends on the design and measurements of the cyclone, the properties of the feed slurry and the operating conditions. The relative importance of these factors is assessed in the following two sections.

2.2.2 Performance analysis

A number of design factors affect the performance of the hydrocyclone. Length, diameter and solid angle of the cydone itself, together with inlet, vortex finder and apex nozzle diameters are all important. Slurry feed pressure also influences the size of separation. Bradley (1965) has collated formulae, derived empirically by various workers, which relate an equilibrium particle size (d_{50}) to the various

parameters of the cyclone. d_{50} is defined as the equilibrium particle size at which half the particles report to the overflow and half to the underflow. All the formulae reduce to basically the same form and only one, that due to Dahlstrom (1949), will therefore be considered.

$$d_{50} = \frac{81\,(be)^{0.68}}{Q^{0.53}} \left[\frac{2.73 - 1.0}{Ps - P}\right]^{0.5}$$

where d_{50} = diameter of particle in microns

b = " " inlet in inches

e = " " vortex finder in inches

Q = flow of slurry in U.S. gals/min.

Ps = density of solid in g/ml

p = " " liquid in g/ml

The right hand side of the formula consists of two products, the second of which is only important when minerals of widely different densities are being hydrocycloned. This often happens in mineral dressing where, under a set of typical operating conditions, the d_{50} value for quartz may be 30 microns but the corresponding figures for columbite and cassiterite would be 18.6 and 16.1 microns respectively. Ore minerals are therefore recovered at smaller particle sizes at the expense of the lighter gangue material. Conversely, in clay separation, a minor advantage of the density factor is that non-clay minerals, which are usually heavier than the clay minerals being separated, are eliminated via the underflow at smaller sizes than the overflow cut-off size for the clay.

Converting the rather mixed units in the Dahlstrom formula to c.g.s. units and assuming a mean (quartz) density of 2.65 for the feed, the expression for d_{50} reduces to:

$$d_{50} = \frac{47(iv)^{0.68}}{F^{0.53}}$$

where d_{50} = diameter of particle in microns

i = inlet diameter in cm

v = vortex finder diameter in cm

F = flow in litres/min.

It would appear from the formula that d_{50} may be decreased by diminishing the diameters of inlet or vortex finder whilst maintaining the flow at a constant value. In practice the variables are inter-dependent. Reduction in size of the inlet reduces the flow, and flow reduction also occurs when the vortex finder diameter is diminished due to the greater back pressure exerted by the cyclone. On balance, as will be seen later, increase in feed pressure does result in a finer separation.

An expression for the diameter of the apex does not appear in the formula. In general, if this is large enough to allow free discharge of coarse material, it has only a minor influence on d_{50}. During correct operation of the hydrocyclone the underflow leaves the apex in an umbrella-shaped discharge. If the feed slurry is too concentrated, or the feed pressure is not sufficient, the underflow forms a ropey discharge and some of the coarser particles may be forced into the overflow. Short-circuiting by the coarser particles may also occur if the diameter of the apex is too small. Reduction in the included angle of the apex results in a finer separation (Naylor, 1958).

Calculated d_{50} values for a range of operating conditions are presented in table 2.1. The equilibrium particle size is seen to decrease both as the slurry feed pressure is increased and also as the

Table 2.1. Equilibrium particle sizes (d_{50}) under different operating conditions. 3 cm cyclone with 0.4 cm inlet and 0.25 cm apex nozzle. Volume ratios of underflow and overflow products and also flow rates at pressures shown were measured with water only

vortex diameter (cm)	volume ratio o/f : u/f	calculated d_{50} at pressures (lbs/sq.in) of: 15	20	25	30	35
0.85	17 : 1	*	7.33	7.05	6.54	6.06
0.60	8 : 1	6.78	6.93	5.88	5.64	5.48
0.42	2.4 : 1	6.00	5.54	5.37	≠	≠

* unsatisfactory apex discharge

≠ vortex finder springs failed

Table 2.2. Equilibrium particle sizes (d_{50}) under different operating conditions. 1.5 cm cyclone with 0.4 cm inlet and 0.13 cm apex nozzle. Volume ratios of underflow and overflow products and also flow rates at 25 lbs/sq.in. were measured with water only.

vortex finder diameter (cm)	volume ratio o/f : u/f	calculated d_{50} at pressure of 25 lbs/sq.in.
0.42	20 : 1	5.63
0.30	7 : 1	5.00
0.21	2.8 : 1	4.40

diameter of the vortex finder is diminished. As feed pressures in excess of 25 lbs/sq. in. could not be used with the 0.42 cm vortex finder (due to failure of the springs connecting this to the main body of the cyclone), the effective difference in d_{50} at maximum pressure between the largest and smallest vortex finders is only 0.6 micron. The overflow to underflow ratio is related to the relative cross-sectional areas of the vortex finder and apex nozzle. As the latter is constant the ratio increases with increase in vortex finder area although this is not a strict proportional relationship due to the variable area occupied by the central air core.

The Dahlstrom formula does not contain an expression for the diameter of the cyclone but, subject to certain qualifications (Naylor, 1958), the smaller the diameter the finer the potential separation. Variation in d_{50} with different vortex finders for a smaller cyclone is shown in table 2.2. Comparing the d_{50} values with those calculated at 25 lbs/sq. in. for the 3 cm cyclone it is seen that finer separations are possible with the smaller cyclone. In practice it was found that the 1.5 cm cyclone would only operate satisfactorily at very low feed concentrations and as this effectively negated one of the advantages of the hydrocyclone for this study no separations were carried out with the smaller diameter cyclone.

Although the Dahlstrom formula is valuable for predicting variations in d_{50} as operating parameters are changed it has, in practice, a number of limitations. Differences in the size distribution of the feed - which undoubtedly influence the size of separation - are not taken into account; neither can the formula predict the maximum size of particle present in the overflow (the cut-off size) or the proportions of the sample, by weight or by volume, discharging at the overflow and underflow. In order to assess the performance of the hydrocyclone it was found necessary to carry out a number of preliminary separations, varying

the important parameters such as feed pressure and vortex finder diameter, and determining the particle size distribution of the resulting products. (Difficulties may be experienced in the particle size analysis of montmorillonite clays and these are discussed in Appendix 3).

2.2.3 Preliminary separation trials

The separation trials described below were conducted with the 3 cm cyclone fitted with a 0.4 cm diameter inlet. Operating variables were essentially vortex finder diameter and nature of the feed slurry.

Figures 2.3a and b illustrate the results from some preliminary separations on two samples which differed appreciably both in mineralogical composition and particle size distribution. Sample A1 consisted predominantly of montmorillonite accompanied by only minor amounts of non-clay constituents. Sample C3 was a mixture of montmorillonite and mica (illite) with calcite, quartz and pyrite. Details of the products from hydrocyclone separation are given in tables 2.3 and 2.4.

For sample A1 the size distributions of the overflow products obtained with both vortex finders are identical (fig. 2.3a curves 2 and 4) in spite of the smaller calculated d_{50} value for the 0.42 cm vortex finder (see table 2.1). When using the smaller diameter vortex finder a larger proportion of the finer material is forced into the underflow (compare curves 3 and 5 in fig. 2.3a). The underflow 'reject' from the separation using the 0.42 cm vortex finder was roughly half the weight of the original sample (table 2.3). If the hydrocyclone is being used to upgrade relatively pure clays, such as this sample, appreciable loss of adventitious fine particles to the underflow would thus inevitably result; on this basis the 0.85cm vortex finder provides a more efficient separation. Repassing the first overflow product reduces the cut-off size of the clay product from 7 to 5 microns (fig. 2.3a, curves 4 and 6) and increases the amount of less than 2 micron

SAMPLE A1

3 cm cyclone
① original sample
0·42cm vortex finder
pressure 20 lbs/sq in
② overflow (48%)
③ underflow (52%)
0·85cm vortex finder
pressure 35 lbs/sq in
④ overflow (62%)
⑤ underflow. (38%)
⑥ overflow from ④ (53%)
⑦ underflow from ④ (9%)

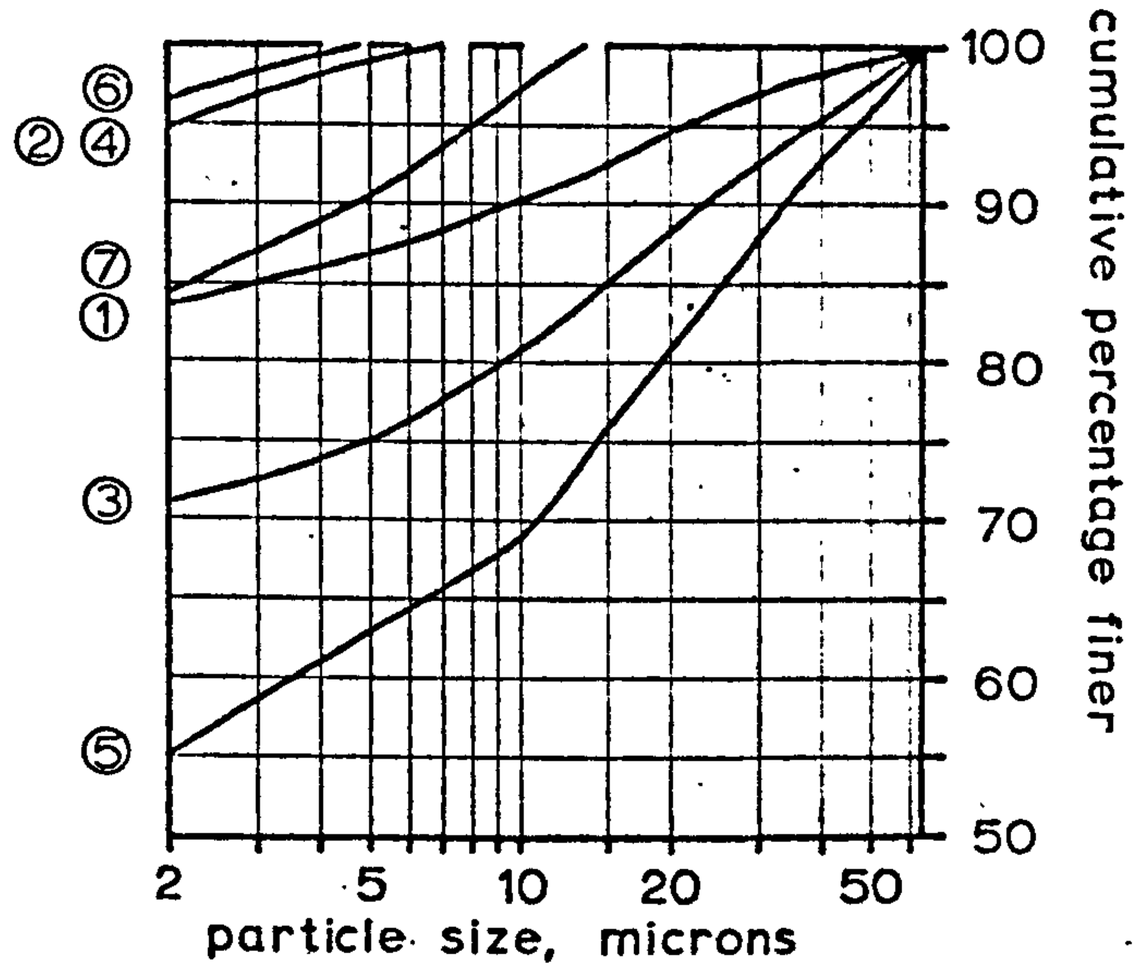

SAMPLE C3

3 cm cyclone
① original sample
⑭ original sample
recalculated from ④ and ⑤
0·42cm vortex finder
pressure 15 lbs/sq in
② overflow (49%)
③ underflow (51%)
0·85cm vortex finder
pressure 35 lbs/sq in
④ overflow (63%)
⑤ underflow (37%)
⑥ overflow from ④ (55%)
⑦ underflow from ④ (8%)

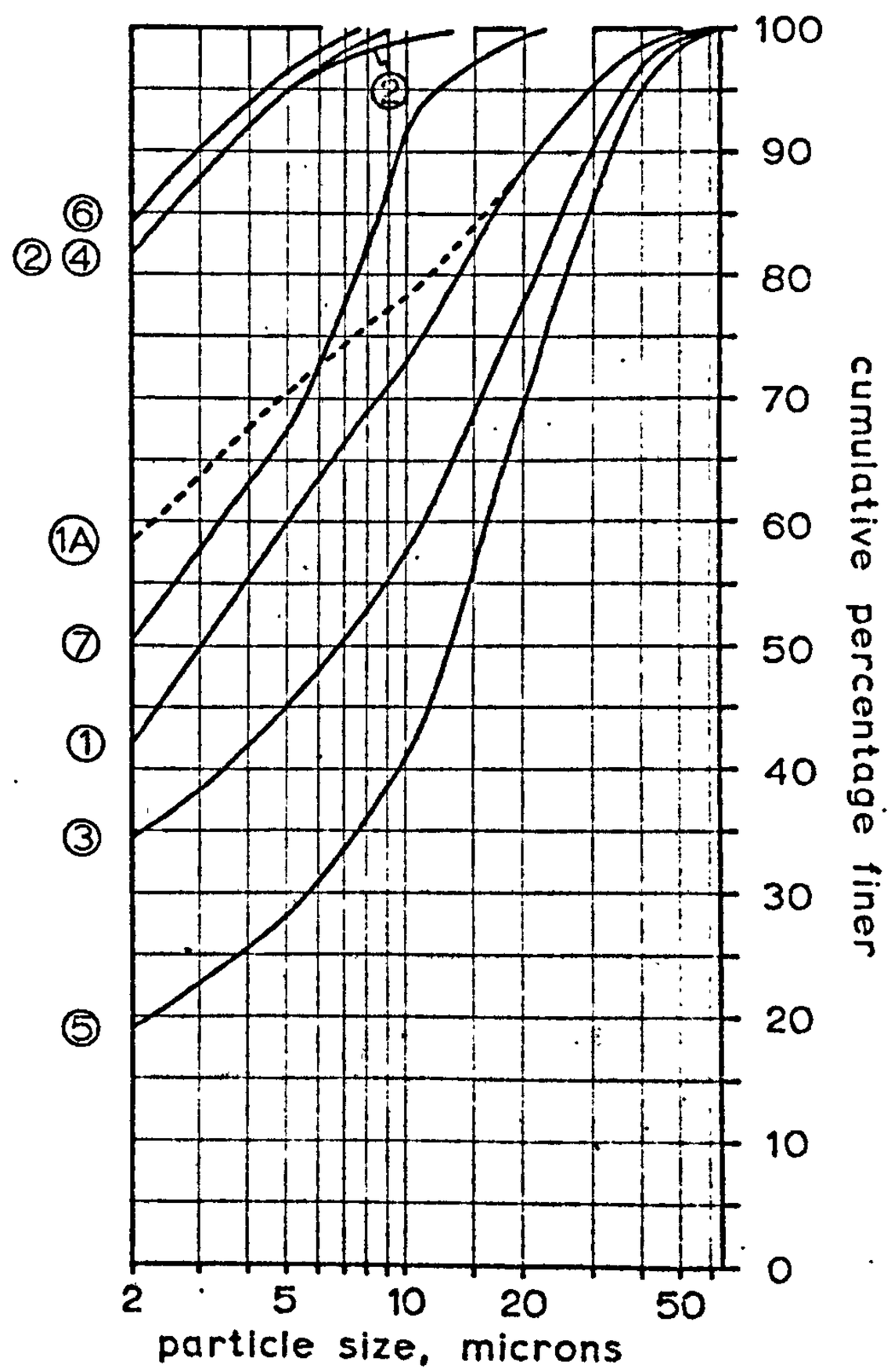

Fig. 2.3 Trial separations with a 3 cm diameter cyclone. Constant inlet diameter (0.40cm) and apex nozzle diameter (0.26cm), other parameters varied as shown. Figures in parentheses refer to % recovery of total solids.

Table 2.3 Trial separations on sample A1 using a 3 cm cyclone with 0.4 cm inlet and 0.26 cm apex nozzle. Details are for products obtained with a 0.85 cm vortex finder (at 35 lbs/sq.in. pressure) and a 0.42 cm vortex finder (at 20 lbs/sq.in. pressure).

Vortex finder diameter (cm)	Volume ratio o/f : u/f	solids weight ratio o/f : u/f	% solids in o/f	% solids in u/f	% recovery of 2 μ
0.85	15.7: 1	1.6 : 1	4	36	74
0.42	2.5: 1	0.9 : 1	4	10	55

Table 2.4 Trial separations on sample C3 using a 3 cm cyclone with 0.4 cm inlet and 0.26 cm apex nozzle. Details are for products obtained with a 0.85 cm vortex finder (at 35 lbs/sq.in. pressure) and a 0.42 cm vortex finder (at 15 lbs/sq.in. pressure).

Vortex finder diameter (cm)	Volume ratio o/f : u/f	solids weight ratio o/f : u/f	% solids in o/f	% solids in u/f	% recovery of 2 μ
0.85	14.6: 1	1.7 : 1	4	30	88
0.42	2.5: 1	1 : 1	4	10	70

material from 94 to 97%. Overall recovery of less than 2 micron material is, as a result, reduced from 74 to 64%.

From tables 2.3 and 2.4 it is seen that the volume and weight ratios of the products obtained from the two samples under comparable conditions are almost identical. The particle distribution curves, however, although illustrating the same general trends, do differ markedly, thus emphasising the influence of the original size distribution of the feed on separation characteristics.

A comparison of curves 2 and 4 in fig. 2.3b shows that for sample C3 use of the smaller diameter vortex finder leads to a much less sharp cut-off for the overflow product. As was found for A1, the 0.42 cm vortex finder is also less efficient in terms of recovery of less than 2 micron material. Recycling the first overflow from the larger diameter vortex finder leads only to a marginal improvement, both in cut-off size and amount of less than 2 micron material, and reduces the overall recovery of particles smaller than 2 microns from 88 to 81%. A comparison of curves 1 and 1A in fig. 2.3b shows that passage through the cyclone has disaggregated particles up to 20 microns in size and, as a consequence, increased the less than 2 micron content from 42 to 58%. Evidence presented later (section 7.3) shows that the latter value is a more accurate indication of the clay content of the sample.

2.2.4 Calculated and observed 'd_{50}' values

Size distribution of the original sample is not taken into account in the Dahlstrom formula; consequently both samples give closely similar calculated d_{50} values for the same operating conditions. These are shown under 'd_{50} calculated' in table 2.5 and are of the same order as those recorded under equivalent conditions in table 2.1. Actual d_{50} values may be obtained from the particle distribution curves of the

Table 2.5. 'Calculated' and 'observed' d_{50} values for samples A1 and C3. (Values used for flow rates were those actually measured.)

Sample	d_{50}	Vortex finder diameter (pressure)	
		0.42 cm (15-20 lbs/sq.in.)	0.85 cm (35 lbs/sq.in.)
C3, A1	calculated	5.6	5.9
C3	observed	3.2	4.7
A1	observed	1.4	1.7

cyclone products and are reported under 'd_{50} observed' in table 2.5. Differences between the observed d_{50} values for the two samples are due to the finer average particle size of A1. The larger d_{50} values observed with the 0.85 cm vortex finder are a consequence of fewer fine particles being lost in the underflow. It is doubtful whether d_{50} values are of much significance when dealing with clays containing large amounts of material smaller than the lowest cut-off size for the cyclone.

3.3 SEPARATION OF CLAY FRACTIONS

3.3.1 General

On the basis of the work described in the preceeding section all the 'clay fractions' for a chemical analysis and detailed mineralogical examination were obtained from a 3 cm diameter cyclone using the 0.85 cm vortex finder at a pressure of 35 lbs/sq. in. When necessary the initial overflow was recycled to give a finer product. Only rarely did the final clay fraction from the montmorillonite and interstratified illite/montmorillonite samples contain particles larger than 10 microns, and in the majority of cases a cut-off at about 7 microns was observed. Clay minerals such as chlorite and kaolinite commonly occur with particles above 2 microns in size and therefore a cut-off at 7 microns would provide a more representative recovery of the mineral (although this may be at the expense of the grade). Even with montmorillonite-rich clays the occurrence of particles larger than 2 microns in the overflow need not necessarily indicate the presence of non-clay minerals. In fig. 2.3a, for example, examination of the recycled overflow by X-ray diffraction identified montmorillonite - a proportion of this mineral must therefore be present as undispersed (polycrystalline) aggregates in the 2-5 micron range.

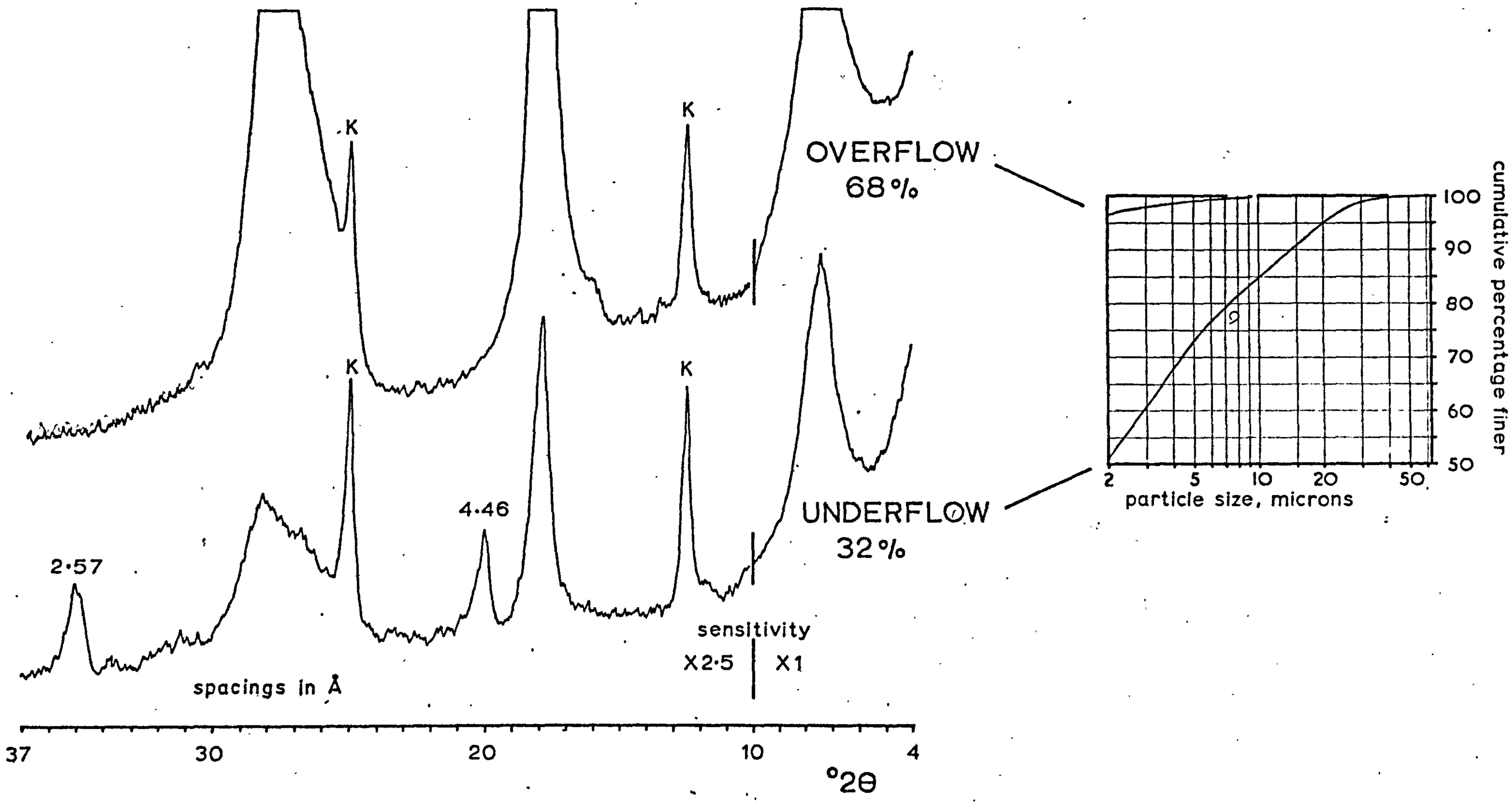

Fig. 2.4

Sample B11: X-ray diffraction traces and particle size analyses of overflow and underflow products. Samples were prepared for X-ray analysis by depositing equal weights (150 mg) on glass slides.

In many cases non-clay minerals comprised only a small proportion of the sample. The underflow products from these consisted mainly of silt-size clay aggregates. With such material a comparison of the physical properties of underflow and overflow products provided information on the susceptibility of various tests to the state of dispersion of the clay. This will be considered in detail in chapter 7 but one simple illustration will be given here. Fig. 2.4 shows the X-ray diffraction traces of oriented overflow and underflow products from sample B11, an interstratified illite/montmorillonite accompanied by small amounts of kaolinite. Calcite is the only other mineral present in significant amounts but was eliminated by screening at 240 mesh. The overflow product consists of 97% particles smaller than 2 microns whereas the underflow contains almost 50% incompletely dispersed aggregates in the fine to medium silt size range. Although the same weight of clay was used in both cases to prepare the oriented slides, the dispersed nature of the overflow product results in much enhanced diffraction effects. The appearance of two non-basal peaks at 4.46A (020, 110) and 2.57A (200, $13\bar{1}$) on the trace for the underflow product confirms the aggregated nature of this material. Kaolinite might be expected to concentrate in the coarser fractions but it is unsafe to draw any conclusions from the present diffraction traces as oriented samples are unreliable for quantitative measurements (Gibbs, 1965).

2.3.2 Species differentiation during hydrocycloning

Species differentiation is here defined as the preferential concentration of a clay mineral, by virtue of its size, in either overflow or underflow products. The critical size for the hydrocyclone is in the region of 5 microns. As clay minerals, aggregated or otherwise, occur usually below, but often above, this figure a certain amount of

species differentiation was expected. As mentioned above oriented slides are unsuited for accurate monitoring of any variation in amount of a particular clay mineral and the following discussion is based on information obtained from randomly-oriented X-ray diffraction traces of the hydrocyclone products.

Kaolinite, chlorite and detrital mica were all concentrated in underflow products, although for kaolinite this effect was often marginal (as, for example, in B11). Chlorite was noticeably concentrated in the underflow from B14. Detrital mica was present in significant amounts in B13, C1 and C2; in the latter two samples high recoveries of this mineral were noted in the underflow products.

Particle size analyses of hydrocyclone products from C1 are shown in fig. 2.5. Diffraction traces from most of the randomly oriented products are also shown in the figure and the peak heights of the first order montmorillonite, mica, and kaolinite reflections are recorded in table 2.6. Peak heights for quartz, the only other mineral present in significant amount, are not given in the table. The increase in clay mineral content of overflow 2 and underflow 2 is due to the concentration of quartz in the coarser sizes, e.g. underflow 1. From table 2.6, however, it is seen that the montmorillonite content of overflow 2 is more than double that of the original sample whereas kaolinite has increased only one and a half times. This, together with the erratic distribution of mica between the products shows that species differentiation is taking place. Examination of the peak height ratios for the clay mineral pairs (in table 2.7) shows that mica, and to a lesser extent kaolinite, are concentrated in the second underflow product and montmorillonite is concentrated in the final overflow.

McAtee (1958) has shown that after supercentrifuging montmorillonite with a mixed cation assemblage, Ca and Mg were found to be the predominant cations of the coarser montmorillonite whereas Na-montmoril-

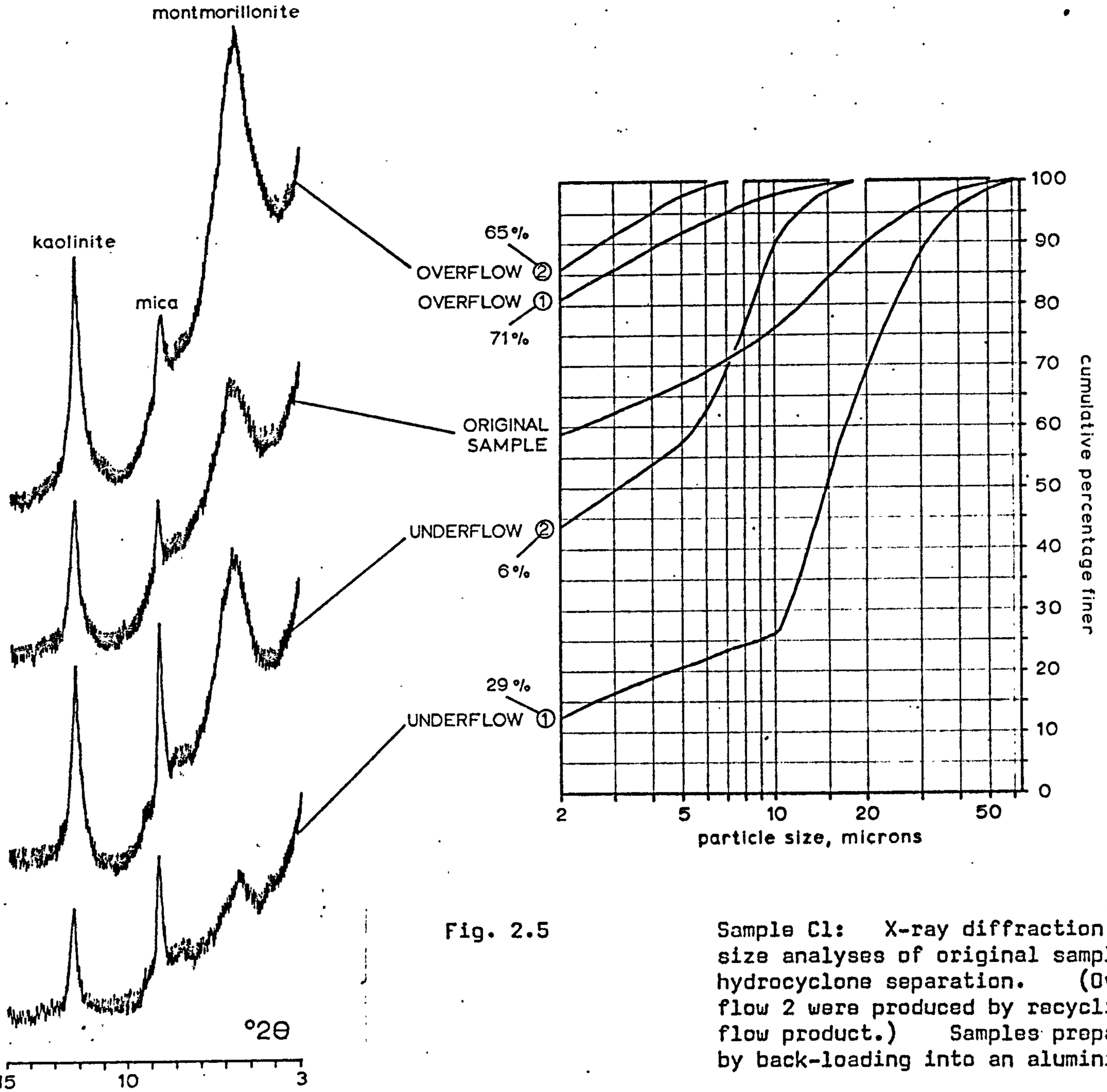

Fig. 2.5

Sample C1: X-ray diffraction traces and particle size analyses of original sample and products from hydrocyclone separation. (Overflow 2 and underflow 2 were produced by recycling the first overflow product.) Samples prepared for X-ray analysis by back-loading into an aluminium holder.

Table 2.6. Sample C1: peak heights from first order reflections (d_{001}) for the constituent clay minerals

Product	peak heights (cm)		
	montmorillonite	mica	kaolinite
o/f 2	12.5	5.0	9.5
u/f 2	8.0	8.3	8.2
orig. sample	5.7	4.2	6.0
u/f 1	2.6	5.7	4.3

Table 2.7. Sample C1: peak height ratios (d_{001}) for the clay mineral pairs.

Product	Ratios		
	mica/mont.	kaolinite/mont.	mica/kaolinite
o/f 2	0.40	0.80	0.53
u/f 2	1.03	1.03	1.01
orig. sample	1.39	1.05	0.68
u/f 1	2.19	1.65	1.32

lonite concentrated in the finer fractions. The critical size at which differentation occurred was in the region of 0.15 microns (Mungan and Jensen, 1963). In the present study no differences were observed in the exchangeable cation assemblage of montmorillonite in overflow or underflow products although as Ca and Mg are the dominant cations in the samples it would be difficult to detect any small variations in exchangeable cation content even if these did occur. In the single sample which contains significant amounts of exchangeable Na (see table 2.8) there is no evidence of the concentration of this element in the overflow product No differences either in exchangeable cation composition or d-spacing (which would indicate a change in illite/montmorillonite ratio) were observed between overflow and underflow products from the interstratified clays: the main criterion determining the appearance in either product depends, as with montmorillonite, on the state of aggregation of the clay.

2.3.3 Shearing effect of the hydrocyclone

Although mechanical agitation in water and subsequent passage through a 240 mesh screen is an adequate preliminary to hydrocyclone separation (see Appendix 2) the resulting suspensions are by no means fully dispersed - the appearance of silt-size clay aggregates in the underflow product from most of the samples confirms this. The existence of intense shearing forces within the cyclone has already been noted, the shear rate being at a minimum near the wall of the cyclone while increasing towards the centre. Potential underflow particles would thus undergo the least shear although with a recirculatory period before underflow and overflow products are withdrawn the chances of aggregate breakdown are obviously increased.

It has already been demonstrated that the hydrocyclone is responsible for aggregate breakdown in the fine- to medium-silt size range

Table 2.8. Sample A4: liquid limits and exchangeable cation assemblages of original sample and overflow product

	Liquid limit	Exchangeable cations			
		Ca^{2+}	Mg^{2+}	K^{+}	Na^{+}
Original sample	209	65.2	39.4	2.5	5.5
Overflow product	292	66.3	39.2	3.2	5.9

(fig. 2.3a and discussion). What is not immediately apparent is that exposure to the high-shear conditions of the hydrocyclone may, for montmorillonite, also result in appreciable disruption of interparticle associations in the sub-micron size range. This phenomenon may be illustrated with reference to sample A4, a pure montmorillonite with 99% particles less than 2 microns. The increase in liquid limit from 209 for the original sample to 292 for the overflow product (table 2.8) must be due to increased dispersion in the less than 2 micron size range. From table 2.8 it is obvious that variation in the exchangeable cation content of original sample and product is not responsible for the increase. Liquid limit values of 307 and 314 were obtained from the original sample after subjecting it to the (?comparable) high-shear conditions of a Braun liquidiser. Enhancement of physico-chemical properties, such as liquid limit, from original sample to overflow product will be dealt with in detail in chapter 7.

CHAPTER 3

MINERALOGICAL EXAMINATION OF THE CLAY FRACTIONS

3.1 X-RAY DIFFRACTION

3.1.1 General

X-ray diffraction was used extensively in the initial stages of the work in determining the mineralogical composition of the original untreated samples. In Chapter 2 it was employed to characterise and evaluate various products from hydrocyclone separations. The present discussion is concerned exclusively with the examination of the purified clay products obtained from these separations. The amount of useful data which could be obtained from X-ray examination varied. For the fuller's earth-type montmorillonites the initial problem was that of identifying small amounts of non-clay impurities. Randomly oriented powders were used for this purpose. On the other hand oriented slides were used in the examination of the mixed-assemblage clays because in this instance the problem was that of identifying, and distinguishing between, a number of different clay minerals. Diffraction traces were made of the air-dried and glycerolated clays and also of heated material.

Of necessity a large part of this chapter is devoted to the X-ray examination of the interstratified illite/montmorillonites and of clays from associated horizons. For the former, traces were made of oriented air-dried, glycerolated and K-saturated material, from which the relative proportions of the two interstratified components could be determined. A limited amount of information was also obtained from traces of randomly oriented air-dried clays. Examination of the associated clay horizons was accomplished using oriented slides.

Sample preparation techniques and X-ray equipment constants are recorded in Appendix 4.

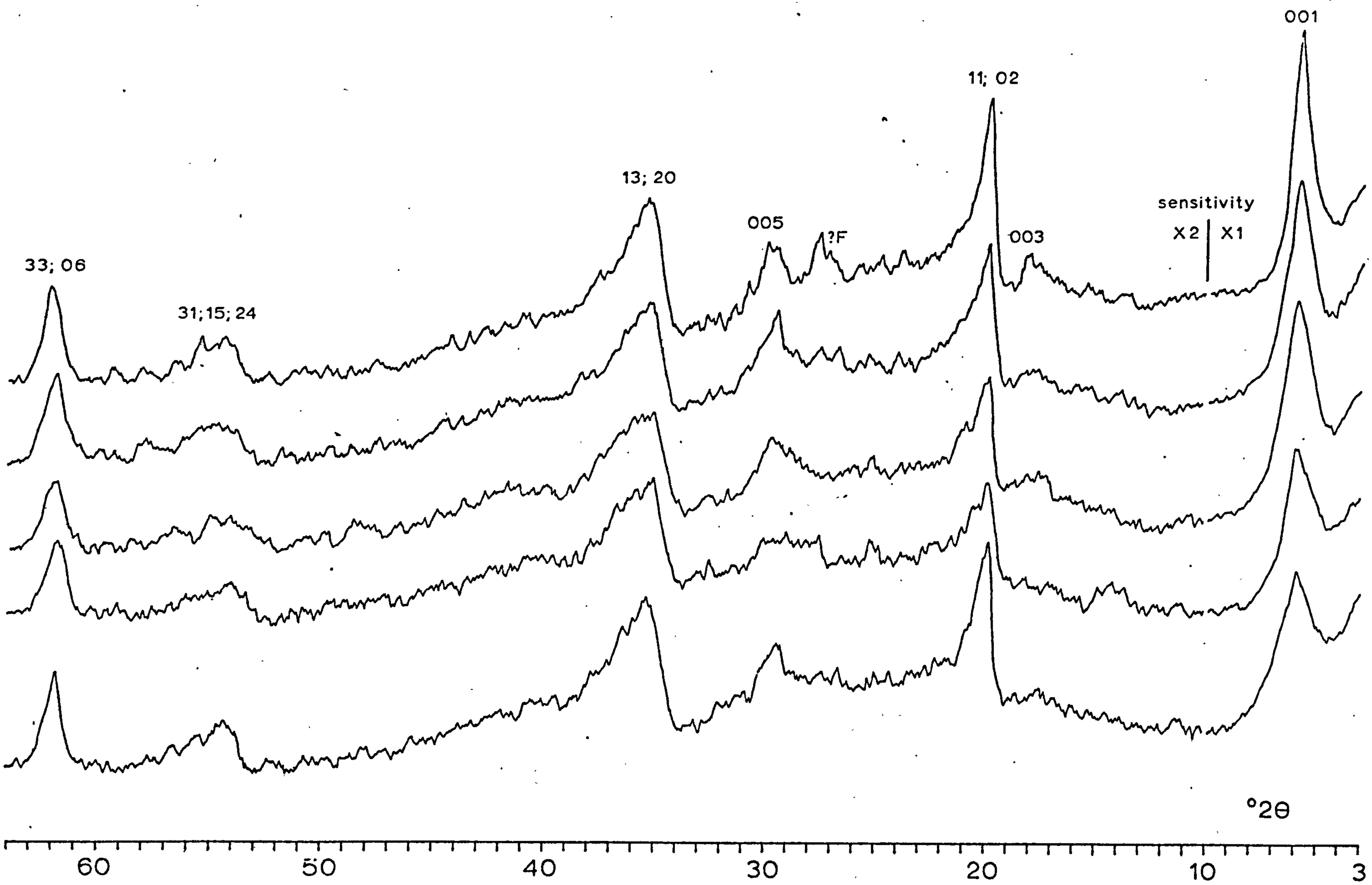

Fig. 3.1 Diffraction traces of randomly oriented montmorillonites (all hydrocyclone overflow products). Peak marked ?F on trace of sample A15 is probably due to feldspar.

3.1.2 Montmorillonites

X-ray diffraction patterns of montmorillonites show two distinct types of reflections (MacEwan, 1961). The first type are asymmetric with a sharp inner edge and a gradual fall in intensity on the side furthest from the undeviated X-ray beam. These are hk bands and result from the non-regular superposition of individual montmorillonite layers. Reflections of the second type are sharp and are exact sub-multiples of a fairly high spacing, usually in the range 10-18 A. These reflections are given by planes parallel to the layers (basal planes), the first (and subsequent) order reflections being susceptible both to the nature of the interlayer cation and the state of hydration of the clay.

Diffraction traces of a selection of randomly oriented montmorillonites are illustrated in fig. 3.1; indices assigned to the diffraction bands are those of an ortho-hexagonal unit cell (MacEwan, 1961). These traces would appear to confirm the essentially monomineralic nature of these particular upgraded clay products. However when calculating a structural formula from the chemical analysis of A15, satisfactory charge balances could only be achieved by assuming the presence of approximately 5% feldspar in the clay. Feldspar was only tentatively identified on the trace for A15 (peak marked ?F in fig. 3.1). Also, up to 0.5% quartz and 1% feldspar impurity could occur in A7 (from structural formula calculations) but no indication of the presence of these minerals was obtained from the trace in fig. 3.1. It must be assumed that under the conditions used trace amounts of mineral impurities could have remained undetected in these clay products.

Diffraction traces of oriented montmorillonite clay products were also made. All showed first order montmorillonite d-spacings in the range 15-15.4 A which signified that the interlayer exchange positions were occupied mainly by divalent cations. No other data were obtained from these traces.

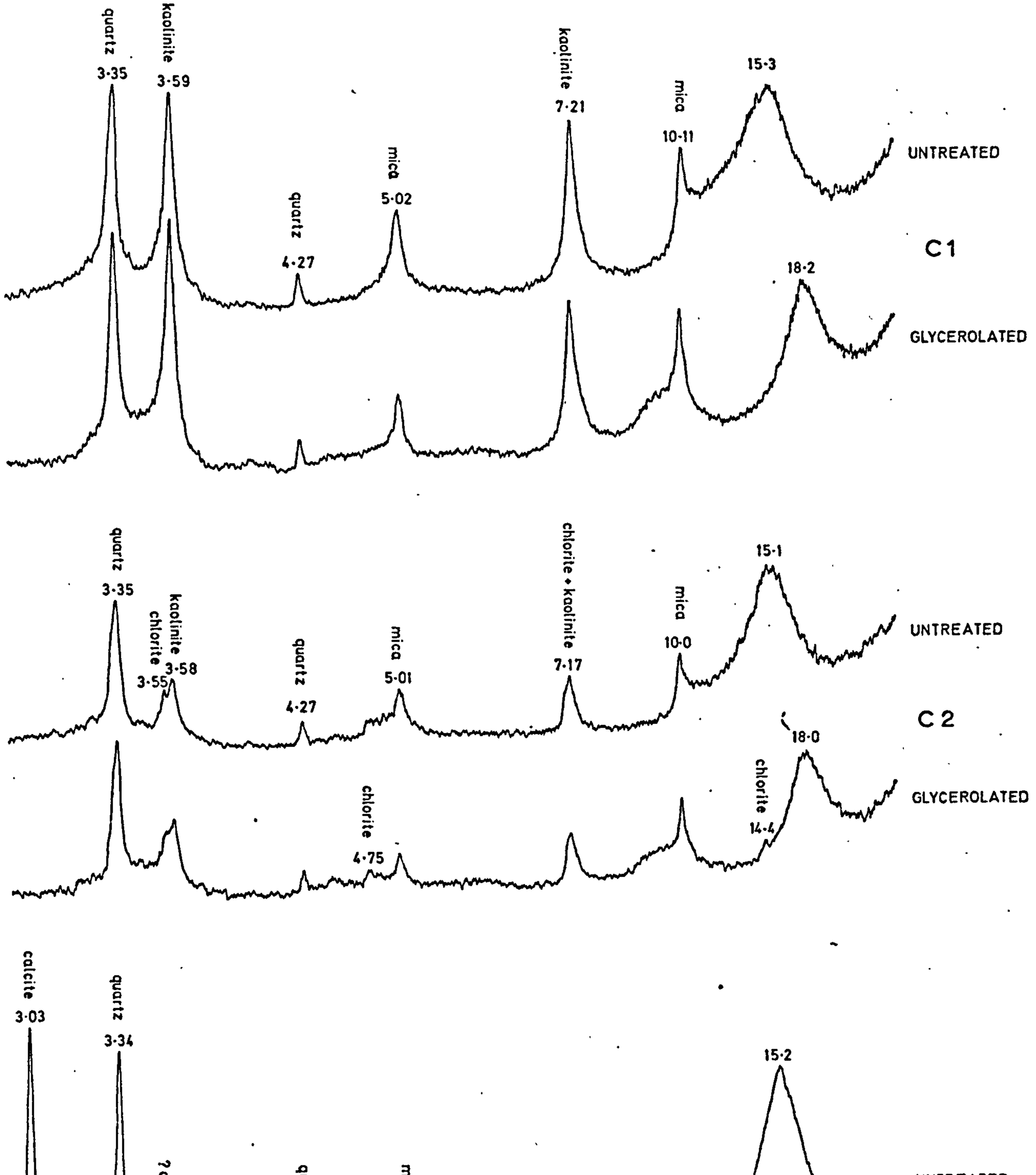

Fig. 3.2 Diffraction traces of hydrocyclone overflow products from the mixed-assemblage clay samples. Peaks at approximately 15A (in untreated products) and 18A (glycerolated products) are due to montmorillonite, others as labelled.

3.1.3 Mixed-assemblage clays

The hydrocyclone overflow products from the three samples in this group contain appreciable quantities of non-clay material and also, as may be seen from the traces reproduced in fig. 3.2, a distinct and varied clay mineral assemblage. Montmorillonite is dominant in all three samples, the first order spacing at 15A suggesting that the exchange positions on this mineral are occupied mainly by divalent cations (this was confirmed later - see table 5.9). On glycerolation the montmorillonite expands to 18A and the second order reflection at 9A is also visible on these traces. Appreciable amounts of kaolinite are present in C1; smaller amounts of this mineral also occur, together with chlorite, in C2. Resolution of second order kaolinite and fourth order chlorite reflections is shown for C2 and there was consequently no need to heat this sample to 600°C (see Appendix 4). Heat treatment of C3 could only indicate that chlorite might be present but this provisional identification is supported by the values of the small ?second and ?fourth order reflections at 7.06 and 3.52A on the trace of the air-dried clay (the first and second order kaolinite peaks tend to be at higher d-spacings - see, for instance, the trace for C1).

The mineral responsible for the 10A peak in these clays is, for convenience, described as mica. On the trace for C1 the spacing of 10.11A is too high for a well-crystallised mica and the presence of 'illite' in this sample seems likely. A DTA curve (described later) provided some evidence to support this contention. Well-crystallised mica, recognisable on microscopic evidence, occurs in the silt fractions of C1. As the overflow product contains particles ranging from 15 microns down to sub-micron size, it appears that both well-crystallised mica and illite phases are present. Whether these two phases exist independently or are part of a mica degradation sequence is not answered by the present

data. In samples C2 and C3 the 10A phase is present in smaller amount and the d-spacing is nearer that of a well-crystallised mica.

The small peak at 4.47A on the trace for C3 is a non-basal prism reflection and is due to the less than complete orientation of the clay components.

3.1.4 Interstratified illite/montmorillonites

3.1.4.1 General

The theory underlying the diffraction behaviour of interstratified clays has been summarised by MacEwan, Ruiz-Amil and Brown (1961). Methods for interpreting diffraction patterns are described in detail but there are limitations to the use which can be made both of the theoretical diffraction curves and peak migration curves presented by these authors, as in most instances they were calculated on the basis of completely random interstratification of the two components. Recent work on illite/montmorillonite interstratification has involved the comparison of theoretical one-dimensional diffraction profiles (computed with increasing degrees of sophistication) with the observed diffraction traces of clays from a number of localities (Sato et al., 1965; Reynolds, 1967; Morelli et al., 1967; Reynolds and Hower, 1970). From these studies it has become apparent that some degree of statistical order is common near the illite end of the interstratified sequence. Reynolds and Hower (op. cit.) have stated that in systems containing less than 40% montmorillonite layers ordered interstratification - involving an illite-montmorillonite superlattice (IM) - is almost always present. A further superlattice arrangement (IMII) is confined to samples containing 5-10% montmorillonite layers. These authors have also presented a number of calculated diffraction profiles for illite/montmorillonite interstratifications in which both the proportions of the two components

and also the ordering relationships between these vary. As the profiles were for ethylene glycol-saturated clays only qualitative comparisons could be made with the traces of the glycerol-saturated clays described here.

When discussing the diffraction traces of interstratified clays it is convenient to label the various non-integral peaks with respect to the peaks of the pure phases between which they migrate. Thus the index $(002)_{10\text{Å}}$ $(004)_{18\text{Å}}$ refers to the peak intermediate to 5 and 4.5Å - the actual position depends on the ratio of the two components. In this composite index the lower spacing component is always represented first (MacEwan et al., 1961). For interstratified systems where (a) the illite component is in excess, (b) no montmorillonite layers are contiguous, and (c) segregation is absent, interstratification is essentially between illite (I) and illite-montmorillonite (IM) units. Peak migration should then be considered with respect to I and IM entities (see Reynolds and Hower, op. cit.). For instrance, in the glycerol-saturated clay, the index $(001)_{10}/(001)_{28}$ should be used in preference to $(001)_{10}/(001)_{18}$. In practice, unless the extent of ordering is known, it is advisable to use the composite index for random interstratification (as is followed in the next section) subject to the rider that some of the peaks so indexed may be modified by a higher order reflection from the superlattice.

From a preliminary examination of the diffraction traces of the present samples it was established that in all but two (B12, 13) the illite component of the interstratified clay was dominant. Diffraction traces from samples of the larger group will be discussed first.

3.1.4.2 Diffraction traces of oriented clays from samples B1-11, 14, 15

Peak migrations resulting from variations in relative amounts of the two components are illustrated for a sequence of air-dried and

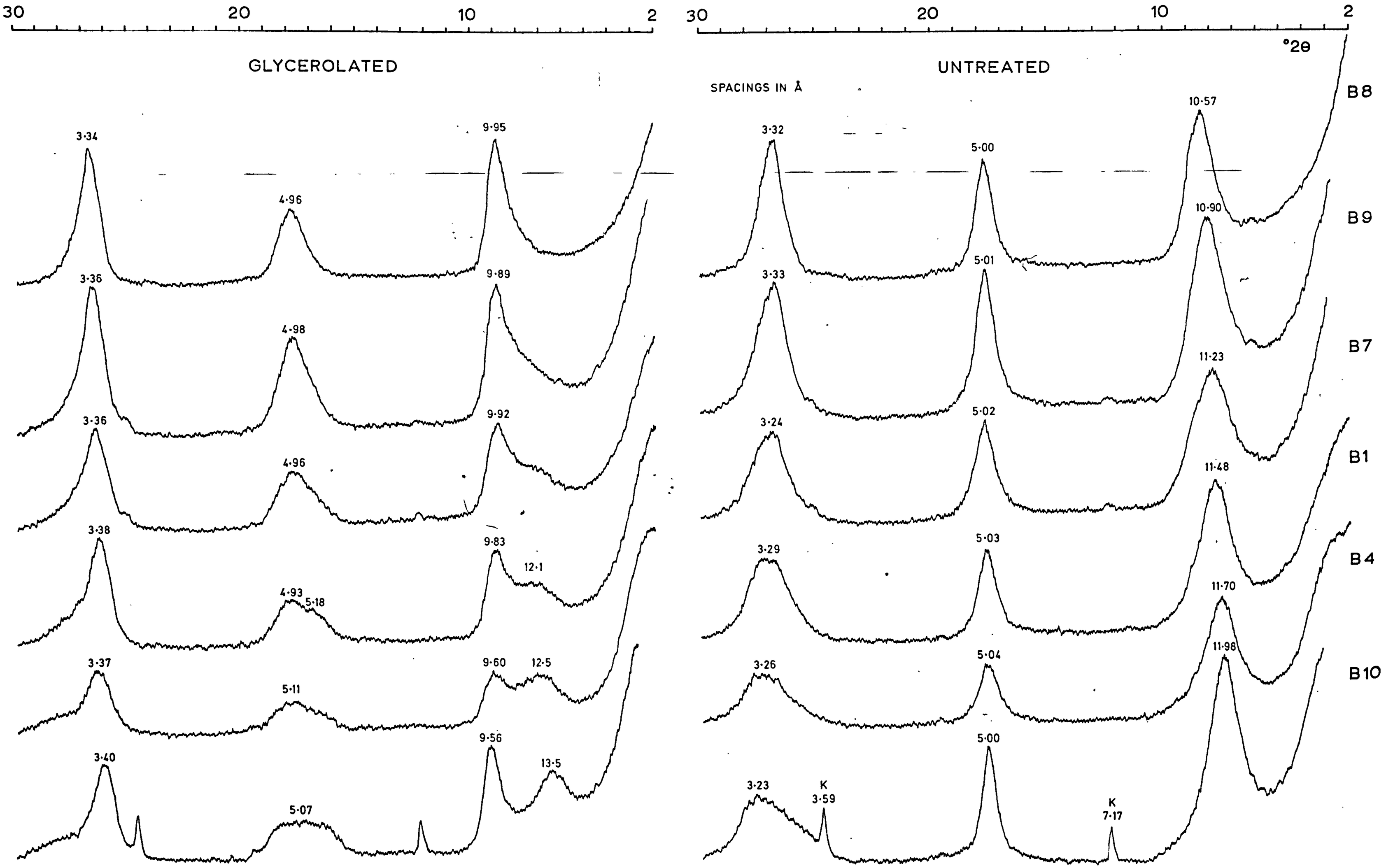

Fig. 3.3 Diffraction traces of interstratified illite/montmorillonites (all hydrocyclone overflow products). Traces are arranged so that the amount of montmorillonite component increases downwards from B8 to B10.

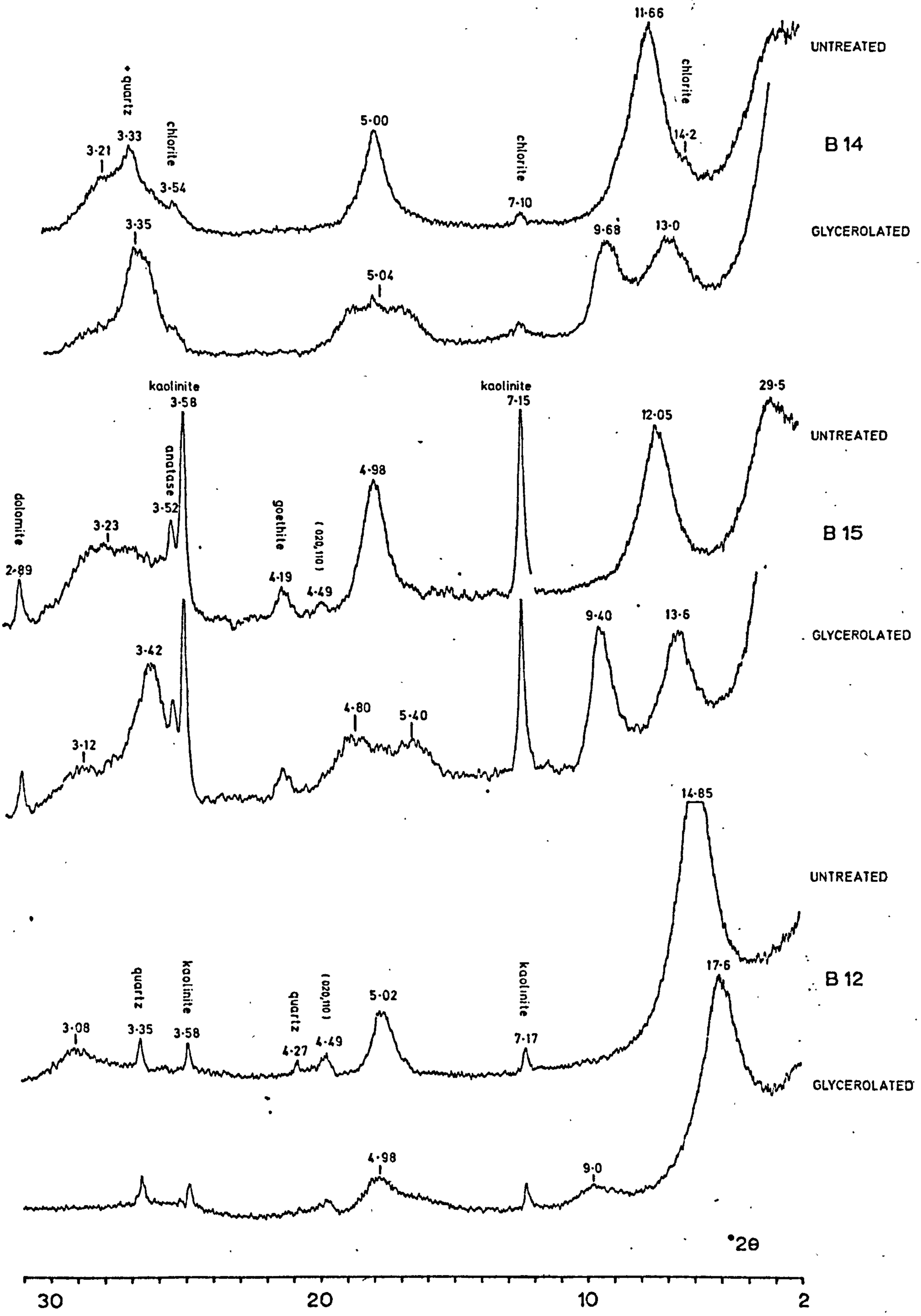

Fig. 3.4 Diffraction traces of interstratified illite/montmorillonites containing appreciable amounts of impurities (all hydrocyclone overflow products). Unassigned peaks are due to the interstratified clay, others as labelled.

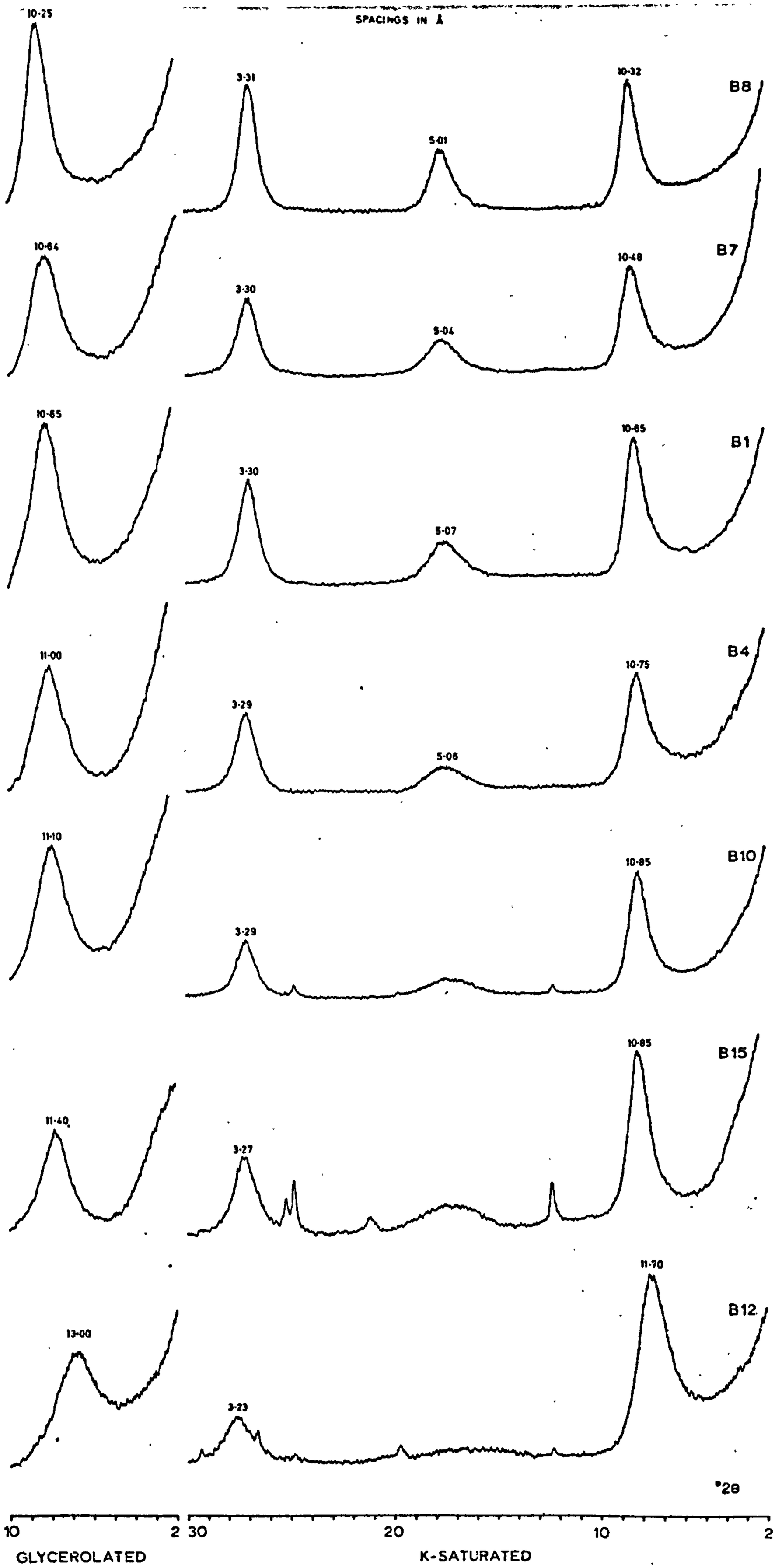

Fig. 3.5 Diffraction traces of K-saturated interstratified illite/ montmorillonites (all hydrocyclone overflow products).

glycerolated clays by the series of diffraction traces in fig. 3.3 (arranged so that the amount of illite component decreases towards the bottom of the page). In passing it may be mentioned that traces for B14 and 15 (fig. 3.4) can also be placed in this series but have been kept separate because peaks due to both clay and non-clay impurities are present. Kaolinite occurs in B10 (fig. 3.3). Small 'humps' at 7A on the traces of B7 and 9 could not be assigned with certainty to either kaolinite or chlorite although heating tests showed that the latter mineral was the most likely in B7.

Relative proportions of the two components of an interstratified sequence - and also the precise ordering relationships between these - may be determined by calculating Fourier transforms from the observed peak spacings and their intensities (MacEwan, 1956). With the possible exception of B15, lack of resolution between certain sets of composite peaks precluded calculation of Fourier transforms from the traces of the present samples and the relative amounts of the two components had to be determined from the peak migration curves (for random interstratification) presented in MacEwan et al. (1961). Results are shown in table 3.1. and for most samples the mean value for montmorillonite interlayering agrees closely with that expected from a comparison of the relevant diffraction trace with published traces for which the amount of montmorillonite component is known (e.g. Morelli et al., 1967; Reynolds and Hower, 1970). Some bias is present in a few of the mean results in table 3.1 (for B9, 14) due to incomplete data. For each sample discrepancies between the values obtained from different migration curves are often quite marked, especially where the proportion of montmorillonite layers exceeds 25%. The glycerolated trace of B15 shows resolution of all the composite peaks up to 003/006 and the amounts of montmorillonite interlayering corresponding to the d-spacings of these peaks (from migration curves in MacEwan et al., 1961) are shown in table

Table 3.1. Amount of montmorillonite interlayering (%) calculated from peak migration curves for randomly interstratified systems (in MacEwan et al., 1961).

sample	1a	1b	2a	2b	3a	3b	mean
B8	17	13	17	-	20	17	17
B9	-	-	20	-	25	21	(22)
B7	20	17	22	32	24	21	23
B1	27	17	24	20	29	23	23
B14	-	-	26	-	33	-	(29)
B4	30	21	26	27	35	24	27
B10	33	21	28	33	40	30	31
B15	33	25	29	-	44	40	34
B12	60	-	60	-	-	-	(60)

1. From 001/001(a) and 003/004(b) peak migration curves for 10/12.4A random interstratifications.

2. From 001/001(a) and 003/003(b) peak migration curves for 10/15.4A random interstratifications.

3. From 001/002(a) and 003/005(b) peak migration curves for 10/17.5A random interstratifications.

Table 3.2. Sample 815. Peak spacings taken from diffraction chart together with corresponding amounts of montmorillonite interlayering obtained from peak migration curves for 10/17.5A random interstratifications (in MacEwan et al., 1961). Figures in parentheses were obtained from the diffraction trace of the Kinnekulle type II clay figured by Morelli et al. (1967).

Composite peak	d-spacing	amount of mont. interlayering (%)
001/002	9.40 (9.5)	44 (42)
002/003	5.40 (5.40)	40 (40)
002/004	4.80 (4.72)	26 (30)
003/005	3.42 (3.43)	40 (41)
003/006	3.12 (3.13)	50 (50)

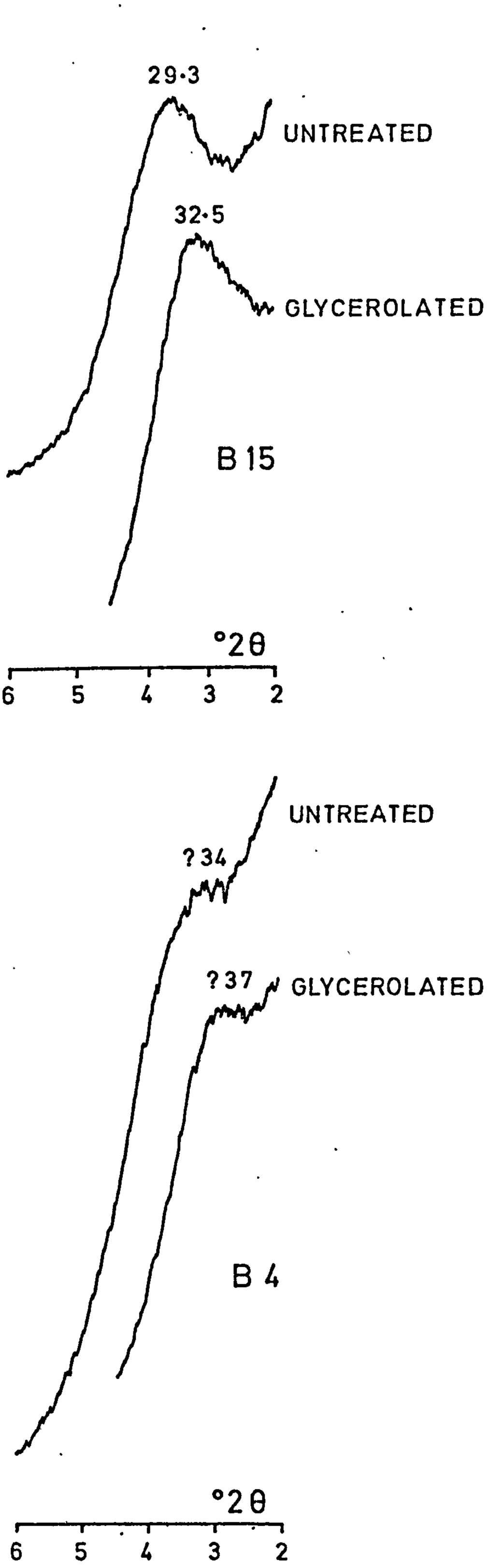

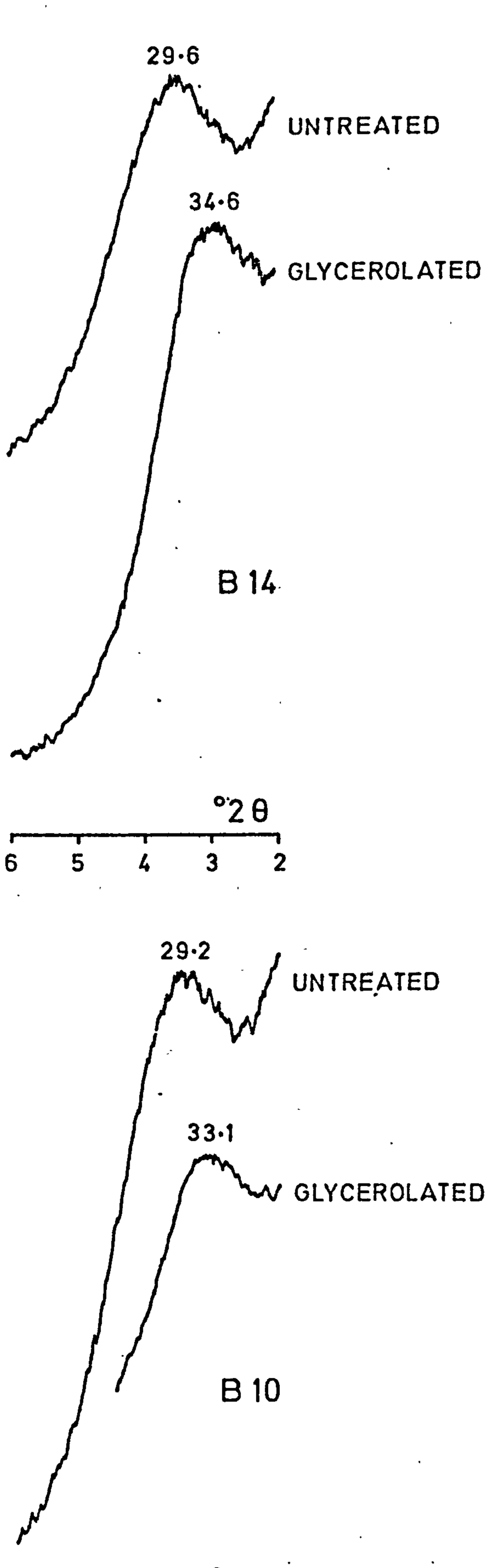

Fig. 3.6 Diffraction traces (low-angle region only) of four inter-stratified illite/montmorillonite hydrocyclone overflow products

3.2. Similar inflated values are given by Kinnekulle sample II, which contains 33% montmorillonite layers (Morelli et al., op. cit.) and gives a diffraction trace identical to that of B15.

Use of peak migration curves calculated on the basis of random interlayering is not strictly justified as the present samples exhibit at least some degree of ordering. Reynolds (1967) has shown that the presence of a peak between 8 and $6^{o}2\theta$ (Cu-radiation), or any asymmetry on the low-angle side of the first order 'illite' peak, for ethylene glycol (and also, presumably, glycerol) saturated clays is an indication of regular interstratification. Both phenomena are visible on the traces of the glycerol-treated samples in fig. 3.3 and 3.4. A second indication of ordering is the presence of peaks in the region of 30A. These are clearly visible on some of the traces in figs. 3.3 and 3.4. To improve resolution of these low angle peaks the samples were also examined under longer wavelength Co-radiation. High d-spacings were found for samples B4, 10, 14 and 15 (which contained between 27 and 34% montmorillonite layers). The relevant portions of the diffraction traces are shown in fig. 3.6. The rapidly increasing effect of Lorentz and polarisation factors causes a false peak shift towards lower diffraction angles - this effect is more marked as the breadth of the peak increases (Reynolds, 1967). The actual d-spacings are thus lower than recorded in fig. 3.6. In a comparable case Hower (1968) found that the observed d-spacings for air-dried and glycerolated clays (approximately 29 and 31A respectively) changed to 25 and 27A after correction for the Lorentz-polarisation factors. These d-spacings are compatible with the presence of an IM superlattice. The spacings of the glycerolated clays (fig. 3.6) apparently increase as the amount of montmorillonite interlayering decreases and only a poorly-defined peak or shoulder appears on the trace for B4. Similar observations

were made by Hower (op. cit.) for a series of ethylene glycol-saturated clays. The absence of peaks in this region for samples containing less than 27% montmorillonite layers may be due to the combination of the Lorentz-polarisation effect with the decreasing intensity of possible superlattice reflections.

3.1.4.3 Diffraction traces of oriented clays from samples B12, 13

The following discussion concentrates entirely on the X-ray diffraction behaviour of the clay product from sample B12 as the illite/montmorillonite from B13 showed identical diffraction characteristics. The trace of the air dried sample (fig. 3.4) appears no different from that of a montmorillonite (ss) although discrepancies are apparent after glycerolation. The peak at 4.98A on the trace of the glycerolated sample is undoubtedly aberrant as montmorillonite (ss) would give a third order reflection at approximately 6A and a fourth order at 4.5A. (Even assuming the presence of interstratification it is still difficult to assign a convincing composite index to this particular peak). Observations which confirm the interstratified nature of the sample may be summarised viz:

(i) Diffraction behaviour after K-saturation (fig. 3.5)

(ii) The K_2O figure of 2.23% (table 5.3) which cannot be accounted for by discrete mica or feldspar.

(iii) Similarity of the diffraction trace of the randomly oriented sample to the traces of the other undoubtedly interstratified clays (fig. 3.7).

About 60% montmorillonite layers are present in this sample (table 3.1) - interstratification is therefore probably random (Reynolds and Hower, 1970).

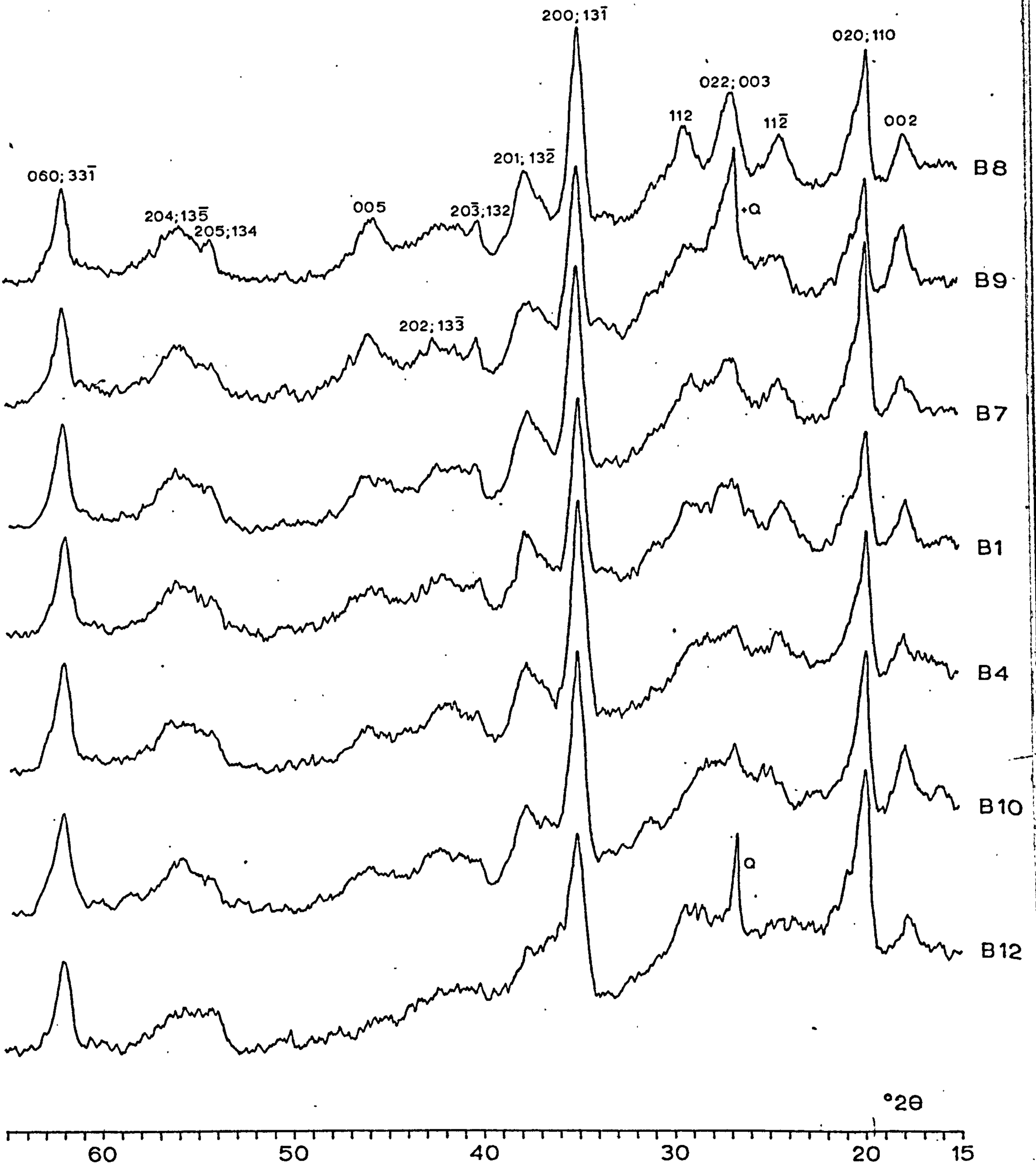

Fig. 3.7 Diffraction traces of randomly oriented interstratified illite/montmorillonites (all hydrocyclone overflow products). Traces are arranged so that the amount of montmorillonite component increases downwards from B8 to B12. Peaks marked Q on traces for B9 and B12 are due to quartz.

3.1.4.4 Diffraction traces of the randomly oriented clays

All the traces show reflections characteristic of the 1M mica polymorph and in fig. 3.7 the trace for B8 is indexed on this basis. The traces of the remaining samples show a progressive loss of definition in the region between 22 and $34^{o}2\theta$ as the amount of montmorillonite interlayering increases. This region includes the $11\bar{2}$ and 112 reflections, the intensities of which were shown by Yoder and Eugster (1955) to diminish from well crystallised 1M mica to the 1Md polymorph. (No quantitative 1M-1Md distinction was defined by these authors however). For B8 the extent of the $11\bar{2}$ and 112 peak development would suggest a high degree of stacking order. Even for B12 (60% montmorillonite layers) a significant amount of stacking order remains - compare the sharpness of the peak at $35.5^{o}2\theta$ with the corresponding montmorillonite (ss) hk bands in the same angular range in fig. 3.1.

The 060 spacings all fall within 1.500 $\pm$ 0.002A which is in keeping with the predominantly dioctahedral nature of the clays.

Quartz was identified on the traces of B9 and 12 and this mineral may also be present in B10.

3.1.4.5 Additional data

Some additional points arising from the X-ray investigation of the clays are noted here but discussion of these is deferred until Chapter 6.

(i) With one exception (see (ii) below) clays from localities where two or more horizons were sampled (ie Llangibi, Woodbury and Penny Hill) showed identical illite:montmorillonite ratios.

(ii) At Overbury the clays from two closely adjacent horizons were found to contain 31% (B10) and 60% (B12) montmorillonite interlayers. Bystrom (1956) recognised two distinct types of illite/montmorillonite

interlayering in her account of the Kinnekulle, Sweden, interstratified clay occurrences. One horizon, 2 m thick, was composed of interstratified clay in which the illite and montmorillonite components were in the ratio 40:60 (proportions from a later, more detailed, X-ray study of this clay by Hower and Mowatt, 1966). Higher in the succession occurred thinner horizons in which the illite and montmorilonite components of the clay were in the ratio 67:33 (proportions from a later study of the clay by Morelli et al., 1967). Similarities with the Overbury occurrence are marked and would tend to support the suggestion of Bystrom (op. cit.) that certain stable arrangements of illite and montmorillonite layers exist.

(iii) Studies on the illite/montmorillonite horizons of the US have shown that weathered illite/montmorillonite clays give both broader peaks and larger 001/001 d-spacings than fresh material from the same horizon (Huff, 1963; Mossler and Hayes, 1966). The conclusion drawn from these observations was that weathering leached 'fixed' K from the clay lattice, thus increasing CEC and amount of montmorillonite interlayering. Neither peak broadening or increase in 001/001 d-spacing was observed on comparing X-ray diffraction traces of weathered and fresh clay from the Woodbury section although at this locality exposure of clay to sub-areal weathering conditions had only taken place over the last ten years or so.

3.1.4.6 Diffraction traces of clay fractions from reworked illite/montmorillonite horizons

The top three traces in fig. 3.8 were obtained from the clay fraction of a reworked mudstone (possibly from the Lower Ludlow Shale Group) occurring between 89.50 and 89.53 m in the IGS Dean Borehole, Brosely, Salop. The trace of the untreated clay shows reflections of chlorite (14.13, 7.07, 4.71, 3.57 and 3.53A), detrital mica (9.95, 4.97

and, in part, 3.33A), quartz (4.24 and, in part, 3.33A), plagioclase feldspar (3.19A) and calcite (3.03A). Most of the calcite present in the sample occurs as an alteration product of plagioclase. In addition to the more abundant detrital chlorite, pseudomorphs of chlorite after an unknown ferromagnesian mineral occur in this sample but on the diffraction trace only the fourth order reflections (3.57 and 3.53A) of the two chlorite species are resolved. (Acid dissolution tests showed that kaolinite was absent.) An interstratified illite/montmorillonite phase gives a broad 001/001 peak at 11.32A and on glycerolation new 001/001 and 001/002 reflections appear (arrowed on trace). Dissimilarities between the traces of untreated and glycerolated clays are also apparent in the 17-19 and 24-28^{o}2θ regions. The amount of montmorillonite component in the interstratified phase would appear to lie between 20 and 25%. Heating the sample at 600^{o}C causes the 001 chlorite peak to shift from 14.13 to 13.85A and also results in the virtual disappearance of all succeeding chlorite reflections. Contraction of the illite/montmorillonite phase to approximately 10A on heating enhances the first, second and third order mica reflections.

Traces similar to those described above were given by the clays from the upper portions of the thickest Woodbury illite/montmorillonite horizon and also by the fossiliferous grey mudstone band occurring 3m above this (section 1.5.3).

3.1.4.7 Diffraction traces of shales adjacent to illite/montmorillonite horizons

The bottom three diffraction traces in fig. 3.8 were obtained from the clay fraction of a compact green mudstone occurring 1m below an illite/montmorillonite horizon (sample 696A in this study) in the IGS Manor Farm Borehole No. 1, Walsall. (Identical traces were given by a moderately plastic, pale green clay collected from a surface exposure of

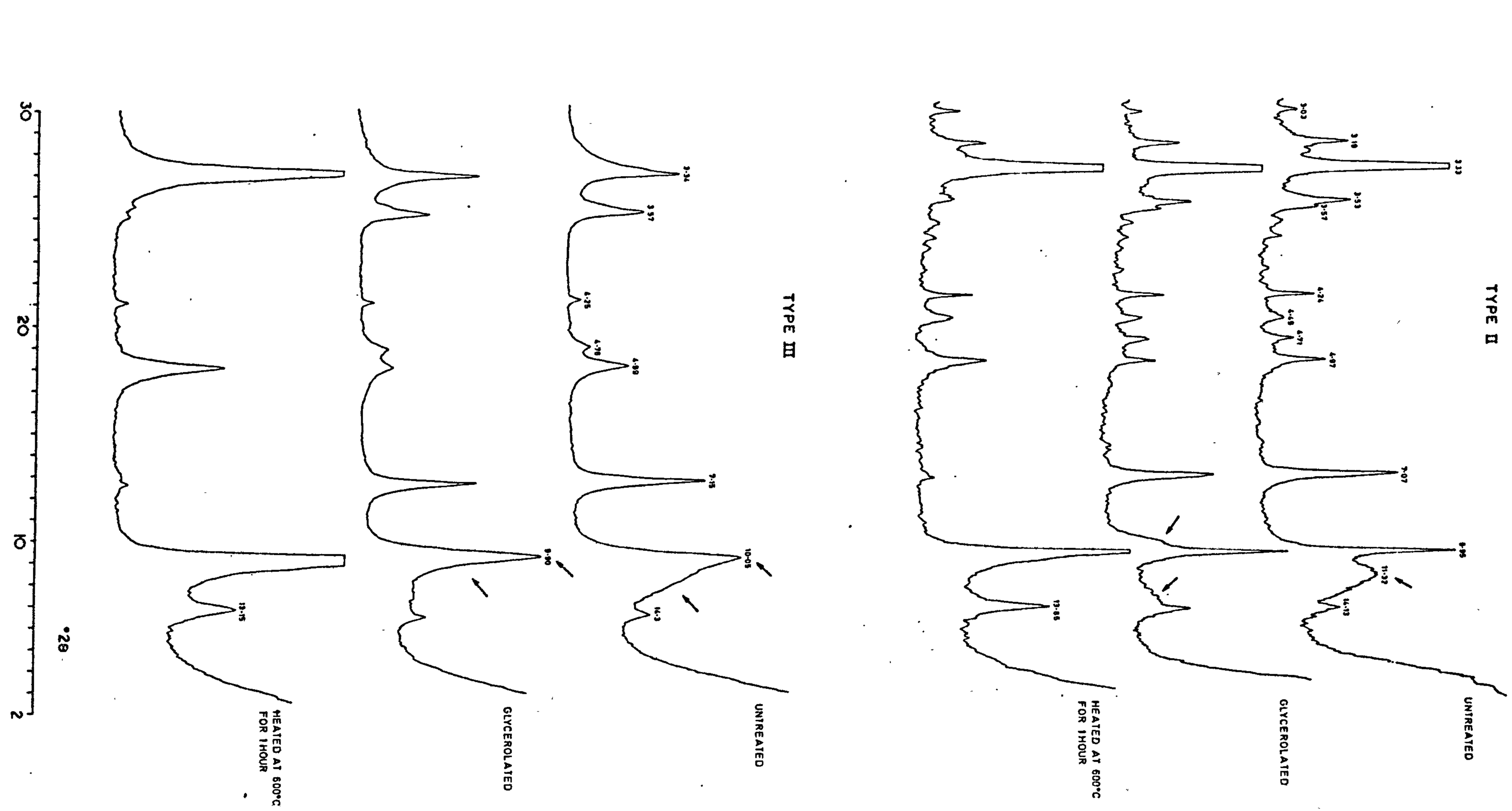

Fig. 3.8 Diffraction traces of clays associated with the 'pure' interstratified illite/montmorillonite horizons. Top three traces: hydrocyclone overflow product from reworked illite/montmorillonite horizon. Bottom three traces: hydrocyclone overflow product from shale underlying an illite/montmorillonite horizon.

Wenlock strata at Lincoln Hill, Ironbridge, Salop.) 'Mica' (10.05, 4.99 and, in part, 3.34A), chlorite (14.3, 7.15, 4.76 and 3.57A) and quartz (4.25 and, in part, 3.34A) were the only constituents identified on the trace of the untreated clay. A marked asymmetry is apparent on the low angle side of the first order 'mica' peak and on glycerolation a sharpening of this peak, and a shift in d-spacing from 10.05 to 9.90A, is observed. X-ray diffraction examination of the randomly oriented clay suggested that the 'mica' is the 2M polymorph.

Heller-Kallai and Kalman (1972), in a study of Palaeozoic sediments from the Negev, Israel, described a clay showing identical diffraction behaviour, in the 6-10^{o}2θ region, to the present sample. They concluded that both apparent sharpening and shift of the 'mica' peak after glycerolation would be caused by a mixture of discrete illite (? mica) and a randomly interstratified illite/montmorillonite in which the amount of montmorillonite component did not exceed 20%. It is unlikely that the present sample contains both discrete mica and interstratified illite/montmorillonite as the diffraction traces given by such a mixture would be markedly different (see top two traces in fig. 3.8). ~~Rather it is~~ Tenatively this suggested that interstratification is contained wholly within the miea phase and results from modification of the mica structure (? expansion via frayed edges) during weathering and subsequent transportation. Sharpening of the first order 'mica' peak after glycerol or glycol treatment is common in detrital assemblages (Triplehorn, 1970).

3.2 THERMAL EXAMINATION

3.2.1 General

Thermal methods were used in the mineralogical investigation of the original untreated samples both in identifying small amounts of

sulphides and carbonates and providing quantitative data for the latter. Initially it was hoped that those differences in structural properties of the clay minerals which could be monitored by thermal means (eg normal v. abnormal dehydroxylation) might be related to differences in physico-chemical behaviour. Consequently, comprehensive thermal data were obtained for the montmorillonite and interstratified illite/montmorillonite clay products. However it will be shown in Chapter 7 that the extent of particle disaggregation of these clays is the major factor influencing the development of most of the physico-chemical properties investigated and therefore the effect of any subtle variation in clay type could not be assessed.

In the first part of this section DTA curves of dioctahedral montmorillonites are discussed in some detail and various attempts at classification, based on thermal behaviour, are reviewed. The use of thermogravimetry for measuring the structural water content of montmorillonite is also assessed. DTA curves of the interstratified illite/montmorillonite overflow products are presented and compared with published curves. The suggestion that the termperature of the dehydroxylation peak may give some indication as to origin (Cole and Hosking, 1957) is reviewed. Simultaneous DTA was carried out in conjunction with thermogravimetric analyses and the TG/DTA curves for four montmorillonites and four interstratified illite/montmorillonites are illustrated and discussed.

Descriptions of the conditions under which DTA and simultaneous TG/DTA were carried out are given in Appendix 4.

3.2.2 DTA Curves of montmorillonites

DTA curves of montmorillonites are usually divided into three regions: (a) a low temperature region (ambient to 300°C), (b) the dehydroxylation region (400 to 750°C), and (c) a high-temperature region

(above 800°C). The approximate temperature ranges in parentheses apply at a heating rate of 10°C/min.

3.2.2.1 DTA curves - low temperature region

The most prominent feature on montmorillonite DTA curves (air-dried or equilibrated at 52% RH) is a large endotherm with a peak at about 140 to 150°C. This endotherm may show a subsidiary peak or shoulder at approximately 120°C. Nemecz (1962) has suggested that the main endotherm is due to expulsion of water present in the interlaminar region of the montmorillonite whilst the lower temperature component results from release of water sorbed on the surface of montmorillonite aggregates. Montmorillonites containing divalent exchangeable cations (and Li-saturated varieties) also show an endothermic peak at about 200°C resulting from expulsion of water molecules coordinated to the cation.

3.2.2.2 DTA Curves - dehydroxylation region

Montmorillonites may be described as 'normal' or 'abnormal' depending on the temperature range in which dehydroxylation occurs. Normal montmorillonites show a dehydroxylation endotherm at approximately 700°C, abnormal varieties either a single endotherm at approximately 550°C or a dual endothermic system with peaks at approximately 550 and 650°C. No significant differences between the dehydroxylation peak areas of normal and abnormal varieties were found by Mackenzie (1961).

The reasons for the observed differences in dehydroxylation behaviour have not yet been explained satisfactorily. Mackenzie (1970) stated that variation in dehydroxylation temperature must be related in some way to the energy with which the hydroxyl groups are bound in the lattice, earlier having stated (1957) that subtle variations in distribution of octahedral cations (with respect to hydroxyl ions) may be

responsible for these differences in lattice bonding energy. It is unlikely that dual dehydroxylation endotherms result from 'mixing of layers' as Grim and Kulbicki (1961) suggest, or are related to an asymmetric layer charge distribution within the montmorillonite structural unit (Tettenhorst and Johns, 1966). Schultz (1969), reviewing variations in montmorillonite bulk chemistry, stated that the major structural ions (Al, Mg, Fe, and Si) do not seem to influence dehydroxylation temperature by more than $\pm$ 50^{o}C. This statement is questionable. The evidence presented by Schultz to the effect that abnormal montmorillonites contain structural water in excess of that required by the $O_{20}(OH)_4$ structural unit is not conclusive and will be discussed further in section 3.2.3. The existence of 'structural defects' in montmorillonite may be related to dehydroxylation behaviour (Greene-Kelly, 1957), some support coming from Schultz's observations that the sharpness and intensities of X-ray reflections (especially 02) are weaker in abnormal montmorillonites.

3.2.2.3 DTA Curves - high temperature region

This region of the DTA curve shows an endothermic peak (at approximately 850^{o}C) either followed immediately by an exotherm (giving as S-shaped peak system), or the endothermic and exothermic effects may be separate and differ in peak temperature by up to 200^{o}C. The endotherm at 850^{o}C represents heat absorbed in the transition from an ordered to a disordered or amorphous state (Early et al., 1953). Grim and Kulbicki (1961) placed montmorillonites into gwo groups (Wyoming- and Cheto-type) on the basis of the nature of the endo-exothermic peak system and the high-temperature phases formed up to 1500^{o}C. Those of the Wyoming-type show an S-shaped endo-exothermic inversion and simultaneous crystallisation of both mullite and cristobalite about 200^{o}C after this event.

(In high-Fe Wyoming types mullite does not form). In Cheto-type montmorillonites, where the endothermic and exothermic peaks are separate, Grim and Kulbicki related crystallisation of β-quartz with the exothermic effect The β-quartz inverts to β-cristobalite above 1100°C and cordierite crystallises above 1200°C. In contrast to the Wyoming-type montmorillonites, crystallisation of all phases in the Cheto-types could be correlated with the high temperature exothermic peaks on the DTA curve. In both types of montmorillonite the nature of the exchangeable cation influences the size and shape of the DTA peak system between 800 and 1100°C (Mielenz et al., 1955) and the extent of the high temperature phase development.

The classification of Grim and Kulbicki does appear to reflect fundamental differences in montmorillonite type. Cheto-type montmorillonites show higher Mg for Al substitution leading to high lattice charges and CECs (114-133 meq/100g). In contrast Wyoming-type montmorillonites give maximum CECs of 111 meq/100g. X-ray powder photographs of the latter also show somewhat better-defined prism reflections (Grim and Kulbicki, op. cit.).

Classifications based on DTA behaviour can be carried to extreme lengths. Schultz (1969) accepted the classification into normal and abnormal montmorillonites, although using the terms ideal and non-ideal for reasons explained in his paper. He further separated the former group into four types - Wyoming, Otay, Tatatilla, and Chambers - on the somewhat doubtful criteria of exact dehydroxylation peak temperature (within the range 660 to 725°C) and shape of the high temperature endothermic-exothermic peak system.

3.2.2.4 DTA curves of the present samples

Curves for a selection of montmorillonite overflow products are given in fig. 3.9. For the Lower Greensand and Jurassic montmorillonites

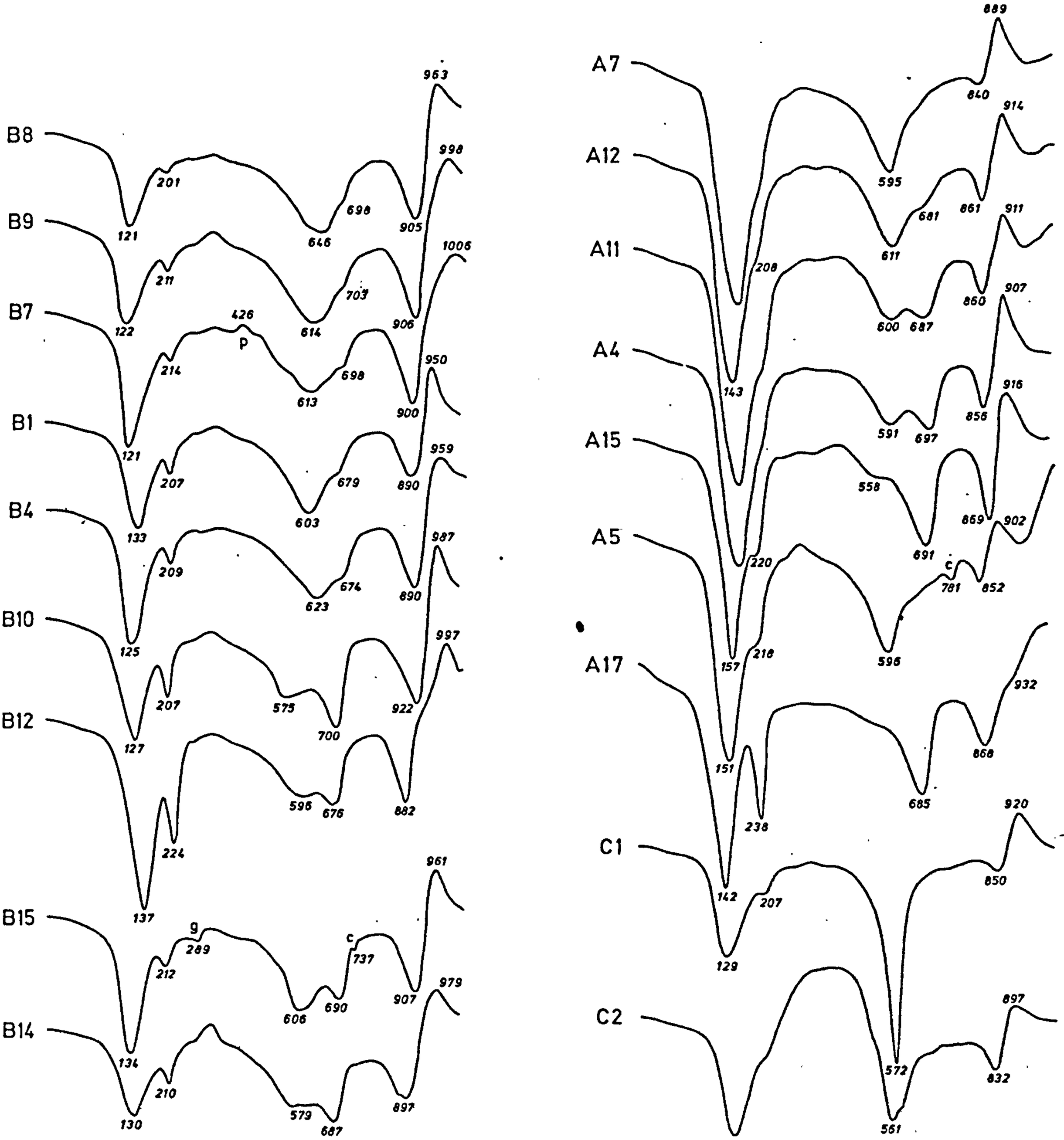

131

temperatures in °C

Fig. 3.9 Left hand side: DTA curves of interstratified illite/montmorillonites (from B8 to B12 these are arranged so that the amount of montmorillonite component increases downwards). Right hand side: DTA curves of montmorillonites (A7 down to A17) and mixed-assemblage clays (C1 and C2). All curves of hydrocyclone overflow products except that of A17 which is of the original sample. Peaks marked P, g and c on curves are due to pyrite, goethite and calcite respectively.

(A7 down to A5) release of cation-coordinated water is represented only by a poorly defined shoulder on the high-temperature side of the main endotherm. Sample A17 shows a sharp peak at a considerably higher temperature (238^{o}C). Lack of definition of the cation-coordinated water peak may be due partly to the masking effect of the much larger adsorbed water endotherm. Even allowing for this effect the difference in definition and temperature of this peak between A17 and the rest of the samples is significant and must reflect differences in cation-water bonding energies

Differences in dehydroxylation behaviour are apparent and, for these samples, A7 and A15 may be regarded as exemplifying abnormal and normal dehydroxylation behaviour respectively. Inflexion points are present on the high-temperature side of the dehydroxylation endotherm of A7 and on the low-temperature side of the dehydroxylation endotherm of A15 and therefore these samples are not pure end-members of the abnormal-normal dehydroxylation series. (See also discussion of simultaneous TG/DTA curves in section 3.2.3.2.)

The high-temperature peak system is S-shaped in all the samples except A17 where the presence of large amounts of discrete iron oxide/ hydroxide minerals encourages fusion at relatively low temperatures. In A7 the virtual absence of an endotherm, and the lower temperature of the exothermic component of the high-temperature peak system, is probably related to the high structural Fe-content.

3.2.3 Thermogravimetric examination of montmotillonites

3.2.3.1 Review

A typical montmorillonite thermobalance trace may be divided into three regions. (It should be noted that this three-fold division is

based on different criteria from those used to divide montmorillonite DTA curves into three regions). In the first region of the trace a sharp weight loss occurs between 100 and 250°C- this is due to loss of adsorbed, interlayer, and the bulk of the cation-coordinated water. A gently sloping 'plateau region' follows and this may extend to 550°C. The remainder of the cation-coordinated water is lost in this region, the slope of the plateau being greater for divalent as opposed to monovalent cation-saturated montmorillonites (Mielenz et al., 1955; Mackenzie, 1964). Dehydroxylation commences at some point on the plateau before loss of cation-coordinated water is complete; the main dehydroxylation loss (in the third region of the trace) is essentially complete by 700°C although a small rate of weight loss may be observed up to 900°C.

The plateau region is critical in any attempt to determine the structural (hydroxyl) water content of montmorillonite by thermogravimetric means. Various authors have tried to separate cation-coordinated water loss from dehydroxylation either by varying experimental conditions such as heating rate, or, artifically, by constructions on the thermobalance traces (see, for instance, Neumann, 1964). Even at slow heating rates of 0.4°C/min the plateau region has a pronounced slope (Neumann, op .cit.) and the first approach does not appear feasible. (For the present samples maintaining isothermal conditions at various temperatures within the plateau region also met with no success). Schultz (1969) arbitrarily chose the mid-point of the plateau on the traces of a number of montmorillonites with different dehydroxylation characteristics and expressed the weight losses above this point on an ignited weight basis. He concluded, on the strength of these results, that the presence of structural water in quantities greater, and possibly even less, than the exact amount required by the $O_{20}(OH)_4$ structural unit appeared to be the major factor controlling dehydroxylation (normal v.

abnormal) behaviour. Such conclusions are questionable in view of (a) the arbitrary nature of the point on the thermobalance trace at which dehydroxylation was assumed to begin (see also discussion in the following section) and (b) the buoyancy corrections which have to be made to any weight loss measurement (which are considerable when compared to the relatively small dehydroxylation loss). The use of thermobalance data by Mielenz et al. (1955) to support the existence of tetrahedral hydroxyl groups in montmorillonite is open to the same criticism.

3.2.3.2 Results for present samples

Four montmorillonites, for which the amount of structural water had already been calculated, were examined by simultaneous TG/DTA. The TG/DTA traces are illustrated in fig. 3.10. Arrows on the TG curves indicate start of evolution of (a) H_2O^+ (water loss above 105^oC obtained from static heating) and (b) H_2O^+ corrected (water loss above 105^oC corrected for cation hydration water by the method of Mackenzie, 1961). The actual positions of the arrows were obtained by back calculation from the ignited weight. H_2O^+ (corrected) corresponds to the hydroxyl water content of the montmorillonite.

In table 3.3 the temperatures corresponding to the implied start of evolution of hydroxyl water (H_2O^+(corrected)) and the temperatures at the mid-points of the plateau region on the thermobalance traces (Schultz, 1969) are compared with the temperatures at which the dehydroxylation endotherm commences on the respective simultaneous DTA curves. (All temperatures were taken from the original charts). From the table it is seen that the plateau region begins at approximately the same temperature for all four montmorillonites and the mid-point temperature increases as the dehydroxylation character becomes more normal. Comparison of the last two columns in table 3.3 shows that for three montmorillonites

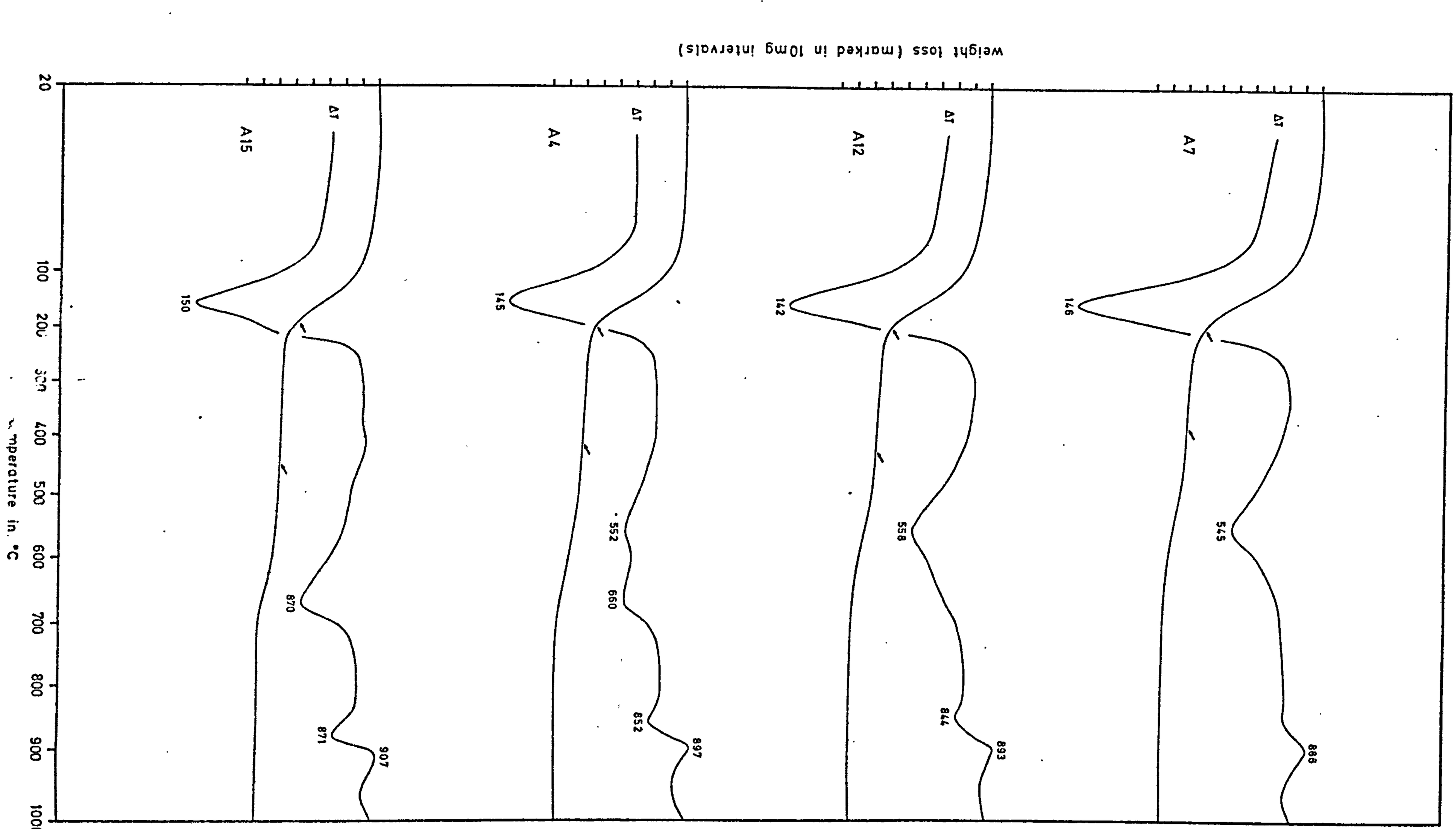

Fig. 3.10 Simultaneous TG/DTA curves of four montmorillonite hydrocyclone overflow products. Arrows on TG curves indicate start of evolution of H_2O^+ and H_2O^+ (corrected by Mackenzie's method).

Table 3.3. Start-of-dehydroxylation temperatures (in °C) for montmorillonites

Sample	Temp. range of plateau	Temp. at mid-point	Start of dehydroxylation endotherm on DTA curve	Temp. on TG curve corresponding to start of H_2O+ (corr.) evolution
A7	260-445	352	340	373
A12	260-485	372	360	420
A4	250-490	369	414	414
A15	260-520	390	425	445

Table 3.4. Dehydroxylation of montmorillonites: percentages of structural water (H_2O^+ corr.) corresponding to (discrete) endothermic effects on DTA curves.

Sample	Dividing or inflexion point on dehydroxylation endotherm	structural water first loss (%)	second loss (%)
A7	600	72	28
A12	606	61	39
A4	597	44	56

the start-of-dehydroxylation temperatures from the DTA curves are lower than the temperatures corresponding to the beginning of evolution of H_2O^+(corrected) on the TG traces. This is to be expected if the weight losses due to loss of cation-coordinated water and dehydroxylation overlap. No meaningful deductions can be drawn from the figures in table 3.3 in view of the uncertainty introduced by superposing data obtained by a static method, i.e. H_2O^+(corrected), on to TG traces which were obtained by dynamic means. All that can be stated is that, at a heating rate of 6^oC/min, dehydroxylation of abnormal montmorillonites may commence as low as 340^oC whereas for normal montmorillonites the start-of-dehydroxylation temperature may be in excess of 400^oC.

For the three Cretaceous montmorillonites, A4, 7, and 12, the dehydroxylation endotherm is either undoubtedly dual (with a dividing point at approximately 600^oC) or is single with an inflexion point or shoulder at this same temperature. From the corresponding TG traces the proportion of structural water lost below 600^oC (table 3.4) shows a strong negative correlation with octahedral Al content of the montmorillonite. The data further suggests that abnormal dehydroxylation characteristics would more or less be lost when the number of octahedral Al ions exceeds three. This may well be valid for the present montmorillonites but it is very unlikely that normal v. abnormal dehydroxylation behaviour depends solely on the number of Al-OH bonds. (The beidellite examined by Weir and Greene-Kelly, 1962, showed a dehydroxylation endotherm at approximately 500^oC yet contained nearly the full complement of octahedral Al).

3.2.4 Thermal examination of the interstratified illite/montmorillonites

The selection of DTA curves in fig. 3.9 is arranged in order of increasing montmorillonite interlayering from B8 down to B12; samples

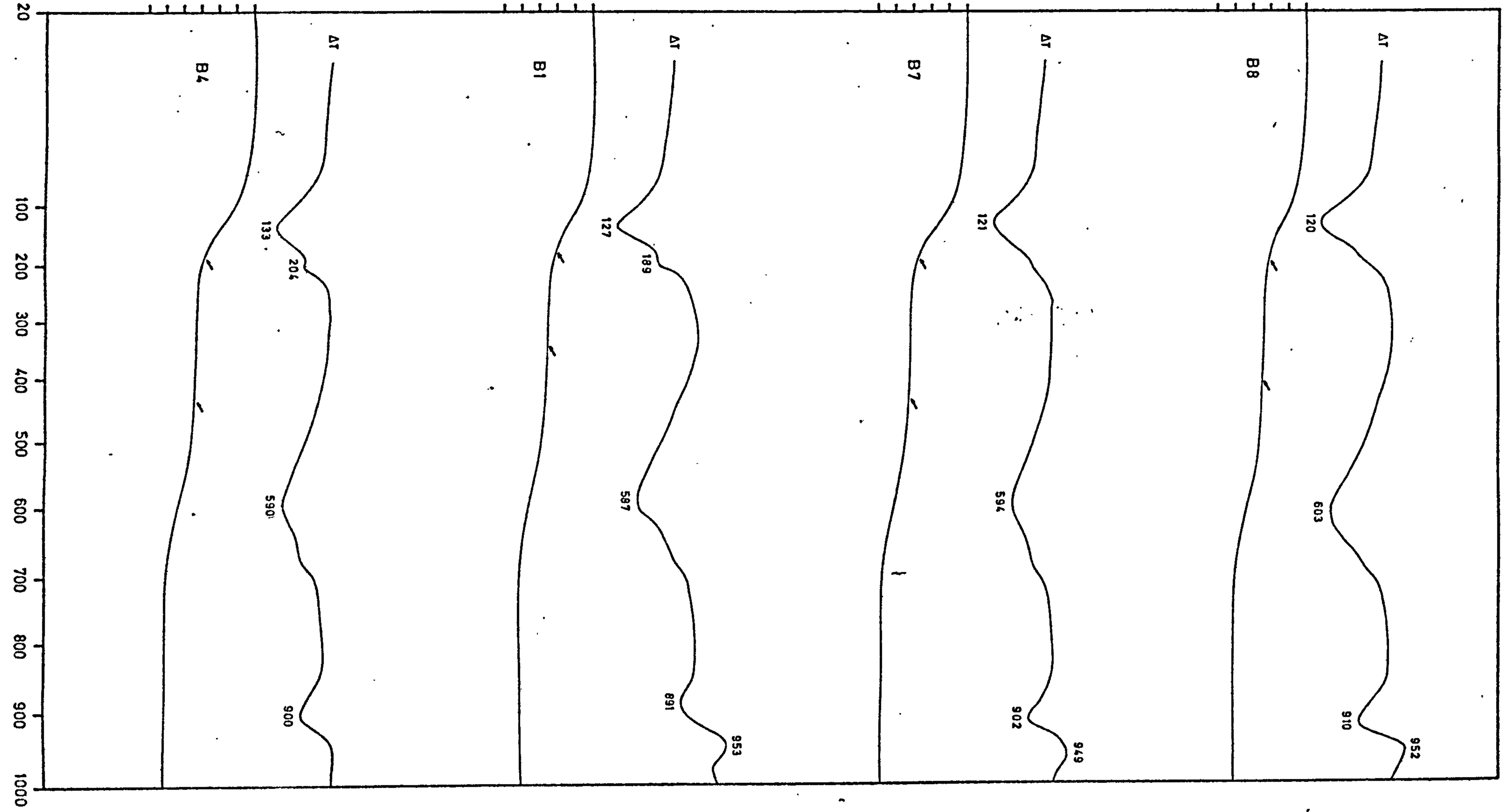

Fig. 3.11 Simultaneous TG/DTA curves of four interstratified illite/montmorillonite hydrocyclone overflow products. Arrows on TG curves indicate start of evolution of H_2O^+ and H_2O^+ (corrected by Mackenzie's method).

Table 3.5. Start-of-dehydroxylation temperatures (in ^{o}C) for interstratified illite/montmorillonites

Sample	Temp. range of plateau	Temp. at mid-point	Start of dehydroxylation endotherm on DTA curve	Temp. on TG curve corresponding to start of H_2O+ (corr.) evolution
B8	221-448	334	361	402
B7	237-480	359	405	424
B1	204-426	315	332	332
B4	215-467	341	371	424

Table 3.6. Dehydroxylation of interstratified illite/montmorillonites: percentages of structural water (H_2O^+ corr.) corresponding to main and subsidiary endothermic effects of DTA curves

Sample	inflexion point on high temperature side of dehydroxylation endotherm	structural water	
		first loss (%)	second loss (%)
B8	659	77	23
B7	676	76	24
B1	637	77	23
B4	646	72	28

B14 and 15 are separated from this series as they contain clay mineral impurities which modify the shape of the curve in the dehydroxylation region. Relatively few DTA curves of interstratified illite/montmorillonites are available for comparison in the literature. Bystrom (1956) has presented DTA curves for a number of Kinnekulle samples and Slansky (1961) figured eight curves for interstratified illite/montmorillonites (accompanied by small amounts of kaolinite) occurring in Carboniferous sediments of Czechoslovakia.

In fig. 3.9 the peaks between 200 and 225°C (due to expulsion of cation-coordinated water) increase in size as the amount of montmorillonite interlayering increases. In the dehydroxylation region samples B8 down to B4 (all from the Abberley district) show a broad endotherm with a peak between 600 and 650°C and a shoulder at 670 to 700°C. Reference to table 3.6 shows that the main endotherm corresponds to the loss of about three-quarters of the structural water. Dehydroxylation appears to commence at temperatures ranging from 330 to 400°C (table 3.5). DTA curves of the Abberley clays are similar, especially in the dehydroxylation region, to curves of the Kinnekulle clays recorded by Bystrom (op. cit.). In contrast clays from Overbury (samples B10 and 12, fig. 3.9) exhibit a well defined dual-peak dehydroxylation system in which the higher temperature component is dominant. Curves for these samples show more similarities to the curves figured by Slansky (op. cit.). All the samples, except B12, give an S-shaped endothermic-exothermic peak system, the amplitude of which varies quite markedly (compare B1 and B7). An inflexion point between the two components of the high-temperature peak system is present on the curve for B12.

Cole and Hosking (1957) divided published DTA curves of illites and montmorillonites into two series. In the first series the main endothermic dehydroxylation peak lay between 525 and 625°C, in the second between 650 and 725°C. These authors suggested that the first series

represented illite in the course of transition to abnormal montmorillonite and the second series the gradual transition of montmorillonite to abnormal illite. According to this hypothesis it should be possible to determine whether interstratified illite/montmorillonites were originally montmorillonite- or mica-like simply from the dehydroxylation peak temperature. Mossler and Hayes (1966), for instance, stated that the dehydroxylation peak temperatures of their Ordovician clays 'indicate that the mixed-layer mica/montmorillonite has proceeded through a montmorillonite stage and has become more mica-like by K-fixation in interlayer positions'. Of the present samples, B8 down to B4, together with B15, appear to belong to the first series of Cole and Hosking whereas samples B10, 12 and 14 definitely belong to the second series. Two contrasting modes of formation for the present samples are therefore suggested but in view of the similarity in field occurrence, X-ray behaviour etc. this is extremely unlikely. It appears unwise to use criteria such as dehyroxylation peak temperatures for such a purpose when the factors governing DTA peak configuration in the 500-750^{o}C temperature range have not been explained satisfactorily (section 3.2.2.2).

3.2.5 Thermal examination of the mixed-assemblage clays

The amount of information which can be obtained from DTA curves of mixed assemblage clays is limited.

DTA curves of two of the samples from this group are shown in fig. 3.9. For C1 the large narrow endotherm with a peak at 572^{o}C suggests that appreciable amounts of kaolinite are present (in agreement with previous X-ray diffraction results). Both low-temperature and high-temperature sections are compatible with the presence of montmorillonite or 'illite'. In C2 large amounts of organic material are present, its combustion producing the large exothermic effect on the curve. Sample C3 gives a similar curve except that, in addition, a large endothermic peak, resulting from dissociation of calcite, occurs at 820^{o}C.

CHAPTER 4

MINERALOGICAL EXAMINATION OF THE ACCESSORY MINERALS

4.1 INTRODUCTION

Data are presented for the accessory minerals, occurring mainly in the sand size fractions (> 240 mesh), of the Lower Greensand fuller's earths and the Silurian interstratified illite/montmorillonites.

A considerable amount of information on the accessory mineralogy of the UK fuller's earths already exists in the literature and is summarised here. No attempt was made to duplicate this work but it was felt that certain aspects, relating mainly to the origin of the deposits, should be investigated in detail and the results are considered in this chapter. In contrast, the accessory minerals of the Silurian interstratified illite/montmorillonites have received very little attention, only Butler (1937) having dealt with this topic in any detail. Consequently the accessory minerals of the present samples were investigated and each species is dealt with individually.

It should be emphasised that the accessory mineral assemblage of the sand size fraction is not necessarily representative of the total sample. It was mentioned in chapter 2 that quite large amounts of aggregated clay were present in the silt size range. Difficulties were experienced in separating even coarse silt-size accessory mineral fractions free of clay and only limited data were obtained for such fractions.

Descriptions of the techniques used in the separation and examination of the accessory minerals are given in Appendix 4 (section X4.3).

4.2 ACCESSORY MINERALS OF THE LOWER GREENSAND FULLER'S EARTH SAMPLES (A1-12, 868)

4.2.1 Summary of published information

A detailed study of the accessory minerals of the fuller's earths was carried out by Newton (1937). In the light fractions (SG < 2.9) this author identified quartz, calcite, and both plagioclase and alkali feldspar ($Or_{36}Ab_{53}An_{11}$ from chemical analysis). This latter feldspar Newton termed anorthoclase although on strict compositional grounds (see, e.g., Deer, Howie and Zussmann, vol. 4, 1962) it would appear to be a sanidine. Among the heavies (SG > 2.9) Newton found, in roughly decreasing order of abundance, sphalerite, sphene, baryte, apatite, epidote, tourmaline, zircon, staurolite, biotite, hornblende, galena, pyrite, magnetite and ilmenite. The heavies were found to comprise much less than 0.1% of the original clay. The euhedral nature of some of the accessory minerals, e g. sphene, apatite, sphalerite and 'anorthoclase', led Newton to suggest that they had been precipitated from solution under the same conditions as the montmorillonite - i.e. they were of authigenic or (in the sense used by Millot, 1970) of neoformed origin. Other minerals such as tourmaline, epidote and staurolite were assumed, because of their worn appearance, to be of detrital origin. This two-fold division into minerals of authigenic and detrital origin was confirmed by Wood (1956). Hallam and Selwood (1968) also recorded the presence of an unidentified zeolite in the Surrey deposits; this was later shown to be a member of the clinoptilolite/heulandite series by Bain et al. (1971). Cowperthwaite et al. (1972) divided the accessory minerals of the fuller's earth deposits into three groups.

(i) unworn grains and crystals of calcite, glauconite, apatite and feldspar of diagenetic (or authigenic) origin

(ii) Worn grains of a variety of heavy minerals, feldspars, quartz and glauconite of detrital origin.

(iii) Unworn crystals of apatite, zircon, sphene and biotite which had been derived directly from a volcanic source.

These authors considered that arguments in favour of direct derivation from a volcanic source appeared particularly strong for minerals of this third group: zircon is never authigenic, sphene is very rare in detrital suites and chloritised biotite is unlikely to be authigenic.

Similar mineral assemblages were recorded from the fuller's earths selected for the present study but some new or particularly important features warrant further discussion.

4.2.2 Siderite

No record of the occurrence of siderite as an accessory mineral in the Lower Greensand fuller's earths exists in the literature. This is surprising as most of the heavy fractions separated from the present samples contained this mineral. Siderite, occurring as pale orange-brown rhombohedra, was especially abundant in samples A11 and 12, in the latter comprising over 5% of the total sample. The mineral is of diagenetic origin.

4.2.3 Ilmenite

Ilmenite was only a minor constituent of the heavies separated from the present samples and was concentrated in the more magnetic fractions (see section X4.3). It occurred as black, lustrous grains of sharp outline, some of which showed platy euhedral form. The fresh appearance, complete lack of any surface abrasion, and angular nature of these ilmenite grains would tend to rule out a detrital origin (but see Newton, 1937; Wood, 1956). The ilmenite could, however, be of pyroclastic origin.

4.2.4 Alkali feldspar

Alkali feldspar was found in all the present samples although it was noticeably more abundant in samples from Nutfield and Woburn. The mineral was concentrated in the fractions of SG 2.3-2.61. Under the binocular microscope the feldspar appeared clear, glassy and unaltered. Grains were of irregular platy to prismatic form and were generally angular but showed only rare crystal faces (where present these appeared to be terminal on prismatic grains). In transmitted light the grains showed refractive indices of between 1.518 and 1.527 and a low negative 2V. Grains showed no evidence of twinning or of exsolution lamellae. An X-ray diffraction trace of the 2.3-2.61 SG fraction from sample A7 showed that the feldspar was monoclinic; from the position of the $(\bar{2}01)$ and (400) spacings (Orville, 1967, p. 76) it appeared to have a composition of $Or_{56}Ab_{44}$.

Monoclinic alkali feldspars may crystallise in a high-temperature magmatic environment or form authigenically under earth surface conditions (Deer, Howie and Zussmann, vol. 4, 1962). Previous workers assumed that the alkali feldspar of these deposits formed authigenically although there appears some disagreement as to whether both feldspar and montmorillonite formed contemporaneously (Newton, 1937) or whether formation of feldspar postdated that of montmorillonite (Hallam and Selwood, 1968). The possibility that the feldspar might have had a volcanic origin does not appear to have been considered. Very little information is available on authigenic alkali feldspars. There is some doubt as to whether intermediate members of the alkali feldspar series may crystallise under earth surface conditions (Baskin, 1956). Only end members of the series were identified in a group of 40 authigenic alkali feldspars examined by this author (Na_2O contents of the K-feldspars did not exceed 0.3% and the K_2O contents of the Na-feldspars did not exceed 0.2 and 0.4% respectively). Features of these authigenic feldspars noted by

Baskin were their submicroscopic to microscopic size, fresh unaltered appearance and rhombohedral outline (adularia habit?). Baskin also found that they almost always possessed a detrital core, usually a minute and well-rounded clastic feldspar grain.

Morphological features of the present feldspar do not appear fully in accord with an authigenic origin. This mineral does occur as clear unaltered grains but these are angular (? broken, see Newton, op. cit., p. 195) and certainly do not possess the good crystal outline which would be expected if crystallisation had occurred in situ. (However Newton did find a few grains which were rhombic to rectangular in shape). On compositional grounds an igneous origin appears more likely. The apparent lack of exsolution phenomena in the feldspar grains could also be cited as evidence in favour of a high-temperature origin.

4.2.5 Zeolite

The zeolite clinoptilolite/heulandite was found to be common in the fuller's earths from Nutfield, Woburn and Baulking. At the last-named locality the zeolite also occurred in arenaceous sediments adjacent to the fuller's earth horizons (Bain et al., 1971). The zeolite was concentrated in the sand fractions of SG < 2.3 although in these it was accompanied by the bulk of the undispersed clay aggregates. X-ray powder photographs of some separated grains showed patterns almost identical to those given by Brown et al. (1969). A DTA curve of a relatively pure zeolite concentrate showed only a broad endothermic peak at $180^{o}C$; using the criteria of Alietti (1967) the zeolite would appear to be nearer clinoptilolite in composition. The zeolite occurred mainly as aggregate grains but occasionally as discrete euhedral prisms less than 100 microns long. Aggregates were of irregular shape but were generally platy: their typical surface morphology is illustrated

Fig. 4.1 Scanning electron microscope photographs of zeolite aggregate grains from sample A7.

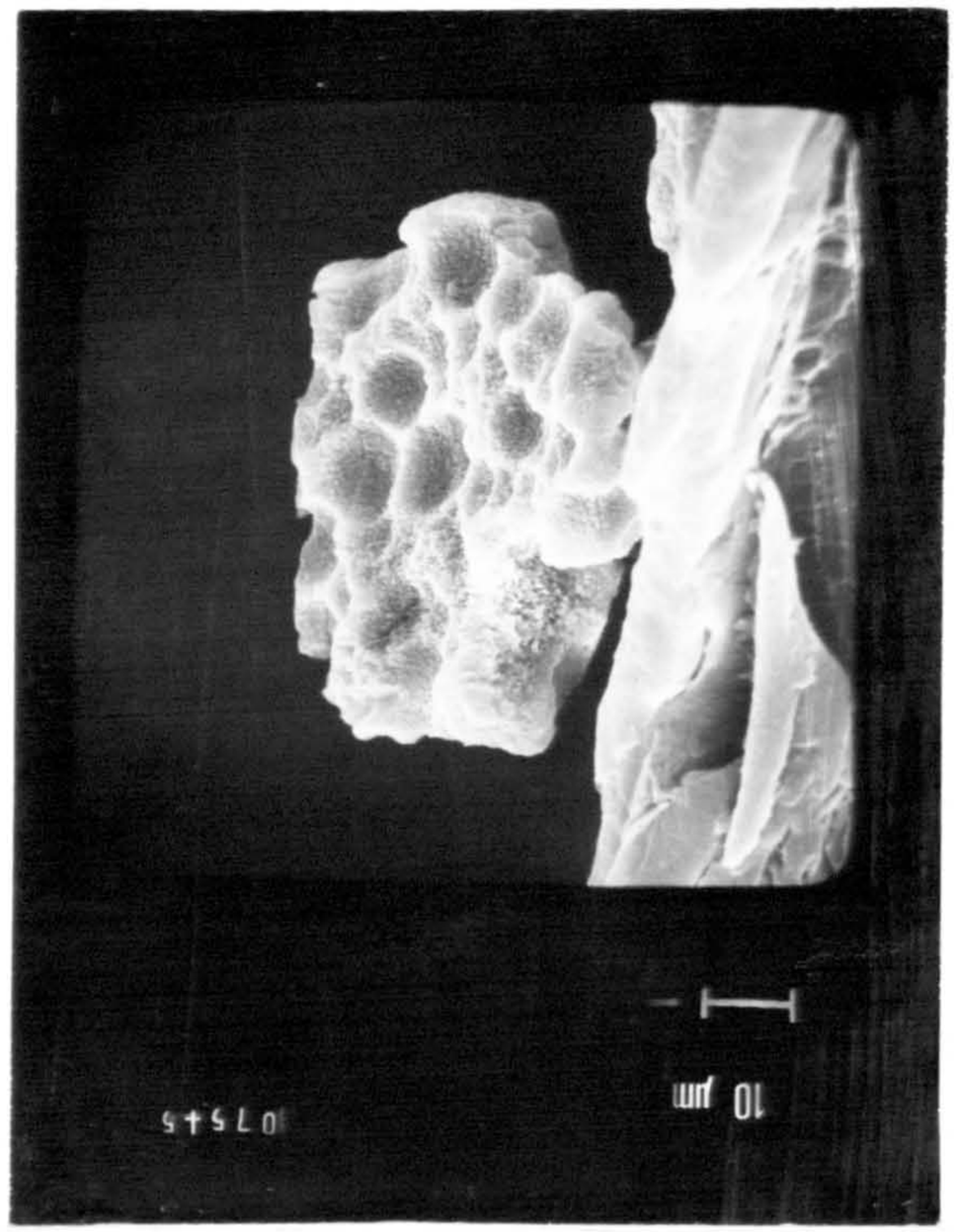
10 μm
0754S

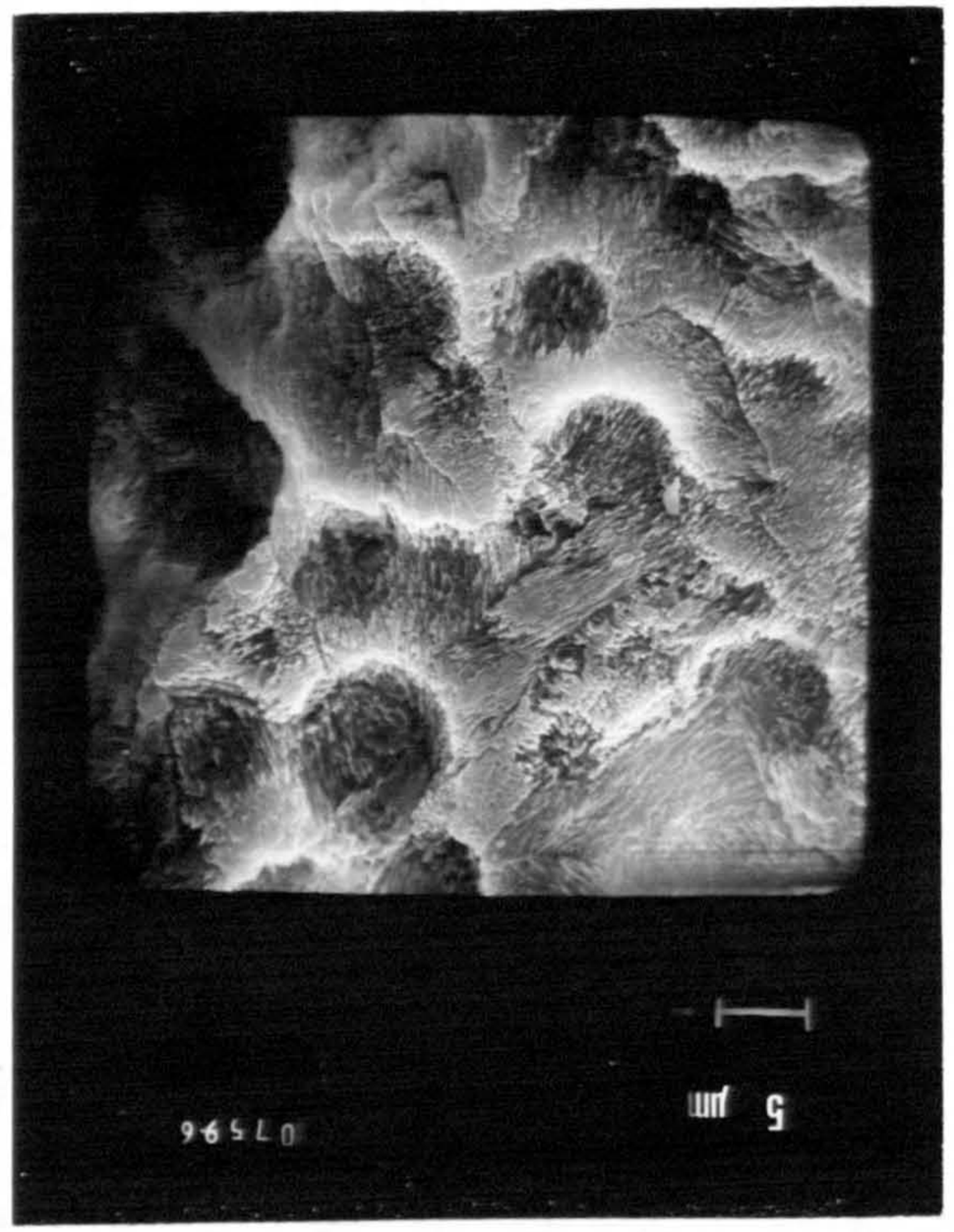
5 μm
07596

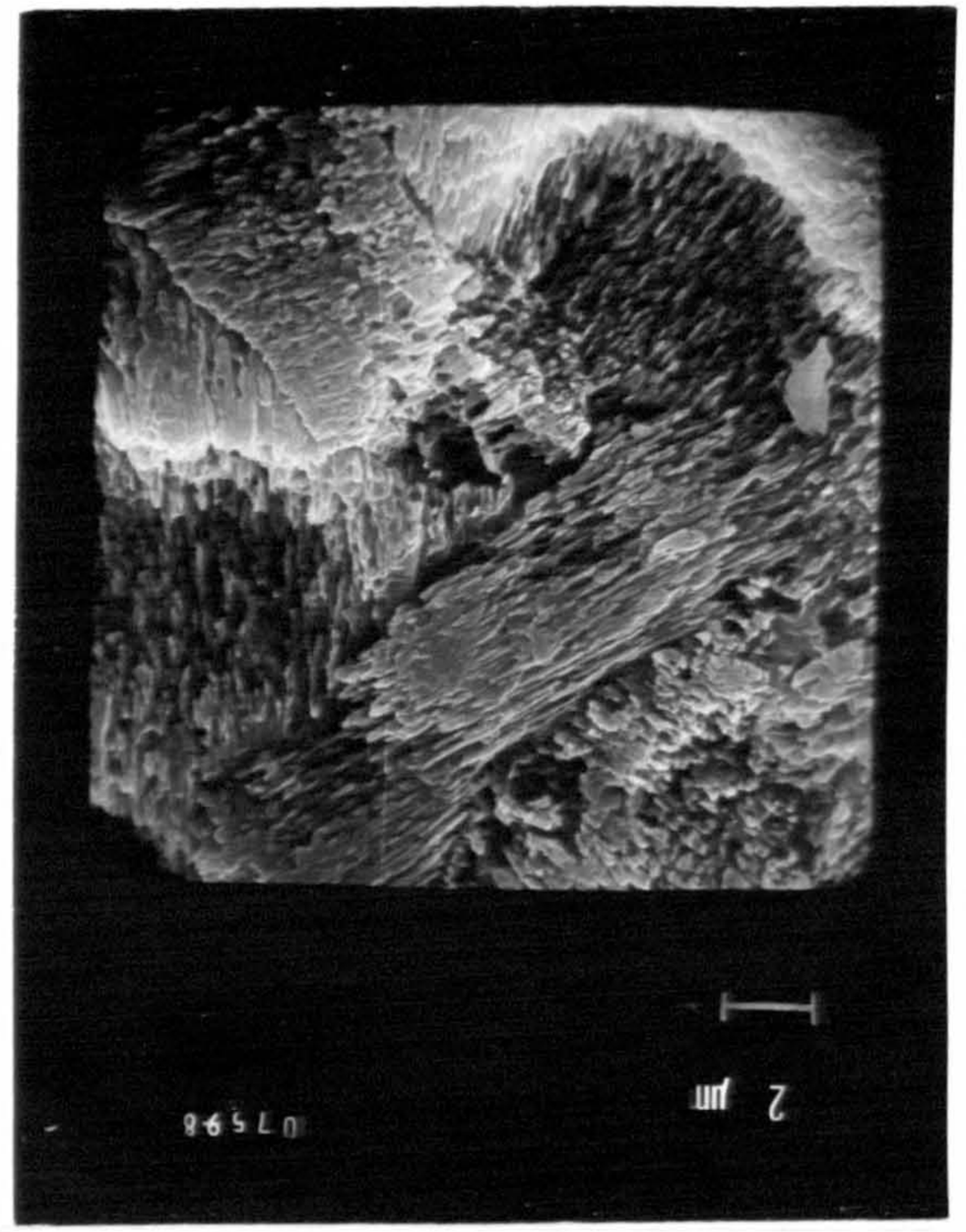
2 μm
07598

in fig. 4.1. The surface of the aggregate is pitted by ovoid depressions of somewhat variable diameter (fig. 4.1a, b). The aggregates themselves are composed of randomly oriented parallel growths of lath-shaped crystals (fig. 4.1c).

The clinoptilolite/heulandite occurring in Jurassic to Palaeocene sediments of south-east England was considered by Brown et al. (1969) to have formed authigenically, the necessary constituents perhaps being provided by the dissolution of flint, biogenic opal and carbonate and the leaching of glauconite, micas and feldspar. Poole and Kelk (1971a) suggested that the clinoptilolite/heulandite of the Baulking fuller's earth deposits formed in a similar manner. However, zeolites of this composition may also form during the diagenetic alteration of volcanic glass (Mason and Sand, 1960). It is impossible to prove conclusively whether the clinoptilolite/heulandite of the present samples is of neoformed origin or whether it is an alteration product of volcanic glass. The surface morphology of the zeolite aggregate grains might suggest that these formed as casts or moulds but the lack of symmetry in disposition of the concavities would tend to rule out any connection with an organic body. Such morphology could result from the direct replacement of vesicular volcanic glass.

4.3 ACCESSORY MINERALS OF THE SILURIAN INTERSTRATIFIED ILLITE/MONTMORILLONITE SAMPLES (B1-14)

4.3.1 Quartz

Almost invariably quartz was found to be the dominant mineral in the sand size fractions of these clays, occurring as rounded grains up to 2 mm in size. Many features of the quartz grains observed under the binocular microscope (fig. 4.2a) are in keeping with a volcanic origin. Grains displaying the high-temperature β-quartz habit (hexagonal

Fig. 4.2 (a) Quartz grains showing β-quartz habit and evidence of magmatic corrosion (oblique incident light, x 40). (b) Quartz grains showing embayments (transmitted light, x 100). (c) Linear surface features on quartz grains (transmitted light, x 300). (d) Linear surface features on quartz grains (transmitted light, x 750).

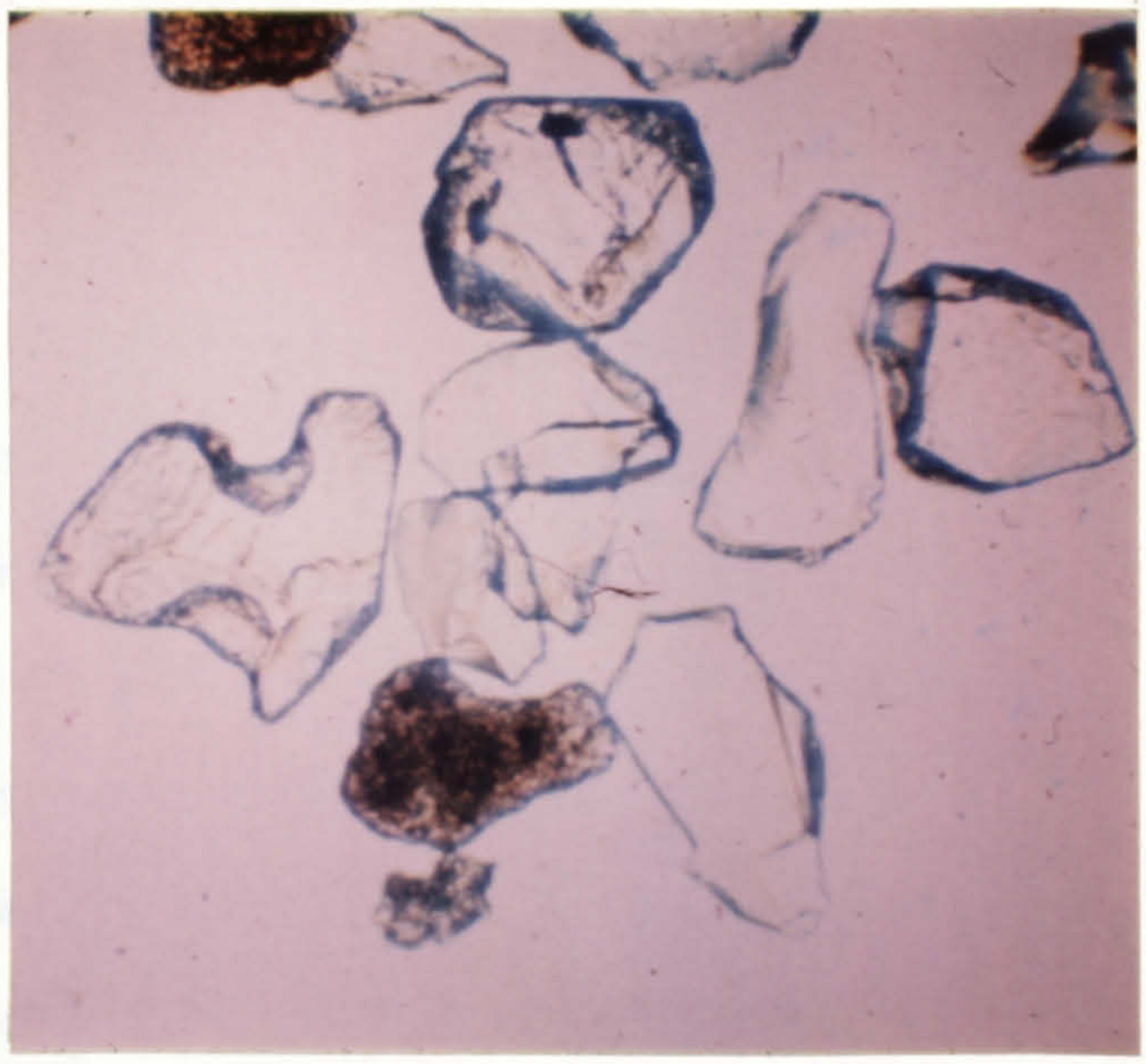

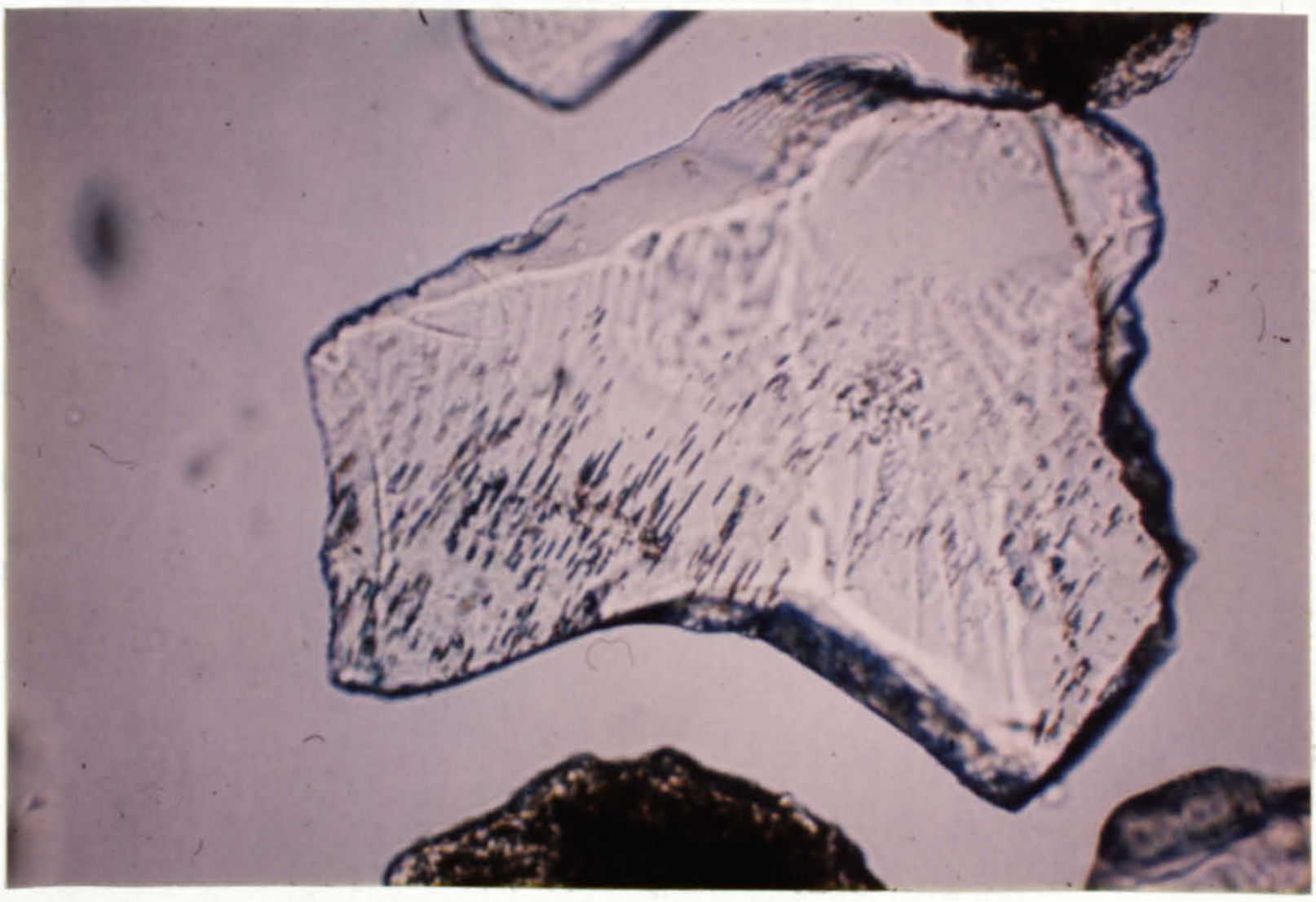

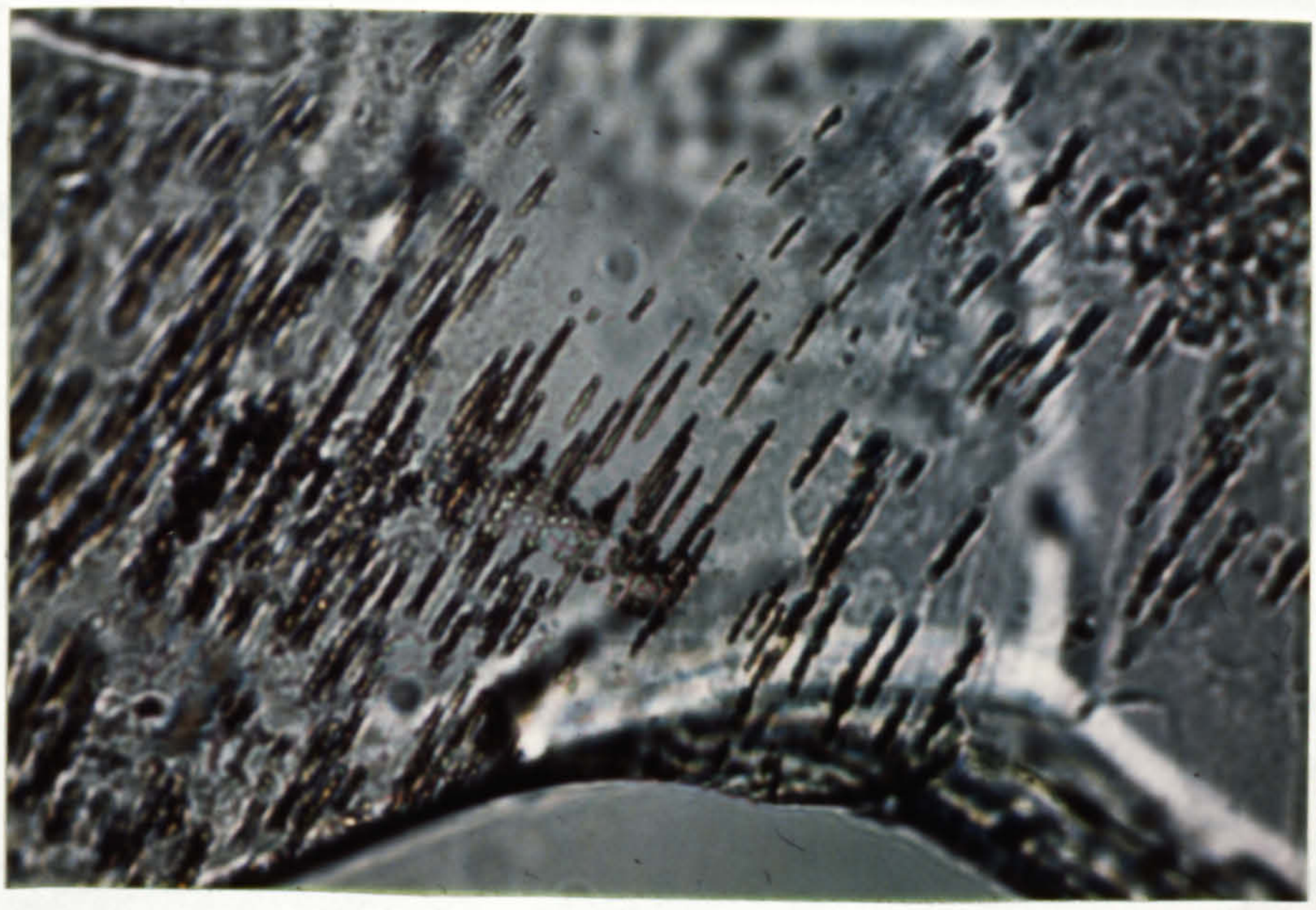

bipyramids with no prism faces) were common and some were embayed in ways reminiscent of magmatic corrosion. The quartz did not show any evidence of strain extinction under crossed polars. The presence of linear surface features on some of the grains was also noted during transmitted light examination. These features (fig. 4.2c) invariably emanated from a wedge-shaped edge or, more commonly, from a pointed intersection of surfaces. They were not continuous along the length of the grains but tended to occur in dense arrangements at one end or at either end. Under high power (fig. 4.2d) these features appeared to be made up of joined segments. A possible interpretation of these linear features is that they represent annealed glass spherule trails which formed on the quartz grains immediately after eruption as a result of their rapid rise through a cloud of fine glassy dust. If this interpretation is correct it is perhaps surprising that these features have persisted through subsequent alteration of the enclosing vitric ash to clay. Further examination of the quartz grains by electron microscopy is proposed.

4.3.2 Feldspar

Plagioclase feldspar was found to be a common accessory mineral in these clays. It was concentrated in the sand fractions of SG 2.61-2.7. X-ray diffraction examination of these suggested that the plagioclase had a composition near andesine-oligoclase (this was confirmed during subsequent optical examination). The plagioclase grains showed subhedral to anhedral outline; replacement by carbonate was common, often to the extent that only cores or corners of grains remained unaffected. After dilute acid treatment of the 2.61-2.7 SG fractions to dissolve carbonate large numbers of plagioclase grains of skeletal aspect were observed.

X-ray diffraction examination of the sand fractions of SG < 2.61

showed that feldspar was again present. However the diffraction pattern of this feldspar differed significantly from that of the andesine-oligoclase of the heavier SG fractions. The best fit of the diffraction pattern of this lighter feldspar was to that of albite. For reasons which will become apparent this identification could not be confirmed by optical means. In the < 2.61 SG fraction from sample B6 X-ray diffraction showed that the 'albite' was accompanied by a roughly equivalent amount of quartz and minor amounts of illite/montmorillonite. Under the petrological microscope this fraction was seen to consist almost exclusively of microcrystalline aggregates. Some of these aggregates appeared fresh, others showed variable degrees of cloudiness: in none were individual grains large enough for determination of any diagnostic optical data. However from X-ray evidence these aggregates must be composed of quartz and albite. (Under crossed polars the fresh aggregates appeared identical to the quartzo-feldspathic aggregates featured by Smith (1967, fig. 4) although this author considered that the feldspathic component of these aggregates was sanidine). Discrete albite was also not detected during optical examination of the equivalent SG fractions from samples B1 and B2 in spite of prior identification of this mineral by X-ray diffraction (from the diffraction traces both albite and quartz were seen to be subordinate in amount to illite/montmorillonite). Under transmitted light these fractions were seen to consist only of colourless to pale brown platy grains, clouded with dusty material, which showed low-order aggregate birefringence under crossed polars. Refractive indices of these platy grains were in the range shown by clays of the montmorillonite group. In these fractions it must be assumed that both quartz and albite are present in the clay phase. The resistance to dispersion shown by the clay aggregates (assumed because of their persistence in the sand sizes) could be due to finely particulate secondary quartz and albite acting as cementing agents (see also Bystrom, 1956;

Smith, 1967).

Plagioclase would appear to have been a constituent of the parent ash of the illite/montmorillonite deposits. The 'albite' is of later diagenetic origin, its formation perhaps being related to the alteration of the plagioclase.

4.3.3 Biotite

Biotite was identified in the sand fractions of all the illite/montmorillonites, this mineral occurring at a noticeably larger average grain size than the other minerals of the sands. Under the binocular microscope biotite was seen to occur as thin (sometimes buckled) to stout dark brown hexagonal flakes, often with somewhat rounded corners. Some flakes were broken and angular, some showed an embayed outline. Slender prismatic inclusions with hexagonal cross-section (? apatite) were frequently observed. Rare strongly green coloured irregularly-shaped flakes were also noted, these being assumed to represent biotite in an advanced state of alteration to chlorite. Biotite flakes exhibiting many of the features described are shown in fig. 4.3a. The euhedral nature and embayed outline of many of the biotite flakes is strong evidence in favour of direct derivation from an explosive volcanic source.

Biotite comprised about 5% by weight of the thickest illite/montmlrillonite horizon at Woodbury Quarry. Biotites occurring near the top of this horizon exhibited a range of specific gravities, the mineral being found in the 2.61-2.7, 2.7-2.86 and >2.86 SG fractions separated from the sands. Under the binocular microscope biotite flakes from all three SG fractions were found to be identical with respect to colour and shape and no obvious surface alteration or exfoliation were noted in flakes of the lighter SG fractions. Under transmitted light only minor differences in optical properties were shown by biotites of different SGs. Flakes of SG > 2.86 appeared reddish brown in colour and showed refractive

indices ($\gamma \simeq \beta$) of about 1.625. Biotites of SG < 2.7 were lighter in colour, some flakes giving RIs as low as 1.605. In addition these biotites showed wavy extinction, presumably due to deflection of light waves by buckled crystals, and interference figures less well defined than those of biotites of SG > 2.86 (no significant differences in 2V values being noted). X-ray diffraction examination of the biotites from the upper part of the thickest Woodbury horizon showed that they were in fact altered, those of the lighter SG fractions quite extensively. An X-ray diffraction trace of a biotite concentrate of SG 2.7-2.86 is shown in fig. 4 4 (trace 1). The two sharp peaks at 7.14 and 3.57A are due to the alteration product. It may be noted that the intensities of these two peaks relative to the first and second order biotite peaks, at 10.05 and 3.35A respectively, increased in traces of the lighter flakes and decreased in traces of biotites of greater SG. On heating at 550^{o}C for one hour intensities of the 7.14 and 3.57A peaks diminished by about half (trace 2) but these reflections were still not completely eliminated after a further hour at 600^{o}C.(trace 3). A weak 13.8A peak gradually appeared on heating (traces 2-4). On the basis of this evidence the impurity in the biotite is probably an Fe-rich chlorite or septechlorite. The latter would appear more likely from the DTA curve (trace 5). The weight loss associated with the dual endothermic peak system (450 to 700^{o}C) was 5.7% which would be equivalent to a 'septechlorite' content of approximately 50%.

Alteration of biotite to vermiculite was also observed. It was noted in section 1.5.3 that flakes of biotite were common on the surface of the shaly limestone underlying the illite/montmorillonite horizon at Shaver's End Quarry. A diffraction trace of a bulk sample of this biotite is given as trace 7 in fig. 4.4. The broad biotite peaks at 10.1 and 3.36A contrast strongly with the sharp peaks of the chloritised biotite in trace 1 of the same figure. On the trace of the

Fig. 4.3 (a) Biotite flakes showing euhedral form, occasional embayed outline and presence of ?apatite inclusions (oblique incident light, x 30). (b) Apatites, mainly stumpy euhedra with single or double terminations. Some crystals show central cavities (oblique incident light, x 40). (c) Zircon, doubly terminated prisms (oblique incident light, x 80).

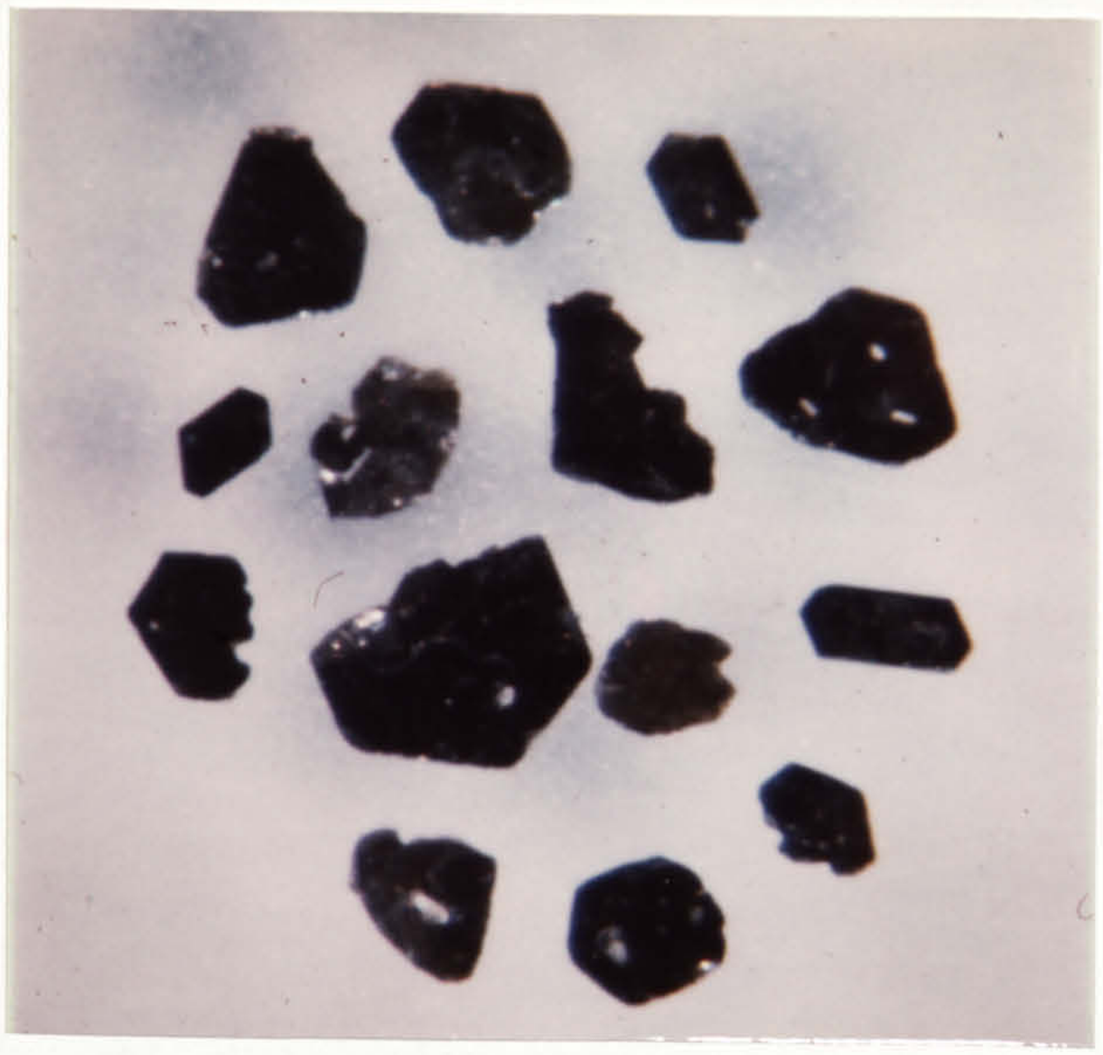

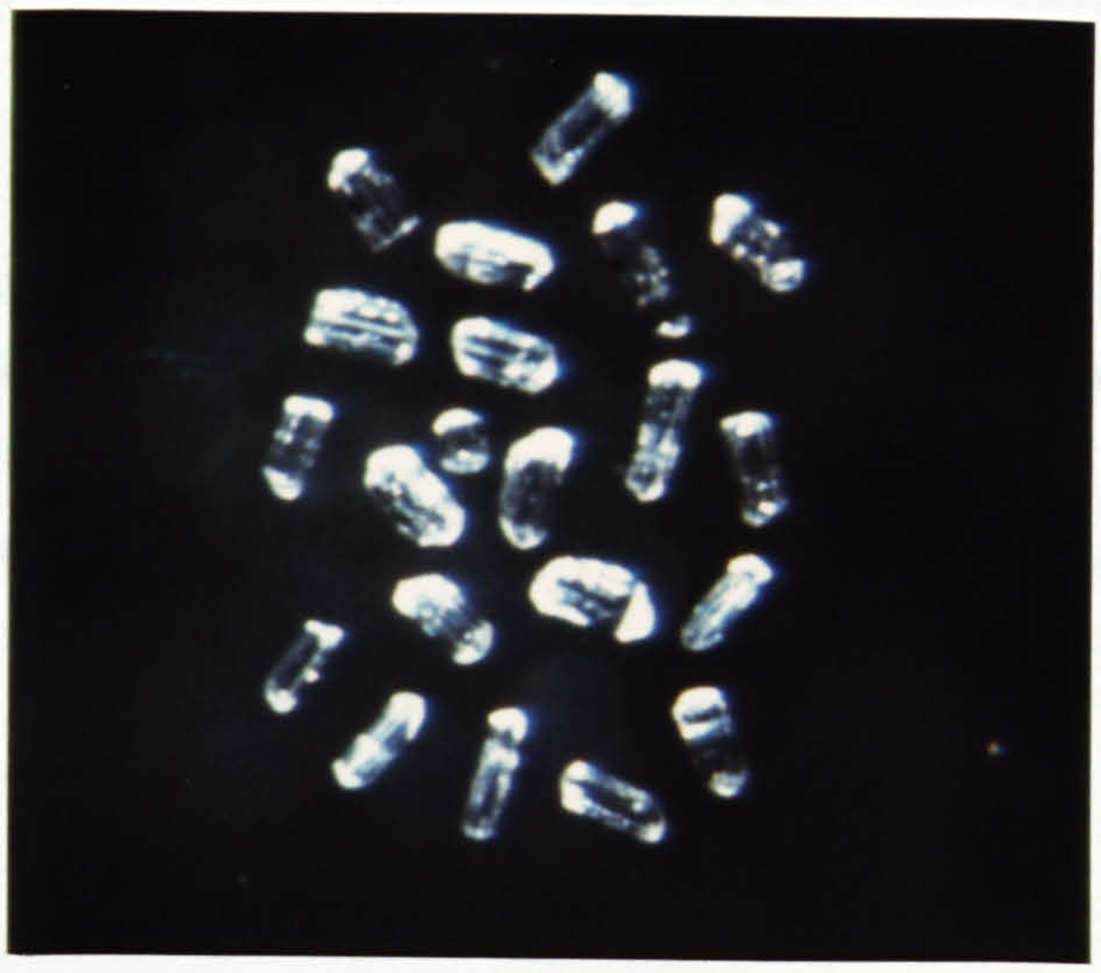

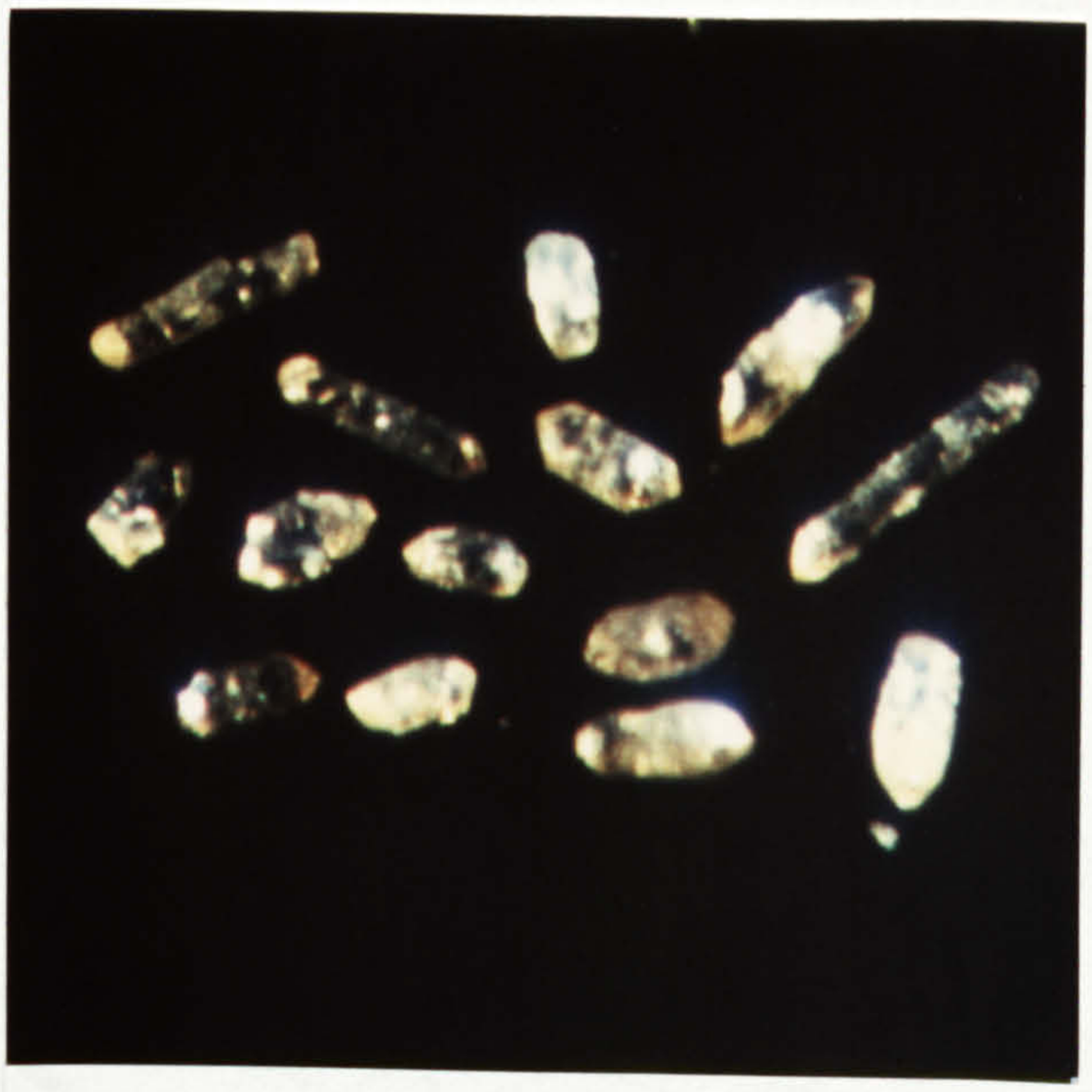

Fig. 4.4 X-ray diffraction traces of altered biotites. Traces 1-4: biotite from thickest illite/montmorillonite horizon at Woodbury quarry (trace 5, DTA curve). Traces 6-9: biotite from base of illite/montmorillonite horizon at Shavers End quarry.

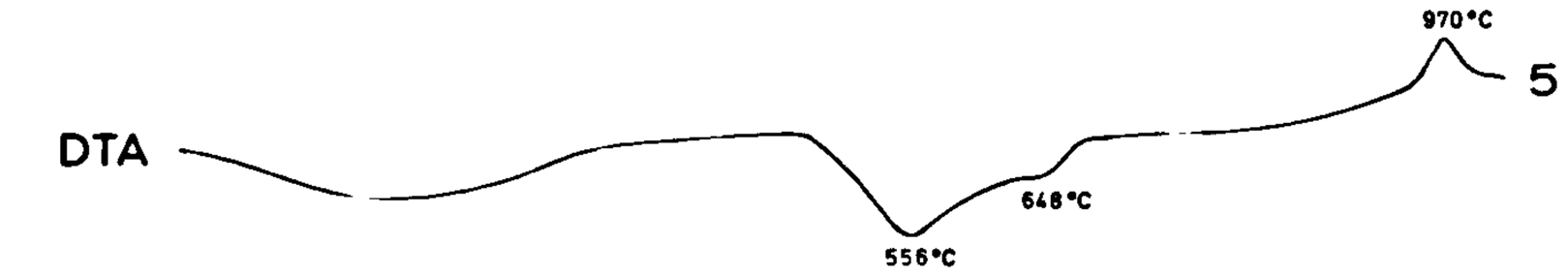
DTA
970°C
5
648°C
556°C

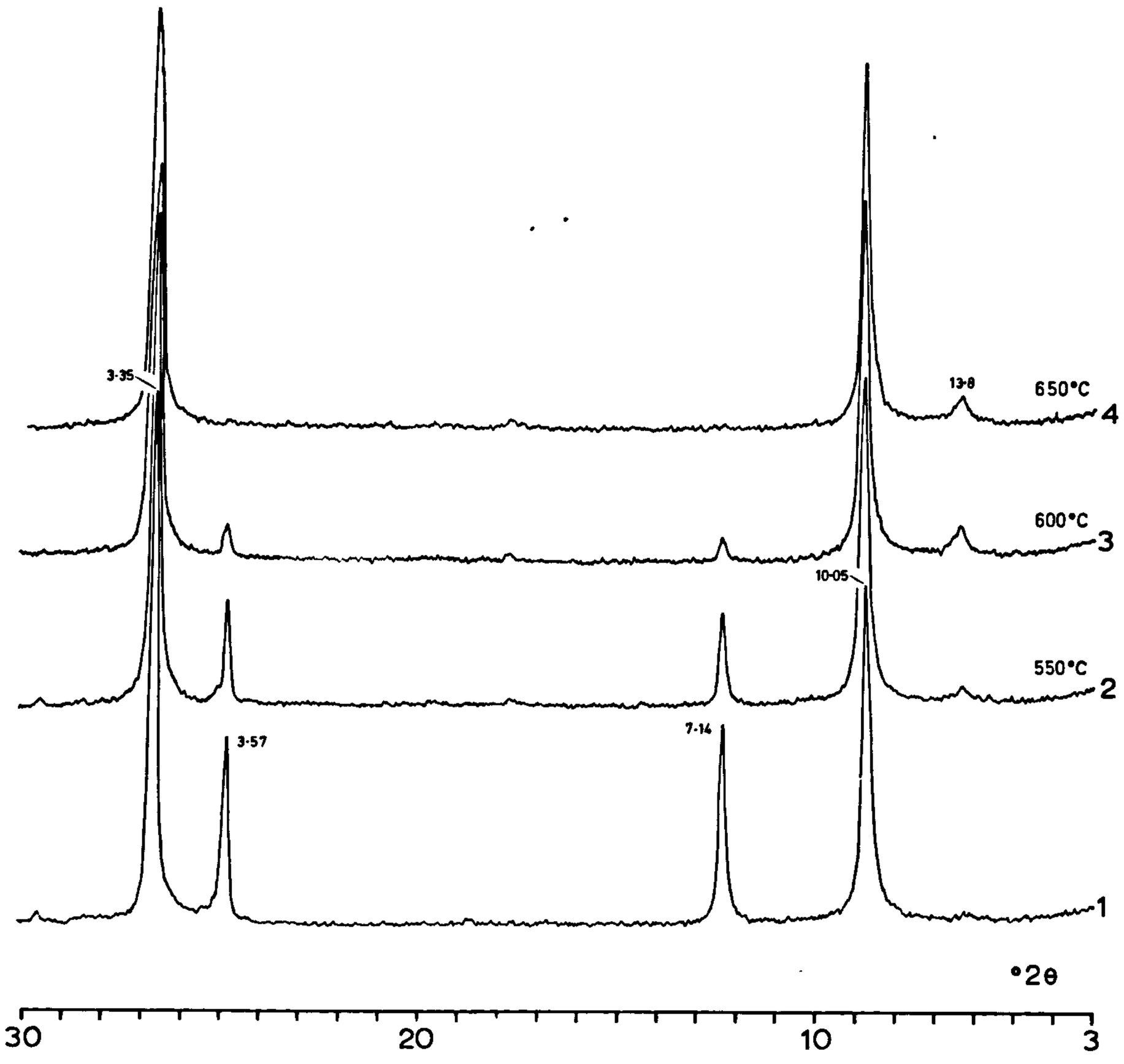
3·35
13·8
650°C
4
600°C
3
10·05
550°C
2
3·57
7·14
1
°2θ
30
20
10
3

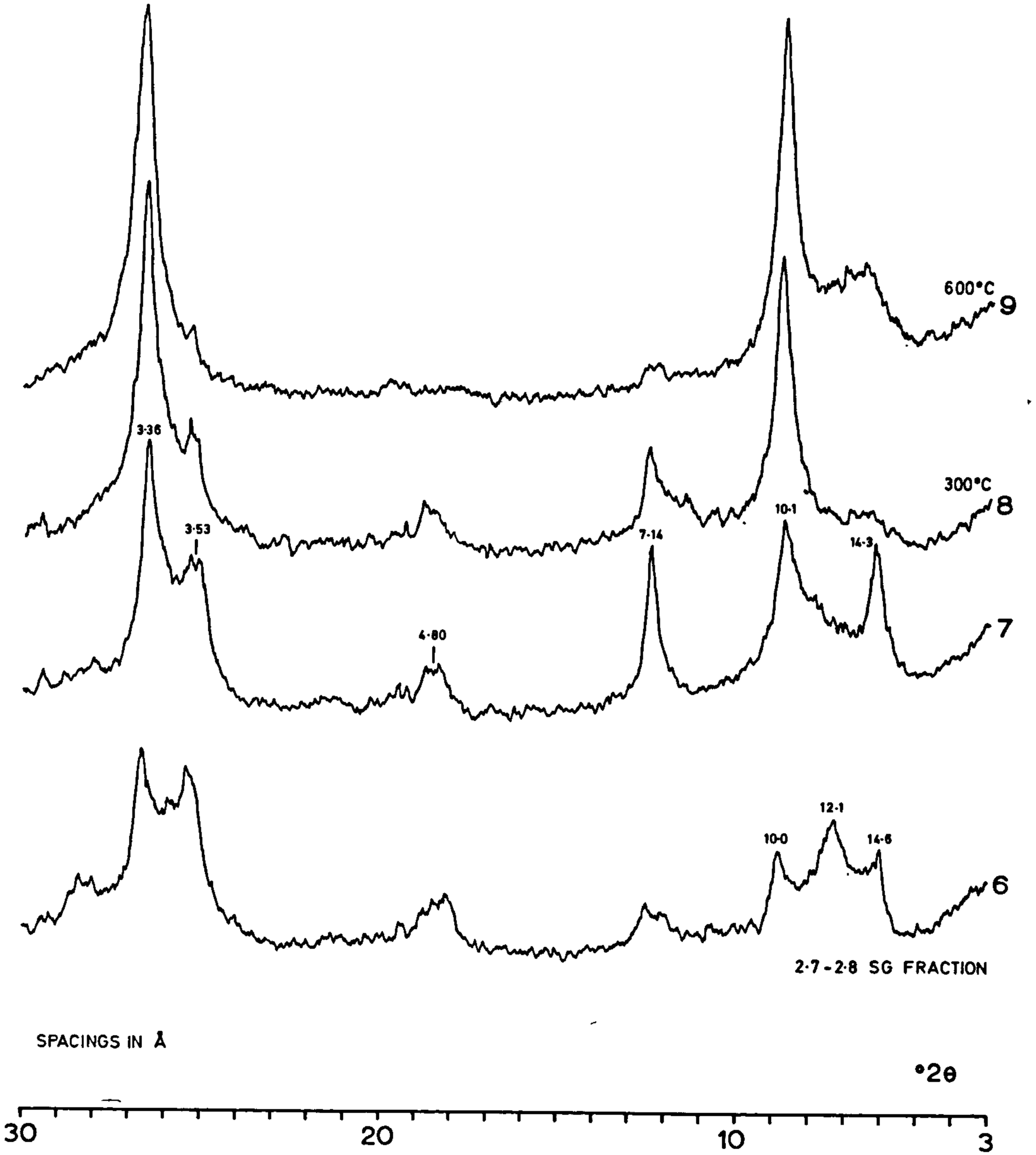
600°C
9
3·36
300°C
8
3·53
10·1
14·3
7·14
4·80
7
12·1
10·0
14·6
6
2·7-2·8 SG FRACTION
SPACINGS IN Å
°2θ
30
20
10
3

Shaver's End biotite the additional peaks at 14.3, 7.14, 4.80 and 3.53A could be due to vermiculite or chlorite. The disappearance of the 14A peak on heating to 300°C (trace 8) would suggest vermiculite; however the appearance of a broad 14A peak after further heating to 600°C (trace 9) would suggest that some chlorite is also present. A diffraction trace of biotite flakes of SG 2.7-2.86 (trace 6) showed an additional peak at 12.1A which is probably the second order reflection of a 1:1 regular biotite/vermiculite interstratification (hydrobiotite). The strata at Shaver's End show high dips. Alteration of the biotite was probably caused by solutions percolating down the plane of contact of the illite/montmorillonite horizon and the underlying limestone. Interlayer hydration of the biotite appears to have proceeded via an intermediate hydrobiotite stage.

4.3.4 Apatite

Apatite occurred in all the sand fractions, mainly as clear, stumpy euhedral prisms (elongation ratios between 2:1 and 3:1), doubly or singly terminated by a basal pinacoid. Prisms were often slightly rounded and many showed distinct cross-fractures. Occasional crystals showed overgrowths in optical continuity. Inclusions were common and could be divided into three types:

(i) Euhedral zircons, generally present near the edges of the crystals

(ii) Broad tubular cavities running the whole length of the crystal, often filled with cryptocrystalline aggregates of low birefringence and with an RI less than apatite. Some cavities did not run the whole length of the crystal but were open at one end.

(iii) Tubular elongate inclusions, similar to those described above but smaller and enclosed. These appeared to be gas- rather than liquid-filled. Ovoid inclusions also occurred.

Fig. 4.3b shows a selection of apatites some with tubular cavities.

The presence both of tubular cavities and gas-filled inclusions is strong evidence for a primary igneous origin (Wyllie et al., 1962) although overgrowths noted on some grains may signify a degree of later authigenic addition. Apatites separated from the Gaspe, Canada, illite/montmorillonites (Smith, 1967) show many similarities with those described above notably in their stout prismatic habit and the presence of cavities parallel to the c-axis.

4.3.5 Zircon

Zircon was identified in the sand fractions of all the illite/montmorillonites and occurred as pale pink to colourless doubly terminated prisms, generally less than 100 microns in size (fig. 4.3c). Opaque inclusions were sometimes noted and, very rarely, prisms were seen to be zoned. Broken prisms and anhedral grains also occurred.

Smith (1967) dealt at length with the significance of the wide range of habits shown by zircons from the Gaspe illite/montmorillonites. Zircons from the present samples showed a much smaller range of habits all of which however, using Smith's criteria, are compatible with an igneous origin.

4.3.6 Titanium minerals

The heavies from most illite/montmorillonites contained discrete grains of rutile. This mineral occurred as dark red prismatic grains usually showing markedly acicular form (in B1, 2, 4) although occasional rounded grains were noted (in B12). Irregularly shaped blue grains of anatase also occurred in some heavy fractions. Broken euhedral ilmenite was noted in the heavies from sample B5.

Secondary titanium minerals were common. Numerous white to pale blue powdery grains of somewhat sugary texture were observed in the

Fig. 4.5 (a) Cryptocrystalline aggregates of anatase, 2.86-3.3 SG fraction, B5 (oblique incident light, x 50). (b) Cryptocrystalline anatase, 2.86 SG fraction, B8 (oblique incident light, x 50). (c) Sphalerite and pyrite, the latter mineral occurring in the form of cubic crystals, some interpenetrant, and lath-shaped forms (oblique incident light, x 40). (d) Sphalerite and galena (oblique incident light, x 40).

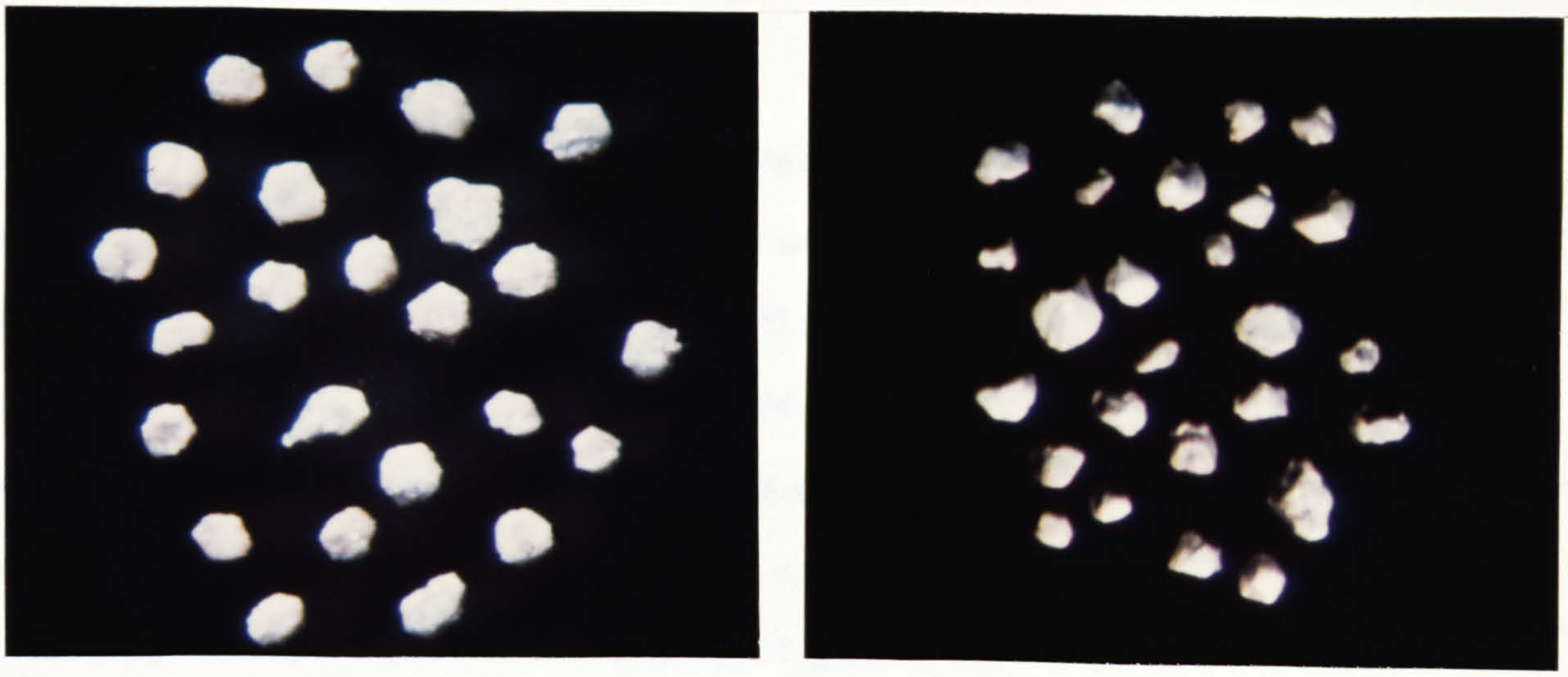

heavies from samples B10 and 12. Under transmitted light these grains were seen to consist of aggregates of fine-grained material enclosing a separate dispersed phase of very high RI. An X-ray powder photograph showed kaolinite and anatase, the latter mineral presumably being responsible for the bluish colour of these grains. In sample 85 white porcellaneous cryptocrystalline grains with ?orthorhombic/monoclinic form (fig. 4.5A) comprised a significant proportion of the 2.86-3.3 SG fraction. These grains were shown by X-ray powder photography to consist of anatase only and may be referred to as leucoxene. Anatase occurred also in sample 88 in the form of greyish to orange brown finely crystalline grains of tetragonal bipyramidal aspect. These are illustrated in fig. 4.5b.

The primary titanium minerals described above could all have been constituents of the original volcanic ash. Some of the cryptocrystalline anatase could have formed as an alteration product of ilmenite. No explanation can be advanced regarding the origin of the kaolinite/anatase grains.

Records of the occurrence of titanium minerals in other illite/montmorillonite deposits are sparse. Euhedral rutile and brookite were identified in the Gaspe deposits by Smith (1967) and Huff (1963) noted the presence of leucoxene in the Kentucky illite/montmorillonite.

4.3.7 Sulphides

Brassy greenish yellow framboidal aggregates of pyrite were common in the sand size heavies; in weathered illite/montmorillonites these aggregates often showed evidence of alteration to secondary iron oxides. Occasional lath-shaped forms were noted (fig. 4.5c), these probably resulted from fragmentation of the larger framboidal (or marcasitic) aggregates. In the heavies from the thickest Woodbury horizon fresh euhedral pyrite exhibiting cubic form and interpenetrant

twinning was common (fig. 4.5c); occasional dodecahedra also occurred.

Sphalerite, although present in the heavies from all the samples, was especially abundant in those from B6 and 7. Here it occurred as large euhedral crystals up to 200 microns in size (figs. 4.5c, d). Crystals, often twinned and in clusters, were dark smoky brown to amber in colour (even, rarely, bright orange), translucent and of resinous lustre.

Galena was common in the heavies from samples B4, 5, 6 and 7. This mineral was found as soft grey irregular masses in a carbonate matrix and also as single crystals, some showing ?modified cubic form.

A diagenetic origin for all three sulphides is indicated. Sphalerite, galena and possibly pyrite could have formed from elements present in the original volcanic ash.

4.3.8 Carbonates and sulphates

Small pink calcite fragments were noted in the light fractions of the sands from a number of illite/montmorillonites, usually those collected from horizons which contained a basal layer of pink calcite (section 1.5.2). White, massive, anhedral calcite was common in all samples and the mineral was also found as an alteration product of plagioclase feldspar (section 4.3.2).

Only minor amounts of dolomite were present in most of the clays. An exception was sample B9 where small (less than 75 microns) white to cream rhombohedra comprised the bulk of the $>$ 2.86 SG fraction.

Baryte was uncommon except in sample B8 where it occurred as white porcellaneous platy grains with irregular outline.

Gypsum was present, often as white surface efflorescences, in the weathered illite/montmorillonite horizons.

4.3.9 Others

A number of other minerals were identified in the heavies. Pink sugary grains of monazite were found in samples B1 and 2. Tourmaline was present in small amount in most samples but was especially noticeable in B1, 8, 10 and 12. This mineral occurred as light green to smoky-brown rounded prisms, often broken. Pale to deep pink anhedral garnet grains were noted in samples B1 and 5. Black octahedra of magnetite were found in B2 and 5. Rounded grains and broken prismatic fragments of green hornblende occurred in small amount in most samples. Rounded pale green epidotes were identified in B5.

The lack of crystal form shown by both monazite and garnet could be cited in support of a detrital origin although, for the latter mineral especially, this could be a result of magmatic corrosion (Smith, 1967). Tourmaline, epidote and hornblende are most likely of detrital origin.

CHAPTER 5

CHEMICAL DATA

5.1 INTRODUCTION

Following a brief review of the chemical structural relationships within the montmorillonite group, and the relevance of K-fixation studies on clays of this type to the problem of the natural formation of interstratified illite/montmorillonites, the remainder of this chapter is devoted to the presentation and discussion of a large amount of analytical data for all three groups of samples. Complete chemical analyses of four purified montmorillonites and four purified illite/montmorillonites are given together with partial analyses of some additional illite/montmorillonites. Structural formulae calculated from these analyses are presented and those for the Jurassic and Lower Greensand montmorillonites are compared with formulae given by previous workers. Results for interstratified illite/montmorillonites from UK localities are few so that, in this case, comparisons are also made with formulae presented by Hower and Mowatt (1966) who analysed similar clays from the USA and Sweden.

In view of the importance of the amount and type of exchangeable cations in interpreting differences in physico-chemical properties, individual exchangeable cations present in a selection of original samples and their respective hydrocyclone products are recorded.

Finally, trace element assemblages of most of the original montmorillonite and interstratified illite/montmorillonite samples have been determined to complete the geochemical record. In an attempt to determine the location of these elements (with regard to the mineral host) additional, but more limited, trace element data were obtained on the sand-size heavy mineral fractions from some of these clays and also on some of the purified clays themselves. Allocation of some trace elements

to a host mineral phase is, of necessity, tentative and in many instances purely speculative.

Analytical methods used are described in Appendix 5.

5.2. REVIEW OF CHEMICAL/STRUCTURAL RELATIONSHIPS WITHIN THE MONTMORILLONITE GROUP

5.2.1 General

The most widely accepted structure for montmorillonite is based upon that of pyrophyllite from which it differs only in the distribution of the constituent ions and in the superposition of the multiple layers (MacEwan, 1961). The montmorillonite structure (fig. 5.1) consists of superposed layers each containing a plane of Al, Mg ions sandwiched between two inward pointing sheets of linked SiO_4 tetrahedra. Hydroxyl ions lie in the same plane as the apical oxygens of the SiO_4 tetrahedra; these, together with the Al, Mg ions, may be regarded as forming a central octahedral sheet. For the structure to be electrically neutral either Al must occupy two-thirds of the available octahedral sites (as in pyrophyllite itself) or Mg must occupy all the octahedral sites (as in talc). Substitution in octahedral positions (divalent for trivalent cations) and in tetrahedral positions (trivalent cations for Si) results in the montmorillonite structure having a net negative charge. This negative charge is neutralised by cations present in the interlayer space, these being generally exchangeable (e.g. Na^+, Mg^{2+}, Ca^{2+}) although some may be more strongly bound or 'fixed' (e.g. K^+ - see section 5.2.3). Monovalent exchangeable cations usually have a single layer of water molecules associated with them in the interlayer space and the repeat distance along the c-axis of the montmorillonite structure is 12.6A. A double layer of water molecules is associated with divalent exchangeable cations and in this case the repeat distance is 15.4A.

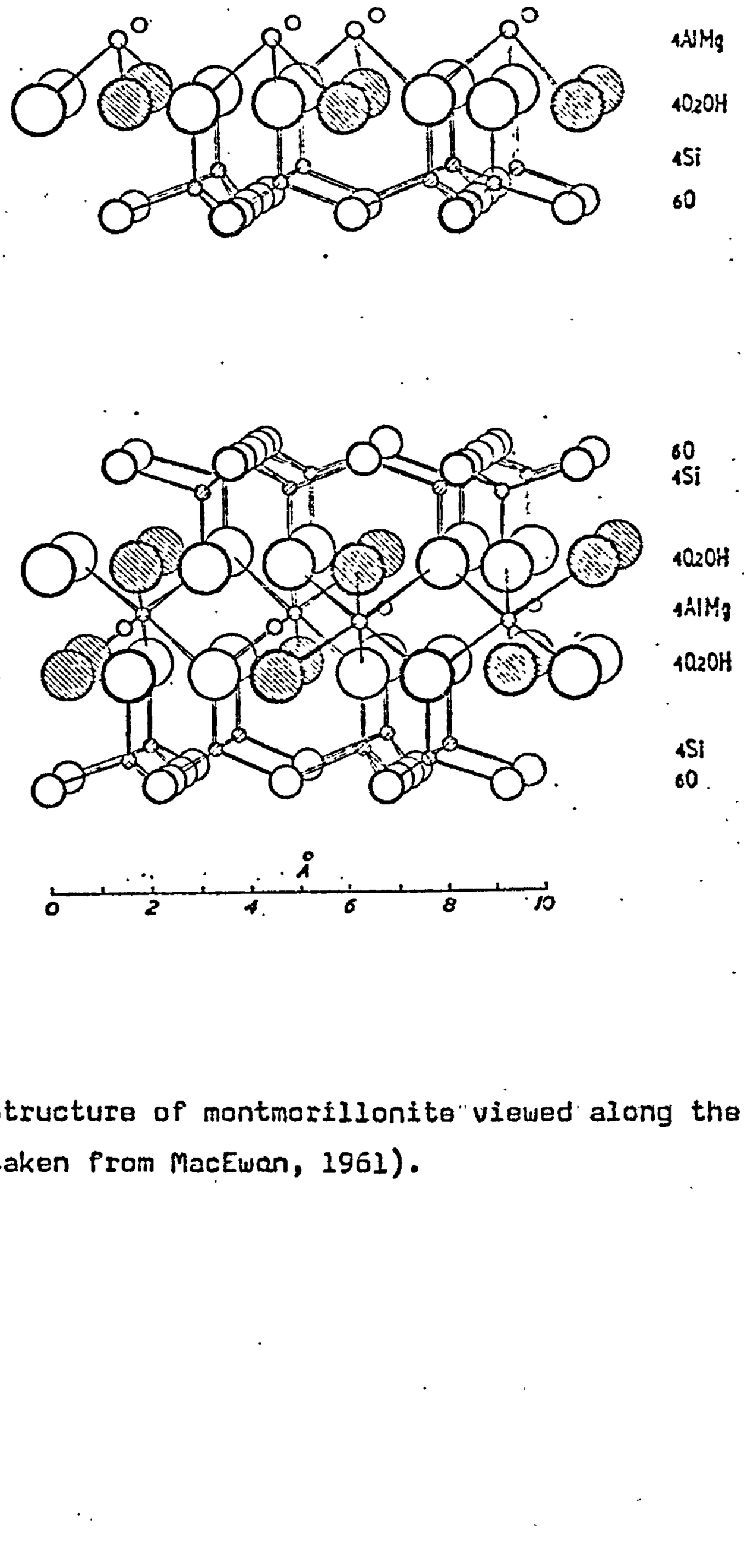

Fig. 5.1 Structure of montmorillonite viewed along the a-axis (taken from MacEwan, 1961).

A number of more or less theoretically distinct species belong to the montmorillonite group and these may be placed in one of two series depending on whether a di- or trivalent cation is the main occupant of the octahedral lattice positions. The dioctahedral series - montmorillonite s.s., beidellite, nontronite - will be discussed below. Most UK montmorillonites belong to this series. The trioctahedral series comprises stevensite and saponite (Mg-rich), hectorite (Mg, Li-rich), sauconite (Zn-rich), and a number of other varieties rich in the less common cations such as Cr, Ni, Cu, Mn, and V. This series is not discussed further as only minor occurrences of trioctahedral montmorillonites have been recorded from the UK.

5.2.2 The dioctahedral series (montmorillonite s.s., beidellite, nontronite)

Montmorillonite s.s. is the most important member of the dioctahedral series. In this mineral Al is the major occupant of the octahedral positions although replacement by Mg and Fe (II and III) invariably occurs. Some substitution of Al (and Fe III) for Si in the tetrahedral sheet is usual. When no substitution occurs in the latter the charge on the lattice is due entirely to the deficit in positive charge resulting from substitution of divalent for trivalent cations in the octahedral sheet.

An isomorphous series is considered to exist between montmorillonite and beidellite (Weaver and Pollard, 1973). In the beidellite examined by Weir and Greene-Kelly (1962), and regarded by these authors as an end-member of the series, virtually all the octahedral sites were occupied by Al and the lattice charge originated from Al for Si substitution in the tetrahedral sheet. In analyses of other Al-rich montmorillonites quoted by Weaver and Pollard (op. cit.) the sum of the octahedral cations was found to be appreciably in excess of the theoretical four per structural unit resulting in a positive charge for the octahedral

sheet. These authors could not decide, however, whether such high octahedral occupancy was real. Although the status of near end-member beidellites may be, in some instances, doubtful, the concept of the isomorphous series between this species and montmorillonite is a useful one if only to emphasise that as the beidellitic character increases so does the contribution to total lattice charge from tetrahedral substitution. (Weir and Greene-Kelly suggested that montmorillonites and beidellites should be divided at the composition at which the contributions to total lattice charge from octahedral and tetrahedral sources are equal.)

Nontronite is the third member of the dioctahedral series. In this species Fe (III) dominates the octahedral positions and may also replace Si in the tetrahedral sheet (Osthaus, 1954). Some Al is always present in tetrahedral substitution and the lattice charge originates primarily from this source. Analyses presented by Weaver and Pollard show that octahedral Fe and Al form a continuous series and a strict demarcation cannot be made between montmorillonite and nontronite.

5.2.3 Potassium fixation by montmorillonite: interstratified illite/montmorillonites.

Cations such as Na^{+}, Ca^{2+}, and Mg^{2+} present in the interlayer space of montmorillonite are readily exchangeable. In contrast K^{+}, once introduced into the interlayer space, often becomes unexchangeable or 'fixed', possibly because the cation is just the right size to fit within the pseudohexagonal holes on the montmorillonite layer surface. Fixation of some of the K in a K-exchanged montmorillonite may take place simply on air-drying the clay and up to 35% K may be rendered unexchangeable after repeated cycles of wetting then drying at 105°C (Mackenzie, 1957b). The proportion of the montmorillonite lattice charge originating in the tetrahedral layer is believed by many authors to influence the extent of K-fixation. This is because, to quote

Mackenzie (1963), 'with Al- for Si substitution the seat of the charge on the layer is nearer the surface and consequently the charge distribution along the layer surface would be expected to be markedly larger at points where this occurs than where the charge arises from, say, Mg-for-Al substitution in the centre of the layer.' However Weir (1965) found no correlation between K-fixation and tetrahedral substitution in a group of five montmorillonites but showed that the amount of K fixed by these clays increased with increase in total lattice charge.

Occupation of all the exchange sites on the surfaces of adjacent montmorillonite layers by fixed K should, theoretically, lead to a collapse of the interlayer space and result in a non-expandable 10A phase akin to illite. Complete contraction has not been observed experimentally however, Weaver and Beck (1971) noting that 'typical' montmorillonite (montmorillonite s.s.) could not be converted entirely to a 10A phase even under quite drastic laboratory conditions.

Natural interstratified illite/montmorillonites exhibit the following features

(i) a well-defined positive relationship between amounts of fixed K and non-expanding (10A) layers;

(ii) appreciably more Al in tetrahedral substitution than most montmorillonites;

(iii) much higher lattice charges than most montmorillonites;

(iv) a tendency for both the amount of Al in tetrahedral substitution and the magnitude of the lattice charge to increase in sympathy with amount of fixed K.

These features have some bearing on the origin of illite/montmorillonite clays and will be discussed in detail in Chapter 6.

Table 5.1 Chemical analyses of four purified montmorillonites.
(Analyses carried out on air-dried samples)

	A4	A7	A12	A15
SiO_2	51.85	49.24	50.79	51.27
TiO_2	0.45	0.46	0.58	0.56
Al_2O_3	16.77	13.71	14.77	18.09
Fe_2O_3	5.10	8.84	5.84	1.63
FeO	1.06	0.14	1.34	1.65
MnO	0.00	0.00	0.01	0.00
MgO	3.32	2.70	3.33	2.82
CaO	1.67	1.97	2.15	2.26
Na_2O	0.21	0.14	0.05	0.26
K_2O	0.21	0.19	0.23	0.79
H_2O+	6.13	6.49	6.19	6.78
H_2O-	13.59	15.89	14.75	13.36
P_2O_5	0.02	0.03	0.02	0.03
SO_3	0.02	0.00	0.03	0.18*
	100.40	99.80	100.08	99.68
dithionite/citrate extractable Fe_2O_3	0.31	1.17	0.55	0.14

* Sample A15 contained trace amounts of pyrite - some of the S in this mineral may be reported as SO_3.

Table 5.2. Chemical analyses of four purified interstratified illite/montmorillonites. (Analyses carried out on air-dried samples).

	B1	B4	B7	B8
SiO_2	50.40	50.84	51.66	51.20
TiO_2	0.23	0.09	0.37	0.16
Al_2O_3	24.49	23.48	23.66	24.39
Fe_2O_3	2.44	1.69	0.29	1.82
FeO	0.39	0.31	0.75	0.46
MnO	0.00	0.00	0.00	0.00
MgO	2.68	3.33	3.70	3.23
CaO	0.83	0.93	0.65	0.64
Na_2O	0.03	0.03	0.08	0.06
K_2O	6.29	5.77	5.86	6.90
H_2O+	5.75	5.72	5.62	5.35
H_2O-	6.36	7.69	6.96	5.60
P_2O_5	0.00	0.00	0.03	0.01
SO_3	0.00	0.00	0.16*	0.12
	99.89	99.88	99.79	99.94
dithionite/citrate extractable Fe_2O_3	0.24	0.10	0.00	0.33

* Sample B7 contains trace amounts of pyrite and sphalerite - some of the S in this mineral may be reported as SO_3

Table 5.3. Partial chemical analyses of some additional purified inter-stratified illite/montmorillonites. (Analyses carried out on air-dried samples).

	B9	B10	B12	B15
TiO_2 *1	nd	nd	nd	3.9
Fe_2O_3 *2	nd	1.26	2.30	5.93
MgO	nd	2.73	2.82	3.37
CaO	nd	1.94	2.82	2.20
Na_2O	nd	0.05	0.09	0.03
K_2O	6.09	5.22	2.23	3.93
H_2O-	5.12	4.80	8.94	5.26
P_2O_5	nd	0.01	0.01	nd

*1 by XRF

*2 total iron as Fe_2O_3

5.3 CALCULATION OF STRUCTURAL FORMULAE

5.3.1 General

Calculation of structural formulae for both montmorillonites and interstratified illite/montmorillonites followed the method of Mackenzie (1960). The original analyses (tables 5.1 and 5.2) were corrected, where necessary, for feldspar, quartz, gypsum, pyrite, apatite, free iron oxides, Ti-minerals and 'excess water', and an allowance was also made for Mg in exchange positions. Some of the mineral impurities were detected by X-ray diffraction or DTA; the presence of others was suspected from a careful perusal of the analysis itself (as illustrated in Mackenzie, op. cit.). Other corrections were less straightforward and are discussed in some detail below.

5.3.2 Source of Ti in the analysed clay products

Some TiO_2 is usually present in analyses of purified montmorillonite and related clays and there is often doubt as to whether Ti occurs as a component of the clay lattice or in discrete mineral impurities such as anatase, ilmenite etc. Generally Ti is omitted in structural formula calculations for montmorillonites and interstratified illite/montmorillonites (Osthaus, 1955; Mackenzie, 1960; Hower and Mowatt, 1966; Weaver and Pollard, 1973). In layer silicates such as biotite, where TiO_2 contents of 3% or more are common, Ti is assumed to occupy octahedral sites. According to some authors (e.g. Deer, Howie and Zussmann, vol. 3, 1962) this element may also replace Si in small amounts although Hartman (1969) has reasoned that in silicates Ti generally prefers octahedral to tetrahedral co-ordination. Dolcater et al. (1970) subjected a number of layer silicates to a selective dissolution technique (using hydrofluotitanic acid) in order to determine the relative amounts of Ti

in isomorphous substitution in the silicate mineral and in discrete accessory minerals. In the montmorillonites examined these authors concluded that a larger proportion of Ti was present in substituted form. In calculating the structural formulae of a number of illites, Gaudette et al. (1966) apportioned quite large amounts of Ti to the octahedral sheet of the clays. However one of the clay samples was subsequently examined by Dolcater et al. (op. cit.) who found that most of the Ti was, in fact, present in rutile. In their survey of interstratified illite/montmorillonites Hower and Mowatt (1966) analysed a number of different size fractions from selected clays and noted a rapid decrease in TiO_2 content with decrease in particle size of the clay fractions. According to these authors this suggested that Ti occurred as a discrete phase.

Although much TiO_2 recorded in clay analyses may thus, on closer inspection, be assigned to a Ti-bearing mineral impurity, there is also evidence that the element may occur in octahedral lattice positions in the clay. The present purified montmorillonites and interstratified illite/montmorillonites contain up to 0.58 and 0.37% TiO_2 respectively. In preliminary structural formulae calculations from the analyses recorded in tables 5.1 and 5.2 it was found that if all the Ti was assigned to octahedral positions it was often impossible to achieve a satisfactory charge balance between lattice and exchangeable cations. When this element was omitted from the calculations a better agreement was obtained and also the total number of cations in octahedral positions became closer to the theoretical 4.00/unit cell. On these grounds alone the final structural formulae recorded in tables 5.4 and 5.6 were calculated on the assumption that Ti was not a lattice constituent. Discrete Ti-minerals were not detected mineralogically in any of the analysed clay products although there is much indirect evidence for their presence. Sphene, anatase and ilmenite have been identified in the sand and coarser silt size fractions of the Lower Greensand montmorillonites (Newton, 1937; Wood, 1956; also

this study) and these minerals may also occur in the finer silt and coarse clay sizes. It was shown in section 4.3.6 that anatase, rutile and ilmenite are present in the sand fractions of the Silurian illite/montmorillonites. Anatase occurs as fairly soft cryptocrystalline aggregates and in this form may well extend downwards into the coarse clay sizes. (That anatase may be common in the fine silt to clay size range is illustrated by the X-ray diffraction trace of the hydrocyclone overflow product from B15 (fig. 3.4). This product contained 3.9% TiO_2 however.)

5.3.3 Corrections for free iron oxides

Free Fe_2O_3 was determined by the sodium dithionite/citrate method of Mehra and Jackson (1960). Figures for free Fe_2O_3 were subtracted from total Fe_2O_3 figures prior to calculation of structural formulae for the eight analysed clay products.

Mehra and Jackson showed that fine-grained crystalline iron oxides and hydroxides are dissolved both quickly and efficiently by the dithionite/citrate technique. The hydrocyclone overflow product from B15 was shown to contain about 5% goethite by simultaneous TG/DTA. Most, if not all, of the Fe present in the goethite was removed by a single dithionite/citrate leach (table 5.7). The small quantity of additional Fe removed by a second leach (see table 5.7) could have resulted from some inefficiency in the first leach or, alternatively, from attack on the illite/montmorillonite clay lattice. Mehra and Jackson considered that the near neutral conditions (pH 7.2) under which the dithionite/citrate leach was carried out ensured that only negligible amounts of lattice Fe were removed from minerals of the montmorillonite group, quoting a loss of 0.5% Fe_2O_3 for nontronite when subjected to this procedure. However work by Ritchie et al. (1969), and the limited results recorded in table 5.7, would suggest that significant amounts of lattice Fe are in fact removed during dithionite/citrate treatment of montmorillonites. In table 5.7 the figures for the

amount of Fe_2O_3 removed from sample A7 and hydrocyclone products following a single dithionite/citrate leach could signify either that the amount of free Fe_2O_3 increases with decrease in particle size of the clay product or thatthe finer, less aggregated, clay is more susceptible to lattice attack. Results from a second leach favour the latter alternative.

The dithionite/citrate extractable Fe_2O_3 figures recorded in tables 5.1 and 5.2 therefore contain an unknown contribution from lattice Fe. For montmorillonite samples A4, 12 and 15, and also illite/montmorillonites B1, 4, and 8, this is small and subtraction of the whole of the dithionite/citrate extractable Fe_2O_3 figures from the total Fe_2O_3 figures does not seriously affect the validity of the eventual structural formulae. However for A7 this operation is almost certainly responsible for the low octahedral cation total (table 5.4) as the dithionite/citrate extractable Fe_2O_3 figure contains an appreciable contribution from lattice Fe.

Dithionite/citrate leaches were carried out on samples A8 (pale blue in colour) and A9 (pale yellow) order to establish whether free iron oxides were responsible for the colour difference (the two clays are closely associated in the field). The data in table 5.7 suggest that this hypothesis is correct.

5.3.4 Corrections for 'excess water'

'Excess water', i.e. the proportion of the water loss above 105°C (H_2O^+) not attributable to dehydroxylation, was calculated by Mackenzie's (1957) method. In montmorillonites and related clays the excess water is usually equated with the water of hydration of divalent exchangeable cations. The analysed montmorillonites gave excess water figures ranging from 2.10 to 2.90% but these showed no correlation with total, or relative proportions of, exchangeable Ca and Mg. For the four interstratified illite/montmorillonites analysed the amount of excess water decreased from 1.50 to 1.10% as the montmorillonite component (and total

exchange capacity) decreased. Extrapolation of this data strongly suggested that excess water would still be present in the theoretical illite end-member of the series. This is in agreement with observations made by Hower and Mowatt (1966) who suggested that the excess water noted in their illite end-member was present as neutral molecules trapped in non-expanding layers. In view of the aggregated nature of most of these clays (both montmorillonites and illite/montmorillonites) it could not be assumed that drying at 105°C expelled all the interlaminar water (see also section 3.2.2.1). Therefore it is not surprising that water in excess of that resulting from dehydroxylation and dehydration of exchangeable cations is present in the H_2O^+ figure.

5.4. DISCUSSION OF STRUCTURAL FORMULAE

5.4.1 Montmorillonites

Structural formulae of the four analysed montmorillonites are given in table 5.4. All the montmorillonites show low Al for Si substitution in the tetrahedral layer and are consequently montmorillonites s.s. Rather high lattice charges are shown but as there is good agreement between CEC calculated from lattice charge and amount of exchangeable cations there is no reason to question their validity. The discrepancy between lattice charge CEC and methylene blue CEC will be discussed in section 7.2.2.

As sample A4 comes from a new deposit no analyses are available for comparison in the literature. A sample from the same locality as A7 (Woburn, Bedfordshire) has been analysed by Mackenzie (1960). The structural formula of this sample (table 5.5, column 1) shows higher tetrahedral substitution but a larger proportion of octahedral Mg which together with the high octahedral cation total accounts for the lower

Table 5.4 Structural formulae and charge distribution for the analysed montmorillonites (on $O_{20}(OH)_4$ basis).

		A4	A7	A12	A15
tetrahedral	Si	7.78	7.84	7.86	7.77
	Al	0.22	0.16	0.14	0.23
sum		8.00	8.00	8.00	8.00
octahedral	Al	2.74	2.42	2.55	3.04
	Fe III	0.54	0.94	0.61	0.18
	Fe II	0.13	0.02	0.17	0.20
	Mg	0.60	0.60	0.71	0.60
sum		4.01	3.98	4.04	4.02
total lattice charge		-0.92	-0.84	-0.90	-0.97
% charge originating in tetrahedral layer		24	19	16	24
exchangeable	Ca	0.26	0.34	0.35	0.38
	Mg	0.15	0.07	0.07	0.09
	Na	0.06	0.01	0.01	0.01
	K	0.04	0.02	0.05	0.04
total interlayer charge		+0.92	+0.85	+0.90	+0.99
CEC from lattice charge (meq/100g)		122	112	120	129
total exchangeable cations (meq/100g)		119	112	117	130
methylene blue CEC (meq/100g)		95	91	91	88

Table 5.5. Published structural formulae for UK montmorillonites. On $O_{20}(OH)_4$ basis.

		1	2	3	4	5	6	7	8
tetrahedral	Si	7.77	7.97	7.80	7.89	7.80	7.70	7.85	7.78
	Al	0.16	0.03	0.20	0.11	0.12	0.30	0.15	0.22
	(Fe)	0.07							
sum		8.00	8.00	8.00	8.00	8.00	8.00	8.00	8.00
octahedral	Al	2.60	2.51	2.55	2.55	2.96	2.74	2.51	3.02
	Fe III	0.72	0.52	0.50	0.55	0.66	0.60	0.74	0.40
	Fe II	0.05	0.21	0.12	0.17			0.03	
sum		4.10	3.99	3.99	4.00	4.46	4.14	4.06	4.06
total lattice charge	−	0.70	1.02	1.17	1.01	*1	*1	0.78	*1
total interlayer charge	+	0.71	0.98	1.14	1.02	*2	*2	0.79	*2

*1 could not be calculated due to unknown oxidation state of lattice Fe

*2 uncertain values given in original data

1. Montmorillonite, Woburn, Bedfordshire (Mackenzie, 1960). < 2 micron fraction. 1% quartz, 2.3% free iron oxides, 0.2% feldspar, 0.1% anatase subtracted from original analysis.

2.4. Montmorillonites, Nutfield, Surrey (Brammell and Leech, 1940). < 5 micron fractions. Up to 20% impurities present in original analyses.

5, 6. Montmorillonites, Nutfield, Surrey (Kerr et al., 1950). About 20 and 10% impurities subtracted from respective original analyses.

7. Montmorillonite, Redhill, Surrey (Weir, 1965). < 0.2 micron fraction.

8. Montmorillonite, Combe Hay, Somerset (Kerr et al., 1950). About 6% impurities subtracted from original analyses.

Table 5.6. Structural formulae and charge distribution for the analysed interstratified illite/montmorillonites (on $O_{20}(OH)_4$ basis)

		B1	B4	B7	B8
tetrahedral	Si	7.12	7.22	7.29	7.16
	Al	0.88	0.78	0.71	0.84
sum		8.00	8.00	8.00	8.00
octahedral	Al	3.19	3.14	3.22	3.17
	Fe III	0.23	0.17	0.03	0.16
	Fe II	0.05	0.04	0.08	0.05
	Mg	0.55	0.69	0.71	0.66
sum		4.02	4.04	4.04	4.04
total lattice charge		-1.42	-1.39	-1.38	-1.43
% charge originating in tetrahedral layer		62	56	51	59
interlayer (fixed)	K	1.12	1.03	1.03	1.22
exchangeable	Ca	0.13	0.14	0.10	0.08
	Mg	0.02	0.02	0.07	0.02
	Na	0.01	0.01	0.01	0.01
	K	0.01	0.02	0.03	0.01
total interlayer charge		+1.44	+1.38	+1.41	+1.44
CEC from lattice charge (meq/100g)		39	47	45	27
total exchangeable cations (meq/100g)		41	44	48	27
methylene blue CEC (meq/100g)		41	46	44	31

Table 5.7. Removal of iron oxides from selected samples by sodium dithionite/citrate

SAMPLE	% Fe_2O_3 removed 1st treatment	2nd treatment
Nontronite, Manito, Washington (30% Fe_2O_3)	1.66	0.71
A7 orig	1.02	0.29
u/f	0.88	0.18
o/f	1.17	0.34
A8 orig	0.49	nd
A9 orig	0.97	nd
B15 o/f	3.53	0.23

orig = original sample
o/f = hydrocyclone overflow product
u/f = hydrocyclone underflow product

nd = not determined

lattice charge when compared with A7. Both the present structural formula and that of Mackenzie for the Woburn clay are in agreement with respect to the large amount of octahedral Fe (III). Mackenzie also found, using the Osthaus (1954) acid digestion technique, that this montmorillonite contained significant amounts of tetrahedral Fe.

The structural formula of A12 is closely similar to the formulae given by Brammall and Leech (1940) for montmorillonites from Nutfield, Surrey (table 5.5, columns 2-4). Differences are apparent between these structural formulae and those given by Kerr et al. (1950) for montmorillonites from the same locality (table 5.5, columns 5, 6), mainly with respect to Al (both tetrahedral and octahedral) and Mg. The high octahedral cation totals shown by the clays analysed by Kerr et al. cast doubts on the validity of these formulae however. Structural formulae of A15 and the montmorillonite from the same locality, Combe Hay, Somerset, analysed by Kerr et al. (table 5.5, column 8) are virtually identical.

If the structural formulae of the montmorillonites from Nutfield presented by Kerr et al. are disregarded, both present and published analyses of the Lower Greensand montmorillonites are broadly similar. Compared with most of the montmorillonites surveyed by Schultz (1969) the Lower Greensand montmorillonites appear unusual in showing both low Al (< 2.80) and high total Fe (> 0.60) in the octahedral layer. This combination only appeared in a small group of montmorillonites which Schultz noted also exhibited non-ideal (abnormal) thermal dehydroxylation behaviour. The abnormal thermal behaviour of the Lower Greensand montmorillonites has already been mentioned (section 3.2.2.2).

5.4.2 Interstratified illite/montmorillonites

Structural formulae of the interstratified illite/montmorillonites are given in table 5.6. They differ from the structural formulae of the montmorillonites on three counts, viz:

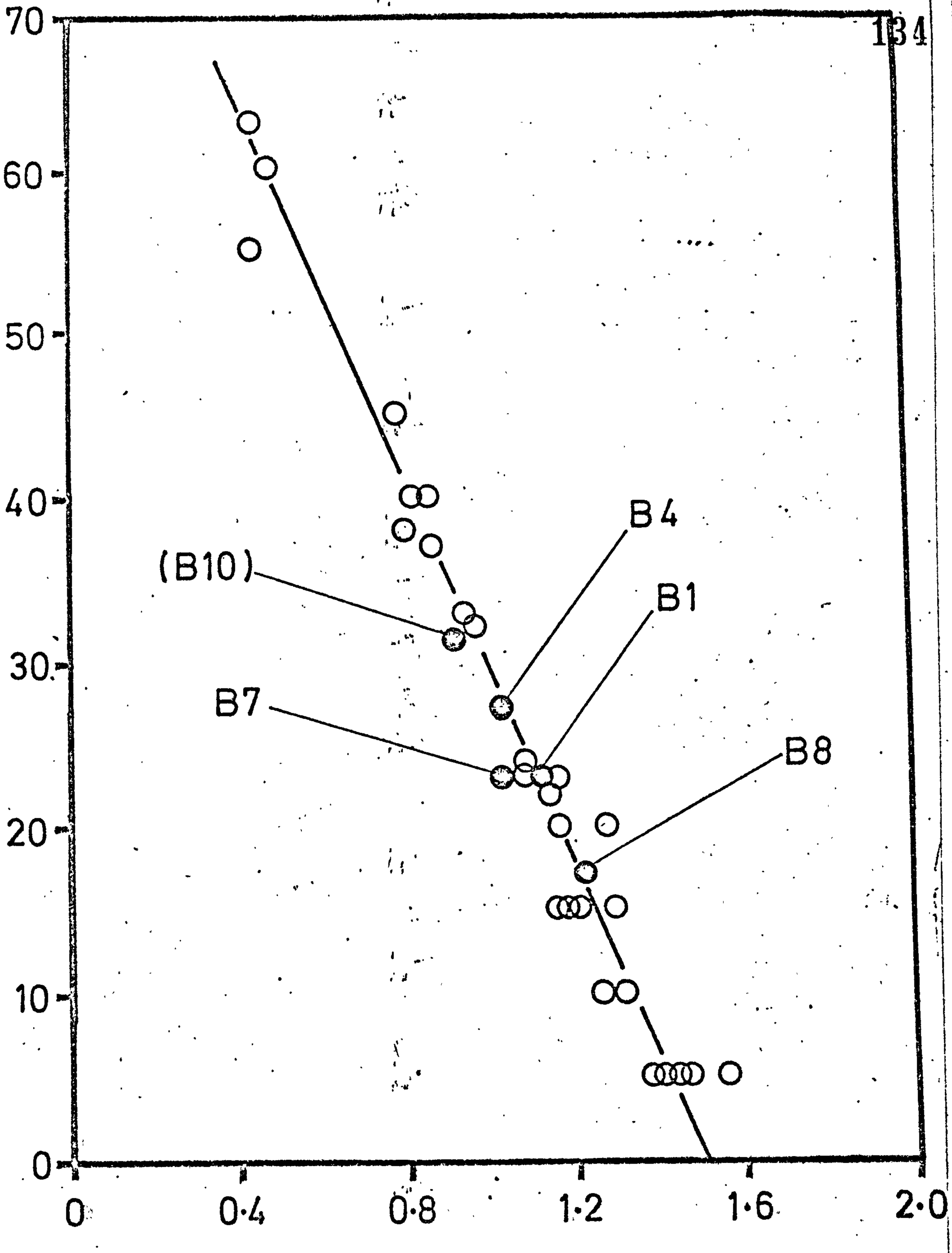

Fig. 5.2 Plot of fixed K v. % montmorillonite interlayers for present illite/montmorillonites and also those analysed by Hower and Mowatt (1966).

1. Greater Al for Si substitution in the tetrahedral sheet

2. Their much higher lattice charges (mainly a consequence of 1)

3. The presence of large amounts of unexchangeable K.

Between 51 and 62% of the total lattice charge originates in the tetrahedral sheet. For samples B8, 1 and 4 (17, 23 and 27% montmorillonite layers respectively) the amount of fixed K decreases as the amount of montmorillonite interlayering increases. These three samples plot well on the regression line of fixed K v. amount of expanding (montmorillonite) layers given by Hower and Mowatt (1966), fig. 7, and illustrated here as fig. 5.2. Sample B7 shows a slightly low fixed K content in relation to the amount of montmorillonite interlayering. Agreement between lattice and interlayer charge for this sample is not quite so good as for the other three and an error in the original analysis cannot be ruled out. Compared with the series of interstratified illite/montmorillonites analysed by Hower and Mowatt (op. cit.) the present samples show consistently higher lattice charges but, as noted above, show similar amounts of fixed K in relation to amount of montmorillonite interlayering. Consequently CECs of the present samples are higher, and on their Fig. 9 would fall on a different regression line of CEC v. amount of expanding layers.

An analysis of an interstratified illite/montmorillonite from Woodbury, Worcs. (same locality as B4) has been presented by MacEwan (1956). The corresponding structural formula shows a larger amount of octahedral Mg and an appreciably smaller amount of fixed K than is shown in table 5.6. Lattice charges are, however, identical. The only other published analysis of interstratified illite/montmorillonite from the Silurian of the UK is found in Gilkes and Hodson (1971). These authors analysed (mainly by XRF and flame photometry) the < 0.02 micron fraction of a clay from Overbury, Herefordshire. Samples from the same locality have also been examined here (B10, 11) but complete chemical

analyses of the hydrocyclone overflow products were not carried out as these were shown to contain appreciable amounts of kaolinite (figs. 2.5 and 3.3). Compared with the structural formulae of the four present illite/montmorillonites (table 5.6) the Overbury clay of Gilkes and Hodson shows a much larger tetrahedral Al content but the total lattice charge is of the same order. The fixed K content is about what would be expected from the amount of montmorillonite interlayering determined for samples B10 and 11 but appears too high for the 41% montmorillonite layers which Gilkes and Hodson maintained were present in their Overbury sample. In fig. 5.2 the position for B10 has been plotted using the value of 31% montmorillonite interlayering obtained from the present study and the figure of 0.91K/unit cell given by Gilkes and Hodson. The partial chemical analysis of B10 (table 5.3) also fails to support the suggestion made by Gilkes and Hodson that significant amounts of a phosphate mineral occur in the finer fractions of the Overbury clay. Both their P_2O_5 and excess CaO figures may be due to calgon treatment of the original sample.

5.5 EXCHANGEABLE CATIONS

5.5.1 General

Cations were displaced from the clays by ammonium acetate; the procedure used is described in detail in Appendix 5. It is generally accepted that repeated extractions with this reagent (as was found necessary for the present samples in view of their aggregated nature) solubilises accessory sulphates and carbonates. In samples where these minerals are present the 'exchangeable' Ca figure therefore contains a contribution from this source. For instance, samples A5 and C3 (tables 5.8 and 5.10, respectively) obviously contain ammonium acetate-soluble minerals.

Table 5.8. Exchangeable cation assemblages of selected montmorillonites

SAMPLE	meq/100g clay (on dried at 105°C basis) Ca^{2+}	Mg^{2+}	K^{+}	Na^{+}
A1 orig	67.2	29.5	4.7	4.1
A2 orig	65.5	30.5	3.3	4.1
A3 orig	68.8	33.6	4.2	4.4
A4 orig	65.2	37.3	3.0	5.8
o/f	66.3	39.2	3.2	5.9
u/f	56.5	35.0	2.7	4.3
A5 o/f	177.2	4.9	1.8	1.2
A6 orig	70.2	14.1	0.8	0.7
A7 orig	79.7	12.6	1.5	1.0
o/f	84.5	16.6	1.5	1.5
u/f	65.0	8.7	1.2	0.8
A10 o/f	119.2	5.2	1.7	0.7
A11 orig	96.1	4.8	1.9	< 1
o/f	109.4	5.5	2.1	< 1
u/f	88.5	3.5	1.8	< 1
A12 o/f	90.7	17.7	2.1	1.2
A15 o/f	93.9	21.5	2.0	<1
u/f	90.3	13.9	1.5	<1

orig = original sample

o/f = hydrocyclone overflow product

u/f = hydrocyclone underflow product

Table 5.9. Exchangeable cation assemblages for selected interstratified illite/montmorillonites

SAMPLE		meq/100g clay (on dried at 105°C basis) Ca^{2+}	Mg^{2+}	K^{+}	Na^{+}
B1	o/f	32.6	5.3	1.6	<1
B3	orig	31.1	9.9	2.2	<1
B4	o/f	34.9	5.7	2.1	0.5
B7	o/f	25.5	17.9	3.4	<1
B8	orig	28.6	4.2	1.3	<1
	o/f	20.2	4.3	1.6	0.2
	u/f	47.3	3.3	0.6	<1
B9	o/f	20.3	8.3	1.7	<1
B10	o/f	51.3	3.1	1.6	<1
B11	o/f	43.4	2.1	1.7	<1
	u/f	44.6	1.2	2.1	<1
B12	o/f	91.9	4.6	1.5	<1
B15	o/f	36.7	23.9	1.9	0.3

orig = original sample

o/f = hydrocyclone overflow product

u/f = hydrocyclone underflow product

Table 5.10. Exchangeable cation assemblages for montmorillonite, mica, kaolinite, chlorite mixtures

		meq/100g clay (on dried at 105°C basis)			
		Ca^{2+}	Mg^{2+}	K^{+}	Na^{+}
SAMPLE					
C1	o/f	21.3	16.0	0.9	< 1
C2	o/f	38.4	19.0	2.7	1.9
C3	orig	280	19.6	1.3	1.8

orig = original sample

o/f = hydrocyclone overflow product

u/f = hydrocyclone underflow product

The hydrocyclone underflow product from B8 (table 5.9) gave a much higher exchangeable Ca figure than the original sample which, in turn, showed more exchangeable Ca than the overflow product. Gypsum is present in B8 and, following hydrocyclone separation, the bulk of this mineral reported in the underflow product Some gypsum is present in the overflow product as is seen from the SO_3 figure in table 5.2. It was suggested in section 2.1.3 that the shear conditions encountered by the sample during hydrocycloning may solubilise minerals such as gypsum. However this effect does not appear as serious as was originally feated; gypsum in the overflow product from B8 may be present by virtue of its size and not necessarily as a result of shear solubilisation and later recrystallisation on drying.

No significant variations, other than those attributable to solubilisation of accessory minerals, were found in the exchangeable cation assemblages of hydrocyclone underflow and overflow products from the same sample.

5 5.2 Montmorillonites

The exchangeable cation assemblage of the Lower Greensand montmorillonites, although dominated by Ca, also contains significant amounts of Mg. Variations in exchangeable Ca/Mg ratios for samples from the same depositional area may be marked (see results for A10, 11 and 12, all from Nutfield, Surrey). About 30% of exchange positions in the Baulking montmorillonites (A1-4) are occupied by Mg and in these samples exchangeable K and Na are also present in greater amount than in montmorillonites from other localities. Clinoptilolite/heulandite has been positively identified in samples A1-3 and, tentatively, in A4; solubilisation of this mineral during the cation extraction procedure could be partly responsible for the high exchangeable K and Na values. Some Ca is also released from this zeolite as a result of the normal exchange

reaction and the exchangeable Ca figures for samples A1-3 certainly contain a contribution from this source.

5.5.3 Interstratified illite/montmorillonites

The presence of appreciable amounts of gypsum in many of the interstratified clays leads to high 'exchangeable' Ca values (notably for B8, 10, 11 and 12). The overflow product from B15 contains fine-grained dolomite and calcite and both exchangeable Ca and Mg figures are enhanced as a result of solubilisation of these minerals. Only a small proportion of the total K in the illite/montmorillonites ie exchangeable (see also table 5.6). About 35% of the exchange positions in B7 are occupied by Mg (this sample also shows the highest amount of exchangeable K). Samples B3 and 9 also contain high exchangeable Mg and it could be significant that B3 contains more exchangeable Mg than B4, its weathered equivalent.

5.5.4 Mixed-assemblage clays

Two features of note from table 5.10 are the high values for exchangeable Mg shown by all three samples and the large 'exchangeable' Ca figure for the original sample C3 which results from solubilisation of gypsum and, possibly, calcite.

5.6 TRACE ELEMENTS

5.6.1 General

Trace element data for a number of fuller's earths and inter-stratified illite/montmorillonites (all original samples) are recorded in tables 5.11 and 5.12. Relevant data from published sources (i.e. Worssam, 1963; Gilkes and Hodson, 1971) are also incorporated in these tables. As a preliminary indication of possible anomalous trace element contents the range of results for each element may be compared with published data for

the average composition of shales - this information is placed at the bottom of table 5.11. As will be seen later particular importance may attach to the high levels of Zr, Nb and the rare earths shown by the present samples.

In the following sections an attempt is made to allocate individual trace elements to their respective mineral hosts. For this purpose they have been placed - not always for sound geochemical reasons - into seven groups. Sources of some of the trace elements were fairly easily found: for example Zn, Pb and Ba appear to be present almost entirely in the accessory minerals sphalerite, galena and baryte. Other elements were not so easily allocated. In order to obtain further information on trace element distribution within these samples the heavies separated from the sands (and some coarse silt fractions) were subjected to XRF scans over the angular range 8-46^{o}2θ. Some attempt was made to quantify the resulting data: elements detected (tables 5.13, 5.14) were regarded as being present in major, minor or trace amounts from a comparison of the heights of their Kα peaks with the height of the Kα peak of either Zn or Zr (the two dominant elements on the traces). In addition, figures for Zr, Nb, Y and La were obtained on four (hydrocyclone-) purified montmorillonites and four purified illite/montmorillonites (table 5.15) to establish whether these elements were depleted or enriched relative to the respective original samples. Enrichment of an element in these purified clays does not necessarily signify that the element is present in, or attached to, the clay lattice. It was shown in Chapter 2 that the hydrocyclone was only separating material finer than 5-7 microns and therefore fine silt size accessory minerals could be present in the purified clays. Care must also be taken to avoid drawing conclusions for the total non-clay assemblage merely from the mineral species identified in the sands; it is quite possible that discrete minerals of the heavier elements such as Sn and Nb would occur only in the silt size range.

Table 5.11. Trace element data for fuller's earths. Values in ppm except those for TiO_2 which are in %. Analytical methods used for each element are described in section X5.3

	Zn	Pb	Cu	V	Cr	Ni	Co	Sc	Rb	Ba	Sr	Zr	Nb	Y	La	Ce	Ga	Be	Sn	U	TiO_2
A2	120	25	15	45	30	15	6	14	10	80	912	500	120	90	215	430	30	3	6	5	1.10
A3	140	30	25	35	15	10	3	12	10	40	856	660	140	90	245	530	40	3	12	7	1.14
A4	100	20	25	30	40	30	6	8	10	40	106	500	60	65	220	520	35	1	7	6	0.73
A6	120	15	30	55	100	15	8	8	10	80	122	420	50	30	185	520	25	<1	3	7	1.09
A7	120	45	20	15	10	20	<3	4	10	900	108	560	160	90	265	470	35	6	7	8	0.60
A8	200	50	30	15	10	80	8	6	10	480	86	1000	200	90	250	700	35	4	6	12	0.92
A9	120	30	40	15	15	20	3	6	11	600	89	800	240	90	270	620	40	6	10	9	0.85
A10	130	40	20	30	15	15	3	7	16	350	106	720	200	80	240	590	35	3	6	9	0.87
A11	160	40	15	20	20	15	3	8	15	380	94	780	240	80	215	480	35	7	10	8	0.86
A12	120	30	20	25	10	100	16	9	10	80	51	560	90	80	195	380	30	<1	8	5	0.95
868	140	20	35	60	80	35	10	7	25	90	67	400	160	50	190	360	30	2	5	4	0.80
A15	120	20	25	<10	10	10	<3	6	25	450	448	900	220	80	270	690	50	3	12	7	0.85
Data from Worssam (1963)																					
Sp190 } Nutfield, Surrey			10	30						2000	100	800	200	50	200		30				
Sp 191 } Nutfield, Surrey			5							500	100	800	100	30			20				
Sp 194 } Nutfield, Surrey										600	100	500	100	70	300		20				
Maidstone, Kent										40	80	700	100	50	100		20				
AVERAGE SHALE	95	20	45	130	90	68	19	13	140	580	300	160	11	32	41	86	19	3	6	4	0.46

Values from Turekian and Wedepohl (1961) except those for Y, La and Ce which are from Herrmann (1970)

Table 5.12. Trace element data for interstratified illite/montmorillonites. Values in ppm except those for TiO_2 which are in %. Analytical methods used for each element are described in section X5.3

	Zn	Pb	Cu	V	Cr	Ni	Co	Sc	Rb	Ba	Sr	Zr	Nb	Y	La	Ce	Ga	Be	Sn	U	TiO_2
B1	50	15	50	10	15	25	3	18	241	90	53	360	45	90	110	280	25	4	9	8	0.32
B4	100	80	25	<10	15	15	3	13	269	50	50	300	50	60	65	170	25	3	8	7	0.19
B6	180	80	20	80	20	60	15	25	208	40	119	500	30	100	125	270	30	2	6	7	0.44
B7	140	50	10	10	10	15	<3	18	302	40	95	380	35	70	165	380	25	4	5	9	0.54
B8	<50	60	10	15	20	10	<3	12	334	70	30	320	40	60	50	100	30	5	8	6	0.24
B9	<50	15	15	20	30	15	3	14	342	60	57	380	30	60	130	340	25	4	3	8	0.24
B10	<50	10	25	<10	20	15	<3	10	168	80	44	240	35	40	95	240	25	3	3	4	0.31
696A	50	10	40	40	15	20	18	25	144	75	76	600	20	80	105	250	20	4	7	6	0.23
696E	80	60	20	25	35	40	6	12	162	150	195	420	40	70	180	360	35	3	8	6	0.47
786A	60	25	15	<10	10	30	<3	13	161	50	73	460	40	70	170	420	25	2	12	4	0.31
Data from Gilkes and Hodson (1971)																					
Woolhope	41	6	4						147		35	225		26			21			2	
Much Wenlock	70	75	37						106		47	202		20			15			2	

Table 5.13. Some trace elements present in the sand size 'heavies' separated from selected montmorillonites. (Analyses by XRF).

sample	elements		
	major	minor	trace
A2	Zr, Sr, Zn	Ba, Nb, Y	Ce, Ag, Rb, Li, Th, Pb, As
A4	Zr, Zn	Nb, Y, Sr	Cd, Ag, Rb, Pb, As
A7	Ba, Zr, Zn	Nb, Y, Sr	Ce, Ag, U, Rb, Th, Pb
A8 (sand)	Ba, Zr, Zn	Nb, Y, Sr	Sn, Cd, Ag, Pb
A8 (coarse silt)	Ba, Zr, Zn	Nb, Y, Sr, Pb	Ce, Sb, Sn, Cd, Ag, Th
A9	Zr	Ba, Nb, Y, Zn	Nd, Ce, La, Ag, Sr, U, Rb, Th, Pb, As
A10	Ba, Zr, Zn	Nb, Y, Sr, As	Ce, Sn, Cd, Ag, Pb
A11 (sand)	Ba, Zr, Zn	Nb, Y	Ce, Cd, Ag, Sr, U, Rb, U, Pb
A11 (coarse silt)	Ba, Zr, Zn	Nb, Y, Pb	Ce, La, Sn, In, Cd, Ag, Sr, As
A15	Ba, Zr, Zn	Nb, Sr	Cd, Ag, Y, Rb, As

Table 5.14. Some trace elements present in the sand size 'heavies' separated from selected illite/montmorillonites. (Analyses by XRF).

	major	minor	trace
B1	Zr	Y, Nb, Zn	Ce, Nd, La, Cd, Ag, Th, Sr
B2	Zn	Zr	Ba, Cd, Ag, Nb, Y, Sr, Th, Pb
B4 (sand)	Zr	Y, Nb, Pb, Zn	Th, Sr
B4 (coarse silt)	Zr	Y	La, Ce, Ba, Sn, Nb, Sr, U, Rb, Th, Pb, As, Zn
B6	Zn	Cd, Zr	Sn, In, Y, Sr, Th, Pb
B7	Ba, Zr	Nb, Y, Sr, Zn	Th, U, Pb
B9	Zr	Y, Zn	U, Ba, Ce, Nb, Sr, Th, As

5.6.2 Zn, Pb, Cu

The fuller's earths contain between 100 and 200 p.p.m. Zn, the interstratified illite/montmorillonites from < 50 (the limit of detection) to 180 p.p.m. Major amounts of this element were recorded in most of the sand size heavy fractions separated from the clays (tables 5.13, 5.14). Sphalerite is common in the heavies; high Zn values shown for instance by illite/montmorillonites B6 and B7 (180 and 140 p.p.m. respectively) correspond with the predominance of sphalerite in the heavies. Most, if not all, of the Zn in these clays is therefore assumed to be present in sphalerite although the possibility that some occurs in octahedral sites in the clay lattice cannot be ruled out. An XRF scan of the heavies from B6 detected minor amounts of Cd - this element probably occurs in solid solution in the sphalerite.

Galena occurs both in the fuller's earths and illite/montmorillonites (Newton, 1937; this study, section 4.5.7). The higher Pb values in tables 5.11 and 5.12 are generally given by samples in which galena was positively identified in the separated sand size heavies (i.e. A7, 8; B4, 6, 7). Galena is therefore assumed to be the main or only source of Pb in these clays.

Cu does not exceed 50 p.p.m. in any of the samples analysed. Rare grains of a secondary Cu-mineral (? malachite/azurite) were seen in the heavies from B1; the original sample had given a Cu-content of 50 p.p.m. This instance apart, there is no direct evidence regarding the source of this element. Pyrite, a common accessory mineral of the clays, could contain Cu in solid solution; some Cu could also occur in octahedral lattice sites in the clay itself.

5.6.3 V, Cr, Ni, Co, Sc

In both groups of samples the individual elements are present in amounts less than 100 p.p.m. The illite/montmorillonites generally

show lower V, Cr, Ni and Co contents (the high V value of 80 p.p.m. shown by B6 is the only notable exception). For Sc, however, the reverse is true: the illite/montmorillonites show 10-25 p.p.m. Sc, the fuller's earths 4-14 p.p.m.

The ionic radii of V, Cr, Ni and Co are such that occupation of octahedral sites in the clay lattice is possible; montmorillonites rich in the first three elements have been described in the literature. The ionic radius of Sc (0.81 A) is too large to allow entry into clay lattice sites. In accessory minerals the substitutions Co, Ni $\rightleftharpoons$ Fe (pyrite) and Co $\rightleftharpoons$ Zn (sphalerite) are also possible.

Amounts of these elements in the fuller's earths appear to be related to the oxidation state of the iron in the sample as a whole. This is especially so for Ni and Co which would be expected to substitute for Fe (II). The highest Ni and Co values are shown by A12. In this sample the montmorillonite has a high octahedral Fe (II) content and siderite and pyrite are prominent accessory minerals. It may also be noted from table 5.11 that sample A8 (blue clay) contains appreciably more Ni and Co than sample A9 (yellow clay). The montmorillonite of sample A7 has a large octahedral Fe (III) content and secondary iron oxides are also present. This sample shows the lowest V, Cr, Co and Sc values and the Ni value is among the lowest recorded for the fuller's earths.

5.6.4 Rb, Ba, Sr

Rb commonly occurs in association with K in minerals. In the fuller's earths values range from <10 (the detection limit) to 25 p.p.m., the element probably being located in K-rich accessory minerals such as feldspar (in sample A15 especially) or muscovite (in sample B68). The illite/montmorillonites contain between 130 and 330 p.p.m. Rb. In these clays Rb contents show a rough correlation with the amount of illite

component. The montmorillonite lattice is capable of fixing substantial amounts of Rb (Mackenzie, 1961). It may be concluded that the Rb in the illite/montmorillonites is immobilised in the 10A (illite) component in sympathy with K.

In the fuller's earths Ba is present in amounts ranging from 40 to 900 p.p.m., this variation being a function of the erratic distribution of baryte in these clays. Baryte also appears the most likely source of the Ba in the illite/montmorillonites. B8 was the only sample in which baryte was positively identified and it may be seen from table 5.14 that this was the only sample in which major amounts of Ba were detected in the sand size heavies.

Geochemically Sr is closely associated with Ca and like Ba commonly forms sulphates and carbonates. Sr levels in the fuller's earths range from 51 to 912 p.p.m. and in the illite/montmorillonites from 30 to 195 p.p.m. Major amounts of Sr were also detected in the sand size heavies from certain of the fuller's earths (table 5.13). No discrete Sr minerals were found in the heavies from either of the two clay groups and the exact location of this element can only be surmised on geochemical grounds. In the fuller's earths some Sr could be present in baryte; in some of these clays and also in some illite/montmorillonites values for Sr are of approximately the same order as those for Ba so it is unlikely that baryte is a major source of the Sr. Sr $\rightleftharpoons$ Ca substitution in carbonate, or even apatite, may occur. Some Sr could also be present in exchange positions on the clay or in the clinoptilolite/heulandite of the fuller's earths.

5.6.5 Zr, Nb

Between 420 and 1000 p.p.m. Zr and 50 and 240 p.p.m. Nb are present in the fuller's earths. A linear relationship exists between the relative concentrations of Zr and Nb in these clays (fig. 5.3), the

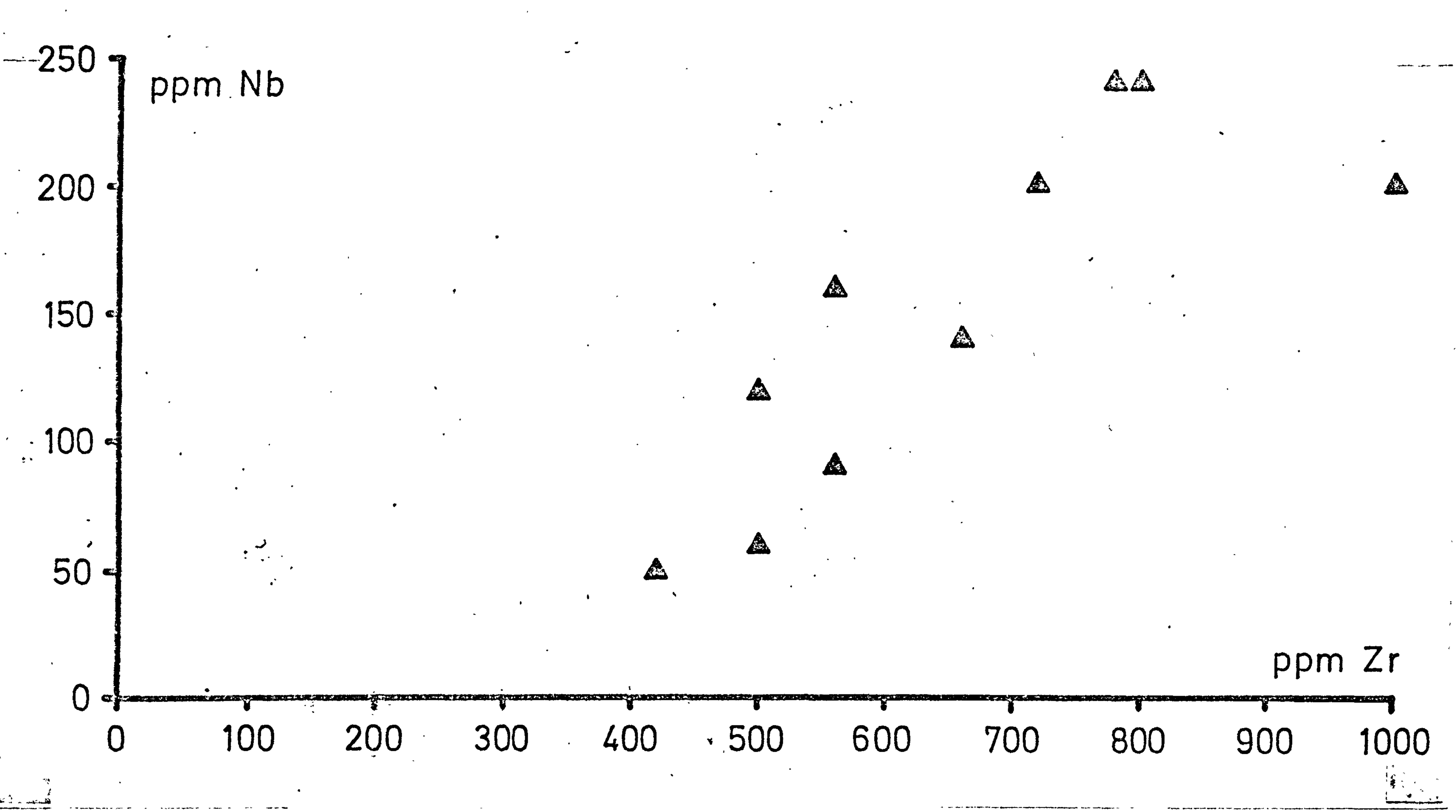

Fig. 5.3 Nb v. Zr contents for Lower Greensand fuller's earths (original samples).

significance of which will be discussed in section 6.1.3. The illite/montmorillonites contain from 240 to 600 p.p.m. Zr and 20 to 50 p.p.m. Nb.

Zircon is a common accessory mineral in both fuller's earths and illite/montmorillonites but only a small proportion of the total Zr can be accounted for by zircon in the sand sizes and Zr values are still high in the clay.fractions (table 5.15). No discrete Nb minerals were identified in the heavies from either clay group but Nb was detected during XRF scans (tables 5.13, 5.14) and the possibility that Nb is present in isomorphous substitution in one or more of the constituents must be considered. Nb may commonly substitute for Ti and Zr (Vlasov, 1966). No correlations were observed between Nb values and total TiO_2 contents of either fuller's earths or illite/montmorillonites. Sphene, ilmenite and ?anatase all occur in the fuller's earths but simple calculations, taking into account the levels of Nb substitution normally observed in these minerals (data from Vlasov, op. cit.) and amounts actually present in the clays, show that they could only be minor sources of Nb. The amount of Nb which can be accommodated in the zircon structure does not exceed 2% (Vlasov, op. cit.). In the fuller's earths Zr/Nb ratios lie between 5:1 and 3:1 and not more than a fraction of the total Nb could occur in this mineral. Using a similar argument zircon could not be more than a minor source of the Nb present in the illite/montmorillonites also.

It is apparent from table 5.15 that the bulk of the Zr and Nb in these clays does not occur in the sand (or coarse to medium silt) size fractions but is associated with the finer sizes. Particles coarser than about 7 microns should not be present in the 'purified' clays - the Zr and Nb recorded in these must therefore occur either in accessory minerals of fine silt (even coarse clay ?) size or as lattice constituents of the clay. It may be noted that the ionic radius of Nb (0.68 A) is very close to that of Mg and there appears no reason why Nb should not

Table 5.15. Trace element contents (ppm) of purified clays and respective original samples (values for the latter, in parentheses, are taken from tables 5.11 and 5.12).

sample	Zr		Nb		Y		La	
A4	495	(500)	80	(60)	70	(65)	200	(220)
A7	550	(560)	155	(160)	80	(90)	160	(265)
A12	500	(560)	70	(90)	60	(80)	85	(195)
A15	1260	(900)	200	(220)	85	(80)	160	(270)
B1	385	(360)	40	(45)	80	(90)	40	(110)
B4	205	(300)	35	(50)	50	(60)	60	(65)
B7	275	(380)	30	(35)	70	(70)	55	(165)
B8	180	(320)	35	(40)	55	(60)	75	(50)

occupy octahedral lattice sites in the clay. Such a location for Zr is less likely however both on valency grounds and in view of the larger radius of this cation.

5.6.6 Y, La, Ce

Y contents of the fuller's earths and illite/montmorillonites all lie between 40 and 100 p.p.m . La contents of the fuller's earths (range 185 to 270 p.p.m.) are generally about double those of the illite/montmorillonites (50-180 p.p.m.). Ce levels in the fuller's earths range from 360 to 700 p.p.m. and in the illite/montmorillonites from 100-420 p.p.m.

No rare earth minerals were identified in these clays apart from a few grains of monazite recorded from the sand size heavies,of illite/montmorillonite B2. All three elements were detected in the heavies separated from clays of both groups (tables 5.13, 5.14). Y was especially prominent, the height of the Kα peak of this element showing a sympathetic relationship with the height of the Zr Kβ peak. Zircon may contain up to 9% Y_2O_3 (Vlasov, 1966) and it is quite possible that this mineral is the source of some of the Y detected in the heavies. An apatite concentrate, hand picked from the sand size heavies of B4, showed a Ce content of the order of 1000 p.p.m. (by XRF). A large proportion of the Ce (probably also La) detected in the heavies could thus be present in apatite. Sphene is the only other mineral identified in the heavies in which the isomorphous replacement Y, La, Ce $\rightleftharpoons$ Ca could occur; normally, however, sphene does not contain more than 1.5% total rare earth oxides.

The 'purified' clays show a marked depletion in La relative to the original samples (table 5.15) and it would appear that the coarser accessory minerals make a significant contribution to total La contents. However appreciable amounts of La, and most of the Y, are associated with material of the clay and fine silt sizes. Again (see previous section)

it cannot be decided whether these elements are present in fine silt size accessory minerals or whether they are present in, or on, the clay lattice. The ionic radii of Y, La and Ce are 0.92, 1.22 and 1.07A respectively. The cations are too large to be accommodated within the montmorillonite lattice but there is no reason why they should not occupy exchange positions on the lattice surface. Roaldset (1973) has shown that a considerable fraction of the rare earth elements present in clays may be surface adsorbed.

5.6.7 Ga, Be, Sn, U

Ga values in these clays are in the range 25 to 50 p.p.m. The close geochemical coherence between Ga and Al is well known, Ga may thus occur with Al in octahedral lattice sites of the clay. Isomorphism between Ga and Zn in sphalerite, again quite common, appears unimportant in the present context in view of the lack of any sympathetic relationship between Zn and Ga values in the clays.

Be contents are low (maximum 7 p.p.m.). This element could conceivably substitute for Si in the clay lattice.

U (Maximum value 12 p.p.m.) could substitute for Zr in zircon or Si in the clay lattice. Similar substitutions are possible for Sn (maximum value also 12 p.p.m.), this element could also be present as cassiterite.

CHAPTER 6

ORIGIN OF THE CLAY DEPOSITS

6.1 ORIGIN OF THE LOWER GREENSAND FULLER'S EARTHS

6.1.1 Introduction

Early Lower Cretaceous (Berriasian to Barremian) sedimentation in the Wealden-Dorset area of southern England was primarily non-marine in character. The area of deposition was bounded to the north by the London Uplands. To the north of this landmass was the Northern Sea, the southern limits of which, during this period, do not appear to have extended much below the present-day southern borders of Lincolnshire and Norfolk. During Lower Aptian times the Wealden-Dorset basin was invaded by a sea advancing either from northern France or in a north-east direction along the line of the English Channel. Initially, the northern limits of this first marine incursion were not very different from those of the original basin. In the Upper Aptian, however, there was renewed marine transgression with the seas lapping on to the southern margins of the London Platform and spreading across Wiltshire, Oxfordshire and into the southern Midlands to link up with the Northern Sea (Kirkaldy, 1963). The fuller's earth deposits are all found near the Upper Aptian coastline (see, for instance, the palaeogeographic map in Kirkaldy, op. cit., p. 143).

It was mentioned in section 1.2.2 that two quite different theories of origin for the montmorillonite of these deposits exist, one involving direct precipitation from solution, the other alteration of volcanic material. Both theories are discussed in detail in the following sections. Some of the features of the deposits which have to be accounted for are listed below.

(i) Their occurrence in isolated basins or troughs of relatively small areal extent (section 1.2.2).

(ii) The thickness of some of the individual fuller's earth horizons (4-5 m at Redhill).

(iii) Their high grade (in terms of montmorillonite) and the absence in them of any other clay minerals.

(iv) The relatively small variation in ionic composition of montmorillonites from different deposits (section 5.4.1).

(v) Certain peculiar features of the trace element assemblage (table 5.11) including the apparent association of Zr, Nb, Y, La and Ce with the fine silt and clay sizes (sections 5.6.6 and 5.6.7).

(vi) Certain unusual features of the accessory mineral assemblage (section 4.2.1).

6.1.2 Origin by precipitation from solution

Cox (1918) suggested that the montmorillonite of the fuller's earth deposits had formed as a direct chemical precipitate under certain peculiar conditions obtaining locally in the Upper Aptian sea. This theory was later adopted by Newton (1937), Wood (1956), Robertson (1961) and Poole and Kelk (1971a, b). From the various suggestions put forward by these authors a composite picture emerges of montmorillonite being precipitated in off-shore, alkaline, shallow-water areas in which, for long periods, detrital sedimentation was negligible. Protection from the current action of the open sea may have been afforded by littoral pebble banks - one of these possibly being represented by the coarse grained facies of the Sandgate Beds of the Guildford region (Newton, op. cit.). Certain accessory minerals of these deposits, such as sphene, apatite, sphalerite, feldspar (Newton) and clinoptilolite/heulandite (Poole and Kelk), were considered to have been precipitated at the same time and under the same conditions as the montmorillonite. It was

assumed that the 'commonplace elements' Fe, Mg, Ca, Al and Si (Poole and Kelk, 1971a) necessary for montmorillonite and accessory mineral formation were readily available in this environment. Most were supplied by rivers draining the adjacent, deeply-weathered land surface (Robertson, op. cit.); these were supplemented by silica and lime resulting from the dissolution of sponge spicules and shell debris within the depositional area.

The assumption that all the elements necessary for montmorillonite formation were (i) available and (ii) present in the right quantities in this environment is questionable. Simultaneous dissolution of both silica and calcium carbonate is unlikely on grounds of pH (Hallam and Selwood, 1970). Finding a source for the aluminium of the montmorillonite also presents problems. The amount of dissolved aluminium which can be carried in solution is markedly dependent upon pH. In the 4.5-8 pH range, within which most river waters fall, solubility of this element is virtually negligible. Therefore even though aluminium would be soluble in the alkaline waters of the depositional area it is unlikely that sufficient could have been introduced in dissolved form by rivers draining the adjacent landmass. There is the possibility (touched upon by Robertson, op. cit.) that aluminium was transported in poorly crystalline aluminosilicates, these having formed as a result of deep weathering of the adjacent landmass. After entering the alkaline depositional area these aluminosilicates could have dissolved. Alternatively they could have reacted directly with cations in solution to form montmorillonite - i.e the montmorillonite would have been synthesised compositionally but not structurally (Mackenzie and Garrels, 1966) within the depositional area. It is extremely unlikely that this process would result in a monomineralic montmorillonite deposit. Moberley et al. (1968) have suggested such an origin for the montmorillonite occurring in Hawaiian off-shore sediments (in Hawaii, weathering of basalts supplies

much 'weakly crystalline to amorphous' material to rivers entering the sea). However these off-shore sediments are far from monomineralic; in them montmorillonite is accompanied by chlorite, kaolinite and illite.

Many authors (see, e.g., Hallam and Selwood, 1968) hold that there is no convincing evidence that montmorillonite may be other than of secondary origin, this mineral supposedly forming only as an alteration product of volcanic material or as a weathering product, under conditions of restricted drainage, of a range of rock types. This is, perhaps, too extreme a view as there have been a number of reports in the literature of the successful synthesis of montmorillonite under conditions approximating those at the Earth's surface. Harder (1972) studied the problem of the low-temperature synthesis of montmorillonite in some detail. He found that (i) amorphous Al, Fe, Mg-hydroxides were capable of coprecipitating silica from dilute solutions and (ii) subsequent aging of these hydroxide/silica precipitates at temperatures between 3 and 20°C resulted in the formation of montmorillonite. (This second conclusion was subject to the obvious condition that the proportions of silica and other elements in the hydroxide/silica precipitates approximated those found in naturally-occurring montmorillonites). Harder also showed that the extent of montmorillonite formation depended both on the Mg-content of the original solution and the pH during precipitation. Under neutral conditions, coprecipitation of Mg and Al hydroxides did occur but these precipitates remained amorphous unless they contained at least 6% MgO. Under basic conditions (pH 10) only 10 p.p.m. Mg in solution was necessary for the eventual formation of montmorillonite. The mineral was not obtained from solutions which did not contain Mg. Magnesium thus appears to adopt two roles in montmorillonite formation. The first is to precipitate silica from solution; the second may be in enabling Al to take sixfold co-ordination under basic conditions (Dekimpe et al., 1961). At low temperatures Al tends to assume sixfold co-

ordination in an acid environment and fourfold in a basic environment. In the latter a certain amount of Mg (which exhibits sixfold co-ordination only) may be necessary to nucleate the montmorillonite octahedral sheet.

Although the feasibility of the precipitation process has been demonstrated experimentally, surprisingly few occurrences of montmorillonite, apart from those under discussion, have been attributed to this mechanism. Of minor interest only (in the present context) are the observations of Jeans (1968) and Millot (1970) that the montmorillonite of the Chalk is of primary origin. Millot also considered that the montmorillonite occurring in dominantly alkaline sediments occupying the sites of littoral and interior basins of Eocene age in West Africa had been precipitated from solution. During the Eocene land adjacent to these basins was of low relief and, according to Millot, contributed little other than dissolved material to the depositional environment (obvious parallels with the supposed conditions in the Wealden basin in Upper Aptian times). In these sediments montmorillonite is, however, accompanied by attapulgite, sepiolite, carbonate, phosphate and chert and a progressive dominance offshore from aluminous montmorillonite through aluminomagnesian montmorillonite to sepiolite may be recognised. The lack of any indications of detrital inheritance from rock or soil, or any evidence of volcanic material, led Millot to assume that all these minerals were essentially chemical precipitates. An observation by this author is worth quoting viz: 'neoformed attapulgites, sepiolites and montmorillonites seem to be indifferent to the salinity of their genetic environment. They occur in calcareous or hypersaline lakes as well as in calcareous or hypersaline seas. The abundance of the Na and K salts has no influence on the mechanism of their growth, but an alkaline environment is necessary.' Bischoff (1972) has shown that a montmorillonite-type mineral is being precipitated at present in the

Red Sea, its formation apparently being directly associated with the discharge of brine on the sea floor. The montmorillonite mineral occurs as the main solid constituent of a dark brown mud 5 km thick which is distributed over an area of 56 km^2. Structural formulae of various montmorillonites from the deposit showed that the mineral was intermediate between nontronite and the theoretical trioctahedral ferrous iron member of the montmorillonite group. Bischoff suggested that the precipitation mechanism required a combination of cooling of the brine and subsequent mixing with the Red Sea bottom waters. All components appeared to have come from the brine which contained approximately 60 p.p.m. dissolved silica and 80 p.p.m. Fe(II), as well as other metals such as Zn and Cu which Bischoff assigned to octahedral sites in the montmorillonite lattice. As the brine discharged on the sea floor it cooled, thereby making the dissolved silica supersaturated. During mixing with sea water a portion of the Fe(II) was oxidised and the (proto-) montmorillonite precipitated as a mixture dominantly of Fe(II), Fe(III) (? hydroxides) and silica. Bischoff did point out that the montmorillonite was unstable in the presence of sea water and a trend towards equilibrium would probably involve K-fixation and consequent formation of glauconite.

The 'direct chemical precipitation' theory of origin is unable to explain many of the features of the Cretaceous fuller's earth deposits. These may be accounted for in a much more satisfactory manner by the 'alteration of volcanic ash' theory described in the next section.

6.1.3 Origin by alteration of volcanic ash

The possibility that the Lower Greensand fuller's earths might have been derived from volcanic material was first advanced by Kerr (1932) who noted the presence of supposed glass shard fragments in the Woburn deposit. At the time this theory attracted little support, mainly because no instances of contemporaneous volcanic activity were known but

also, perhaps, because the climate of opinion was then very much in favour of an origin by direct precipitation from solution. Newton, the main proponent of the precipitation theory, maintained that the fragments described by Kerr could either have been sponge spicules or crystals of authigenic 'anorthoclase' and there the matter rested. Only recently has this theory been revived (Hallam and Selwood, 1968; Cowperthwaite et al., 1972). According to these authors the parental material of the fuller's earth deposits originated in distant explosive volcanic eruptions and was transported to the depositional site by high altitude jet-stream winds. After deposition some redistribution of the fine-grained (vitric) ash took place. Cowperthwaite et al. considered that fuller's earth beds up to 1m thick could have been derived directly from a single major ash fall; thicker beds formed from ash deposits which had previously been concentrated in the basin of deposition, perhaps as a result of rapid erosion of ashfalls covering adjacent landmasses. The source of the volcanicity was considered by Hallam and Selwood to be in the eastern Atlantic to the west of Britain. Cowperthwaite et al. favoured the same general area but placed the source nearer the present day coastline of Britain, suggesting that the Wolf Rock (~~in the approaches to the Bristol Channel~~) may be the basal wreck of one of the volcanoes.

One of the main arguments against this theory invokes the absence, in the deposits, of any remnant tuffaceous texture or of any material of undoubted volcanic origin. Cowperthwaite et al. did, however, note that electron micrographs of peels taken from the surface of specimens of the Redhill fuller's earth showed pores reminiscent of those in volcanic glass. It has been noted in the present investigation (section 4.2.5) that certain morphological features of the zeolite aggregate grains suggest the presence of an original vesicular glassy phase. Cowperthwaite et al. considered that sphene, biotite and some zircon and apatite were constituents of the parent ash; ilmenite and alkali feldspar could

possibly have had a similar origin (this study, sections 4.3.2 and 4.2.4). The assemblage of minerals of assumed volcanic origin gives little indication as to the composition of the original ash, although the absence of quartz may be significant. According to Cowperthwaite et al. 'the mineralogical and petrographical characteristics of the English fuller's earths suggest that they have been very largely derived from the alteration of undersaturated and/or basic alkaline volcanic ash.' This statement appeared to be based wholly on the absence of free silica in these clays!

Certain anomalous aspects of the trace element chemistry of the fuller's earths (table 5.11) can only be explained by assuming direct alteration from material of igneous origin. Between 420 and 1000 p.p.m. Zr are present in these deposits. Zr values of this magnitude may be shown by sedimentary rocks but are more common in sandstones than in finer grained sediments. Nb values for the fuller's earths (50-240 p.p.m.) are completely outside the range quoted for sedimentary rocks (according to Turekian and Wedepohl (1960) the average Nb content of a sandstone is <1 p.p.m. and shales and deep sea clays show average Nb contents of 11 and 14 p.p.m. respectively). Rare earth values of the order of magnitude shown by the fuller's earths (Y 30-90 p.p.m., La 185-270 p.p.m., Ce 360-700 p.p.m.) are also uncommon in sedimentary rocks. For a group of European shales Herrmann (1970) quoted average Y, La and Ce values of 32, 41 and 86 p.p.m; a similar group of North American shales gave essentially similar values although a much larger group of Russian shales showed Y, La and Ce values of 53, 61 and 120 p.p.m. respectively. Zr, Nb, Y, La and Ce values in the range exhibited by the fuller's earths are not uncommon in igneous rocks, especially those of an acid or alkaline nature. At this stage it should be noted that both the major and trace element chemistry of an igneous rock may be markedly affected by a variety of secondary processes such as late deuteric

alteration, alteration in a marine environment, devitrification and low-grade regional metamorphism. Cann (1970) has shown that in ocean floor basalts the abundance of the more refractory trace elements (Y, Zr, Nb and Ti) seems to be little changed by such processes. In these basalts Cann found high positive correlations between element pairs such as Y/Ti and Zr/Ti and suggested that these relationships 'might be a very powerful method of identifying ocean floor basaltic rocks as such even after the operation of profound secondary processes.' On the basis of Cann's observations it would appear reasonable to assume that montmorillonite deposits derived from volcanic ash would contain Nb, Zr, Y etc. in essentially the same quantities as the parent ash and it should therefore be possible to determine the composition of the parent material from the actual amounts of these elements present in the clays.

Ranges of values for Zr, Nb, Y, La and Ce are very similar to those shown by trachytic members of the alkali-basalt association of oceanic regions (Engel et al., 1965) and also the trachytes and pantellerites of the peralkaline series of lavas of the East African Rift System (Weaver et al., 1972; Gibson, 1972). In the East African lavas Weaver et al. noted the existence of linear relationships between the relative concentrations of Zr, Nb, La and Ce. The latter were considered to have behaved as residual elements, i.e. they were completely retained in the liquid phase of the magma during any solid/liquid reactions prior to eruption. Although a linear relationship of sorts exists between the relative concentrations of Zr and Nb in the fuller's earths (fig. 5.3) - this could be used as further evidence in favour of direct derivation from igneous material (Cann, Weaver et al., op. cit.) - it does not necessarily prove that Zr and Nb were present as residual elements in the original material as corresponding linear relationships between other element pairs were not found. However the association of Zr, Nb, Y, La and Ce with the finer grained material of the present deposits (sections

5.6.5, 5.6.6) might be expected if they were present as residual elements in the parent ash.

During alteration of ash to montmorillonite it may be assumed that the Al_2O_3 content remained more or less constant on the grounds of the low solubility of this oxide (see, e.g., Smith, 1967). By comparing particular element/Al_2O_3 ratios of the montmorillonite with ash of chosen composition the amount of material added or removed during the course of alteration may be calculated. For ash of trachytic composition the most significant changes would have been the addition of Mg (perhaps from sea water) and the removal of K and Na. No free silica (apart from that present in trace amount in the form of sponge spicules) is present in these deposits. The montmorillonites show SiO_2/Al_2O_3 ratios of 3.13 to 3.53 and these are within the range quoted for trachytes (see for instance the analytical data on trachyte flows presented by Engel and Engel, 1964). SiO_2/Al_2O_3 ratios of the montmorillonites could thus be a reflection of the ratios in the parental pyroclastic material.

Cowperthwaite et al.'s suggestion that the original pyroclastic material of the Cretaceous fuller's earths stemmed from volcanicity associated with the Mesozoic rifting of the North Atlantic is therefore supported by the evidence presented here.

6.2 ORIGIN OF THE SILURIAN INTERSTRATIFIED ILLITE/MONTMORILLONITES

6.2.1 Introduction

It has been noted (section 1.4.1) that interstratified illite/montmorillonite deposits of the potassium-bentonite type found in Lower Palaeozoic strata of the United States, Canada and Scandinavia are considered to represent the alteration products of fine-grained, wind-transported volcanic ash which had settled in a shallow-water marine

environment. The close similarities between these deposits and the illite/montmorillonite horizons occurring in Silurian strata of the Welsh Borderlands have been emphasised at various points in the present text (mode of occurrence, section 1.5.2; clay mineralogy, section 3.1.4; accessory mineralogy, sections 4.3.1 to 4.3.5; clay chemistry, section 5.4.2). Thus there appears no doubt that the parent material of the Silurian illite/montmorillonites was also of volcanic origin - a view shared by the few workers (e g. Butler, 1937; Trewin, 1971) who have examined these occurrences in any detail. However there are still a number of points which need clarification. Evidence of volcanicity in the area of the Welsh Silurian Geosyncline is sparse; in the following section the recorded instances are described and an attempt is made to suggest a possible source (or sources) for the parental material of these clay horizons. Controversy also exists over the nature and exact sequence of reactions involved in the transformation of ash to illite/montmorillonite, in particular the factor or factors controlling the eventual ratio of illite to montmorillonite layers in these clays. In section 6.2.3 this problem is discussed in some detail.

6.2.2 Nature and possible source of the original ash

Turner (1937) showed that the recorded instances of Silurian volcanism were distributed in a narrow belt extending from the Dingle Peninsula in south west Ireland, through Pembrokeshire and the Bristol district across to the mainland of Europe. This author suggested that the distribution of the Silurian volcanic centres was related to a subsequent trend of Variscan (Armorican) folding. Holland (1969) disagreed, considering rather that these occurrences were related to the marginal tracts of the Welsh geosyncline, the south eastern margin of which curved towards a westerly, or even north westerly, orientation in southern Ireland.

The succession at Dingle begins low in the Wenlock and extends into the Middle Ludlow (Holland, op. cit.). Rhyolitic lavas, agglomerates and ashes are intimately associated with the marine sedimentary sequence. Zeigler et al. (1969) have shown that the succession at Skomer Island and the Marloes Peninsula, Pembrokeshire, the top 1000 m of which is of Silurian age, includes basic lava flows, flow-banded rhyolites, ignimbrites and tuffs. This suite was assigned to the alkali-basalt - trachyte - sodium-rhyolite series and, according to these authors, formed in an oceanic environment with continental affinites. The volcanic rocks of the Mendip Hills and Tortworth area, Gloucestershire (Van De Kamp, 1969) are mainly rhyodacites, latites and andesites which occur both as ash flows and pyroclastics. These are all of the calc-alkaline type and would appear to have been formed in an orogenic continental environment.

Thus, during the Silurian, explosive volcanic activity did take place on the margins of the Welsh geosyncline and possibly also on the adjacent cratonic block. All the illite/montmorillonite horizons examined occur in facies of the shelf-sea type which had been deposited on the south eastern margins of the geosyncline. However as only the shelf sea environment would have provided conditions suitable for the accumulation of substantial quantities of ash this observation cannot necessarily be taken to signify that the volcanic sources were also located in the shelf area.

It has been shown in sections 4.3.1 to 4.3.5 that many accessory minerals of these clays were derived directly from the volcanic source. The presence of appreciable amounts of quartz in the assemblage of minerals of volcanic origin would indicate a source of acid to intermediate composition. From mineralogical evidence alone it is impossible to be more specific than this. However the range of values for the trace elements

Nb, Y, La and Ce (table 5.12) would suggest that the original pyroclastic material was derived from a source with alkaline affinities. Mineralogical and chemical evidence together would suggest that the parental material of the clay horizons had a composition near that of an alkaline rhyolite or, perhaps, a quartz-trachyte. The centres at Pembrokeshire, and possibly Dingle, could have provided pyroclastic material of this composition. (At Marloes, Pembrokeshire, the volcanic sequence is followed, unconformably, by the Wenlock Coralliferous Series, the basal 80 m of which contains fifteen illite/montmorillonite horizons (Ziegler et al., op. cit.)). Although the Tortworth, Gloucestershire, centre is nearest geographically to the illite/montmorillonite deposits of the Welsh Borderlands it is unlikely that this, or the Mendips centre, was a source of the ash. Van De Kamp (op. cit.) has presented trace element analyses of the various rock types present at these localities. Values for Nb, Y, La and Ce are much lower than shown by the illite/montmorillonite deposits and V, Cr, Ni and Co are markedly higher.

6.2.3 Alteration of the ash to illite/montmorillonite

Any model describing the sequence of reactions involved in the transformation of the ash to illite/montmorillonite has to account for the apparently contradictory observations noted as points (i) and (ii) in section 3.1.4.5. Features of the lattice chemistry of illite/montmorillonites in general (mentioned as points (i) to (iv) in section 5 2.3) also have to be explained.

The simplest model would involve alteration of the ash on the sea floor directly to a high-charge (beidellitic) montmorillonite. In this event the extent of K-fixation, and consequently the ratio of illite to montmorillonite layers, could have been determined once and for all by the composition of the montmorillonite - i.e. the higher the lattice charge the more K would be fixed (see Weir, 1965). The source of the

K could have been the ash itself; alternatively this element could have been extracted from the surrounding sea water. Bystrom (1956) suggested that thinner ash beds would have been more accessible to the overlying sea water and consequently could have fixed more K. The nature of the interstratified clays at Kinnekulle would appear to support this suggestion: the thicker beds are composed of illite/montmorillonite containing about 0.43K/unit cell whereas the thinner beds contain about 0.86K/unit cell (Bystrom, op. cit.)

There are, however, many reasons for regarding models of formation in which all processes occur essentially during the halmyrolitic stage as invalid (Hower and Mowatt, 1966). It is also unlikely that the ash altered directly to illite/montmorillonite. Potassium/argon dating carried out on minerals from the Kinnekulle clay horizons suggests that formation of illite/montmorillonite occurred long after deposition of the ash. Biotite, an original constituent of the ash, gave an age of 480 m.y., the enclosing illite/montmorillonite an age of 331 m.y., suggesting later incorporation of K (Bystrom-Asklund et al., 1961). A model more in keeping with current thinking would involve alteration of the ash first to montmorillonite. This process may well have been initiated during the halmyrolitic stage but would probably not have been completed until some point during the shallow burial stage (Muller, 1967). With deeper burial the montmorillonite would undergo a progressive reorganisation of lattice chemistry, notably an increase in Al-for-Si substitution in the tetrahedral sheet and/or increase in total lattice charge (see points (ii) to (iv) in section 5.3.2). With increase in charge more K would have become fixed: this element could have been present in sea water trapped in the original ash deposit but the main source would probably have been the ash itself, the K-bearing minerals of which breaking down with increasing depth of burial. A number of

authors have observed that interstratified illite/montmorillonite may form as a result of the diagenetic alteration of montmorillonite brought about by deep burial. Although these observations refer solely to the alteration of previously formed montmorillonite they do provide information on the later stages of the supposed transformation ash → montmorillonite → interstratified illite/montmorillonite and consequently are considered in some detail below.

Outcropping Tertiary and Cretaceous rocks and soils adjacent to the Texas Gulf Coast of the USA are dominantly montmorillonitic. Rivers draining this area contain appreciable amounts of montmorillonite in suspension and this mineral, together with variable amounts of detrital mica, quartz and feldspar, is deposited offshore. Perry and Hower (1970) and Weaver and Beck (1971) have monitored the mineralogical and chemical changes in the resulting sediments down to a depth of 8,000 m. Both sets of authors found that during the initial burial stages montmorillonite showed a progressive increase in amount of 'illite' layers until a fairly stable product containing 70-80% illite interlayers was formed. This occurred at temperatures in the region of 100°C: above this temperature the main diagenetic change appeared to be an increase in regularity of the interlayering. Weaver and Beck suggested that a further modification of the montmorillonite could involve the formation of interstratified illite/chlorite/montmorillonite and these authors saw the whole alteration process as part of a persistent evolution towards an equilibrium suite of muscovite, chlorite and quartz. According to Weaver and Beck the original montmorillonite may have adsorbed some K from seawater during the transport and deposition process although during the early diagenetic stages K was obtained from solution of feldspar. Perry and Hower, however, considered that breakdown of detrital mica during early diagenesis was the most likely source of the K. The increase in lattice charge, which these authors stressed was a necessary

concomitant to the transformation of montmorillonite to illite/montmorillonite was ascribed to (i) increase in Al-content of the tetrahedral sheet and (ii) valency reduction of octahedral Fe. The former process involved migration of interlayer Al through the ditrigonal holes in the basal oxygen planes and subsequent expulsion of an equivalent amount of Si from tetrahedral sites.

It was noted in section 3 1.4.5 (observation (i)) that at many localities in the Abberley district two or more clay horizons occurred within a vertical distance of a few metres, illite/montmorillonite ratios of clays from all horizons at a particular locality being identical. However the actual illite/montmorillonite ratio varied from locality to locality even though these were only a few kilometres apart. These observations can be explained by the 'progressive modification with depth' model. Ash horizons separated by only a few metres of intervening sediment would have been subject to essentially the same burial conditions and the resulting clays would therefore be expected to show identical illite/montmorillonite ratios. In the Abberley district faulting is extensive, bringing into contact sediments which may have been exposed to different burial conditions. This is probably the reason for the variation in illite/montmorillonite ratios of clays from different localities within this district. (To what extent these later tectonic events, with their attendant intense, if short-lived, temperature/pressure conditions, modified the diagenetic changes resulting from deep burial alone is, however, open to question). Two clay horizons containing different illite/montmorillonite ratios occur in the sequence at Overbury quarry (observation (ii), section 3.1.4.5) and this appears to be at variance with the 'progressive modification with depth' model. It could be that even under the same burial conditions thinner ash beds were more susceptible to diagenetic change. Differences in SiO_2/Al_2O_3 ratios of the original ash deposits and, possibly, the availability of K during

burial could also have influenced the eventual illite/montmorillonite ratios in these clays.

CHAPTER 7

THE USE OF CERTAIN PHYSICO-CHEMICAL PROPERTIES IN THE QUANTITATIVE EVALUATION OF MONTMORILLONITIC CLAYS

7.1 INTRODUCTION

In the preliminary stages of the evaluation of a montmorillonite deposit an assessment of the grade, i.e. montmorillonite content, of a large number of samples is normally required. The most accurate results would undoubtedly be obtained by applying some combination of chemical and mineralogical techniques - possibly, by very careful standardisation of operating conditions, even from the latter alone - but this approach is time consuming and in practice recourse has to be made to simple, rapid tests which can be applied on a routine basis. The use of such tests in the evaluation of a recently discovered montmorillonite deposit in the neighbourhood of Baulking and Fernham, Berkshire, has been described by Bain et al. (1971) and Bain and Morgan (1971). Tests used to good effect in the assessment programme included cation exchange capacity measurements by the methylene blue dye adsorption method and Atterberg plastic and liquid limits both before and after sodium-exchange (the latter evaluating the 'quality' of the clay as well as the grade). In this chapter three tests, surface area, methylene blue cation exchange capacity and liquid limit, are investigated in detail, mainly with reference to their relative merits in assessing the grade of a montmorillonite-bearing clay. Development of the physico-chemical properties of montmorillonite is influenced largely by the degree of dispersion of the clay. Sansom and White (1970) (1971) have stressed that identical pretreatments do not necessarily bring different montmorillonite to the same state with regard to interparticle association

(according to these authors few pretreatments do break down particle associations completely). Consequently emphasis is placed on the type of pretreatment used prior to testing and also its efficiency in disrupting interparticle associations. In this respect testing the hydrocyclone overflow and underflow products - which represent two opposite extremes of particle association within a particular sample - was especially productive.

When assessing the economic potential of montmorillonites of the fuller's earth-type an important factor is the ease with which the divalent exchangeable cations may be replaced by sodium. This process may give a product similar to a natural bentonite and extend appreciably the range of possible uses of the original clay. In this chapter liquid limits, together with some viscosimetric measurements, are used to monitor the response of selected samples to step-wise addition of sodium carbonate up to, and above, the amount required to satisfy the exchange capacity of the clay. Methods normally used in the laboratory for the preparation of sodium-exchanged clays (see, for instance, Van Olphen, 1963) are too lengthy and tedious when used on a large scale (Bain, 1971). The exchange procedure used both in industry (Hofmann, 1959; Grim, 1962) and in laboratory evaluation tests (Bain and Morgan, op. cit.) simply involves the addition of powdered anhydrous sodium carbonate to the dry clay, this being followed by a period of grinding to ensure intimacy of mixing. When water is added sodium carbonate goes into solution and sodium occupies the exchange positions on the clay surfaces. The divalent cations liberated are then precipitated as carbonates. The effectiveness of other soluble salts of sodium which also form insoluble calcium salts - i.e. the tungstate, oxalate and molybdate - has been assessed by viscometry (Ritchie and Gregg, 1965) and liquid limit determinations (Bain, op. cit.). By both methods these salts were shown to be inferior to sodium carbonate.

Appendix 6 contains descriptions of the various tests mentioned in this chapter.

7.2 MONTMORILLONITES

7.2.1 Surface areas

Variability in published values (750-810 m^2/g) for the theoretical surface area of montmorillonite is due mainly to uncertainty as to the precise contribution to total surface from the edges of montmorillonite particles. Isomorphous substitution within the montmorillonite lattice, which affects both dimensions and weight of the unit cell, may also be a minor contributing factor as not all authors have chosen identical type formulae for this mineral. The calculation of theoretical surface area for montmorillonite is described by Van Olphen (1963).

The use of the BET method for measuring montmorillonite surface area is limited. Non-polar molecules, such as N_2 and CO_2, cannot penetrate the montmorillonite lamellae to any great extent and only the surface external to crystal aggregates is determined. An extreme case has been recorded by Greene-Kelly (1964). Films of Na- and Ca-forms of the same montmorillonite showed surface areas of 5 and 30 m^2/g respectively to N_2 and it was apparent that little more than the external surfaces of the films themselves were being measured. The larger value obtained from the Ca-montmorillonite film was due to its greater porosity (Greene-Kelly, op. cit.). In compressed-core samples of Na- and Cs-montmorillonite Aylemore et al. (1970) found that the presence of some residual water molecules enhanced both N_2 and CO_2 penetration of montmorillonite lamellae. On completely outgassed samples surface areas were affected both by the nature of the exchangeable cation - Cs-montmorillonites forming a more open matrix and thus giving larger values - and the size, and apparent affinity for the clay

surface, of the adsorbate molecules. The highest value recorded by these authors was only 215 m^2/g (for CO_2 on Cs-montmorillonite). Application of the BET theory to water vapour adsorption on montmorillonite might be expected to provide a figure close to the theoretical surface area due to the polar nature of the water molecule. In practice results are rarely reproducible and considerable hysteresis occurs between adsorption and desorption. Values no higher than 250 m^2/g have been reported for the surface area of Na-montmorillonite by this method (Johansen and Dunning, 1959).

Methods based on the adsorption of highly polar organic molecules, such as ethylene glycol or ethylene glycol monoethyl ether (EGME), are far more promising and do provide realistic values for the surface area of montmorillonite. These methods depend on the formation of a stable monolayer of adsorbate molecules on the montmorillonite unit cell surface; experimental details are given in Dyal and Hendricks (1950) and Carter et al. (1965). The amount of time needed to reach equilibrium varies enormously with different adsorbate molecules. For EGME, equilibrium is reached in a number of hours. It is doubtful whether ethylene glycol actually forms a stable monolayer cover on montmorillonite, and readings, taken over a period of days, have to be extrapolated to obtain an 'equilibrium value'. In order to obtain a surface area value the amount of adsorbate retained by the clay at equilibrium is multiplied by a conversion factor. This, in turn, is calculated from the amount of adsorbate retained at equilibrium by a pure montmorillonite of known structural formula (from which the theoretical surface area is calculated).

The amount of adsorbate retained by montmorillonite has been shown by a number of authors to depend to some extent on the nature of the exchangeable cation. Eltantawy and Arnold (1973) have also suggested that some procedures used for surface area measurements by EGME produce incomplete unimolecular layers in which the extent of EGME retention is

almost certainly determined by exchangeable cation-EGME interaction and not by the real extent of the clay surface.

EGME surface areas of the present samples were determined by the procedure of Carter et al. (op. cit.). Results for original samples and respective hydrocyclone products are given in table X6.1. The montmorillonite overflow products gave surface areas in the range 721 to 820 m^2/g. Those showing values in the lower part of the range contained impurities - for example, sample A5 (721 m^2/g), which contained gypsum and calcite, and sample A15 (745 m^2/g), which contained about 5% feldspar and traces of sulphide. It is unlikely that any single factor is responsible for the variation in the upper part of the range (i.e. 770-820 m^2/g). Experimental error of the method, the presence of small amounts of impurities, differences in the exchangeable cation assemblage and variation in montmorillonite surface morphology may all be important. Experimental error (precision of measurement) is within $\pm$ 1%. From mineralogical and chemical evidence no more than 2% total non-clay impurities appear to be present in these particular overflow products. Significantly lower EGME surface areas have been reported for Mg- as opposed to Ca-saturated montmorillonites (Davis et al., 1971): surface areas of the present clays might therefore be expected to reflect differences in exchangeable Ca/Mg ratios. This does not appear to be the case. Sample A4, with over a third of the exchange sites occupied by Mg, gave a surface area of 785 m^2/g; both higher and lower values were shown by samples containing less exchangeable Mg.

For all overflow products showing surface areas in the upper part of the range described above, the actual surface area value was assumed to represent 100% montmorillonite. Amounts of montmorillonite in original samples and underflow products were then obtained by comparison of their surface areas with those of the respective overflow product. In this way a measure of the extent of upgrading produced by hydrocycloning

each sample was obtained. An estimate of montmorillonite content of some of the lower grade samples from which no overflow products were produced was made by assuming a surface area of 785 m^2/g for the montmorillonite constituent. Sample A16, for instance, gave 42% montmorillonite by this procedure; the only other mineral present in the sample was calcite for which thermogravimetry gave a figure of 56 %. Montmorillonite percentages of original samples and hydrocyclone products, obtained as described above, were also used in assessing the dispersion-dependency of other physico-chemical tests described later in this chapter as interlayer penetration by the polar EGME molecule is independent of the dispersed state of the clay.

7.2.2 Methylene blue cation exchange capacities

When discussing the structural formulae of the analysed montmorillonites(table 5.4) it was noted that the cation exchange capacities (CECs) measured by methylene blue dye adsorption did not exceed 82% of the CEC calculated from the lattice charge. The methylene blue cation is raft-shaped and may assume three different orientations at a solid surface (Kipling and Wilson, 1960). If adsorbed 'edgewise' or 'on end' the cation occupies 75 or 39.5 A^2 respectively. On clays it is usually assumed to be adsorbed 'flat', occupying an area of 135 A^2. It is the large size of the methylene blue cation in relation to the area available at each exchange site on the surface of the montmorillonite unit cell particle which is primarily responsible for the deficit noted above. Bodenheimer and Heller (1968) have shown that the extent of methylene blue adsorption is also influenced by the state of dispersion of the montmorillonite. The mechanism of dye sorption by montmorillonite will be examined below, sample A4 being used as an example. In this section CEC refers to the property measured by dye sorption unless specified otherwise.

The overflow product from sample A4 gave a CEC of 91.2 meq/100g. The original sample had given a CEC of only 72.6 meq/100g in spite of a montmorillonite content in excess of 98%. However, CECs of between 90 and 92 meq/100g were eventually obtained from the original sample after this had been subjected to ultrasonic and high shear dispersion. By using the value of 92 meq/100g - which appears to represent the maximum amount of dye which can be adsorbed - in conjunction with the EGME surface area of 791 m^2/g it may be shown that each methylene blue cation (lying flat) occupies 144 A^2 on the clay surface. This is greater than the area assigned to each exchange site on the basis of lattice charge CEC, the latter being of the order of 110 A^2. Replacement of exchangeable cations by methylene blue apparently ceases when the montmorillonite surface is covered by a monolayer of flat-lying methylene blue cations even though the lattice charge CEC has not been satisfied. Results for sample A4 are in very close agreement with observations made by Hang and Brindley (1970). These authors also found that adsorption stopped on a Ca-montmorillonite at 90 meq/100g dye following monolayer formation. For the Na-exchanged clay, however, dye adsorption up to the lattice charge CEC of 120 meq/100g was noted. From an X-ray study of interlayer spacings of the Na-montmorillonite/dye complex Hang and Brindley suggested that 'edgewise' adsorption of the methylene blue cation occurred - the alternative would have been to postulate formation of multilayers of flat-lying cations.

In fig. 7.1 CECs of the original samples and hydrocyclone products are plotted against percentage montmorillonite (determined from surface area measurements as described in section 7.2.1). The bold line running from the origin to 97 meq/100g represents theoretical maximum cover of methylene blue cations, adsorbed flat, for any particular percentage montmorillonite. In order to obtain this line a value of 785 m^2/g was taken as the average montmorillonite surface area. The other two lines

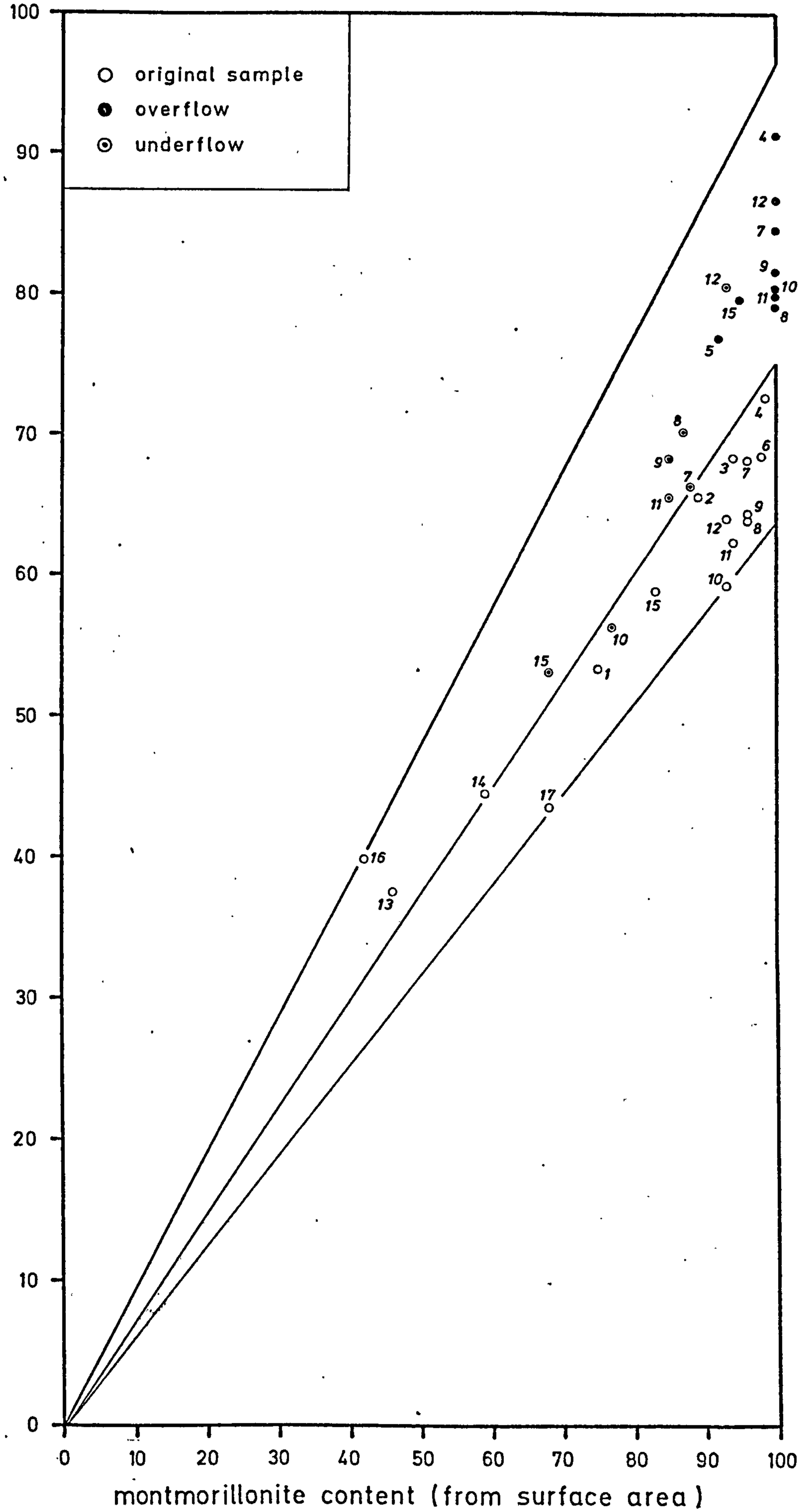

Fig. 7.1 Plot of CEC v. montmorillonite content for montmorillonite original samples and hydrocyclone products

on the diagram are arbitrary. The middle line is the regression from 75 meq/100g (previously assumed by Bain et al. (1971) to be the maximum CEC shown by Ca, Mg-montmorillonites under normal preparative techniques) to the origin. This line is discussed below in relation to the quantitative assessment of montmorillonite. The bottom line is also useful in this respect as, for the present samples, it defines an upper limit to the experimental error in such quantitative determinations.

The four chemically analysed montmorillonite overflow products showed quite large variations in lattice charge CEC (table 5.4). The range of methylene blue values shown by these overflow products plotting at 100% montmorillonite in fig. 7.1 is, however, mainly a function of degree of dispersion of the clays prior to CEC determination. Sample A4 approaches 'perfect' dispersion. For the original samples dispersion is less efficient (but more uniform?) than in corresponding overflow products which have been subjected to the shearing forces of the hydrocyclone. Semi-quantitative measurement of montmorillonite in original samples thus appears feasible, although assuming a value of 75 meq/100g for 100% montmorillonite would, on the basis of the present data, lead to underestimation at montmorillonite contents above 70%. The value of 70 meq/100g appears more realistic. Whether 70 or 75 meq/100g is chosen to represent 100% montmorillonite there is is a danger of overestimation at montmorillonite contents below 50%. Compared with the original samples the underflow products show consistently high CECs for a given montmorillonite content. No satisfactory explanation can be given for this phenomenon.

7.2.3 Liquid limits

7.2.3.1 General

Atterberg recognised five distinct stages in the development of a clay-water system from a maximum cohesive condition at low water content to a fluid slip at high water content (Bauer, 1960). The boundaries between these stages were defined empirically. Two of the transition points, now called plastic limit and liquid limit, have found widespread use in characterising soils for civil engineering purposes and standard procedures have been drawn up for their determination (BSS: 1377, 1967). Bain (1971) has shown that, used together, the plastic and liquid limits may be of particular value in the identification and economic assessment of a range of industrial clays. Liquid limits have also been used in assessing the suitability of montmorillonites for foundry use (Navarro and Taylor, 1959).

Liquid limit determinations were carried out on the present samples both in their original state (section 7.2.3.2) and also after Na-exchange (section 7.2.3.3). Plastic limits were not determined because (i) differences between the plastic limits of Ca, Mg- and Na-montmorillonites are of much less diagnostic value than differences between the respective liquid limits and (ii) in contrast to liquid limit measurement, determination of the plastic limit of montmorillonite is a more subjective process and in the case of the Na-exchanged clay, often liable to error.

The liquid limit may be considered a measure of the resistance of a montmorillonite-water paste to external shearing forces. Up to the liquid limit water must be immobilised in the montmorillonite-water paste; at the liquid limit sufficient free water is present to allow this to flow as a mud under a small applied load (section X6.3). Immobilisation of water may either be 'passive' (i.e. resulting simply because the water molecules are trapped within a network of montmorillonite

particles) or 'active' (as a result of interaction between the water molecules and the surface of the montmorillonite particles). Grim has long held that the plasticity of clay-water pastes is due to the non-liquid nature of the water initially adsorbed by the clay surface. According to this author (1962), the liquid limit comprises both the water which can be held with any substantial rigidity on the clay particle surfaces and the water enclosed 'passively' within the pores (at least part of which is in the liquid state). Typical values from the literature (e.g. White, 1958) show that Ca,Mg-montmorillonites may take up to twice, and Na-montmorillonites up to seven or eight times, their weight in water at the liquid limit. In water Na-montmorillonites disperse into particles approaching unit cell thickness which form a rigid network as a result of attraction between positively charged edges and negatively charged faces (Van Olphen, 1963; Mungan and Jessen, 1963). In Ca,Mg-montmorillonites more particles are therefore available to trap water molecules 'passively' and also a larger proportion of the theoretical surface area is available to react with the water molecules. This latter factor is the more important.

Much evidence has been accumulated over the last few years for the alteration of water properties by clay surfaces (see summary by Low and White, 1970). It is generally agreed that the water sorbed by a clay surface has a density greater than liquid water but there is still some controversy over the exact mechanism by which the first few molecules are retained. Ravina and Low (1972) have suggested that an epitaxial relationship exists between the crystal lattices of montmorillonite (in the Na-exchanged form) and adsorbed water. According to these authors the influence of the montmorillonite surface may extend several hundred angstroms into the surrounding water, the exact distance being a function of the deviation of the b-dimension of the montmorillonite unit cell from 9.0A. The influence of the exchangeable cation on the development of

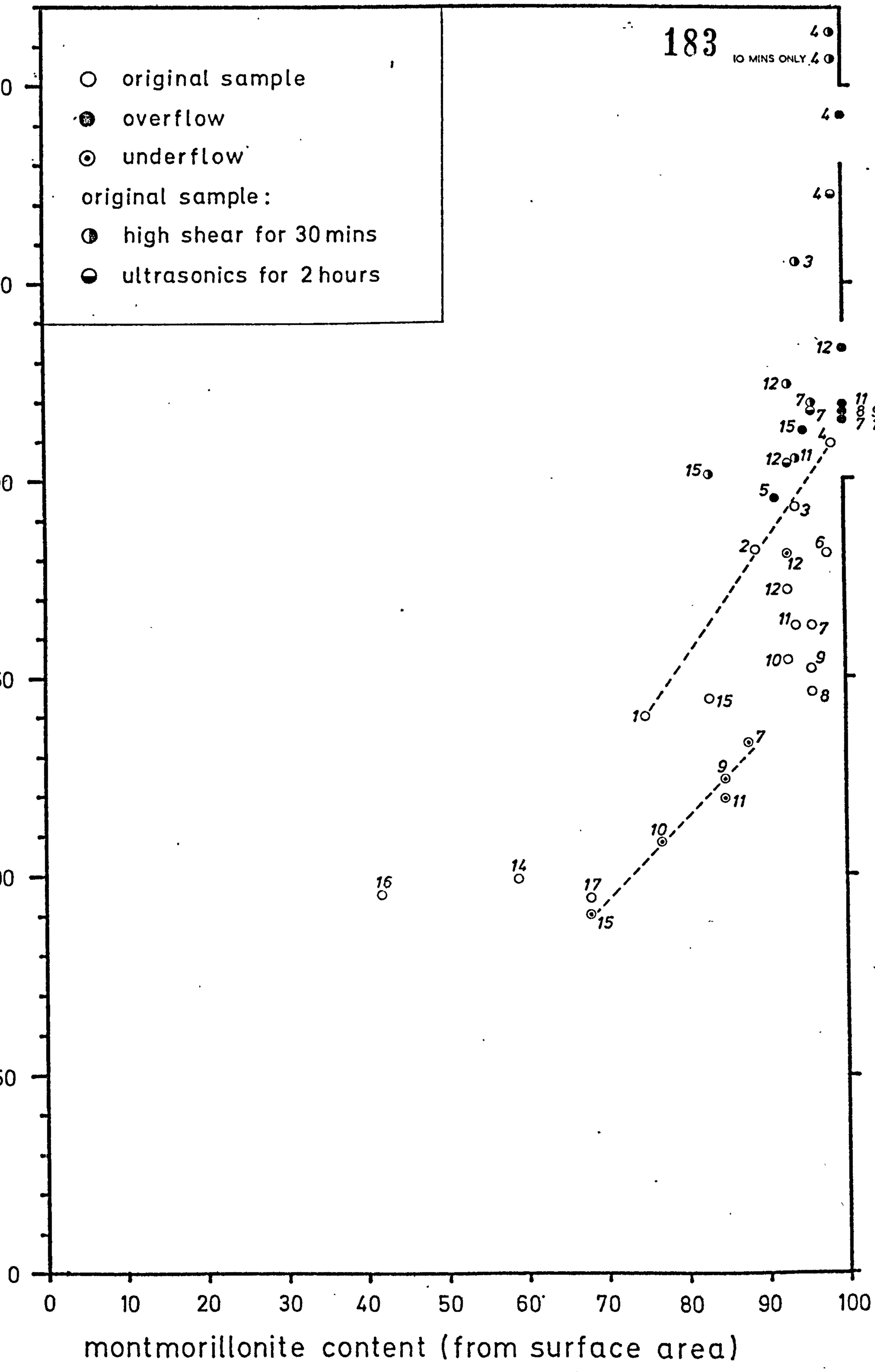

Fig. 7.2 Plot of liquid limit v. montmorillonite content for montmorillonite original samples (some after high-shear and ultrasonic treatment) and hydrocyclone products

the adsorbed water structure on the montmorillonite surface is not clear The Na ion does not exhibit hydration characteristics, and whilst it may not enhance, equally does not hinder the development of adsorbed water layers (Grim, op. cit.). The divalent cations, however, show a marked tendency towards formation of hydration shells which might be expected to disrupt the symmetry of the adsorbed water layers.

7.2.3.2 Original samples and hydrocyclone products.

In fig. 7.2 liquid limits of original samples and hydrocyclone products are plotted against montmorillonite content. At montmorillonite contents exceeding 95% liquid limits range from 146 (A8, original sample) to 314 (A4 subjected to high-shear dispersion). This latter figure is much higher than any previously recorded for Ca,Mg-montmorillonite. Even after taking precautions to minimise the effects of particle aggregation White (1958) found that the highest liquid limits given by <1 micron homoionic Ca- and Mg-montmorillonites were 177 and 199 respectively.

Original samples from Woburn (A7) and Nutfield (A8-12), all containing between 93 and 96 % montmorillonite, gave liquid limits ranging from 146 to 172. No correlation between liquid limit and amount of montmorillonite was apparent. However, linear relationships were found between montmorillonite content and liquid limit of the four Baulking original samples (A1-4) and also (but with a different gradient) all the underflow products with the exception of A12. The respective regression lines are marked in fig. 7.2. Liquid limits of the overflow products from samplea A7-11 cluster between 210 and 220; A12 gives a somewhat higher value of 233, and a liquid limit of 292 is shown by the overflow product from A4.

The large increase in liquid limit from original sample to overflow product, for only a small gain in montmorillonite content, must result from the breakdown of montmorillonite aggregates under the high-

shear conditions of the hydrocyclone separation process. The range of liquid limit values shown by the overflow products suggests that disaggregation had been more successful for some montmorillonites than others. To resolve whether these differences were real, selected original samples were subjected both to the high-shear dispersion conditions of a Braun liquidiser (working at 13,000 rpm) and also to prolonged ultrasonic treatment Liquid limits of these treated samples are also plotted in fig. 7.2 . It should be noted that as the liquid limits are plotted against montmorillonite content of original samples they are not strictly comparable with the liquid limits of the overflow products which contain slightly higher montmorillonite contents. Sample A4 gave a liquid limit of 307 following ten minutes high-shear in the Braun liquidiser; a value of 314 was shown after thirty minutes and this would appear to be the maximum attainable under these conditions. The liquid limit of 292 shown by the hydrocyclone overflow product suggests that comparable disaggregation was being attained by both methods, bearing in mind the shorter time (approximately five minutes) the clay was in the hydrocyclone. Ultrasonic treatment was not as efficient in causing interparticle breakdown but, nevertheless, led to an enhanced liquid limit for A4 (272 compared with 209 for the original sample). High-shear treatment of A3 and A12 resulted in liquid limits in excess of 220, but for the latter sample the overflow product value was not reached - probably because of the presence of 7% sand/silt size siderite in the original sample which had been removed from the overflow product. Ultrasonic dispersion of A12 was even less effective. Both high-shear and ultrasonic treatment of A7 resulted in liquid limits so close to the overflow product value to suggest that a 'steady state' (in the sense of Sansom and White, 1970) had been achieved.

From the above results it appears that the extent of particle association following dispersion is an inherent property of each individual

sample. It is doubtful whether this phenomenon can be related to differences in the exchangeable cation assemblage of the montmorillonite. Table 5.9 shows that the main variation lies in the ratio of exchangeable Ca to Mg In samples A3 and A4, both of which gave maximum liquid limits above 250, about 30% of the exchange positions are occupied by Mg. About 15% exchangeable Mg is present in A12 which had a maximum liquid limit of 233. However, both A7 and A15 gave liquid limits below 220 but contain between 15 and 20% exchangeable Mg. The extent of primary aggregation in the samples may be a function of their geological history, especially compaction due to overburden pressure. It should be emphasised that all liquid limit determinations were carried out on material which had been air-dried, then ground to pass 100 mesh. Simple re-aggregation, consequent only upon drying, did not therefore inhibit development of high liquid limits once the primary aggregates had been dispersed.

7.2.3.3 Sodium-exchanged clays

The response of original samples and respective overflow products to step-wise addition of sodium carbonate is illustrated in fig. 7.3. The maximum liquid limits achieved by the original samples after Na-exchange were found to differ appreciably - the range was 360 to 625. For the overflow products the range was even larger (430 to 760). Most samples developed maximum liquid limits after the addition of between 4 and 5% sodium carbonate. Sample A7, however, showed a markedly slower response and the maximum liquid limit was reached between 5 and 6% sodium carbonate. This could be related to the formation of an impervious skin of Na-exchanged clay on incompletely dispersed aggregates (Ritchie and Gregg, 1965). Addition of sodium carbonate in excess of that required by the CEC of the montmorillonite resulted in a slight reduction in liquid limit for all the samples (see also Bain, 1971). Both a sharper, and larger, reduction might have been expected on the basis of

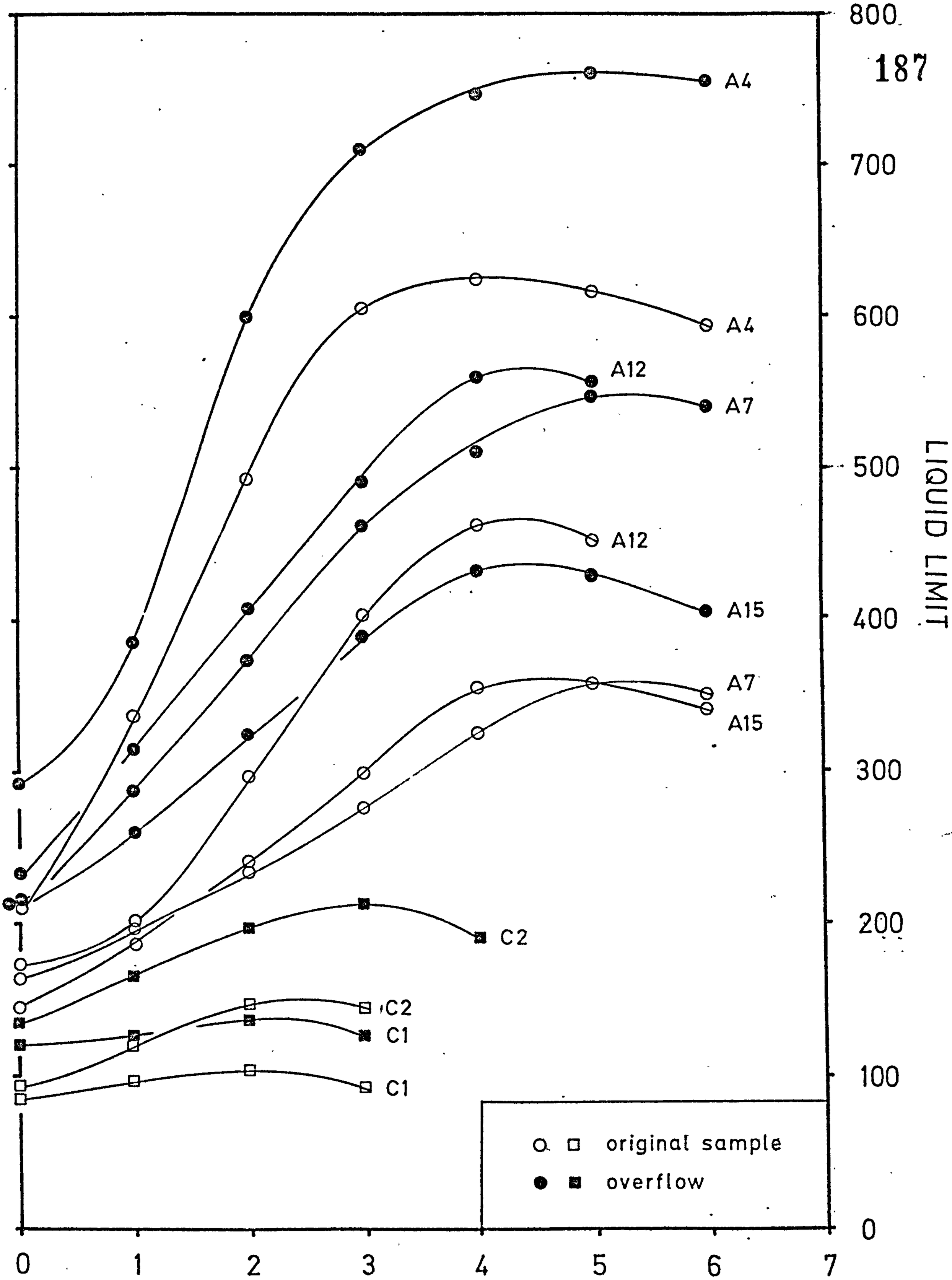

Fig. 7.3 Plot of liquid limit v. % sodium carbonate addition for montmorillonite and mixed-assemblage clay original samples and hydrocyclone overflow products

Table 7.1 Size analyses of montmorillonite hydrocyclone overflow products (calgon used as dispersing agent)

Sample	Cut-off size (microns)	Amount > 2 microns (%)	Amount < 2 microns (%)
A4	? < 2	-	100
A7	8	6	94
A12	< 5	1	99
A15	? > 10	23	77

data presented by Warkentin (1961). This author found that excess sodium chloride, at a concentration of only 0.1N, caused a 50% reduction in the liquid limit of a natural Na-montmorillonite.

Size analyses of original samples A7 and 15 (table X3.3) showed that numerous silt-size montmorillonite aggregates were present. No such aggregates were indicated from the size analyses of samples A4 and 12. The latter clays gave much higher maximum liquid limits. It was noted in the previous section that the shearing action of the hydrocyclone ensured that particle aggregation was much less in overflow products than in corresponding original samples. Size analyses of the overflow products from four of the samples are given in table 7.1. Although the data apply only to the fine-silt size range it is reasonable to assume that they are a reflection of the overall extent of particle association in the overflow products. The amount of particle association in the overflow products thus appears to decrease in the order A15-7-12-4: from fig. 7.3 it is seen that the maximum liquid limits after Na-exchange increase in this order. It is obvious that grade, i.e. montmotillonite content, has little influence on the magnitude of the liquid limit after Na-exchange. The controlling factor is the extent of aggregate breakdown in the montmorillonite. This observation is surprising as it might be expected that after Na-exchange dispersion would be more uniform - perhaps even resulting in particles approaching unit cell thickness - and it is also difficult to reconcile with the fact that maximum liquid limit values were reached following addition of sodium carbonate more or less equal to the amount required for complete Na/Ca, Mg exchange. The conclusion which must be drawn is that the montmorillonite aggregates retain their integrity even after Na-exchange. This being so, the mechanism of sodium carbonate/Ca, Mg-montmorillonite interaction must be more complicated than supposed (see section 7.1), and perhaps involves chemisorption of sodium carbonate on the surfaces of

montmorillonite aggregates as suggested by Szanto et al. (1967).

7.2.4 Viscometry

Measurements were made on suspensions of selected original samples with a Fann viscometer. Preparation of the suspensions (all 5% with respect to the oven-dried clay) is described in section X6.4. Step-wise addition of sodium carbonate was again employed: the figures in table 7.2 are the maximum viscosities obtained for each sample in the range 4 to 6% addition. Above 6% sodium carbonate addition plastic viscosities decreased but apparent viscosities showed considerable fluctuation.

The apparent viscosity of a montmorillonite suspension is made up of two distinct components - the plastic viscosity and the yield value (see Van Olphen, 1963). Plastic viscosity is a mechanical phenomenon and is created by friction between the clay particles, between these and the liquid which surrounds them, and by the shearing of the liquid itself. The yield value is the part of the apparent viscosity which is dependent upon the attractive forces existing between the particles. Thus the plastic viscosity is a measure of the extent of disaggregation of the clay whereas the apparent viscosity also takes into account the electrochemical state of the suspension.

A strict correlation between plastic viscosity and liquid limit after Na-exchange was not shown by the present samples although A4 did give the highest and A15 the lowest values for both parameters. Plastic (and apparent) viscosities were high for A7 in spite of the poor response to Na-exchange as monitored by liquid limit (fig. 7.3). With this exception plastic viscosities increased in the same order as the liquid limits of the original samples after high-shear dispersion. Thus the viscosimetric results support the conclusions drawn in the preceeding section.

Table 7.2 Apparent and plastic viscosities of 5% suspensions of original montmorillonite samples (maximum values recorded after additions of 4-6% sodium carbonate)

Sample	Apparent viscosity cp	Plastic viscosity cp
A3	33	12
A4	42	14
A7	29	12
A11	9	7
A12	12	8
A15	7	6

7.3 MIXED-ASSEMBLAGE CLAYS

This small group of samples was included in the present study in order to obtain some indication of the physico-chemical behaviour of montmorillonite in mixtures containing other clay minerals. For this purpose, figures for the montmorillonite content of the samples were essential. These were obtained by assuming that the total EGME surface area of the samples was due only to montmorillonite, a value of 785 m^2/g being taken for the surface area of this mineral. This operation was thought justified as EGME surface areas of kaolinite rarely exceed 40 m^2/g and values recorded for clay- and silt-size chlorite and mica are of the order of 20 and 10 m^2/g respectively (DJM - unpublished data).

The mixed-assemblage clays gave much higher liquid limits than (impure) fuller's earths containing the same amount of montmorillonite. This is partly a result of the contribution to plasticity from the other clay minerals in the mixed-assemblage clays (the impure fuller's earths examined contained only non-clay impurities with no plastic properties). However the better dispersion of the montmorillonite in the mixed-assemblage clays may be a more important factor. Liquid limits of original samples and hydrocyclone products after step-wise addition of sodium carbonate are recorded in fig. 7.3. The contrast between liquid limits before and after Na-exchange is not as great as might be expected from a comparison with the behaviour of the fuller's earths in the same figure. The overflow products from samples C1 and 2 contain only 38 and 50% montmorillonite respectively. It would appear that significant amounts of other clay minerals interfered with the ability of the Na-exchanged montmorillonite to form a rigid gel.

In fig. 7.4 values for surface area and methylene blue CEC given by sample C3 and hydrocyclone products are plotted separately against % particles less than 2 microns in these (product numbering is the same as in fig. 2.3b). A straight line relationship exists between

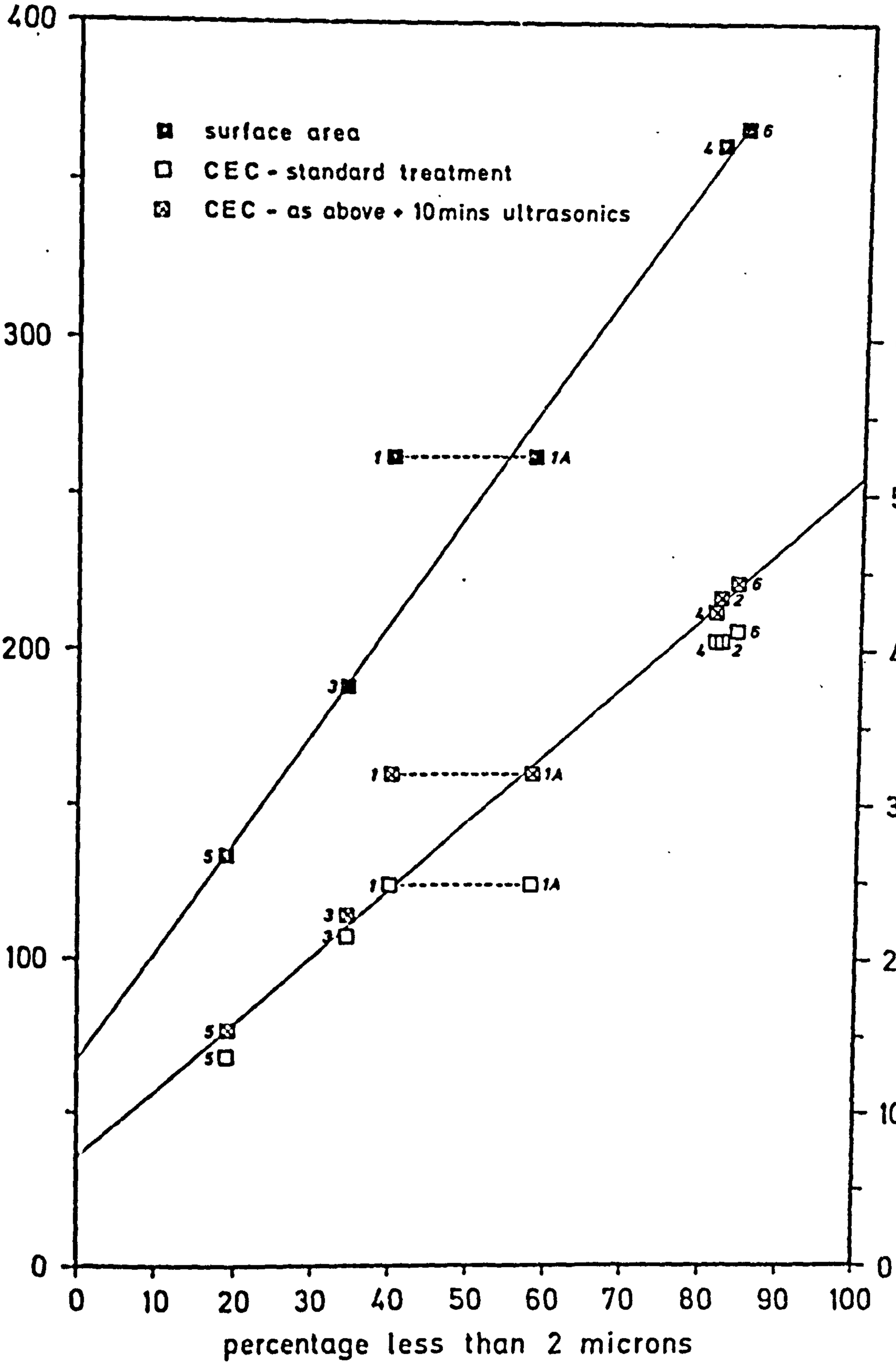

Fig. 7.4 Plots of surface area and CEC v. % particles less than 2microns for sample C3 and hydrocyclone products

surface area and % less than 2 microns It was noted in section 2.2.3 that particle size analysis of the original sample gave a value of 42% less than 2 microns but that the figure back-calculated from % less than 2 microns in hydrocyclone overflow and underflow products was 58%. On the diagram, point 1 is the plot of surface area v. 42% less than 2 microns and point 1A the plot of surface area v. 58% less than 2 microns. It is obvious that the figure of 58% less than 2 microns is the correct one. A linear relationship also exists between CEC and % less than 2 microns. Ultrasonic treatment prior to determination increased the CEC values slightly over those obtained by following the standard pre-treatment (section X6.2); the regression line in the figure is drawn through plots of % less than 2 microns v. CEC after ultrasonics. An interesting point arises in relation to the original sample. Plots of CEC (standard treatment) v. the (false) figure of 42% less than 2 microns and CEC (after ultrasonics) v. the (true) figure of 58% less than 2 microns both fall on the regression line. This would suggest that (i) the amount of methylene blue sorbed is governed by the degree of dispersion of the clay and (ii) essentially similar dispersed states were achieved both by the shear conditions within the hydrocyclone and by ultrasonics. Both regression lines indicate that particles larger than 2 microns are contributing significantly to surface area and CEC. Linear relationships similar to these just described were also found for sample C1 and products. The existence of such proportional relationships in samples of this composition might at first seem surprising; in C1, for instance, the relative amounts of montmorillonite, kaolinite and mica in the hydrocyclone products were shown to vary appreciably (section 2.3.2). However it was noted at the beginning of this section that, compared to montmorillonite, the other clay minerals make only a minor contribution to surface area; the same holds also for CEC. This factor, coupled with the fact that the major variation between the three

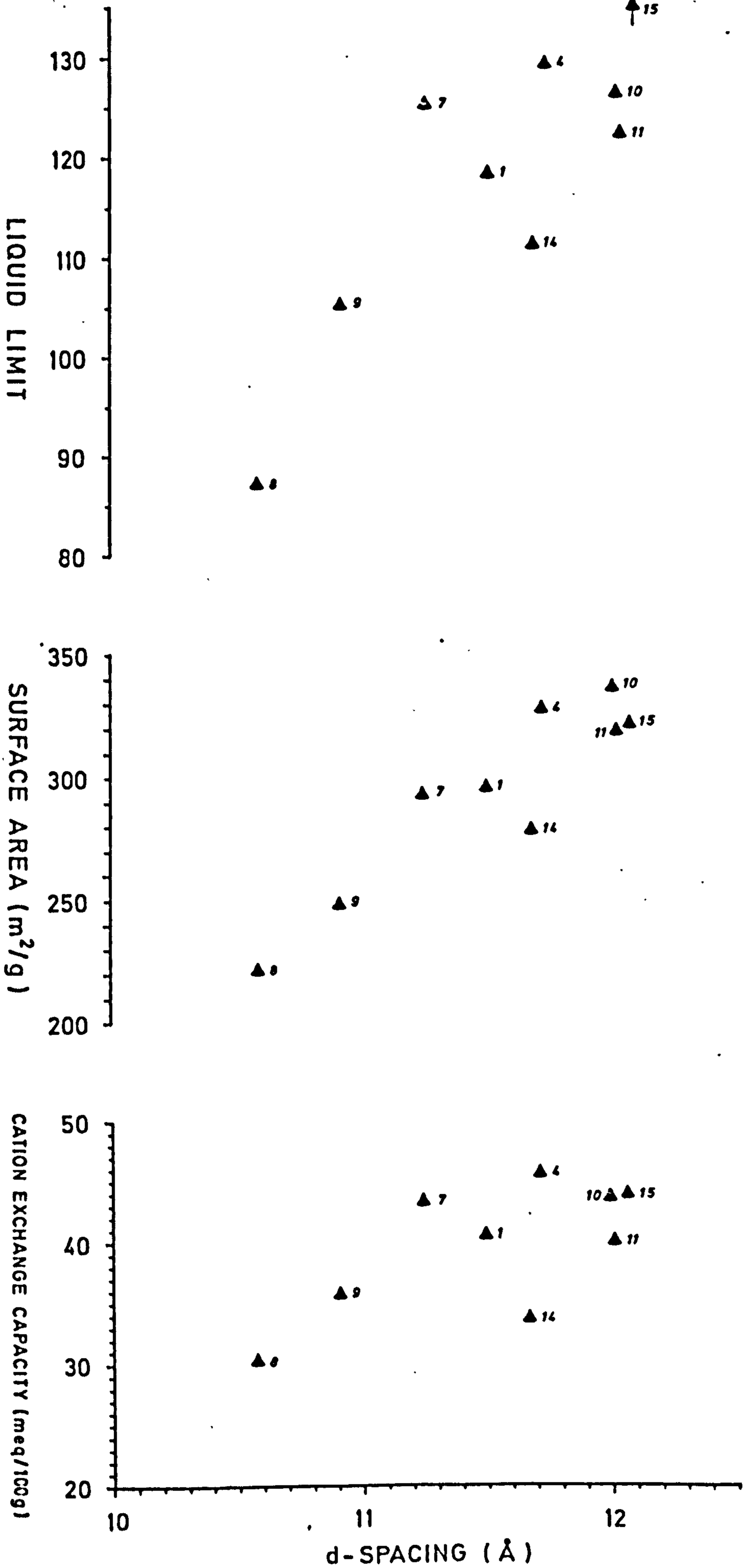

Fig. 7.5 Plots of liquid limit, surface area and CEC v. 001/001 d-spacing for interstratified clay hydrocyclone overflow products

clay minerals occurs in the fine silt sizes, explains the close correlation between these parameters.

7.4 INTERSTRATIFIED ILLITE/MONTMORILLONITES

7.4.1 Dependence of physico-chemical properties on illite/montmorillonite ratios

In fig. 7.5 surface area, methylene blue CEC and liquid limit values are separately plotted against 001/001 d-spacings of the hydrocyclone overflow products. If the low values shown by sample B14 are disregarded (these are caused by the presence of chlorite) then all three properties appear to show a roughly linear response to increase in 001/001 d-spacing. From approximately 10.5 to 13A the 001/001 peak migration curve for 10/15.4A interstratifications (MacEwan et al., 1961, p. 418) is a straight line. Thus surface area, CEC and liquid limit increase linearly with increase in montmorillonite interlayering in these clays. As the 001/001 peak migration curve shows a marked change in slope below 10 and above 40% montmorillonite layers, extrapolation of the regression lines to obtain values for the 'illite' and 'montmorillonite' end-members would not be justified. When percentage montmorillonite layers (values from table 4.1) were plotted against the respective surface area, CEC and liquid limit values straight line relationships were still obtained although the scatter was marked. Extrapolation to the 'illite' end member gave approximate values of 60 m^2/g for the surface area, 6 meq/100g for the CEC, and 30 for the liquid limit. Extrapolation to 100% 'montmorillonite', however, gave unrealistically high values for all three properties.

A complete set of surface area, CEC and liquid limit results for original samples and hydrocyclone products is given in table X6.2.

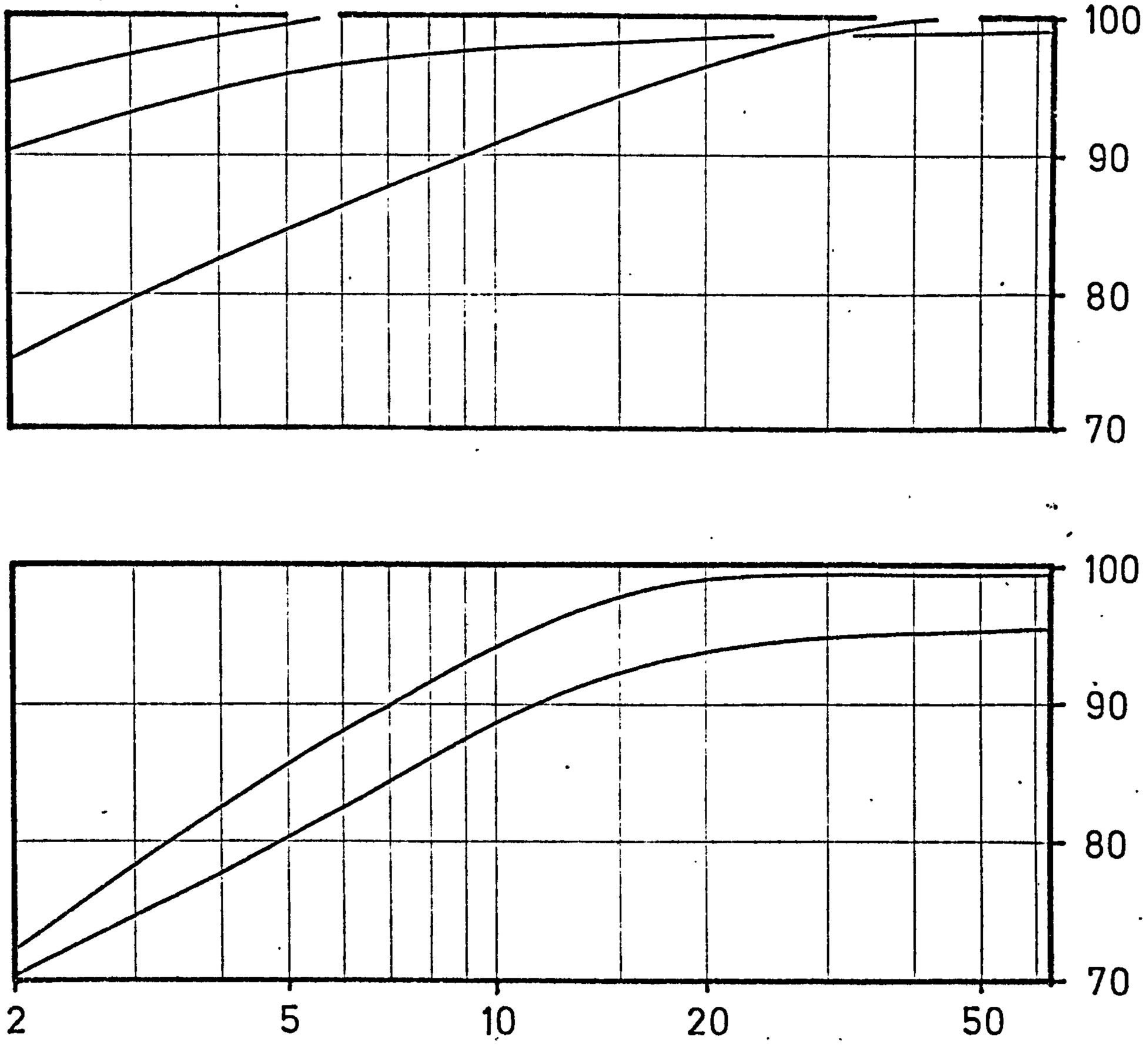

SAMPLE	SURFACE AREA m^2/g	CEC meq/100g	LIQUID LIMIT
B4 orig	317	33·1	100
B4 o/f	327	45·6	129
B4 u/f	298	36·9	88
B3 orig	312	-	79
B5 orig	292	-	74

Fig. 7.6 Particle size distribution curves and tabulated surface area, CEC and liquid limit data for the interstratified clay original samples and hydrocyclone products from Woodbury Quarry

7.4.2 Dispersion-dependency of properties

The dispersion-dependency of both the methylene blue,CEC and liquid limit tests is well illustrated by the results obtained on clays from Woodbury Quarry (samples B3, 4, 5 and products). Particle size distribution curves, together with tabulated values for surface area, CEC and liquid limit, are shown in fig. 7.6. Illite/montmorillonite ratios of the interstratified clays from all these samples and hydrocyclone products were found, by X-ray diffraction, to be identical; the actual interstratified clay contents of these were obtained by comparing their surface area values with that of the overflow product from sample B4 which was assumed, from chemical and X-ray evidence, to consist of 100% interstratified clay. Samples B3 and 4 were collected from the same clay band: B3 was from a freshly exposed face and B4 from its weathered equivalent on the opposite side of the quarry. The marked difference in liquid limits between sample B3 (95% total interstratified clay) and B4 (97% total interstratified clay) must result from the presence in the former of almost 30% fine- to medium-silt size aggregates (see figure). The particle distribution curve for B4 indicates that exposure to sub-areal weathering resulted in the breakdown of most of these aggregates. A disproportionate increase in the liquid limit of B4 occurred after hydrocycloning: this must have been due to further disaggregation below 2 microns. Sample B5, which contained approximately 90% interstratified clay (remainder mainly biotite) showed the same poor dispersion as B3, liquid limits also being comparable. During CEC measurements satisfactory end-points could not be obtained for either samples B3 or 5. This again was due to poor dispersion. The CEC of the underflow product from B4 was greater than that of the original sample in spite of its lower interstratified clay content. This is an unexplained phenomenon which was noted also for montmorillonite (section 7.2.2.).

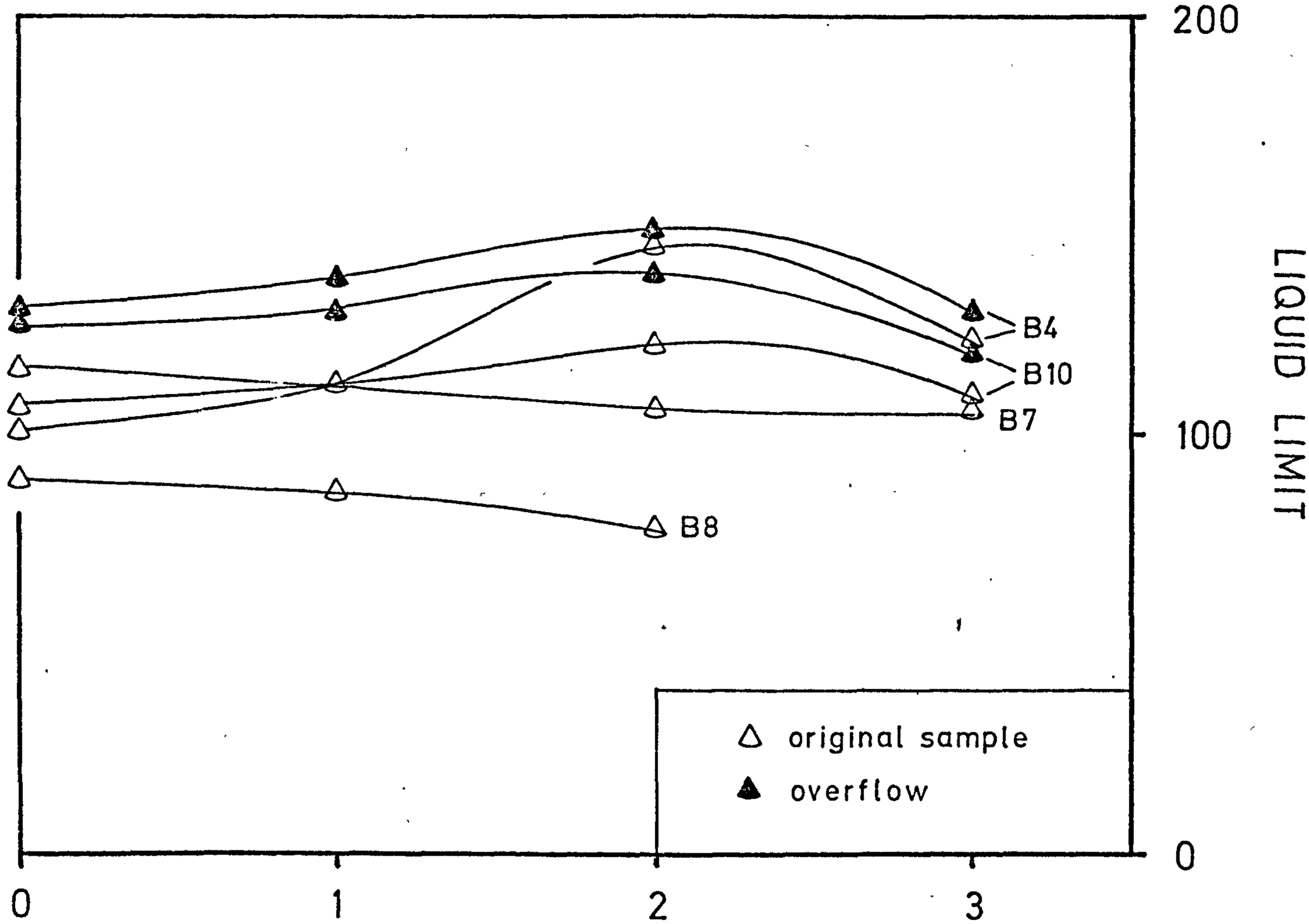

Fig. 7.7 Plot of liquid limit v. % sodium carbonate addition for interstratified clay hydrocyclone overflow products

7.4.3 Response to sodium carbonate

Samples B4 and 10, which contained 27 and 31% montmorillonite interlayers respectively, showed a positive response to sodium carbonate (fig 7.7). Maximum liquid limits were obtained, as would be expected from CEC considerations, after the addition of 2% sodium carbonate. Maximum plastic viscosities of 3-3.5 cp were given by 8% suspensions of these Na-exchanged clays. The fact that apparent viscosities of 5-6 cp were also given showed that some gel strength was being developed. The extent of gel formation compares favourably with that shown by the least dispersed of the fuller's earths (table 7.2). Both sample B7 (23% montmorillonite layers) and B8 (17% montmorillonite layers) showed a decrease in liquid limit after sodium carbonate addition. Low-CEC clays usually show a decrease in liquid limit after the addition of sodium carbonate: possibly a minimum amount of montmorillonite interlayering (% 25%) is necessary before the interstratified clay appears to respond positively to this reagent.

7.5 DISCUSSION

7.5.1 Relative dispersion-dependency of the liquid limit and methylene blue CEC tests

Fig. 7.8 is a plot of liquid limit against methylene blue CEC for original samples and hydrocyclone products from all three groups. Four main features emerge from inspection of the figure and these are listed below.

(i) Most original samples and hydrocyclone overflow products from the interstratified illite/montmorillonite and the mixed-assemblage clays plot in a narrow band passing through the origin.

(ii) The majority of montmorillonite original samples (and the inter-

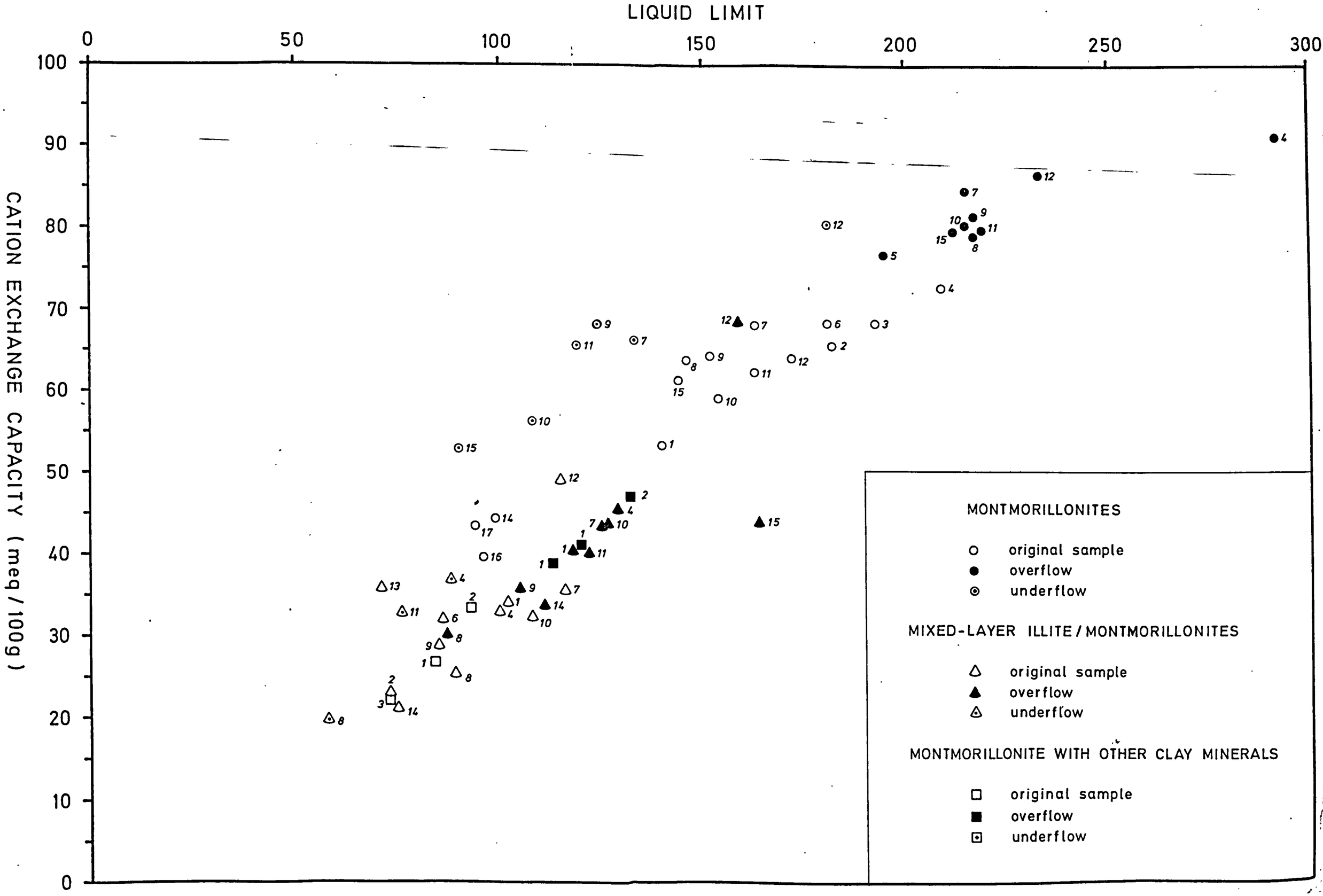

Fig. 7.8 Plot of liquid limit v. CEC for original samples and hydrocyclone products from all three groups

stratified clays B12 and 13) plot on, or just above, a straight line cutting the CEC axis at approximately 20 meq/100g.

(iii) Montmorillonite underflow samples plot on a straight line above that described in observation (ii). This line is of greater slope and cuts the CEC axis at approximately 25 meq/100g.

(iv) The montmorillonite overflow samples, with the exception of A4, plot in a relatively small area at the right hand top corner of the figure.

It may be concluded from observation (i) that the interstratified and mixed-assemblage clays are more or less fully dispersed and allow maximum development of cation exchange and liquid limit properties. The relative position in the band is determined for the interstratified clays primarily by the amount of montmorillonite interlayers and for the mixed-assemblage clays by the amount of discrete montmorillonite present.

The position of the montmorillonite original ,samples on the line described in observation (ii) is mainly determined by grade. For the majority of the original samples (i.e. those actually plotting on the line), dye adsorption and liquid limit show a consistent dispersion-dependency. Original samples A7, 8, 9 and 15, which plot above the line, show a better response to dye adsorption (these samples contain the most resistant montmorillonite aggregates - see section 7.2.3.3). Grade also determines the position of the underflow products on the line described in observation (iii). Here the dispersion-dependency of the two properties is again consistent but, compared to the original samples, the underflow products do show a much greater CEC response relative to liquid limit. From these observations it is apparent that, of the two tests, methylene blue CEC is least affected by the state of aggregation of the montmorillonite.

Both CEC and liquid limits of the overflow products are affected, to a greater or lesser extent, by the state of aggregation of the

montmorillonite. A factor of increasing importance at the higher levels of dye adsorption is the fact that the maximum methylene blue CEC value possible for these purified clays is of the order of 97 meq/100g. No such constraint applies to the development of liquid limit values thus any conclusion drawn from the position of the overflow products in the figure (observation (iv) above) would be suspect.

7.5.2 Summary and conclusions

Differences in unit cell composition, lattice charge and exchangeable cation assemblage undoubtedly influence the physico-chemical behaviour of fuller's earth-type montmorillonites. However in the case of the present samples such influences were more subtle than the effect of interparticle association and it was found that variations in behaviour were due in far greater measure to the extent of disruption of these interparticle associations achieved during separation procedures or other treatments prior to testing. Of the tests used, liquid limit was found to be the most susceptible to this phenomenon; quantitative evaluation of montmorillonite content is impossible using results from this technique. Enhancement of liquid limit values from original samples to purified products resulted primarily from the breakdown of montmorillonite aggregates under the high-shear conditions of the hydrocyclone and not from increase in montmorillonite content. Liquid limits varied from one hydrocyclone-purified montmorillonite to another. A similar variation was observed in liquid limits of original samples themselves after these had been subjected to additional high-shear dispersion procedures and to ultrasonics. The ultimate degree of dispersion attained (as reflected in the maximum obtainable liquid limit value) appeared to be an inherent property of each individual montmorillonite and it was suggested that high-shear dispersion ultimately brings natural Ca, Mg-montmorillonite to a steady state with regard to interparticle association. However in

each montmorillonite the steady state appeared to be represented by a different combination of particles of unit cell thickness, these apparently retaining their integrity even after Na-exchange.

Montmorillonites subjected to high-shear dispersion or to ultrasonics gave methylene blue CECs which were, at best, only 80% of the true (lattice charge) CEC. Dye sorption ceased when the surface of the montmorillonite unit cell particles were covered by a monolayer of flat-lying methylene blue cations, irrespective of whether the lattice charge CEC had been satisfied. Pure montmorillonites show lattice charge CECs of 70 to over 120 meq/100g. The maximum amount of dye which could be sorbed by Ca, Mg-montmorillonite was found, both by calculation and experiment, to be of the order of 97 meq/100g. This technique is also unsuited to the quantitative evaluation pf purified Ca, Mg-montmorillonites. Semi-quantitative estimation of the montmorillonite content of original samples does appear possible, however, provided that the pretreatment procedure is rigidly standardised and high-shear and ultrasonic dispersion is avoided. Only 60-70% of the CEC of the original samples is measured under these conditions.

The measurement of surface area, based on ethylene glycol monoethyl ether (EGME) adsorption, is unaffected by the state of aggregation of the montmorillonite and is not CEC-dependent. The highly polar nature of the EGME molecule enables it to penetrate the montmorillonite crystal aggregates and complete monolayer surface cover is attained under conditions which are easily achieved in the laboratory. Results obtained are both realistic and reproducible. Absolute values may be affected somewhat by the nature of the exchangeable cation assemblage - for instance variation in exchangeable Ca/Mg ratio - but of the three tests used EGME surface area shows by far the greatest promise for quantitative assessment of montmorillonite.

The purified interstratified clays containing 15-35% montmoril-

lonite interlayers showed maximum development of liquid limit and methylene blue CEC, a steady state having been achieved for all samples following exposure to the high-shear environment of the hydrocyclone. Results for surface area, CEC and liquid limit all showed a linear correlation with amount of montmorillonite interlayers. Full development of CEC and liquid limit properties of some of the original samples, especially those collected from freshly exposed horizons, was inhibited by the effects of aggregation. On a practical note, it appeared that the latter could be nullified somewhat by exposing the clay to normal weathering agencies. The effects of interparticle association were pronounced in the two interstratified clays containing 60% montmorillbnite interlayers. In their response to liquid limit and CEC tests both clays showed more similarities to low-grade fuller's earths than to the other interstratified clays described above.

APPENDIX 1

NOMENCLATURE OF MONTMORILLONITE DEPOSITS

X1.1 Bentonite

The term bentonite was originally introduced by Knight (1848) to describe the highly plastic clays, characterised by extreme swelling on wetting, occurring in the Cretaceous formations of Wyoming, USA. Hewett (1917) subsequently showed that these clays formed by the alteration of volcanic ash. Ross and Shannon (1926) defined bentonite as 'a rock composed essentially of a crystalline clay mineral formed by devitrification and accompanying alteration of a glassy igneous material, usually a tuff or volcanic ash', and stated that the characteristic clay mineral of bentonite was a member of the montmorillonite group. Latterly the term bentonite has been applied to (i) alteration products of volcanic material which do not contain montmorillonite (e.g. Schultz, 1963) and (ii) deposits of montmorillonite which have no connection with volcanic material (e.g. Millot, 1970). Millot (op. cit.) did emphasise that the term bentonite should be restricted to montmorillonite-bearing rocks. Those resulting from alteration of volcanic material by hydrothermal action or under sub-areal weathering conditions Millot considered 'true bentonites'; montmorillonite deposits resulting from alteration of volcanic glass in a marine environment were termed 'sedimentary bentonites'. Unfortunately this author extended the latter term to include montmorillonite deposits arising from authigenic neoformation in alkaline and siliceous environments.

X1.2 Terms used to describe the common cationic modifications of montmorillonite

The montmorillonite rock originally termed bentonite by Ross and Shannon contained Na as the principal exchangeable cation. In the

United States Na-montmorillonite clays may be described simply as bentonites. Na-montmorillonite may also be termed Na-bentonite, swelling bentonite (a reference to the pronounced swelling of the Na-clay when in contact with water), or Western bentonite (after the western states where Na-montmorillonites are most common). In contrast montmorillonites containing Ca as the predominant exchangeable cation are called Ca-, non-swelling, or Southern bentonites.

Jurassic and Cretaceous montmorillonite deposits of the UK invariably contain divalent exchangeable cations (dominantly Ca accompanied by some Mg). They are called fuller's earths, this term being derived from the ancient use of the clay for 'fulling' - a method for degreasing wool or woollen cloth by treating it with a clay-water slurry (Hartwell, 1965). Unfortunately, in the past, any clay which had 'fulling' properties was described as a fuller's earth even though montmorillonite may only have been a minor constituent. Problems of nomenclature are further complicated by the established use of the term Fullers Earth for strata of Bathonian age lying between the Upper Inferior Oolite and the Forest Marble. In the United States commercial attapulgite clays are also called fuller's earths.

X1.3 Interstratified illite/montmorillonite clays

In the United States deposits of interstratified illite/montmorillonite are usually described as K-bentonites (Weaver and Bates, 1952). Meta- and sub-bentonites are other descriptive terms, the latter having, on occasion, been applied also to Ca-montmorillonite deposits. The term meta-bentonite has been criticised (e.g. Mossler and Hayes, 1966) on the basis that most illite/montmorillonite deposits do not appear to have been metamorphosed. However Weaver and Beck (1971) have shown that montmorillonite-rich shales may progressively alter to interstratified illite/montmorillonite and then to illite/

chlorite/montmorillonite under deep burial conditions. The point at which these initially diagenetic alterations pass into low-grade metamorphism is open to question.

The use of the term illite for the 10A component of these clays is not universally accepted, many authors, including MacEwan et al. (1961), preferring the term mica. The amount of fixed K in these interstratified clays decreases as the amount of montmorillonite component increases. Extrapolation back to the 10A component shows (Hower and Mowatt, 1966, see also section 5.4.2) 1.6K equivalents per structural unit rather than 2 as in micas. There appears a strong case for using the term illite in this context especially when the undoubted clay size of the material and its disordered nature (section 3.1.4.4) are taken into account.

APPENDIX 2

PRETREATMENT OF SAMPLES

Following collection in the field the clays were kept in sealed plastic bags in order to retain, as far as possible, their field-moist condition. On return to the laboratory a reference sample was transferred to another, smaller, plastic bag and the remainder of the clay air-dried. Obvious impurities such as rootlet matter, portions of adjacent rock horizons, and, in the case of the interstratified illite/montmorillonite clays, discrete veins of calcite, were removed at this stage. The air-dried clays were then jaw-crushed to pass 4 mesh and a portion (100-500 g) of the jaw-crushed material ground to pass 100 mesh. Except for particle size analyses all data on 'original samples' were obtained on this ground material. Particle size analyses were made on 10g sub-samples of the jaw-crushed clay.

Samples for hydrocyclone separation were prepared by shaking 400g of the jaw-crushed material in distilled water using a reciprocal shaker. The resulting slurry was then passed through a 240 mesh screen and, where necessary, material retained on the screen placed in an ultrasonic tank for a short time both to clean the sand grains and break down any sand-size clay aggregates still remaining. The final sand fraction from wet screening was air-dried and then rescreened dry at 240 mesh, additional material passing the screen being added to that resulting from the previous wet screening. The sand fraction was retained for mineralogical study (see Appendix 4, section X4.3). The less than 240 mesh slurry was made up to 4 litres in the hydrocyclone system. Products from hydrocycloning were air-dried then lightly crushed to pass a 4 mesh screen. Portions for particle size analysis were sampled out and the remainder ground through 100 mesh. This material was used for all mineralogical and chemical analyses and determinations of physico-chemical properties.

APPENDIX 3

SIZE ANALYSES OF MONTMORILLONITIC CLAYS

X3.1 General

Particle size analysis data (obtained by the Andreasen Pipette Method) have been used extensively in this study. Montmorillonite, when fully dispersed, exists as particles much smaller than can be detected by size analysis procedures based on unassisted gravitational settling in a liquid medium. However much interest in this study has centred on the silt size-range (2-63 microns) for which, by careful control of experimental conditions, precise and meaningful results may be obtained by the procedures just mentioned. Within this size-range occurred a large proportion of the accessory minerals of the samples and also montmorillonite or illite/montmorillonite particle aggregates which, under normal pretreatment conditions (prolonged shaking in water with a dispersing agent), showed resistance to dispersion. In fact the relative extent of particle aggregation, which has been shown to be the major factor determining the response of the clay to certain physico-chemical tests, was first recognised from particle size analyses of the original samples. Also, when choosing the most suitable operating parameters for the hydrocyclone, comparisons of particle size analyses of original samples and separated products were found to be of critical importance (section 2.2.3). Many difficulties are inherent in the particle size analysis of montmorillonite-rich clays. In view of the fundamental importance of these data to the present study the method used, and in particular the role of the dispersing agent, is discussed in some detail below.

X3.2 Method followed

A 10g sub-sample of the air-dried, jaw-crushed clay was shaken for 4 hours in distilled water to which the requisite amount (see next section) of dispersing agent had been added. The suspension was then wet-screened at 240 mesh, the weight of sand recorded, and the material passing the screen made up to 600 ml in the Andreasen cylinder. The sampling procedure described in British Standard Specification 1377 (1967) p. 68 was then followed, extractions by pipette being carried out at times corresponding to the elimination of particles coarser than 50, 40, 30, 20, 15, 10, 5 and 2 microns. The pipette extracts were dried at 105°C, weighed, and corrected for the amount of dispersing agent (see below). Results were usually expressed as cumulative percentage curves.

X3.3 Importance of the dispersing agent

In the size analysis of montmorillonite-rich clays both the type and amount of dispersing agent added are critical. Sodium hexametaphosphate or 'calgon' was chosen for the present samples following preliminary tests on its effectiveness. The use of calgon as a dispersing agent in size analysis procedures was first suggested by Tyner (1939). Na-montmorillonite suspensions are much more stable, i.e. with respect to flocculation and subsequent settling, than suspensions of Ca, Mg-montmorillonite and the main function of calgon during the mass action displacement of the exchangeable Ca, Mg of montmorillonite by Na is in providing a source of readily available Na ions. However an important advantage which calgon has over other Na salts is the property of sequestration (Daugherty, 1948), which ensures that as Na replaces Ca, Mg these cations are taken up by the phosphate polyanion to form a stable, soluble, complex. A further, although minor, contribution towards suspension stability may result from the reactivity of poly-

phosphate towards Al ions exposed on positively charged edges of clay particles (Van Olphen, 1963). Reversal of edge charge takes place but the magnitude of this effect is likely to be smaller for montmorillonite than, for instance, with kaolinite which has a much higher edge to face area ratio.

For a montmorillonite with CEC of 100 meq/100g 10.2g calgon is theoretically necessary for complete exchange of Ca, Mg by Na. (Comparable figures for sodium carbonate and hydroxide are 5.3 and 4.0g respectively). Potentially large errors may therefore be introduced into the size analysis procedure as the amount of dispersing agent to be subtracted from each pipette extract is a significant fraction of the total weight (the actual amount is Cx where C is the original amount of calgon added and x is the volume ratio of pipette to total suspension in the Andreasen cylinder). The validity of the latter operation depends on the assumption that no precipitation of Ca or Mg as phosphates occurs - which is justified if the phenomenon of sequestration is accepted. However Barshad (1969) reported precipitation of Ca, Mg phosphates following calgon treatment of montmorillonite and tests were carried out on some of the present samples to clarify this point. These are described below.

Copies of the result sheets for two 'size analyses' of sample A4 are shown in fig. X3.1. As this sample contained negligible amounts of sand and silt particles any precipitation of Ca, Mg phosphate should be reflected in a progressive decrease in the weights of the pipette extracts (column 8 on sheets). This is not observed, the results for 1g calgon addition (top result sheet) being well within the limits of error for this method ($\pm$ 1%). Even after adding a large excess of calgon (bottom result sheet) all the phosphate remains in solution.

Samples A1 and C3 were dispersed with different amounts of

SAMPLE A4 (Bowling BH 1, 96-99 ft bulked) 10g air dried

CALGON 1.0g

+240# 0.008g

MEAN TEMPERATURE 23°C

1	2	3	4	5	6	7	8	9	10
PARTICLE DIAMETER	SETTLING VELOCITY	SETTLING DISTANCE	ELAPSED TIME	WEIGHING BOTTLE NUMBER	WEIGHT OF WEIGHING BOTTLE	WEIGHT OF WEIGHING BOTTLE +SAMPLE	WEIGHT OF SAMPLE	−0.0160g CALGON	CUMULATIVE % FINER
50μ	4.25cm	19.7cm	1m 25s	2	23.2831g	23.4362g	0.1531g	0.1364g	99.8
40μ	6.6	19.4	2m 8s	3	21.6008	21.7556	0.1548	0.1381	101.0
30μ	11.6	19.0	3m 40s	4	22.4491	22.6023	0.1532	0.1365	99.9
20μ	26.0	18.6	8m 4s	5	13.8230	13.9760	0.1530	0.1363	99.7
15μ	46.0	18.2	13m 57s	6	13.4431	13.5962	0.1531	0.1364	99.8
10μ	116.0	17.8	34m 25s	7	12.5502	12.7034	0.1532	0.1365	99.9
5μ	420.0	17.4	1h 57m 20s	8	12.4896	12.6422	0.1526	0.1359	99.4
2μ	2670.0	10.0	7h 25m	9	12.2398	12.3929	0.1531	0.1364	99.8
			INITIAL SAMPLE	1	23.8687	24.0221	0.1534	0.1367	100.0

SAMPLE A4 (Bowling BH1, 96-99 ft bulked) 10g air dried

CALGON 2.4g

+240# 0.011g

MEAN TEMPERATURE 23°C

1	2	3	4	5	6	7	8	9	10
PARTICLE DIAMETER	SETTLING VELOCITY	SETTLING DISTANCE	ELAPSED TIME	WEIGHING BOTTLE NUMBER	WEIGHT OF WEIGHING BOTTLE	WEIGHT OF WEIGHING BOTTLE +SAMPLE	WEIGHT OF SAMPLE	−0.040g CALGON	CUMULATIVE % FINER
50μ	4.2 s/cm	19.6cm	1m 24s	2	23.2821g	23.4628g	0.1807g	0.1407g	99.9
40μ	6.6	19.2	2m 7s	3	21.6013	21.7832	0.1819	0.1419	100.1
30μ	11.6	18.8	3m 37s	4	22.4502	22.6314	0.1812	0.1412	100.2
20μ	26.0	18.4	7m 59s	5	13.8228	14.0020	0.1792	0.1392	98.8
15μ	46.0	17.9	13m 42s	6	13.4435	13.6239	0.1804	0.1404	99.6
10μ	116.0	17.5	33m 50s	7	12.5499	12.7318	0.1819	0.1419	100.7
5μ	420.0	17.1	1h 55m 0s	8	12.4901	12.6703	0.1802	0.1402	99.5
2μ	2670.0	10.0	7h 25m	9	12.2404	12.4216	0.1812	0.1412	100.2
			INITIAL SAMPLE	1	23.8680	24.0489	0.1809	0.1409	100.0

Fig. X3.1. Particle size analysis of sample A4 using different amounts of calgon.

Table X3.1. Sample A1: the effect of adding calgon in excess of that required by the CEC of the clay. (Data condensed from a number of complete particle size analyses.)

cumulative	amount of calgon added (g)						from hydrocyclone
% fines	0.4	0.6	0.8	1.0	1.8	2.4	products
10 microns	84.3	90.8	87.7	90.2	88.9	90.5	90.0
5 "	77.9	86.3	84.9	86.2	86.0	86.8	86.2
2 "	64.0	79.2	79.2	80.6	81.5	83.8	82.8

Table X3.2 Sample C3: the effect of adding calgon in excess of that required by the CEC of the clay. (Data condensed from a number of complete particle size analyses.)

cumulative	amount of calgon added (g)			from hydrocyclone
% fines	0.5	1.0	1.5	products
10 microns	68.8	69.9	72.6	78.1
5 "	55.8	55.2	59.9	70.5
2 "	38.1	40.0	42.0	58.5

calgon to examine the effect of adding this reagent in amounts in excess of that required by the CEC of the clay. From table X3.1 it is seen that dispersion of Al is virtually complete following 0.6g calgon addition. Once the necessary amount of calgon is exceeded further increments cause a small increase in less than 2 micron content. The figures in the last column of the table were obtained by back-calculation from the size analyses of the hydrocyclone overflow and underflow products. A comparison of the figures in the last column with those in the preceeding columns would suggest that the sympathetic increase in less than 2 micron content with calgon addition is a real effect and not an artifact introduced by the presence of large amounts of unexchanged calgon in solution.

Table X3.2 illustrates the effect of excess calgon on sample C3. Again there is a progressive increase in the less than 2 micron content as the amount of calgon is increased. (Smaller increments of calgon were added as the CEC of sample C3 is lower than that of Al). From the recalculated size analysis after hydrocycloning it is apparent that, although an excess of calgon does improve dispersion somewhat, this factor is of minor importance compared with the effect of mechanical (shear) forces.

Suspensions for size analysis contained between 1 and 2% (by weight) of clay and even at these low clay/water ratios montmorillonite may exhibit gel formation. Hindered settling of the coarser particles may then occur and an indication of the magnitude of this effect for sample C3 may be obtained from fig. 2.3. The size analysis of the first overflow product (curve 4) suggests that no particles coarser than 10 microns are present. After recycling this product the size analysis of the underflow product (curve 7) shows, however, 8% of particles coarser than 10 microns. As the proportions (by weight) of overflow to underflow products in the second pass were in the ratio 88:12,

approximately 1% particles coarser than 10 microns must have remained undetected in the first overflow product, presumably as a result of hindered settling.

X3.4 Size analysis data on original samples

A record of the amount of sand-, silt-, and clay-size material in the original samples is given in table X3.3. Much of the data has been referred to in chapters 2 and 7. Here it is sufficient to emphasise that a low value for clay-size (i.e. < 2 micron) material does not necessarily indicate low clay mineral content as the standard dispersion treatment prior to size analysis did not necessarily break down all the clay aggregates. These consequently reported as silt during the size analysis (see especially results for samples A7 and A15 which contained about 96 and 83% montmorillonite respectively).

Table X3.3. Particle size analysis data for original samples expressed as % sand (> 63 microns or 240 mesh), silt (2-63 microns) and clay (< 2 microns). (nd = not determined).

SAMPLE	SAND	SILT	CLAY	SAMPLE	SAND	SILT	CLAY
A1	< 1	15	84	B1	2	11	87
2	1	7	92	2	1	40	59
3	1	4	95	3	< 1	26	73
4	< 1	< 1	99	4	< 1	8	91
5	51*	nd	nd	5	5	25	70
6	< 1	< 1	99	6	2	17	81
7	1	56	43	7	< 1	8	91
8	3	16	81	8	< 1	15	84
9	2	11	87	9	< 1	20	79
10	5	13	82	10	3	10	87
11	1	13	86	11	2	12	86
12	8	4	88	12	5	26	69
13	8	nd	nd	13	4	62	34
14	6	nd	nd	14	1	38	61
15	2	63	35	15	19**	36	45
16	3	nd	nd				
17	1	nd	nd	C1	2	39	59
				2	2	37	61
				3	< 1	57	42

* mainly quartz

** mainly ankeritic dolomite

APPENDIX 4

MINERALOGICAL TECHNIQUES

X4.1 X-ray diffraction

X4.1.1 Equipment

Both Siemens and Phillips X-ray generators were used. The following experimental conditions applied:

Siemens: Ni-filtered Cu-radiation at 35kV and 24 mA, time constant 2, 1^{o} divergence slits, 0.3^{o} receiving slits.

Phillips: Ni-filtered Cu-radiation at 40kV and 40mA, time constant 4 (occasionally 1), 1^{o} divergence slits, 0.1^{o} receiving slits.

Co-radiation was used in one instance only (see section 3.1.4.2).

X4.1.2 Techniques

Slides of basally oriented clays were prepared in the following manner. Either 100 or 150 mg of <100 mesh clay were placed in a 4 ml perspex vial and 2 ml distilled water added from a dropping pipette. The vial was held in an ultrasonic tank for 5 mins., removed, and all the suspension taken up in a duplicate dropping pipette. The suspension was then released slowly on to a 38 mm square glass slide (with care a uniform coating of suspension results). The slide was allowed to dry overnight. Duplicate slides were prepared, one was used untreated and then glycerolated, the other was retained in case heating tests (see below) proved necessary.

Attempts to distinguish between peaks due to kaolinite and chlorite on the diffractometer traces of these samples involved, initially, heating the duplicate slide to $600^{o}C$ for 1 hour and then comparing the

intensities of the relevant peaks on the traces of untreated and heated slides. If the results obtained by this procedure proved ambiguous the ground clay was treated with 6N HCl (at 90°C) for 1 hour. The residue was washed, dried, slides were prepared in the manner described above, and diffractometer traces of these compared with the traces of the original sample.

K-saturated interstratified illite/montmorillonites (see fig. 3.5) were prepared by suspending 0.5g clay in 40 ml 1N KCl and agitating ultrasonically. Excess electrolyte was removed by centrifugation. Three consecutive treatments were given and after the final one the clay was washed, dried and oriented slides prepared.

'Randomly oriented' samples were prepared in a standard aluminium holder by back-loading against unglazed paper.

X4.2 Thermal analysis

Netzsch equipment was used for DTA alone. The following experimental conditions applied:

sample pretreatment:	none, except that sample was <100 mesh
sample weight:	0;9-1.0g
inert material:	calcined alumina
sample holder:	Ni-block
temperature rise:	10°C/min (after approximately 100°C)

temperature measured in inert material
T and ΔT recorded on photographic paper

A Stanton Redcroft 1mg sensitivity thermobalance with DTA attachment was used for simultaneous TG/DTA. Sample (approximately 0.4g) and inert reference (calcined alumina) were housed in dimpled platinum crucibles which fitted into an inconel block. The heating rate wsed was 6°C/min and weight loss and DTA were recorded on separate charts which were subsequently superimposed.

X4.3 Procedures used in the examination of the accessory minerals

The sand-size material collected during preparation of the samples for hydrocyclone separation was treated ultrasonically to remove any traces of adherent clay, rescreened at 240 mesh, and then dried. The grains were then separated in bromoform of SG 2.86. Procedures used in the identification of grains from the bromoform 'sinks' and 'floats' varied somewhat and will be discussed separately below.

The bromoform floats were first examined by X-ray diffraction, scans being carried out between 3 and $35^{o}2\theta$ (Cu-radiation) in order to determine relative amounts of, for example, zeolite, alkali v. plagioclase feldspar, quartz and calcite. On the basis of this information further separations were made in bromoform/dimethyl formamide mixtures of SG 2.3, 2.61 and 2.7. The various SG fractions (rarely monomineralic) were then examined with the petrographic microscope under oils.

Bromoform sinks were separated into fractions of different magnetic susceptibility using an Eclipse variable hand magnet. The resulting fractions were examined separately under a binocular microscope and preliminary identifications of grains made on the basis of such criteria as crystal form, colour and occurrence in a particular magnetic fraction. Identifications were checked under transmitted light after immersion of the grains in oils of appropriate refractive indices. Opaque grains, or grains with refractive indices greater than 2, were identified by X-ray powder photography although, in a few instances, a check for major elements by X-ray fluorescence was sufficient.

Non-clay minerals present in the silt sizes were separated from hydrocyclone underflow products. A portion of the latter was dispersed ultrasonically in the presence of excess calgon. After some time (usually at least 1 hour) the clay aggregates were seen to have dispersed, liberating the previously enclosed mineral grains. Successive decantations to remove material finer than 10 microns (with additional ultra-

sonic dispersion where necessary) resulted eventually in a clean medium to coarse silt size non-clay mineral concentrate. After drying bromoform sinks and floats were obtained under centrifugation.

APPENDIX 5

CHEMICAL TECHNIQUES

X5.1 MAJOR ELEMENTS

SiO_2 and Al_2O_3 were determined gravimetrically after sodium carbonate fusion. FeO was determined by the ammonium metavanadate method of Wilson (1955) and H_2O^+ by a modified Penfield tube method.

All other elements were determined on 'solution B' (resulting from digestion of the sample by hydrofluoric and perchloric acids). TiO_2 and P_2O_5 were determined colorimetrically, Na_2O and K_2O by emission flame photometry and CaO, MgO, Fe_2O_3 and MnO by atomic absorption spectroscopy.

X5.2 EXCHANGEABLE CATIONS

Approximately 0.5g air-dried clay was weighed accurately into a 50ml centrifuge tube, 25ml 1N NH_4OAc added, the suspension stirred magnetically for 5 mins then allowed to stand for 1 hour. The suspension was centrifuged for 10 mins and the supernatant liquid collected in a 200 ml volumetric flask. A further 25 ml 1N NH_4OAc was added to the clay in the bottom of the centrifuge tube and the contents again stirred for 5 mins. A total of four such treatments were carried out and the supernatant liquid collected after each centrifugation. For either the second or third treatment the clay was allowed to remain in contact with the NH_4OAc overnight. The leach solution was made up to 200 ml with distilled water and K and Na determined directly by emission flame photometry. Ca and Mg were determined on the diluted solution by atomic absorption spectroscopy.

The NH_4OAc was found to contain significant amounts of Na which varied from batch to batch. This factor was not appreciated during the earlier stages of this study and some values for Na (tables 5.8, 5.9

and 5.10) are only quoted as < 1 meq/100g. A large stock solution of 1N NH_4OAc was subsequently made up and detection of exchangeable Na in these clays improved by running blanks of the solution.

X5.3 TRACE ELEMENTS

Optical spectroscopy was the main technique used. Determination was by DC arc excitation using an Ebert 3.4m grating spectrograph with Pd as an internal standard. For each element intensities of spectral lines were compared, via a computer programme, with the intensities of the lines given by a known amount of the element both in synthetic mixtures of similar matrix characteristics and in standard comparative rocks. Detection limits were:

Zn	50 ppm
V, Cr, Ni, Cu, Ga, Y, Zr, La, Pb	10
Sc, Co, Nb, Sn, Ba	3
Be	1

Sr, Rb and Ce were determined by X-ray fluorescence using a Philips PW 1540 spectrometer with a tungsten tube, LiF crystal and scintillation detector. Samples were pressed into discs. Concentrations were determined by single position counting, Kα lines being used. Background corrections were made by recording the number of c/s $1^{o}2\theta$ either side of the chosen Kα position, taking the mean, then subtracting from the total c/s. Calibration was by standard rock sample G1; matrix variations between this sample and the clays were not taken into account.

Elements recorded in tables 5.13 and 5.14 were detected during an XRF scan over the range 8 to $46^{o}2\theta$. Mineral grains were scattered over a Mylar film stretched over the base of a standard holder.

APPENDIX 6

METHODS USED IN THE PHYSICO-CHEMICAL TESTING OF THE CLAYS

X6.1 Surface areas

The ethylene glycol monoethyl ether (EGME) adsorption method of Carter et al. (1965) was followed closely. Samples were dealt with in batches of five. Approximately 1g of sample was weighed accurately into a tared aluminium container and dried over P_2O_5 in an evacuated desiccator. Three consecutive weighings of the dried clay were taken. Immediately following the final weighing 3 ml of EGME were added to the dried clay and the resulting slurry allowed to stand for 1 hour in a separate desiccator over anhydrous $CaCl_2$. This desiccator was evacuated for 1 hour with a high-vacuum pump and then allowed to stand for a further hour. The vacuum was then released and the aluminium containers and contents weighed as quickly as possible. Surface areas were calculated on the assumption that 2.86×10^{-4}g EGME represents monolayer coverage on $1m^2$ of clay surface (Carter et al.). Values were based on the P_2O_5-dried weight of the clay. Reproducibility of the method was found to be just within 1%: the main source of error was from adsorption of atmospheric moisture during both sets of weighings. Surface area values given in tables X6.1-3 represent the mean of at least two determinations.

X6.2 Cation exchange capacities

The rapid methylene blue dye adsorption method of Jones (1964), as modified by Nevins and Weintritt (1967), was used. Samples were dealt with in batches of ten. Suspensions of 0.6g air-dried clay in 20ml distilled water were shaken for 2 hours on a reciprocal shaker and allowed to stand overnight. In the measurement of dye adsorption a 0.0083N solution of methylene blue was added to the suspension, initially

in increments of 2ml but falling to 1ml as the end-point was approached. Spot testing was carried out in the manner described by Jones (op. cit.) except that a waiting period of up to 30 mins was allowed for completion of dye adsorption at, or near, the end-point. CECs were calculated from the formula given by Nevins and Weintritt (op. cit.) and expressed on an oven-dried basis (the loss at 105°C being determined separately) Reproducibility was within 1ml of methylene blue (equivalent to less than 2 meq/100g) for the montmorillonites and better for the interstratified illite/montmorillonites. All values in tables X6.1-3 are quoted to the first decimal place. The figure following the decimal point has little significance but was retained purely for convenience when plotting these results graphically.

Deviations from the standard method of pretreatment are noted in the text. Ultrasonic dispersion did result in increased dye adsorption (see fig. 7.4 and discussion) but reproducibility suffered.

X6.3 Liquid limits

A description of the apparatus used for liquid limit determinations is given in British Standard Specification 1377 (1967). The procedure used in the present study was as follows. Amounts of clay ranging from 30 to 100g were mixed to a consistency approximating to the liquid limit and stored overnight in a closed, humid container. The following day the paste was placed in the cup of the liquid limit apparatus and the top surface levelled. The special grooving tool was then used to separate the paste into two halves and the cup was 'bumped' a number of times until the two halves met for a distance of approximately 13mm. The number of bumps was noted and the moisture content of the paste determined.Up to 10 readings of moisture content against number of bumps needed to close the groove were made as further water was added to the paste (the number of bumps always falling in the range 60-15). In this

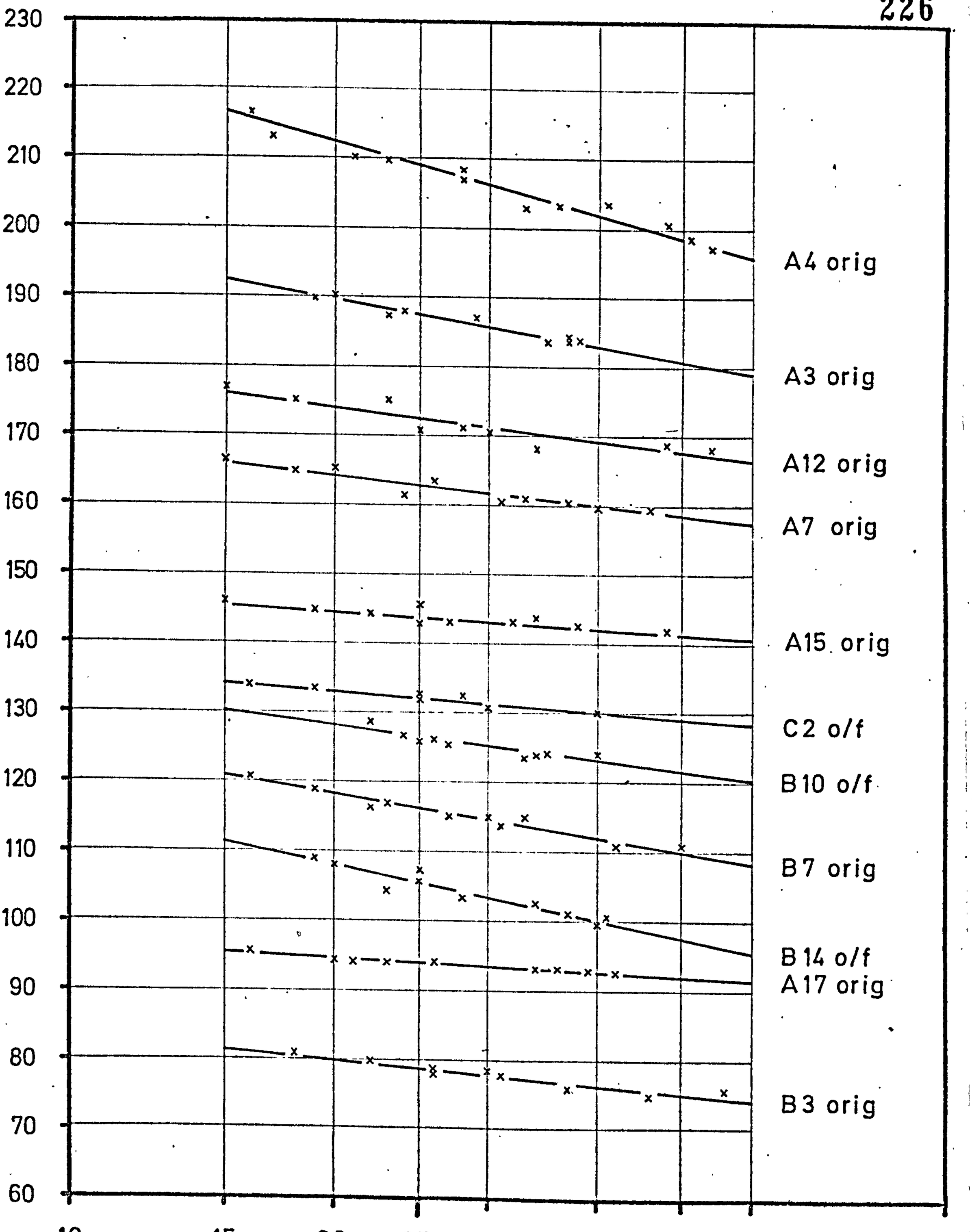

Fig. X6.1. Liquid limit test: 'flow lines' for a selection of samples.

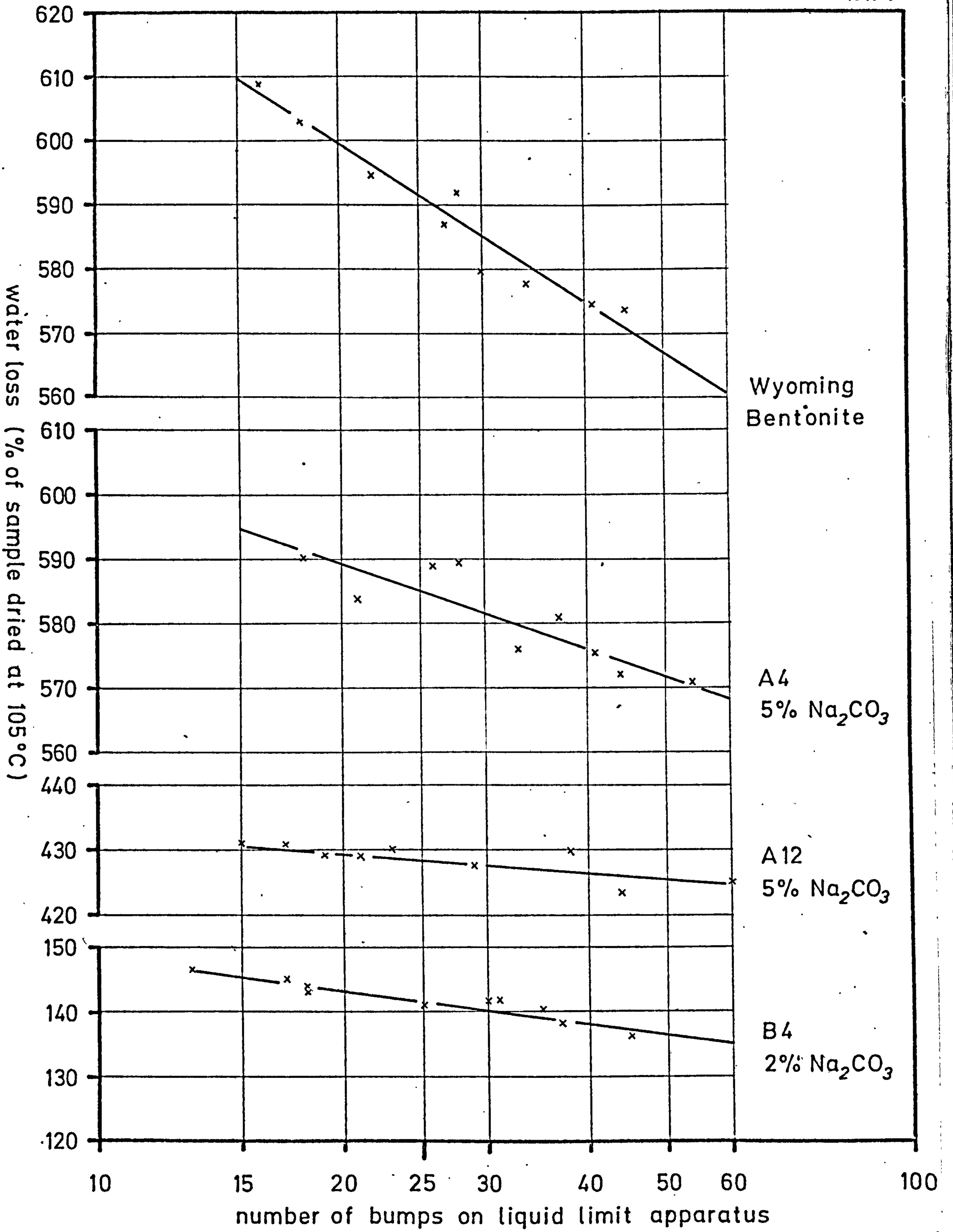

Fig. X6.2. Liquid limit test: 'Flow lines' for a selection of sodium clays.

way 'flow lines' were constructed for each sample and a selection of these are illustrated in figs. X6.1 and 2. The liquid limit (the moisture content at which the two halves of the paste met for the specified distance after 25 bumps) was read directly from the flow lines.

The flow lines of the natural Ca, Mg-clays (both original samples and hydrocyclone products) showed a surprisingly small amount of scatter. At the higher water contents of the Na-exchanged clays much more scatter was apparent but the liquid limit could still be obtained with confidence from the flow line. Slopes of the flow lines did vary between samples and in fig. X6.1 it is seen that the slope does not necessarily increase as the liquid limit increases. The slope of the flow line does appear to be related to the amount of particle aggregation in the clay. Samples A15 and A17, which were extremely difficult to disperse, show very gently-sloping flow lines. Easily dispersible clays such as A4 and B7 show a much greater response to water addition (fig. X6.1) but this response is not comparable with that shown by Wyoming bentonite (fig. X6.2). The very gently-sloping flow curve shown by A12 with 5% Na_2CO_3 may be related to difficulties in the Na/Ca, Mg exchange reaction.

X6.4 Viscometry

In the preparation of samples for viscosity measurement a 5% equivalent oven-dried montmorillonite (or 8% equivalent oven-dried inter-stratified illite/montmorillonite) suspension was mixed for 10 mins in a Braun liquidiser rotating at 13,000 rpm. The requisite amount of sodium carbonate was then added and the suspension remixed for 20 mins and allowed to stand overnight in a closed container. Apparent and plastic viscosities were then measured with the direct-reading Fann viscometer.

Table X6.1. Results of physico-chemical tests on montmorillonite original samples and hydrocyclone products.

SAMPLE	SURFACE AREA m^2/g	CEC meq/100g	LIQUID LIMIT
A1 orig.	594	53.3	140
A2 orig.	705	65.5	182
A3 orig.	744	68.2	193
orig., high shear for 30 mins.	nd	nd	255
A4 orig.	780	72.6	209
o/f	791	91.2	292
u/f	nd	88.5	nd
orig., high shear for 10 mins	782	92.0	307
orig., high shear for 30 mins	793	91.1	314
orig., ultrasonics for 2 hours	nd	90.4	272
A5 orig.	nd	30.2	nd
o/f	721	76.8	195
A6 orig.	776	68.3	181
A7 orig.	785	68.1	163
o/f	819	84.5	215
u/f	724	66.2	133
orig., high shear for 30 mins	nd	nd	219
orig., ultrasonics for 2 hours	nd	nd	217
A8 orig.	774	63.8	146
o/f	803	78.9	217
u/f	698	70.1	nd
A9 orig.	776	64.3	152
o/f	809	81.5	217
u/f	690	68.2	124
A10 orig.	712	59.1	154
o/f	769	80.3	215
u/f	591	56.3	108
A11 orig.	728	62.2	163
o/f	777	79.7	219
u/f	657	65.5	119
orig., high shear for 30 mins	nd	nd	205

Table X6.1 cont.

SAMPLE	SURFACE AREA m^2/g	CEC meq/100g	LIQUID LIMIT
A12 orig.	736	63.9	172
o/f	793	86.6	233
u/f	739	80.5	181
orig., high shear for 30 mins	nd	nd	224
orig., ultrasonics for 2 hours	nd	nd	203
A13 orig.	362	37.4	nd
A14 orig.	468	44.4	99
A15 orig.	654	61.3	144
o/f	745	79.6	212
u/f	537	53.1	90
orig., high shear for 30 mins.	nd	nd	201
A16 orig.	330	39.8	96
A17 orig.	532	43.5	94

orig = original sample
o/f = hydrocyclone overflow product
u/f = hydrocyclone underflow product

nd = not determined

Table X6.2. Results of physico-chemical tests on interstratified illite/montmorillonite original samples and hydrocyclone products.

SAMPLE	SURFACE AREA	CEC meq/100g	LIQUID LIMIT
B1 orig.	261	34.2	102
o/f	295	40.6	118
u/f	217	26.8	nd
B2 orig.	251	23.1	73
B3 orig.	312	nd	79
B4 orig.	317	33.1	100
o/f	327	45.6	129
u/f	298	36.9	88
B5 orig.	292	nd	74
B6 orig.	257	32.2	86
B7 orig.	262	35.6	116
o/f	292	43.3	125
u/f	201	26.9	nd
B8 orig.	196	25.5	89
o/f	220	30.3	87
u/f	165	19.8	58
B9 orig.	220	29.1	85
o/f	247	35.7	105
u/f	158	21.1	nd
B10 orig.	306	32.3	108
final o/f	333	43.6	126
first u/f	286	32.9	nd
second u/f	310	37.8	nd
B11 orig.	303	34.7	nd
o/f	317	40.0	122
u/f	295	33.0	76
B12 orig.	501	49.0	115
final o/f	596	68.4	159
first u/f	466	42.9	nd
second u/f	547	58.5	nd
B13 orig.	429	36.0	71
B14 orig.	195	21.3	75
final o/f	277	33.7	111

Table X6.2 cont.

SAMPLE	SURFACE AREA	CEC meq/100g	LIQUID LIMIT
B15 orig.	nd	21.0	nd
final o/f	320	43.8	164

orig. = original sample

o/f = hydrocyclone overflow product

u/f = hydrocyclone underflow product

nd = not determined

Table X6.3. Results of physico-chemical tests on mixed assemblage clay original samples and hydrocyclone products.

SAMPLE	SURFACE AREA	CEC meq/100g		LIQUID LIMIT
C1 orig.	209	26.8		84
first o/f	297	38.8		113
second o/f	316	41.1		120
first u/f	43	6.8		nd
second u/f	167	21.3		nd
C2 orig.	263	33.4		93
o/f	413	47.0		132
C3 orig.	262	24.8	(32.0)+	73
o/f (2)*	nd	40.6	(43.4)	nd
u/f (3)	189	21.5	(22.9)	nd
o/f (4)	362	40.6	(42.5)	nd
o/f (6)	367	42.5	(44.3)	nd
u/f (5)	134	13.6	(15.4)	nd

orig. = original sample
o/f = hydrocyclone overflow product
u/f = hydrocyclone underflow product

nd = not determined

* figures in parentheses refer to product numbers in fig. 2.3
\+ values in parentheses are those obtained after ultrasonic dispersion

REFERENCES

ALIETTI, A., 1967. Heulanditi e clinoptiloliti. Mineralogica et Petrographica Acta, 13, 119-137.

AYLMORE, L.A.G., SILLS, I.D. & QUIRK, J.P., 1970. Surface area of homoionic illite and montmorillonite clay minerals as measured by the sorption of nitrogen and carbon dioxide. Clays and Clay Min., 18, 91-96.

BAIN, J.A., 1971. A plasticity chart as an aid to the identification and assessment of industrial clays. Clay Min., 9, 1-17.

----- & MORGAN, D.J., 1971. Calcium montmorillonite (fuller's earth) in the Lower Greensand of the Fernham area, Berkshire (Mineralogical Investigation). Rep. No. 71/12, Inst. Geol. Sci., London.

----- MORGAN, D.J. & McKISSOCK, G.M., 1971. Calcium montmorillonite (fuller's earth) in the Lower Greensand of the Baulking area, Berkshire (Mineralogical Investigation). Rep. No. 71/4, Inst. Geol. Sci., London.

BALL, D.F., 1968. Interstratified illitic clay in Ordovician ash from Conway, North Wales. Clay Min., 7, 363-366.

BARSHAD, I., 1969. Preparation of Na-saturated montmorillonites. Soil Sci., 107, 337-342.

BASKIN, Y., 1956. A study of authigenic feldspars. J. Geol., 64, 132-155.

BAUER, E.E., 1960. Amer. Soc. Test Mat. Spec. Tech. Pub. 254.

BIDWELL, J.I., JEPSON, W.B. & TOMS, G.L., 1970. The interaction of kaolinite with polyphosphate and polyacrylate in aqueous solutions - some preliminary results. Clay Min., 8, 445-459.

BISCHOFF, J.L., 1972. A ferroan nontronite from the Red Sea Geothermal System. Clays and Clay Min., 20, 217-224.

BJORLYKKE, K., 1971. Petrology of Ordovician sediments from Wales. Norsk Geol. Tidssk., 51, 123-139.

BODENHEIMER, W. & HELLER, L., 1968. Sorption of methylene blue by montmorillonite saturated with different cations. Israel J. Chem., 6, 307-314

BRADLEY, D., 1965. The Hydrocyclone. Pergamon Press, 320 pp.

BRAMMALL, A. & LEECH, J.G.C., 1940. Montmorillonite in fuller's earth, Nutfield, Surrey. Geol. Mag., 77, 102-112.

BRITISH STANDARD 1377 (1967). Methods of Testing Soils for Civil Engineering Purposes. British Standards Institution, London, 234 pp.

BROWN, G., CATT, J.A. & WEIR, A., 1969. Zeolites of the clinoptilolite-heulandite type in sediments of south-east England. Min. Mag., 37, 480-488.

BUTLER, A.J., 1937. On Silurian and Cambrian rocks encountered in a deep boring at Walsall, South Staffordshire. Geol. Mag., 74, 241-257.

BYSTROM, A.M., 1956. Mineralogy of the Ordovician bentonite beds at Kinnekulle, Sweden. Sveriges Geol. Undersokn., Arsbok 48, Ser. C (1954) No. 5.

CARTER, D.L., HEILMAN, M.D. & GONZALEZ, C.L., 1965. Ethylene glycol monoethyl ether for determining surface area of silicate minerals. Soil Science, 100, 356-360.

CANN, J.R., 1970. Rb, Sr, Y, Zr and Nb in some oceanic floor basaltic rocks. Earth Planet. Sci. Letters, 10, 7-11.

COLE, W.F. & HOSKING, J.S., 1957. Clay mineral mixtures and interstratified minerals. In: The Differential Thermal Investigation of Clays, ed. R.C. Mackenzie, Mineralogical Society.

COWPERTHWAITE, I.A., FITCH, F.J., MILLER, J.A., MITCHELL, J.G., & ROBERTSON, R.H.S., 1972. Sedimentation, petrogenesis and radioisotopic age of the Cretaceous fuller's earth of Southern England. Clay Min., 9, 309-327.

COX, A.J., 1918. Excursion to Nutfield and Redhill. Proc. Geol. Assoc., 29, 150.

DAHLSTROM, D.A., 1949. Cyclone operating factors and capacities on coal and refuse slurries. Trans. Amer. Inst. Min. Engrs., 184, 331-344.

DAUGHERTY, T.H., 1948. Sequestration, dispersion, and dilatancy - lecture demonstrations. J. Chem. Education, 25, 482-486.

DAVIS, C.E., AHMAD, N. & JONES, R.L., 1971. Effect of exchangeable cations on the surface areas of clays. Clay Min., 9, 258-261.

DEER, W.A., HOWIE, R.A. & ZUSSMAN, J., 1962. Rock Forming Minerals: Vol. 3 Sheet Silicates. Longmans, 270 pp.

DEER, W.A., HOWIE, R.A. & ZUSSMAN, J., 1963. Rock Forming Minerals: Vol. 4 Framework Silicates. Longmans, 435 pp.

DE KIMPE, C., GASTUCHE, M.C. & BRINDLEY, G.W., 1961. Ionic coordination in alumina-silicic gels in relation to clay mineral formation. Amer. Min., 46, 1370-1381.

DOLCATER, D.L., SYERS, J.K. & JACKSON, M.L., 1970. Titanium as a free oxide and substituted forms in kaolinites and other soil minerals. Clays and Clay Min., 18, 71-79.

DROSTE, J.B. & VITALIANIO, C.J., 1973. Tioga Bentonite (Middle Devonian) of Indiana. Clays and Clay Min., 21, 9-13.

DYAL, R.S. & HENDRICKS, S.B., 1950. Total surface of clays in polar liquids as a characteristic index. Soil Science, 69, 421-432.

EARLEY, J.W., MILNE, I.H. & McVEAGH, W.J., 1953. Thermal, dehydration, and X-ray studies on montmorillonite. Amer. Min., 38, 770-783.

ELTANTAWY, I.M. & ARNOLD, P.W., 1973. Reappraisal of ethylene glycol mono-ethyl ether (EGME) method for surface area estimations of clays. J. Soil Sci., 24, 232-238.

ENGEL, A.E.J. & ENGEL, C.G., 1964. Igneous rocks of the East Pacific Rise. Science, 146, 477-485.

----- ENGEL, C.G. & HAVENS, R.G., 1965. Chemical characteristics of oceanic basalts and the upper mantle. Geol. Soc. Amer. Bull., 76, 719-734.

FAIRBAIRN, P.E. & ROBERTSON, R.H.S., 1957. Liquid limit and dye adsorption. Clay Min. Bull., 3, 129-136.

GAUDETTE, H.E., EADES, J.L. & GRIM, R.E., 1966. The nature of illite. Clays and Clay Min. (Proc. 13th Conf.) 33-48.

GIBBS, R.J., 1965. Error due to segregation in quantitative clay mineral X-ray diffraction mounting techniques. Amer. Min., 50, 741-751.

GIBSON, I.L., 1972. The chemistry and petrogenesis of a suite of pantellerites from the Ethiopian Rift. J. Pet., 13, 31-44.

GILKES, R.J., 1968. Clay mineral provinces in the Tertiary sediments of the Hampshire Basin. Clay Min., 7, 351-361.

----- & HODSON, F., 1971. Two mixed-layer mica-montmorillonite minerals from sedimentary rocks. Clay Min., 9, 125-138.

GREENE-KELLY, R., 1957. Montmorillonites. In: The Differential Thermal Investigation of Clays, ed. R.C. Mackenzie, Mineralogical Society.

----- 1964. The specific surface areas of montmorillonites. Clay Min. Bull., 5, 392-400.

GRIM, R.E., 1962. Applied Clay Mineralogy. McGraw-Hill, 422 pp.

GRIM, R.E. & KULBICKI, G., 1961. Montmorillonite: high temperature reactions and classification. Amer. Min., 46, 1329-1369.

HAGEMANN, F. & SPJELDNAES, N., 1955. The Middle Ordovician of the Oslo region, Norway: 6, notes on bentonites (K-bentonites) from the Oslo-Asker district. Norsk Geol. Tidssk., 35, 29-51.

HALLAM, A. & SELWOOD, B.W., 1968. Origin of fuller's earth in the Mesozoic of Southern England. Nature, 220, 1193-1195.

----- & SELWOOD, B.W., 1970. Montmorillonite and zeolites in Mesozoic and Tertiary beds of southern England. Min. Mag., 37, 950-952.

HANG, P.T. & BRINDLEY, G.W., 1970. Methylene blue absorption by clay minerals. Determination of surface areas and cation exchange capacities. (Clay-organic studies XVIII). Clays and Clay Min., 18, 203-212.

HARDER, H., 1972. The role of magnesium in the formation of smectite minerals. Chem. Geol., 10, 31-39.

HARTMAN, P., 1969. Can Ti^{4+} replace Si^{4+} in silicates? Min. Mag., 37, 366-369.

HARTWELL, J.M., 1965. The diverse uses of montmorillonite. Clay Min., 6, 111-118.

HELLER-KALLAI, L. & KALMAN, Z.H., 1972. Some naturally occurring illite-smectite interstratifications. Clays and Clay Min., 20, 165-168.

HERRMANN, A.G., 1970. Yttrium and Lanthanides: Abundance in Common Sediments and Sedimentary Rock Types. Handbook of Geochemistry 39, 57-71-K, Springer Verlag.

HEWETT, D.F., 1917. The origin of bentonite. J. Wash. Acad. Sci., 7, 196-198.

HOFMANN, F., 1959. Modern concepts on clay minerals for foundry sands. British Foundryman, 52, 161-170.

HOLLAND, C.H., 1969. The Welsh Silurian geosyncline in its regional context. In: The Pre-Cambrian and Lower Palaeozoic Rocks of Wales, ed. A. Wood. University of Wales Press, Cardiff, 203-217.

HOWER, J., 1968. Order of mixed-layering in illite/montmorillonites. Clays and Clay Min. (Proc. 15th Conf., 1966), 63-74.

----- & MOWATT, T.C., 1966. The mineralogy of illites and mixed-layer illite/montmorillonites. Amer. Min., 51, 825-854.

HUFF, W.D., 1963. Mineralogy of Ordovician K-bentonites in Kentucky. Clays and Clay Min. (Proc. 11th Conf., 1962), 200-209.

JEANS, C.V., 1968. The origin of the montmorillonite of the European Chalk with special reference to the Lower Chalk of England. Clay Min., 7, 311-329.

JOHANSEN, R.T. & DUNNING, H.N., 1959. Water-vapor adsorption on clays. Clays and Clay Min. (Proc. 6th Conf., 1957), 249-258.

JONES, F.O., 1964. New fast, accurate test measures bentonite in drilling mud. Oil Gas J., 62, 76-78.

JORGENSEN, P., 1964. Mineœalogical composition of two Silurian bentonite beds from Sundvollen, Southern Norway. Norsk Geol. Tidssk., 44, 227-234.

KERR, P.F., 1932. Montmorillonite or smectite as constituents of fuller's earth and bentonite. Amer. Min., 17, 192-

----- et alia, 1950. Analytical data on reference clay materials. American Petroleum Institute, Project 49, Preliminary Rept. nO. 7.

KIELING, J.J. & WILSON, R.B., 1960. Adsorption of methylene blue in the determination of surface areas. J. Appl. Chem., 10, 109-113.

KIRKALDY, J.F., 1963. The Wealden and Marine Lower Cretaceous Beds of England. Proc. Geol. Assoc., 74, 127-146.

KNIGHT, W.C., 1848. Bentonite. Engng. Min. J., 66, 491.

LOW, P.F. & WHITE, J.L., 1970. Hydrogen bonding and polywater in clay-water systems. Clays and Clay Min., 18, 63-66.

MACEWAN, D.M.C., 1956. A study of an interstratified illite-montmorillonite clay from Worcestershire, England. Clays and Clay Min. (Proc. 4th Conf., 1955), 166-172.

----- 1961. Montmorillonite Minerals. Chapter IV in: The X-ray Identification and Crystal Structures of Clay Minerals, ed. G. Brown, Mineralogical Society, London.

----- RUIZ AMIL, A. & BROWN, G., 1961. Interstratified Clay Minerals. Chapter XI in: The X-ray Identification and Crystal Structures of Clay Minerals, ed. G. Brown, Mineralogical Society, London.

MACKENZIE, F.T. & GARRELS, R.M., 1966. Silica-bicarbonate balance in the ocean and early diagenesis. J. Sed. Pet., 36, 1075-1084.

MACKENZIE, R.C., 1957. Saponite from Allt Ribhein, Fiskavaig Bay, Skye. Min. Mag., 31, 672-680.

----- b The montmorillonite differential thermal curve, 1. General variability in the dehydroxylation region. Bull. Groupe Franc. Argiles, 9, 7-15. 1957.

----- 1960. The evaluation of clay mineral composition with particular reference to smectites. Silicates Ind., 25, 12-18, 71-75.

----- 1961. The quantitative determination of minerals in clays. Acta Univ. Carolinae, Geol., Suppl., 1, 11-21.

----- 1963. Retention of exchangeable ions by montmorillonite. International Clay Conf., Stockholm, 1, eds. I.T. Rosenqvist and P. Graff-Petersen, 183-193.

MACKENZIE, R.C., 1964. Hydratationseigenschaften von Montmorillonit. Ber. Deut. Keram. Ges., 41, 696-708.

----- 1970. Simple phyllosilicates based on gibbsite- and brucite-like sheets. Chapter 18 in: Differential Thermal Analysis, Vol. 1, ed. R.C. Mackenzie, Academic Press.

MASON, B. & SAND, L.B., 1960. Clinoptilolite from Patagonia: the relationship between clinoptilolite and heulandite. Amer. Min., 45, 341-350.

MCATEE, J.L., 1958. Heterogeneity in montmorillonite. Clays and Clay Min. (Proc. 5th Conf., 1956), 279-288.

MEHRA, O.P. & JACKSON, M.L., 1960. Iron oxide removal from soils and clays by a dithionite-citrate system buffered with sodium bicarbonate. Clays and Clay Min. (Proc. 7th Conf., 1958), 317-327.

MIELENZ, R.C., SCHIELTZ, N.C. & KING, M.E., 1955. Effect of exchangeable cation on X-ray diffraction patterns and thermal behaviour of a montmorillonite clay. Clays and Clay Min. (Proc. 3rd Conf., 1954), 146-173.

MILLOT, G., 1970. Geology of Clays. Chapman & Hall, 429 pp.

MITCHELL, G.H., POCOCK, R.W. & TAYLOR, J.H., 1961. Geology of the Country around Droitwich, Abberley and Kidderminster. Mem. Geol. Surv., HMSO, London

MOBERLY, R., KIMURA, H.S. & MCCOY, F.W., 1968. Authigenic marine phyllosilicates near Hawaii. Geol. Soc. Amer. Bull., 79, 1449-1460.

MORELLI, G.L., FAVRETTO, L. & BYSTROM ASKLUND, A.M., 1967. Determination of the type of stacking in a mixed-layer clay mineral from Kinnekulle. Clay Min., 7, 113-115.

MOSSLER, J.H. & HAYES, J.B., 1966. Ordovician potassium bentonites of Iowa. J. Sedim. Pet., 36, 414-427.

MULLER, G., 1967. Diagenesis in argillaceous sediments. In: Diagenesis in Sediments, eds. G. Larsen and G.C. Chilingar, Elsevier, 127-177.

MUNGAN, N. & JESSEN, F.W., 1963. Studies in fractionated montmorillonite suspensions. Clays and Clay.Min. (Proc. 11th Conf., 1962), 282-294.

MURCHISON, R.I., 1839. The Silurian System.

NAVARRO, J.M. & TAYLOR, H.F., 1959. The significance of liquid limit in evaluating bentonites for foundry use. The British Foundryman, 52, 342-355.

NAYLOR, T.R., 1958. The hydrocyclone in the refining of china clay. Mine and Quarry Eng., 24, 510-513.

NEMECZ, E., 1962. Thermal behaviour of the adsorbed and interlaminar water content of montmorillonite. Acta Geol. Acad. Sci. Hung., 6, 365-387.

NEUMANN, B.S., 1964. The thermal stability of acid extracted montmorillonites. International Clay Conf., Stockholm, 1, eds. I.T. Rosenqvist and P. Graff-Petersen, 183-193.

NEVINS, M.J. & WEINTRITT, D.J., 1967. Determination of cation exchange capacity by methylene blue adsorption. Amer. Ceram. Soc. Bull., 46, 587-592.

NEWTON, E.F., 1937. The petrography of some English Fuller's Earths and the rocks associated with them. Proc. Geol. Assoc., 48, 175-197.

ORVILLE, P.M., 1967. Unit-cell parameters of the microcline-low albite and the sanidine-high albite solid solution series. Amer. Min., 52, 55-86.

OSTHAUS, B.B., 1954. Chemical determination of tetrahedral ions in nontronite and montmorillonite. Clays and Clay Min. (Proc. 2nd Conf., 1953), 404-417.

OSTHAUS, B.B., 1955. Interpretation of chemical analyses of montmorillonites. Clays and Clay Technology, California State Div. Mines, Bull. 169, 95-100.

PERRIN, R.M.S., 1971. The Clay Mineralogy of British Sediments. Mineralogical Society (Clay Minerals Group) London, 247 pp.

PERRY, E. & HOWER, J., 1970. Burial diagenesis in Gulf Coast pelitic sediments. Clays and Clay Min., 18, 165-177.

POOLE, E.G. & KELK, B., 1971a. Calcium montmorillonite (fuller's earth) in the Lower Greensand of the Baulking area, Berkshire. (Geology). Rep. No. 71/4 Inst. Geol. Sci., London.

----- & KELK, B., 1971b. Calcium montmorillonite (fuller's earth) in the Lower Greensand of the Fernham area, Berkshire. (Geology). Rept. No. 71/12 Inst. Geol. Sci., London.

RAVINA, I. & LOW, P.F., 1972. Relation between swelling, water properties and b-dimension in montmorillonite-water systems. Clays and Clay Min., 20, 109-124.

REYNOLDS, R.C., 1967. Interstratified clay systems: calculation of the total one-dimensional diffraction function. Amer. Min., 52, 661-672.

----- & HOWER, J., 1970. The nature of interlayering in mixed-layer illite-montmorillonite. Clays and Clay Min., 18, 25-36.

RITCHIE, J.A. & GREGG, D.R., 1965. Bentonites of Canterbury. Proc. 8th Commonw. Min. metall. Congr., 7 (208), 1-13.

----- GREGG, D.R. & EWART, A., 1969. Bentonites of Canterbury. New Zealand J. Geol. Geophys., 12, 583-608.

ROALDSET, E., 1973. Rare earth elements in Quaternary clays of the Numedal area, southern Norway. Lithos, 6, 349-372.

ROBERTSON, R.H.S., 1961. The origin of English fuller's earths. Clay Min. Bull., 4, 282-287.

ROSS, C.S. & SHANNON, E.V., 1926. Minerals of bentonite and related clays and their physical properties. J. Amer. Ceram. Soc., 9, 77-96.

SANSOM, K. & WHITE, D., 1971. Aggregation and dispersion of clays with particular reference to the montmorillonites. Trans. and J. Brit. Ceram. Soc., 70, 163-166.

SATO, M., OINUMA K., & KOBAYASHI, K., 1965. Interstratified mineral of illite and montmorillonite. Nature, 208, 179-180.

SCHULTZ, L.G., 1963. Non-montmorillonitic composition of some bentonite beds. Clays and Clay Min. (Proc. 11th Conf., 1962), 169-177.

----- 1969. Lithium and potassium adsorption, dehydroxylation temperature, and structural water content of aluminous smectites. Clays and Clay Min., 17, 115-149.

SHERLOCK, R.L., 1922. Geology of the Country around Aylesbury and Hemel Hempsted. Mem. Geol. Surv., HMSO, London.

SLANSKY, E., 1961. The occurrence of mixed-layer clay minerals in some Czechoslovak argillaceous sediments. Acta Univ. Carolinae, Geol., Suppl., 1, 299-306.

SMITH, D.G.W., 1967. The petrology and mineralogy of some Lower Devonian bentonites from Gaspe, P.Q. Can. Min., 9, 141-165.

SPEARS, D.A., 1971. The mineralogy of the Stafford tonstein. Proc. Yorks. Geol. Soc., 38, 497-516.

SQUIRRELL, H.C. & TUCKER, E.V., 1960. The geology of the Woolhope inlier (Herefordshire). Q.J.G.S., 116, 139-181.

SZANTO, F., GILDE-FARKAS, M., VARKONYI, B. & BALAZS, J., 1967. The binding of Na_2CO_3 by bentonite fractions. Acta Geol. Acad. Sci. Hung., 11, 409-418.

TETTENHORST, R. & JOHNS, W.D., 1966. Interstratification in montmorillonite. Clays and Clay Min. (Proc. 13th Conf., 1964), 85-94.

TREWIN, N.H., 1968. Potassium bentonites in the Namurian of Staffordshire and Derbyshire. Proc. Yorks. Geol. Soc., 37, 73-90.

----- 1971. Potassium bentonites in the Wenlock Limestone of Shropshire. Mercian Geol., 4, 1-7.

TRIPLEHORN, D.M., 1970. Clay mineral diagenesis in Atoka (Pennsylvanian) sandstones, Crawford County, Arkansas. J. Sed. Pet., 40, 838-847.

TUREKIAN, K.K. & WEDEPOHL, K.H., 1961. Distribution of the elements in some major units of the earth's crust. Geol. Soc. Amer. Bull., 72, 175-192.

TURNER, J.S., 1935 . Gotlandian volcanicity in Western Europe. Geol. Mag., 72, 145-151.

TYNER, E.H., 1939. The use of sodium metaphosphate for dispersion of soils for mechanical analysis. Soil Sci. Soc. Amer. Proc., 3, 106-113.

VAN DE KAMP, P.C., 1969. The Silurian volcanic rocks of the Mendip Hills, Somerset, and the Tortworth area, Gloucestershire, England. Geol. Mag., 106, 542-553.

VAN OLPHEN, H., 1963. Clay Colloid Chemistry. Interscience, 301 pp.

VLASOV, K.A., 1966. Geochemistry of rare elements. I.P.S.T., Jerusalem, 688 pp.

WALKDEN, G.M., 1972. The mineralogy and origin of interbedded clay wayboards in the Lower Carboniferous of the Derbyshire Dome. Geol. J., 8, 143-160.

WARKENTIN, B.P., 1961. Interpretation of the upper plastic limit of clays. Nature, 190, 287-288.

WEAVER, C.E. & BATES, T.F., 1952. Mineralogy and petrology of the Ordovician metabentonites and related limestones. Clay Min. Bull., 11, 258-264.

WEAVER, C.E. & BECK, K.C., 1971. Clay-water diagenesis during burial; how mud becomes gneiss. Geol. Soc. Amer. Spec. Pap. 134, 96 pp.

---- & POLLARD, L.D., 1973. The Chemistry of Clay Minerals. Elsevier, 213 pp.

WEAVER, S.D., SCEAL, J.S.C. & GIBSON, I.L., 1972. Trace-element data relevant to the origin of trachytic and pantellleritic lavas in the East African Rift System. Contr. Mineral. Petrol., 36, 181-194.

WEIR, A.H., 1965. Potassium retention in montmorillonites. Clay Min., 6, 17-22.

----- & CATT, J.A., 1965. The mineralogy of some Upper Chalk samples from the Arundel area, Sussex. Clay Min., 6, 97-110.

----- & GREENE-KELLY, R., 1962. Beidellite. Amer. Min., 47, 137-146.

WHITE, W.A., 1958. Water sorption properties of homoionic clay minerals. Illinois State Geol. Surv., Rept. of Investigations 208.

WILSON, A.D., 1955. A method for the determination of ferrous iron in rocks. Bull. Geol. Surv. Gt. Britain, 9, 56-58.

WILSON, M.J., 1971. Clay mineralogy of the Old Red Sandstone (Devonian) of Scotland. J. Sed. Pet., 41, 995-1007.

WOOD, G.V., 1956. The heavy mineral suites of the Lower Greensand of the western Weald. Proc. Geol. Ass., 67, 124-137.

WORSSAM, B.C., 1963. Geology of the Country around Maidstone. Mem. Geol. Surv., HMSO, London, 152 pp.

WYLLIE, P.J., COX, K.E. & BIGGAR, G.M., 1962. The habit of apatite in synthetic systems and igneous rocks. J. Pet., 3, 238-247.

YODER, H.S. & EUGSTER, H.P., 1955. Synthetic and natural muscovites. Geochim. et Cosmochim. Acta, 8, 225-280.

ZIEGLER, A.M., MCKERROW, W.S., BURNE, R.V. & BAKER, P.E., 1969. Correlation and environmental setting of the Skomer Volcanic Group, Pembrokeshire. Proc. Geol. Assoc., 80, 409-439.